INTERNATIONAL UNION FOR QUATERNARY RESEARCH

International Inter-INQUA Field Conference and Workshop on Tephrochronology, Loess, and Paleopedology

University of Waikato, Hamilton, New Zealand
7-12 February, 1994

INTRA-CONFERENCE AND POST-CONFERENCE TOUR GUIDES

Edited by

D. J. Lowe

Department of Earth Sciences, University of Waikato, Private Bag 3105,
Hamilton, New Zealand

Bibliographic citation for entire guidebook:

Lowe, D.J. (editor) 1994. Conference Tour Guides. *International Inter-INQUA Field Conference and Workshop on Tephrochronology, Loess, and Paleopedology,* University of Waikato, Hamilton, New Zealand. 186p.

Bibliographic citation for sections within the guidebook (e.g.):

Pillans, B.J.; Palmer, A.S. 1994. Post-Conference Tour Day 3: Tokaanu—Wanganui. *In* Lowe, D.J. (ed) Conference Tour Guides. *International Inter-INQUA Field Conference and Workshop on Tephrochronology, Loess, and Paleopedology*, University of Waikato, Hamilton, New Zealand: 139-156.

Acknowledgements

I thank all the contributors to the guide for their written efforts, and for fine leadership in the field. Ian Nairn (IGNS) is especially thanked for co-leading part of Day 2 of the Intra-Conference Field Trip, and Neill Kennedy (formerly DSIR), Dennis Eden (Landcare Research), and Ron Kimber (CSIRO) are thanked for providing unpublished information. I have appreciated special assistance from Laurence Gaylor (field site preparation), Mike Green (back-up vehicle), Frank Bailey (drafting), Cam Nelson (departmental support) (all University of Waikato), and Carole Mardon and other staff of the University of Waikato Printery. The various people or organisations who hosted or transported the tour parties, or willingly allowed access to private land, are also thanked.

D.J. Lowe (Editor)

Note: Throughout the text, Ma = millions of years before present, ka = thousands of years before present.

TABLE OF CONTENTS

INTRODUCTION TO NEW ZEALAND

Lowe, D.J. 1994. Introduction to New Zealand. In: Lowe, D.J. (ed) Conference Tour Guides. Proceedings International Inter-INQUA Field Conference and Workshop on Tephrochronology, Loess, and Paleopedology, University of Waikato, Hamilton, New Zealand, 4-22.

D. J. Lowe
Department of Earth Sciences
University of Waikato, Private Bag 3105,
Hamilton, New Zealand

NEW ZEALAND'S GEOLOGICAL ENVIRONMENT

New Zealand consists of a cluster of islands, the three largest being North, South, and Stewart, in the southwest Pacific Ocean. They have a total land area of about 270 000 km^2 (similar to that of the British Isles or Japan). The islands are the small emergent parts of a much larger submarine continental mass (Fig. 0.1) that was rafted away from Australia and Antarctica by sea-floor spreading in the proto-Tasman Sea between 85 and 60 Ma. Much of this New Zealand subcontinent is a remnant of the former eastern margin of Gondwanaland, the ancient southern supercontinent. The mainland islands form a long, narrow, NE-SW trending archipelago bisected by an active, obliquely converging, boundary between the Australian and Pacific lithospheric plates (Fig. 0.2), which has evolved over the last 25 million years (Kamp 1992). The plate boundary is marked by active seismicity and volcanic arcs, illustrating New Zealand's position as part of the Circum-Pacific Mobile Belt — the so-called "Pacific Ring of Fire". The NE-SW trend of the modern plate boundary cuts across mainly NW-SE oriented structural features inherited from earlier (mid-Cretaceous) rifting events.

In the South Island, continent-continent convergence across the transcurrent Alpine Fault dominates the tectonic scene, with rapid uplift and jagged relief being the result. Numerous peaks exceed 3000 m in elevation. Rates of rock uplift are most rapid in the central portion of the Southern Alps, currently averaging ≈10 mm/year (Kamp & Tippett 1993; Tippett & Kamp 1993). Over the entire period of uplift, mean rock uplift rates range from ≈1-3 mm/yr — the rate of uplift (and denudation) has thus accelerated towards the present day. Fission track dating shows that uplift of the southern end of the Southern Alps began about 8 Ma, the northern end at 5 Ma, and the southeastern margin at 3 Ma (Kamp et al. 1989; Tippett & Kamp 1993). Because of such rapid uplift, the late Cretaceous-early Cenozoic cover rocks have been largely removed and therefore the landforms are developed in indurated basement rocks (Fig. 0.3; see also Williams 1991).

In the North Island, in contrast, the ocean-continent convergence has commonly produced marine sedimentary basins and has inverted them, and so generally late Cretaceous-Cenozoic rock sequences, including volcanic ones, are dominant. The uplift of the crust of northern and central North Island originates from high heat flows, but in southeastern North Island it is driven by tectonic thickening. An active volcanic arc of andesite and dacite volcanoes runs from White Island to Mt Ruapehu (Fig. 0.2; Cole 1990). To the northwest of this arc is a backarc region characterised by a much-faulted basin-and-range topography involving basement rocks and basic and rhyolitic volcanism. Large multivent calderas, the sources of voluminous rhyolite lava and of pyroclastic deposits in the form of thick sheets of ignimbrites and widely dispersed airfall tephras, occur immediately behind the active volcanic arc (Houghton et al. 1994).

Late Cenozoic intraplate and subduction-related volcanism

The North Island, located on the leading edge of the Australian plate, is being underthrust by the Pacific plate at the Hikurangi Trench with the subducting slab dipping to the NW at c. 50°. Since about 5 Ma, a series of NE-trending frontal arc volcanoes has migrated c. 100 km southeastwards across the central North Island, probably because of gradual steepening of the subducted slab, to reach the present-day locus of activity in the Taupo Volcanic Zone (TVZ) about 2 Ma (Fig. 0.2; Kamp 1984; Tatsumi & Tsunakawa 1992).

Two types of volcanism resulting from this tectonic setting are manifest in the North Island, as follows:

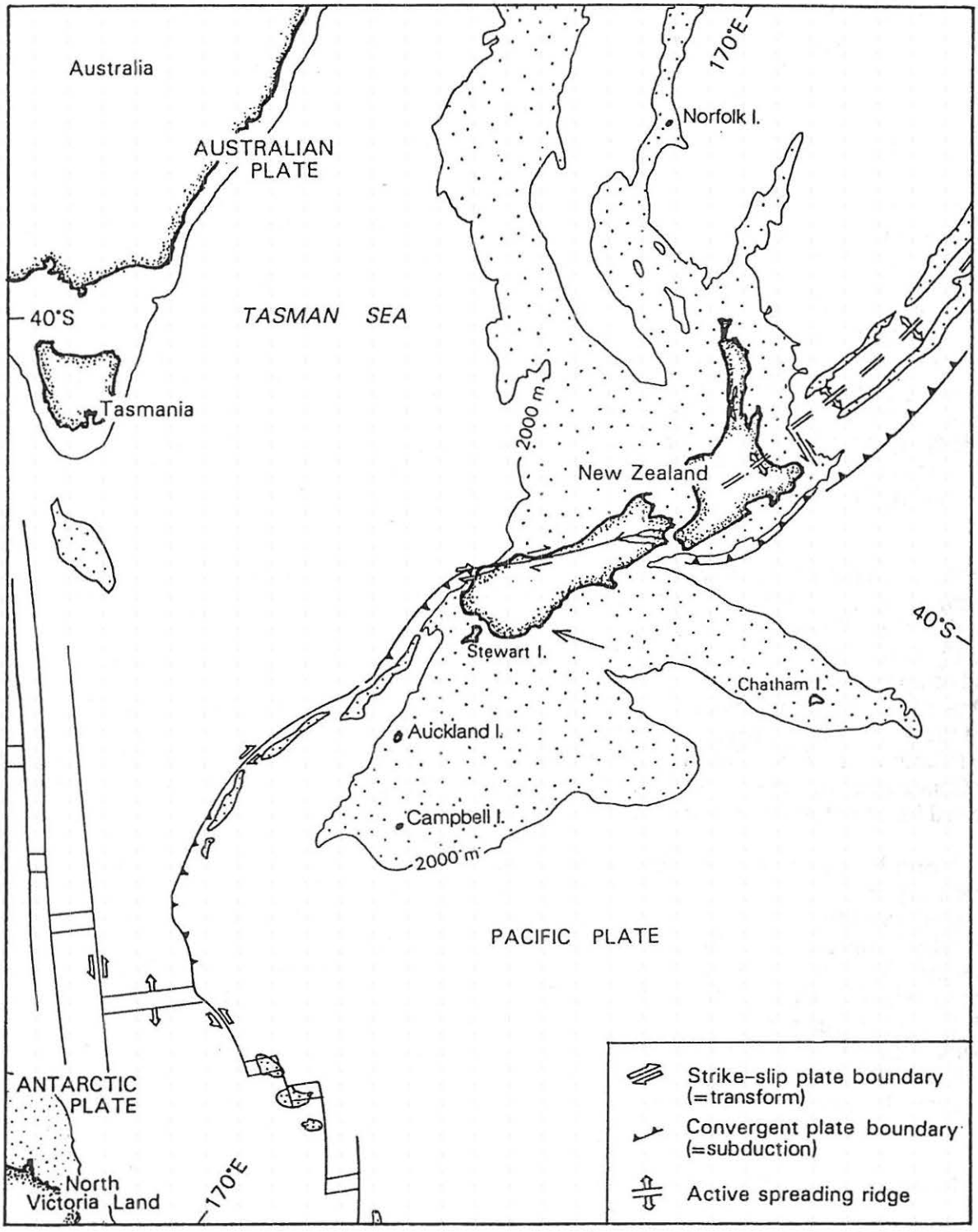

Figure 0.1: Generalised plate tectonic setting of New Zealand and the southwest Pacific. Sparse stipple represents continental sea floor shallower than 2000 m, and defines the New Zealand subcontinent. The active spreading ridge offshore marks the Havre Trough (after Kamp 1986).

(1) Mainly basaltic, intraplate volcanism in the backarc region. Effectively confined to western and northern North Island in seven volcanic fields (Fig.0.2), this volcanism may be caused by the upwelling of asthenospheric materials from deeper parts of the mantle (Fig. 0.4). There is a progressive younging in age of the fields from the Alexandra Volcanics (2.74-1.60 Ma), to Ngatutura (1.83-1.54 Ma), to South Auckland (1.56-0.51 Ma), and to Auckland (0.14 Ma to 600 years) (Briggs et al. 1989; Kermode 1992). However, the Northland fields (numbered 5-7 in Fig. 0.2) show a wide range of ages from c. 10 Ma to c. 1.2 ka.

(2) Mainly andesitic and rhyolitic, subduction-related volcanism along the frontal arc and in the backarc region (collectively referred to as the Central Volcanic Region). Since c. 2 Ma, this volcanism relates chiefly to activity in the TVZ, a relatively narrow (<≈50 km) volcanotectonic depression comprising a young backarc basin — the Taupo-Rotorua Depression — formed within thin continental crust in an area of active extension (rifting) and very high heat flow (700-800 mW/m^2), and the adjacent frontal arc (Cole 1990; Tatsumi & Tsunakawa 1992). The arc extends about 250 km NE-SW from the active volcanoes of White Island in the Bay of Plenty to those of Tongariro Volcanic Centre south of Lake Taupo (Fig. 0.5) (cf. Wilson 1993). It is primarily andesite-dacite in composition, making up about 3% (volumetrically ≈800 km^3) of the TVZ deposits. Very rare basalts (proportionally <1%; ≈2 km^3) also occur in the region (Gamble et al. 1990). The Taupo-Rotorua Depression in the TVZ is evidently the southern extension of active oceanic back-arc rifting along the Havre Trough offshore (Fig. 0.1; Wright et al. 1990), and is currently widening at the rate of 18 ± 5 mm/yr (Darby & Williams 1991). A possible mechanism for this rifting is the injection of asthenospheric materials into the mantle wedge which, together with the subducted slab, is being pushed trenchwards (Fig. 0.4; Tatsumi & Tsunakawa 1992).

A second (part) subduction-related volcanic chain in the backarc region is that of the mainly basaltic Alexandra Volcanics and the andesitic Taranaki volcanoes (aged c. 1.8 Ma to A.D. 1755) in western North Island. These volcanoes are described in Briggs & McDonough (1990), Neall (1979), and Neall et al. (1986).

Taupo Volcanic Zone

The central part of the TVZ, which is comparable in size and longevity to the Yellowstone volcanic area in the United States (Wilson et al. 1984; Houghton et al. 1994), has erupted huge quantities (≈10 000 to 16 000 km^3) of rhyolitic lavas and pyroclastic deposits, including both welded and non-welded ignimbrites, of ≈2 km or more thickness (Wilson et al. 1984; Stern 1987). These silicic materials make up c. 97% of the TVZ deposits, and drillholes reveal that they are underlain in places by andesite lavas locally >1 km thick (Browne et al. 1992). The deposits have been erupted mainly from eight multivent centres marked by large calderas (Fig. 0.5), the earliest known eruptives originating from Mangakino caldera at least 1.6 Ma (Pringle et al. 1992; Soengkono et al. 1992; Briggs et al. 1993). The Taupo volcano is an 'inverse' volcano, so called because it is concave with the flanks sloping gently inwards towards the vent locations (Walker 1984), rather than forming the steep convex cones characteristic of andesite stratovolcanoes (e.g. Mt Taranaki) or rhyolite domes (e.g. Mt Tarawera). This inverted form arises largely because eruptions from rhyolitic volcanoes of this sort are typically so powerful that accumulation of erupted material near the vent is insufficient to counteract subsidence due to caldera collapse because of magma withdrawal and regional tectonic extension, and because later effusion of steep-sided domes is comparatively minor (Wilson 1993). The Mangakino and Kapenga calderas are probably extinct, Rotorua and Maroa may be feebly active, and Taupo and Okataina are very active, the latest eruptions occurring c. 1850 years ago (Taupo) and in A.D. 1886 (Tarawera), respectively. The Whakamaru caldera is probably extinct but intense faulting in the area may be partly due to resurgence (Wilson et al. 1986). Reporoa Caldera, previously described as a fault-angle depression, has recently been recognised as the eighth major rhyolitic centre in TVZ (Nairn et al. in press). It is the source of the Kaingaroa Ignimbrites (0.24 Ma).

The known history of eruptions from these calderas is summarised by Wilson et al. (1984, 1986), Wilson (1986, 1993), Briggs et al. (1993), Houghton et al. (1994), and Nairn et al. (in press). Such eruptions include one of the largest late Quaternary eruptions known, that of the Whakamaru-group ignimbrites and an associated airfall component, the Rangitawa Tephra, from Whakamaru caldera c. 0.35 Ma, producing >≈1200 km^3 of pyroclastic material (Froggatt et al. 1986; Kohn et al. 1992).

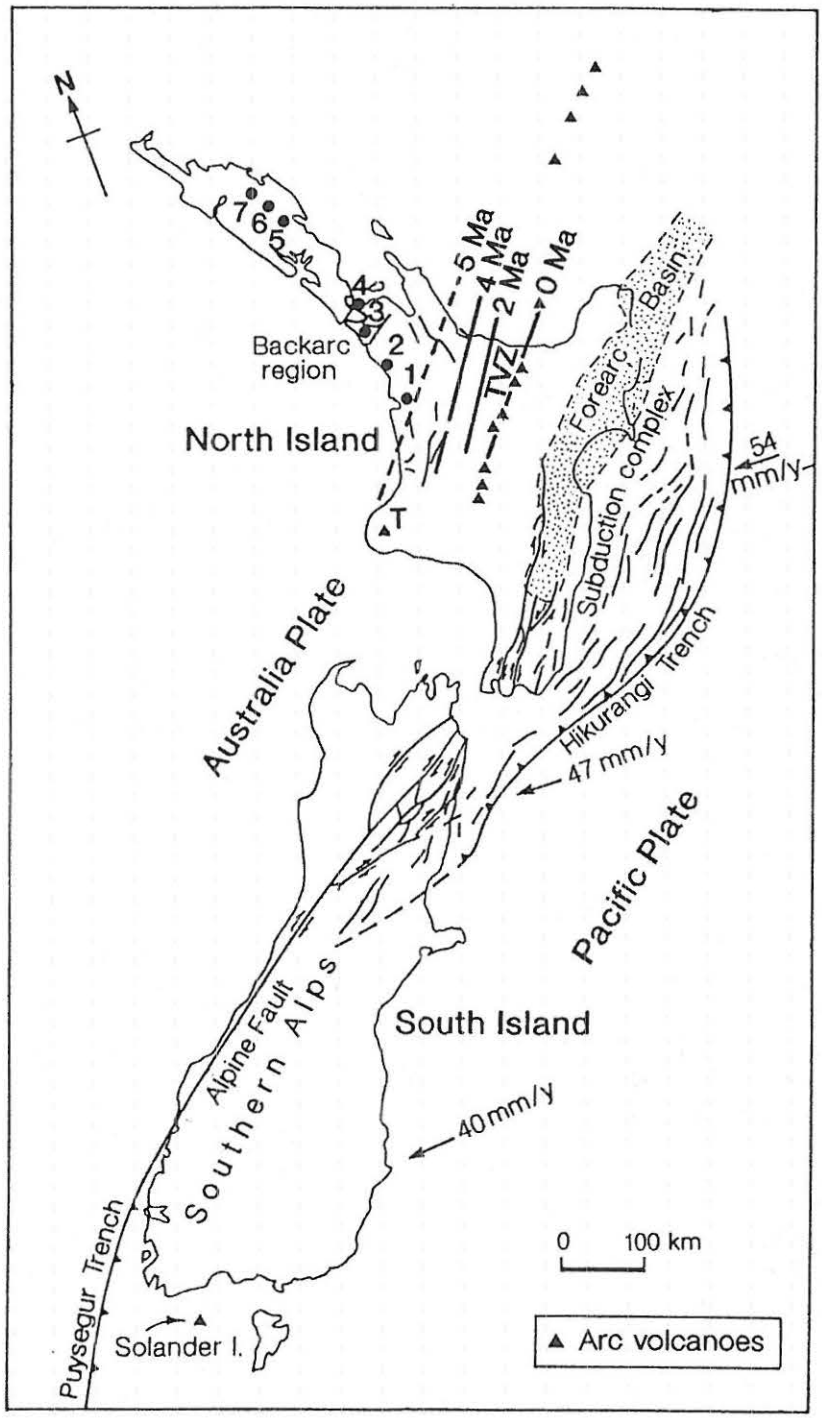

Figure 0.2: The present tectonic character of the obliquely convergent modern Australia-Pacific plate boundary through New Zealand (after Kamp 1992), and the trenchward migration of the arc volcanoes during the last 5 Ma (after Tatsumi & Tsunakawa 1992). TVZ = Taupo Volcanic Zone. Intraplate basalt volcanic fields are: 1, Alexandra (co-existing intraplate and subduction-related eruptives; Briggs & McDonough 1990); 2, Ngatutura; 3, South Auckland; 4, Auckland; 5, Whangarei; 6, Puhipuhi; 7, Kaikohe-Bay of Islands. T = Mt Taranaki.

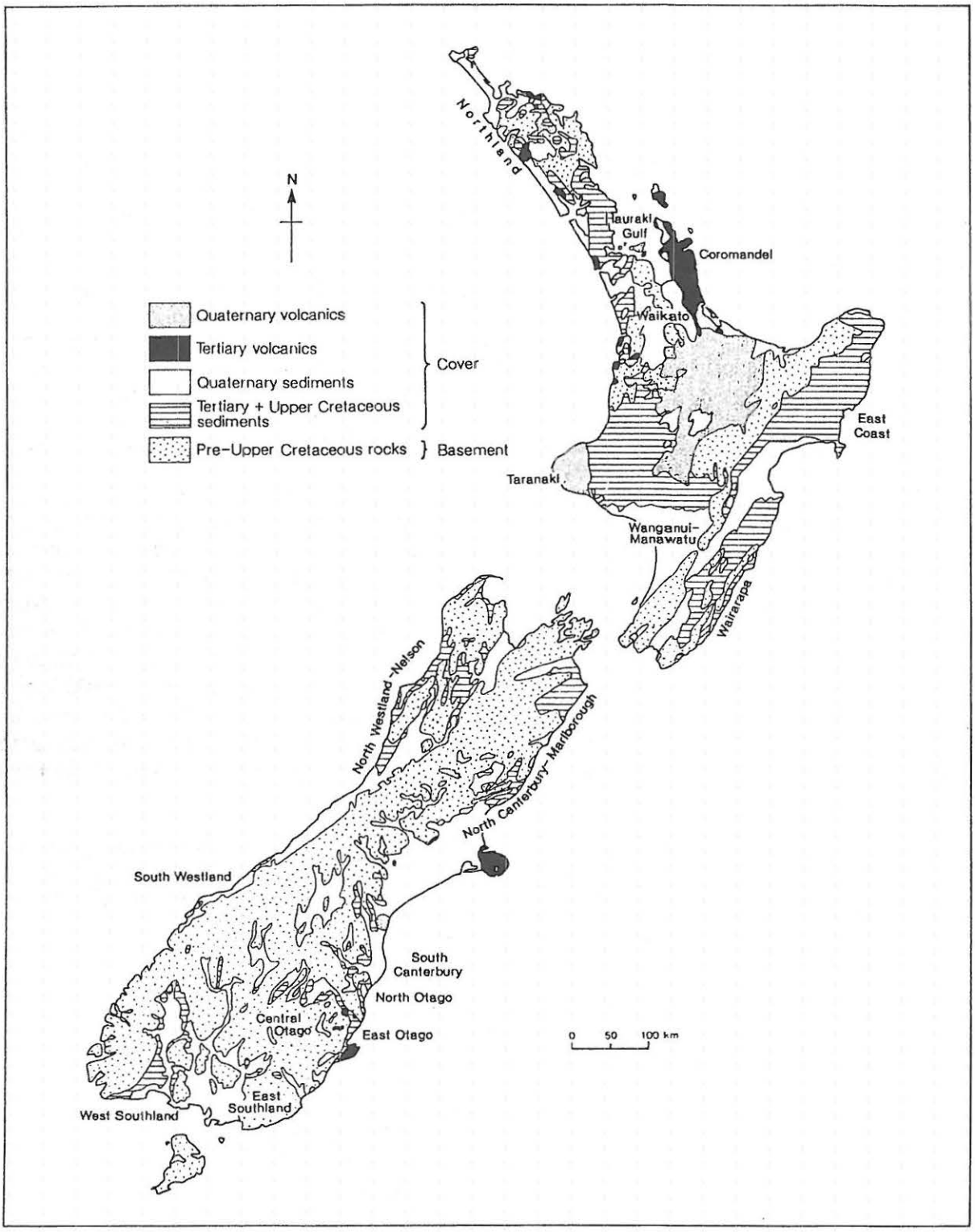

Figure 0.3: Generalised geological map of New Zealand (from Kamp 1992). Quaternary, 2-0 Ma; Tertiary, 65-2 Ma; Upper Cretaceous, 100-65 Ma; Pre-Upper Cretaceous, pre-100 Ma.

Fallout from this eruption probably reached S America, 10 000 km E of New Zealand, and beyond (Froggatt et al. 1986). Another enormous eruption was that of Kawakawa Tephra from Taupo volcano c. 22.6 ka, producing ≈500 km^3 of fall deposits, ≈300 km^3 of ignimbrite, and ≈500 km^3 of intra-caldera fill (Wilson 1993).

Tephrostratigraphy

Pyroclastic fall deposits associated with the central TVZ caldera eruptions are widespread in the North Island, with some forming important stratigraphic markers extending to the South Island and in deep sea cores both west and east of New Zealand (e.g. Nelson et al. 1985b; Barnes & Shane 1992; Pillans & Wright 1992). Apart from a few exceptions, the earliest tephra deposits ('tephra' is a widely-used collective term for all the unconsolidated, primary pyroclastic products of an eruption; Froggatt & Lowe 1990) at distal localities peripheral to TVZ have generally not been well dated. However, recent work using improved fission track dating techniques and the K-Ar and $^{40}Ar/^{39}Ar$ methods, together with paleomagnetism and new stratigraphic work, is making great advances (e.g. Shane 1991; Berryman 1992; Kohn et al. 1992; Pringle et al. 1992; Soengkono et al. 1992; Alloway et al. 1993). In the Waikato region, there are two groups of old, strongly weathered tephra sequences: the Kauroa Ashes (erupted from c. 2.3 to ?1 Ma; Briggs et al. 1989), and the Hamilton Ashes (erupted from c. 0.35 Ma to 0.1 Ma; Selby & Lowe 1992). Both groups have uncertain sources — the Kauroa beds possibly represent very early eruptions from TVZ (?Mangakino caldera), and the Hamilton beds may relate to the eruptions from the Taupo, Whakamaru, or Maroa centres.

Pyroclastic eruptives from TVZ over the past c. 50 ka are much better documented and their chronology (by radiocarbon dating) and distribution are generally well established (Froggatt & Lowe 1990; Lowe 1990; Lowe & Hogg 1992; Wilson 1993). In this time there have been ≈50 or more pyroclastic eruptions from the Taupo and Okataina calderas alone, a mean rate of one every ≈1000 years. Many eruptions produced volumes of deposits >>1 km^3 (cf. the 1980 eruption of Mt St Helens produced ≈1 km^3 of pyroclastic material). The three largest, volumetrically, were the Rotoiti (240 km^3), Kawakawa (800 km^3), and Taupo (90 km^3) eruptive episodes, with the total volume of rhyolitic material erupted from TVZ in the past c. 50 ka conservatively estimated at ≈800 km^3 of airfall tephra, 540 km^3 of ignimbrite, and 550 km^3 of extrusive lava, together equivalent to more than 700 km^3 of magma (Froggatt & Lowe 1990; Wilson 1993). Correlation techniques using discriminant function analysis have been successfully applied to late Quaternary tephras by Stokes & Lowe (1988) and Stokes et al. (1992).

Numerous andesitic tephras have been erupted from the Tongariro Volcanic Centre in late Quaternary times (e.g. Topping 1973; Cole et al. 1986; Lowe 1988; Donoghue et al. 1991, in press), and from Taranaki/Egmont Volcanic Centre (e.g. Neall 1972, 1979; Alloway 1989; Alloway et al. 1992a).

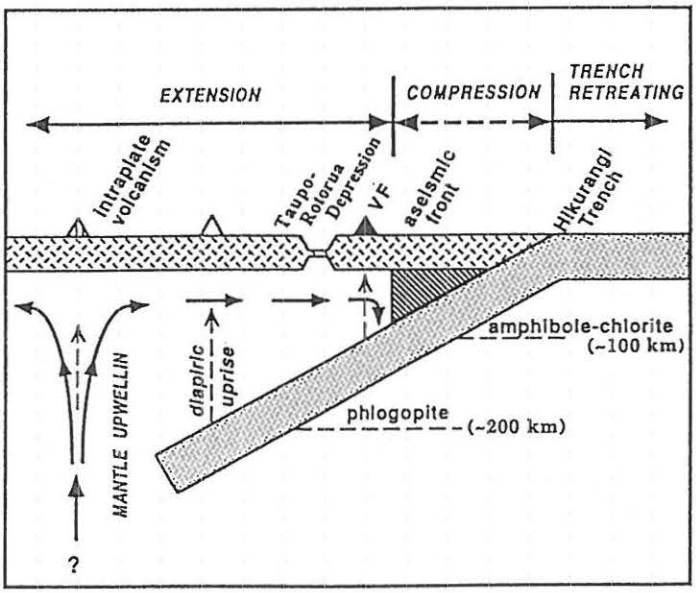

Figure 0.4: Model for the origin of backarc rifting and pattern of stress in North Island as related to intraplate and subduction-related volcanism (from Tatsumi & Tsunakawa 1992). VF = volcanic front (TVZ); hatching = forearc mantle wedge.

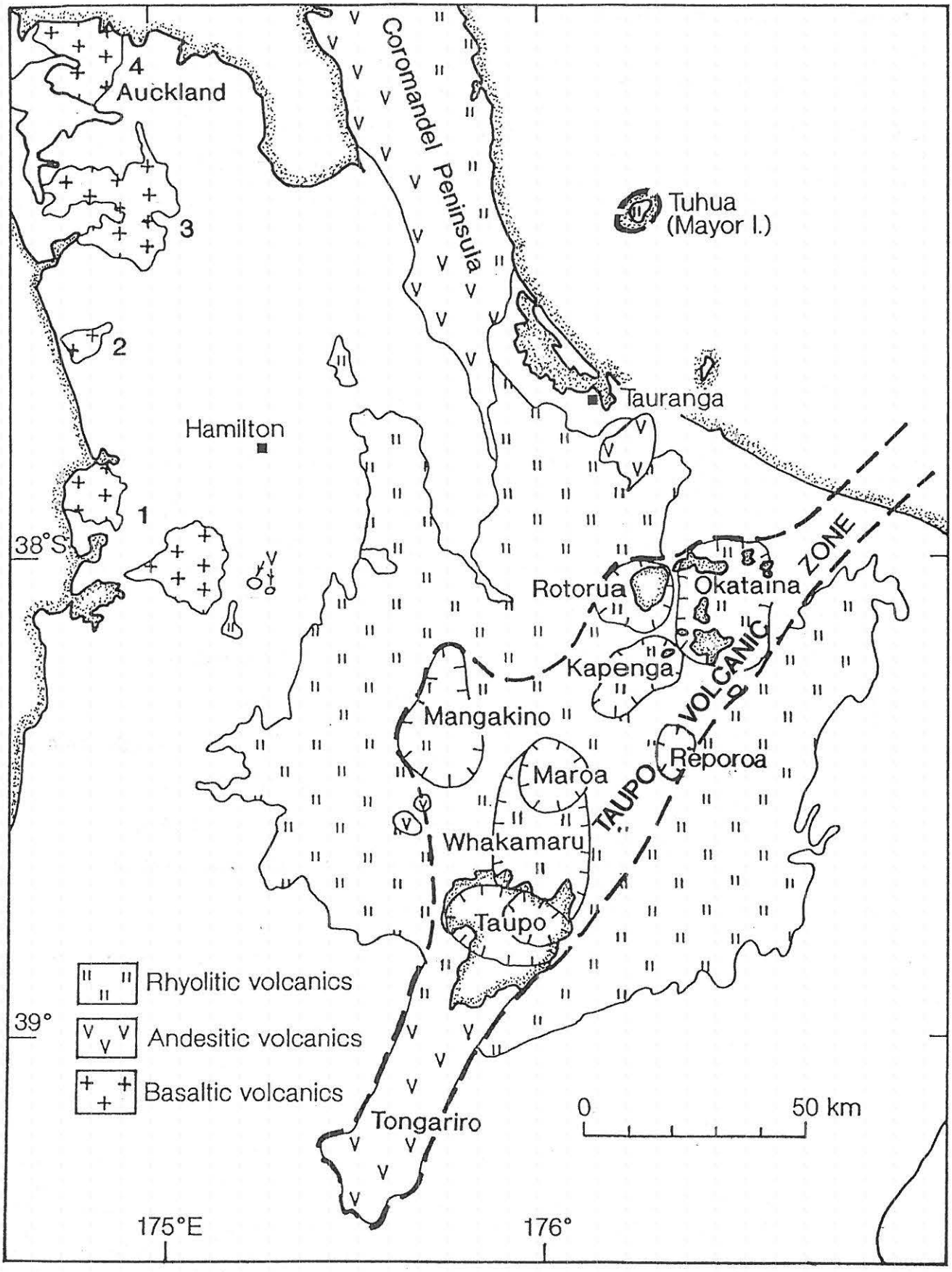

Figure 0.5: Generalised distribution of basaltic, andesitic, and rhyolitic volcanics (including welded ignimbrites) in central North Island, and the locations of eight multivent calderas and Tongariro Volcanic Centre in the Taupo Volcanic Zone (after Briggs et al. 1993 and Nairn et al. in press). The TVZ forms the eastern part of the geologically and geophysically distinct wedge-shaped Central Volcanic Region. The Tuhua volcano of Mayor Island is a peralkaline caldera complex most recently active in the Holocene (Houghton et al. 1992). The Coromandel Peninsula lies in the Coromandel Volcanic Zone, an area of active volcanism in Miocene-Pleistocene times (Skinner 1986). Intraplate basalt fields (numbered) are as in Fig. 0.2.

Quaternary events and deposits

The stratigraphy of the New Zealand Quaternary has recently been reviewed by Pillans (1992), who prepared a generalised map of Quaternary deposits (Fig. 0.6). Time-stratigraphic subdivsions of New Zealand Quaternary strata, based on marine biostratigraphy and climatostratigraphy, has resulted in a series of locally defined stages and substages (Table 0.1). The Plio/Pleistocene boundary as defined at Vrica, Italy, and dated at c. 1.63 Ma, lies near the top of the Nukumaruan Stage in New Zealand. The first faunal evidence of cooling in New Zealand Plio/Pleistocene sequences occurs much earlier, at the base of the Nukumaruan Stage c. 2.4 Ma, with the appearance in central New Zealand of the subantarctic taxa *Chlamys delicatula* and *Jacquinotia edwardsii.*

TABLE 0.1. New Zealand Quaternary stages and substages with boundaries as defined in Wanganui Basin (from Pillans 1992, p. 407.)

Epoch	Series	Stage	Substage	Boundary position
				Present day
PLEISTOCENE	WANGANUI	Haweran		
				Top Putiki Shellbed
		Castle-cliffian	Putikian	
				FAD *Pecten*
			Okehuan	
				Base Butlers Shell Conglomerate
			Marahauan	
PLIOCENE		Nukumaruan		Base Ohingaiti Sand
			Hautawan	
				Base Hautawa Shellbed
		Mangapanian		
				Base Mangapani Shellbed
		Waipipian		

New Zealand's maritime mid-latitude location has made it particularly sensitive to the climatic fluctuations and associated glaciations and sea level changes of the Quaternary Period. Glaciations have had their greatest influence in the South Island where the tectonic uplift produced elevated areas for snow accumulation and the relief and structural features necessary for alpine ice caps and major valley glacier systems to develop. Analysis of cores from DSDP Site 594 southeast of New Zealand (Fig. 0.6) has shown that the South Island glaciations were in phase with those of the Northern Hemisphere (Nelson et al. 1985a; see also Nelson et al. 1993). During the maximum of the last glacial (c. 23-13 ka), an almost continuous glacier complex stretched nearly 700 km along the Southern Alps with snowlines lowered around 800 m below those of the present (Porter 1975). Sea levels were lowered by about 120 m (Pillans et al. 1992).

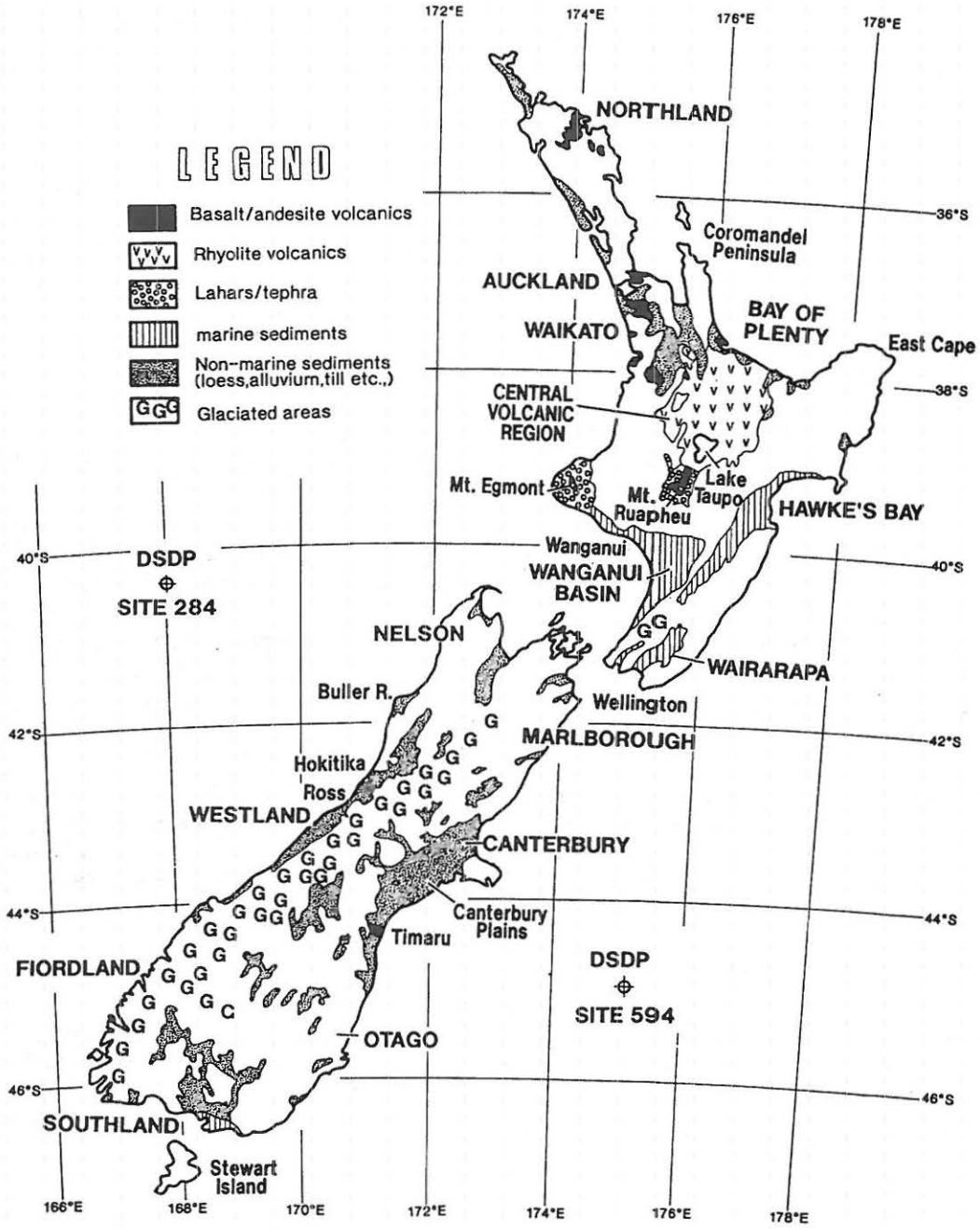

Figure 0.6: Generalised distribution of Quaternary deposits in New Zealand (from Pillans 1992, p. 406).

The estimated drop in annual temperature (ignoring regional variations and assuming similar precipitation levels to those of today) is 4.5 to 5.0°C (McGlone 1988). Cold temperatures, high winds, severe frosts, and droughty conditions were prevalent (Alloway et al. 1992b; Nelson et al. 1993; Pillans et al. 1993).

During the periods of glacial advance and retreat, erosion debris of glacial drift, outwash gravels, and loess was deposited in large quantities in inland basins and on both coastlines, with loess deposits especially abundant on the eastern side of the South Island (e.g. see papers in Eden & Furkert 1988; Pillans 1992).

By comparison with the South Island, glaciation in the North Island was minor with cirques and small valley glaciers occurring in the Tararua Range, and a small ice field on the volcanoes in central North Island. Periglacial activity, including severe fluvial and wind erosion at times, occurred in much of the North Island with the notable exception of the Northland peninsula. Loess sheets were deposited in the southern half of the North Island (Milne & Smalley 1979; Eden & Furkert 1988; see Post-Conference Tour Guide). Dating of these sequences has been mainly by radiocarbon, tephrochronology, and, most recently, thermoluminescence analysis (e.g. Berger at al. 1992). In parts of central North Island, at elevations >400 m, tephric loess was deposited between airfall tephra units during the colder periods (Kennedy 1988, in press).

The dominantly hilly and often mountainous nature of much of New Zealand (around 50% is classed as steep, 20% moderately hilly, and 30% rolling or flat), coupled with a generally high rainfall and the widespread occurrence of highly jointed basement rocks and soft sedimentary rocks that are very susceptible to erosion, has produced generally very fast rates of denudation, especially through landsliding, either as deep rock and debris slides or as shallow, regolith slides. Denudation rates in the Southern Alps range from ≈2.5 mm/yr to ≈0.5 mm/yr with increasing distance from the Alpine Fault across the Alps to the east (Kamp & Tippett 1993). The landsliding is evidently an episodic process controlled chiefly by the frequency of earthquakes and high magnitude climatic events such as rainstorms (Williams 1991; Crozier et al. 1992). In the last millennium human activities, especially deforestation, both by Polynesian and European settlers, have tended to increase rates of erosion (McGlone 1989; McSaveney & Whitehouse 1989).

Thus active tectonism, volcanism, generally abundant rainfall, and high rates of erosion in New Zealand have resulted in a dynamic, sharp textured, and youthful landscape with great landform variety. Almost all of the present landscape has developed within the past two million years, indeed much of it in the second half of the Pleistocene or in the Holocene (Pillans et al. 1992).

SOILS

The soil pattern associated with the New Zealand landscape is complex, partly because of the many different kinds of parent materials, and partly because of the varied conditions under which they have been transformed into soils (Soil Bureau Staff 1968; Molloy 1988). All the orders of *Soil Taxonomy* (Soil Survey Staff 1992) are represented in New Zealand, but Mollisols and (especially) Vertisols are very rare (Hewitt 1992).

Northern North Island, which largely escaped the effects of the glacial periods (Newnham et al. 1993), is warm and humid, and many soils are old, deeply weathered, and clayey, forming mainly Ultisols and some Oxisols (Fig. 0.7). Spodosols, commonly associated with forest species that produce an acid litter (e.g. kauri, rimu), are also represented. Elsewhere in New Zealand the soils are almost all relatively young because of the effects of tectonism, land instability, and the Pleistocene glaciations (especially influential in the South Island). In central and western North Island large areas of soils (and buried paleosols) are developed on the sequences of airfall tephra deposits, forming mainly Udands and Vitrands dominated by short-range order clays. Parts of southern North Island, and eastern South Island, often experience seasonal moisture deficiencies (ustic moisture regimes) and the soils typically are Alfisols or Inceptisols. The very dry inland basins of the South Island (Central Otago) contain Aridisols, whilst in the very high rainfall areas of western South Island, Spodosols, often Aquods, predominate (Fig. 0.7).

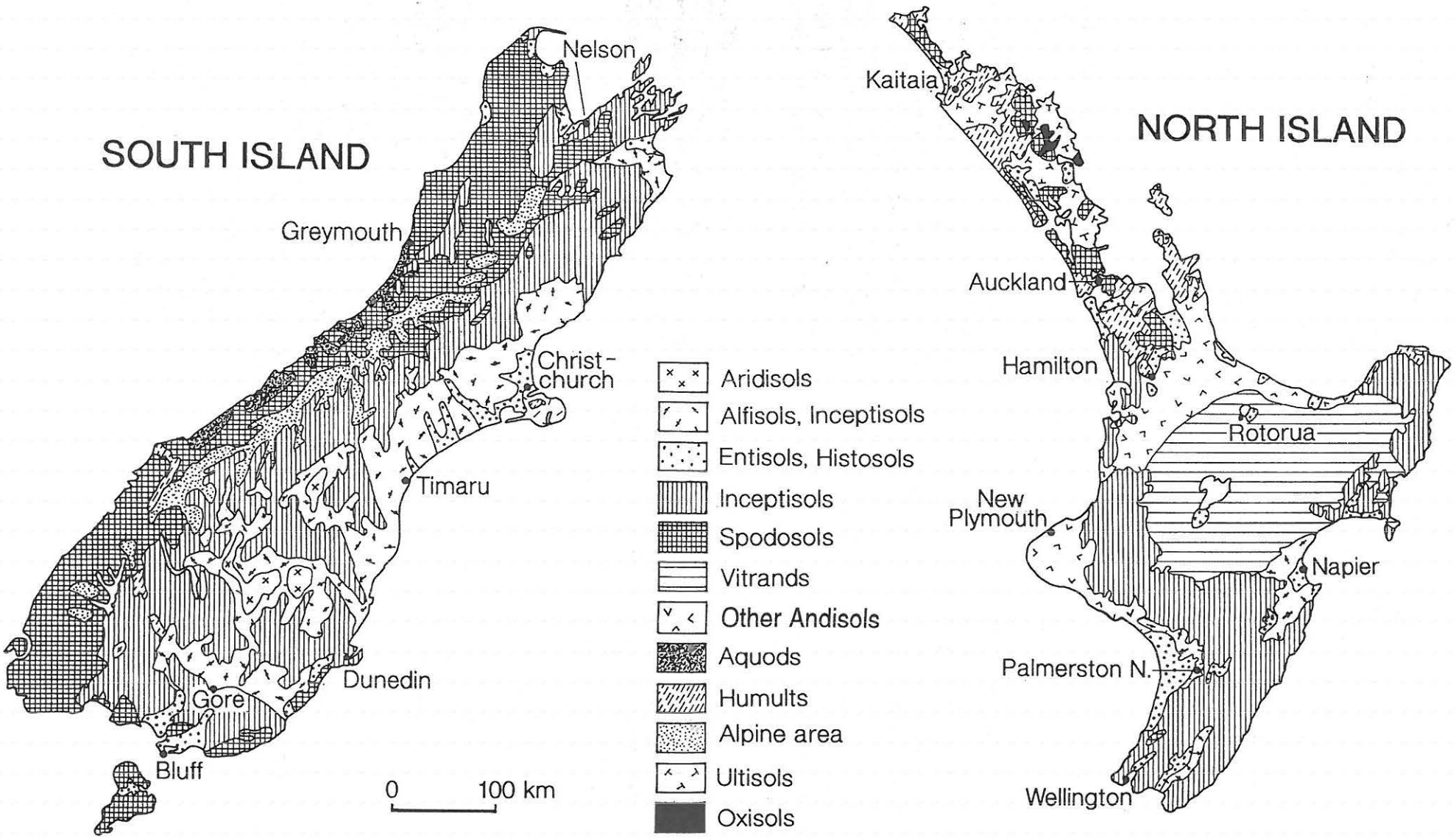

Figure 0.7: Generalised soil map of New Zealand (after Soil Bureau Staff 1968 and Hewitt 1992).

Paleosols

Paleosols, or soils of an environment or landscape of the past, have been differentiated into buried paleosls and relict paleosols (including exhumed paleosols) in New Zealand (Gibbs 1971, 1980). There are numerous paleosols buried under tephra, loess, colluvium, and alluvium deposits of Quaternary age; surface (paleo)soils with relict characteristics are less common.

A review of paleosols in New Zealand was published by Campbell (1986); other New Zealand work of note includes papers by Goh (1972), Birrell & Pullar (1973), Leamy et al. (1973), Runge et al. (1974), Tonkin et al. (1974), Leamy (1975), Kirkman (1976), Birrell et al. (1977), Limmer & Wilson (1980), Stevens & Vucetich (1985), Lowe (1986), Hodder et al. (1990), Lowe & Percival (1993), and Kimber et al. (in press).

CLIMATE

New Zealand lies within the zone of mid-latitude westerly winds extending from 70° to 30°S. These strong, consistent winds are moisture laden after their passage over the surrounding ocean, but moderated in temperature. The main climatic features of the country result from interaction of this air flow with the substantial barrier of the northeast-trending mountain chains (Tomlinson 1975). Because few areas are more than 100 km from the coast, oceanic influence is dominant and the climate is generally moist, windy, and with low annual cloudiness. Most of New Zealand can be classified as warm or cool temperate (McGlone 1988). Annual mean temperatures vary from about 15°C in northern North Island to about 9°C in southern South Island, with summer temperatures relatively cool and winter conditions generally mild. Westerly winds predominate for most of the year although there may be considerable modification by local topography. In many North Island areas, southwesterly flows predominate. In the past few years, mean monthly temperatures have been about 0.5°C lower than normal, and winds generally more southerly, because of the influence of the El Nino phenomenon (ocean surface temperature anomalies of the equatorial Pacific) and fine ash fallout from the Pinatubo eruption in the Phillipines in mid-1991.

Rainfall is highly variable and strongly related to the topography, ranging from more than 7000 mm in the central Southern Alps to 350 mm in inland Central Otago east of the main mountain ranges. The average for the whole country is probably >2000 mm but for much it lies between 600 and 1600 mm. Day-to-day weather variation is high and is controlled by a progression of eastward-moving anticyclones and depressions, with associated cold and warm fronts, at approximately 5 to 10 day intervals (Tomlinson 1975). Persistent weather patterns are rare. Sunshine levels are relatively high with much of the country receiving >2000 hours per year.

FLORA AND FAUNA

Fossil remains show that New Zealand has long been forested, and recognisable ancestors of some present-day trees such as rimu (*Dacrydium cupressinum*), kahikatea (*Dacrycarpus dacrydioides*), totara (*Podocarpus totara*), matai (*Prumnopitys taxifolia*), miro (*Prumnopitys ferruginea*), and kauri (*Agathis australis*) extend back 250 Ma (Bishop 1992). At that time, New Zealand was part of Gondwanaland. Ancestors of various ancient or 'archaic' animals — the tuatara, native frogs, and giant land snails — lived in New Zealand as far back as 150 Ma. The ancestors of the moas and kiwis, southern beeches (*Nothofagus*), and rewarewa (*Knightia*) were also present when New Zealand first began to separate from Antarctica and Australia c. 85 Ma. When this happened many previously dominant plants and animals became extinct. Dinosaurs and other giant reptiles, many marine invertebrates, and some of the fern-like plants and gymnosperms, were lost as climates changed and new life forms evolved. For the plants and animals left 'aboard' New Zealand when it drifted away from Gondwanaland, the islands became both a paradise and a prison (Bishop 1992). Only a trickle of new plants and animals has subsequently arrived from across the sea. Thus New Zealand's early separation and long isolation have provided opportunities for the evolution of peculiar endemic plants and animals. Since then the country's turbulent geological development, involving tectonism, volcanism, and climate change, has further influenced evolution and extinction in New Zealand (McGlone 1985).

The impact of humans or other exotic invaders (especially mammals) has occurred only very recently, being restricted to the last 1000 years or so (Caughley 1989). However, the forests have changed significantly in this relatively short time. About 75% of the land was covered in forest in pre-Polynesian times but this was reduced to about 55% by the time European settlement began about 150 years ago. This reduction in forest cover is attributed largely to Polynesian firings (McGlone 1983, 1989). Since European arrival, forest cover has been further reduced to about 25%, with practically all lowland areas being cleared for agriculture.

An inevitable result of deforestation on this scale, together with the introduction of carnivorous and herbivorous mammals such as rats, stoats, pigs, deer, and possums, has been the extinction of unique native plants and animals, particulary from the lowland forests, through competition, predation, and disease (Towns & Atkinson 1991). A large proportion of the extinctions can be attributed directly to the loss of habitat or to the reduction of forested areas to patches too small to provide adequate resources for survival of populations. Nearly 25% of all the endangered species of birds listed from around the world are from New Zealand, and over 300 of the flowering plants and ferns (10-15% of the total) are currently at risk (Hackwell 1983). Those offshore islands free of introduced pests have assumed special significance as 'safe havens' to transfer native animals whose existence is threatened elsewhere. Such transference to offshore islands, together with programmes of pest eradication on them, now form the mainstay of New Zealand's threatened species management (Towns & Atkinson 1991; Bishop 1992).

Flora

The flora of New Zealand is not rich as the total number of higher plants — slightly more than 2000 — is small compared with other countries of similar size and latitude. However, c. 85% of species and c. 10% of genera are found nowhere else, including one endemic genus of fern and 38 endemic genera of flowering plants. Twenty-four of these 39 endemic genera are represented by a single species (Hackwell 1983). The early naturalist Sir Joseph Banks, visiting New Zealand in 1769 with Captain Cook, remarked that "The entire novelty of what we found recompensed us as natural historians for the want of variety". About 80% of New Zealand's higher plant genera are found also in Australia, but the most distinctive and widespread Australian genera, *Eucalyptus*, *Acacia*, and *Banksia*, do not occur in New Zealand (McGlone 1988).

New Zealand forests are of two major types, dominated either by (1) conifers (podocarps, 'cedar', kauri) and broadleaf 'hardwood' (e.g. tawa, taraire, rata, kamahi, rewarewa) trees, or (2) by one or more of the four southern beeches. Conifer-broadleaved forests are very diverse, occurring throughout the country under all climates but are best developed on warm, fertile, lowland sites. Beeches tend to occupy sites climatically less favourable for plant growth than those dominated by conifer-broadleaved forests, hence are concentrated in cooler, southern regions, and in uplands rather than lowlands (McGlone 1988). The largest tree, kauri (*Agathis australis*), occurs only in warmer regions north of latitude 38°S; it rarely exceeds heights of more than 30 m but has massive, cylindrical boles normally up to 3 m in diameter but some may be as large as 7 m.

As a whole, New Zealand forests are quite different from those of the Northern Hemisphere and other temperate regions, resembling tropical rain forest in many ways: they are moist, dense, and evergreen with many multi-storied vegetation layers, and both the forest floor and trees are often covered in mosses and ferns, with the trees also carrying vines and other plants on trunks and upper branches. Other characteristics include a dearth of deciduous species or annuals; trees frequently have differing juvenile and adult forms; many shrubs and juvenile trees have divaricating forms with widely-angled branches and a tangled growth habit; flowers are usually inconspicuous and lack bright colours; many plants produce colourful, bird-dispersed, small fleshy fruits; and an unusually high proportion (c. 12%) of native species have male and female flowers on separate plants (Hackwell 1983). Finally, New Zealand forests differ from all others in that they have developed in the absence of herbivorous mammals, and hence they more closely resemble the ancient forests of Gondwanaland than those of any other southern continent. New Zealand also has the world's largest buttercup (*Ranunculus lyallii*), the smallest member of the pine family (*Lepidothamus laxifolius*), the largest tree fern (*Cyathea medullaris*), tree-sized daises (*Olearia, Senecio*), mosses 0.3 m high (*Dawsonia superba*), and numerous cushion plants including the huge 'vegetable sheep' of the South Island mountains (*Haastia, Raoulia*).

Fauna

Like the flora, the fauna of New Zealand is a curious mixture of 'archaic' animals of Gondwanaland lineage and later arrivals from more recent times, mostly from Australia. Only a few examples are described here. Among the birds, there has been an evolutionary trend towards increasing size, loss of flight, and dark plumage. Kiwis (*Apteryx*), together with the now extinct moas (*Dinornis*), are endemic representative of the ratites, which also include the emu, cassowary, rhea, and the ostrich. Until recently, both kiwis and moas were thought to have become flightless on Gondwanaland, but new work has suggested that kiwis are of more recent origin than moas, their lineage dating back only 40 million years. If so, how the kiwi's ancestors reached New Zealand, well isolated from Gondwanaland by then, is a puzzle (Bishop 1992). Kiwis, of which four species are known (more probably exist), are unusual amongst living ratites because of their small size and adaptation to life on the forest floor. They are nocturnal and feed on small insects and other invertebrates. Their long beak has nostrils at the tip and cat-like sensory hairs at the base. Moas were herbivores of different sizes, the largest being over 2 m tall and weighing c. 200 kg, and the various species may have browsed in different habitats (see Caughley 1989).

One of New Zealand's rarest flightless birds is the bright green kakapo or New Zealand ground parrot (*Strigops habroptilus*), the world's largest parrot. It has evolved a solitary, nocturnal existence and sometimes climbs trees to get its food. Other flightless herbivorous birds include the rare takahe (*Porphyrio mantelli*), formerly widespread but now restricted to parts of Fiordland, and the weka (*Gallirallus australis*), an opportunist feeding on a variety of animal and vegetable matter (Bishop 1992).

The tuatara (*Spenodon punctatus*) is the sole remaining species from a family of reptiles (Sphenodontida) with a lineage going back more than 225 million years and little changed from its ancient predecessors. It resembles a lizard and a crest of fexible spines along the back, the shape of the skull and jaw, and the enlarged pineal gland suggestive of a 'third eye' are among its special features.

Another distinctive animal, the 'velvet worm' or peripatus (*Peripatoides novaezelandiae*), occupies what appears to be a half-way position in the evolutionary scale between worms and insects. It has the soft, flexible, unjointed body of a worm yet clawed feet and air-conducting tracheae of an insect (Bishop 1992).

The ancestors of New Zealand's three native frog species (*Leiopelma*) probably date back to Gondwanaland times. They are considered to be the most primitive of all living frogs. They lack vocal sacs hence are non-croaking, have tail-wagging muscles but no tail, and have fish-like vertebrae. Lacking fully webbed feet for swimming, they deposit eggs in moist ground or seepages rather than in water. The young of Hamilton's frog (*L. hamiltoni*) are hatched as virtually tailed froglets which then crawl onto the moist back of the adult male to complete development (Bishop 1992).

Perhaps the most 'deadly' archaic animals of the forest floor are the giant snails (*Powelliphanta*) that grow up to 10 cm in diameter. These members of the ancient Gondwanaland snail family, Rhytididae, are voracious carnivores and hunt earthworms, slugs, and smaller snails which are consumed with the hundreds of tiny dagger-like teeth covering their radula, or tongue (Bishop 1992).

REFERENCES

Alloway, B.V. 1989: The late Quaternary cover bed stratigraphy and tephrochronology of north-eastern and central Taranaki, New Zealand. Unpublished PhD thesis, Massey University, Palmerston North.

Alloway, B.V.; McGlone, M.S.; Neall, V.E.; Vucetich, C.G. 1992a: The role of Egmont-sourced tephra in evaluating the paleoclimatic correspondence between the bio- and soil-stratigraphic records of central Taranaki, New Zealand. *Quaternary international 13/14*: 187-194.

Alloway, B.V.; Stewart, R.B.; Neall, V.E.; Vucetich, C.G. 1992b: Climate of the last glaciation in New Zealand, based on aerosolic quartz influx in an andesitic terrain. *Quaternary research 38*: 170-179.

Alloway, B.V.; Pillans, B.J.; Sandhu, A.S.; Westgate, J.A. 1993: Revision of the marine chronology in the Wanganui Basin, New Zealand, based on the isothermal plateau fission-track dating of tephra horizons. *Sedimentary geology 82*: 299-310.

Barnes, P.M.; Shane, P.A.R. 1992: Late Neogene unconformity-bounded tuffaceous sequences: northwestern Chatham Rise, New Zealand. *New Zealand journal of geology and geophysics 35*: 421-435.

Berger, G.W.; Pillans, B.J.; Palmer, A.S. 1992: Dating loess up to 800 ka by thermoluminescence. *Geology 20*: 403-406.

Berryman, K. 1992: A stratigraphic age of Rotoehu Ash and late Pleistocene climate interpretation based on marine terrace chronology, Mahia Peninsula, North Island, New Zealand. *New Zealand journal of geology and geophysics 35*: 1-7.

Birrell, K.S.; Pullar, W.A. 1973: Weathering of paleosols in Holocene and late Pleistocene tephras in central North Island, New Zealand. *New Zealand journal of geology and geophysics 35*: 1-7.

Birrell, K.S.; Pullar, W.A.; Searle, P.L. 1977: Weathering of Rotoehu Ash in the Bay of Plenty district. *New Zealand journal of science 20*: 303-310.

Bishop, N. 1992: Natural History of New Zealand. Hodder & Stoughton, Auckland. 199 p.

Briggs, R.M.; McDonough, W.F. 1990: Contemporaneous convergent margin and intraplate magmatism, North Island, New Zealand. *Journal of petrology 31*: 813-851.

Briggs, R.M.; Itaya, T.; Lowe, D.J.; Keane, A.J. 1989: Ages of Pliocene-Pleistocene Alexandra and Ngatutura Volcanics, western North Island, New Zealand, and some geological implications. *New Zealand journal of geology and geophysics 32*: 417-427.

Briggs, R.M.; Gifford, M.G.; Moyle, A.R.; Taylor, S.R.; Norman, M.D.; Houghton, B.F.; Wilson, C.J.N. 1993: Geochemical zoning and eruptive mixing in ignimbrites from Mangakino volcano, Taupo Volcanic Zone, New Zealand. *Journal of volcanology and geothermal research 56*: 175-203.

Browne, P.R.L.; Graham, I.J.; Parker, R.J.; Wood, C.P. 1992: Subsurface andesite lavas and plutonic rocks in the Rotokawa and Ngatamariki geothermal systems, Taupo Volcanic Zone, New Zealand. *Journal of volcanology and geothermal Research 51*: 199-215.

Campbell, I.B. 1986: Recognition of paleosols in Quaternary periglacial and volcanic environments in New Zealand. *In* Wright, V.P. (ed) Paleosols - Their Recognition and Interpretation. Blackwell, London: 208-241.

Caughley, G. 1989: New Zealand plant-hervivore systems: past and present. *New Zealand journal of ecology (supplement) 12*: 3-10.

Cole, J.W. 1990: Structural control and origin of volcanism in the Taupo volcanic zone, New Zealand. *Bulletin of volcanology 52*: 445-492.

Cole, J.W.; Graham, I.J.; Hackett, W.R.; Houghton, B.F. 1986: Volcanology and petrology of the Quaternary composite volcanoes of Tongariro Volcanic Centre, Taupo Volcanic Zone. *Royal Society of New Zealand bulletin 23*: 7-20.

Crozier, M.J.; Gage, M.; Pettinga, J.R.; Selby, M.J.; Wasson, R.J. 1992: The stability of hillslopes. *In* Soons, J.M.; Selby, M.J. (eds) Landforms of New Zealand 2nd Edition. Longman Paul, Auckland: 63-90.

Darby, D.J.; Williams, R.O. 1991: A new deodetic estimate of deformation in the Central Volcanic Region of the North Island, New Zealand. *New Zealand journal of geology and geophysics 34*: 127-136.

Donoghue, S.L.; Stewart, R.B.; Palmer, A.S. 1991: Morphology and chemistry of olivine phenocrysts of Mangamate Tephra, Tongariro Volcanic Centre, New Zealand. *Journal of the Royal Society of New Zealand 21*: 225-236.

Donoghue, S.L.; Neall, V.E.; Palmer, A.S. in press: Late Quaternary andesitic tephrostratigraphy and chronology, Tongariro Volcanic Centre, New Zealand. *Journal of the Royal Society of New Zealand*

Eden, D.N.; Furkert, R.J. (eds) 1988: Loess: Its Distribution, Geology and Soils. Rotterdam, A.A. Balkema.

Froggatt, P.C.; Lowe, D.J. 1990: A review of late Quaternary silicic amd some other tephra formations from New Zealand: their stratigraphy, nomenclature, distribution, volume, and age. *New Zealand journal of geology and geophysics 33*: 89-109.

Froggatt, P.C.; Nelson, C.S.; Carter, L.; Griggs, G.; Black, K.P. 1986: An exceptionally large late Quaternary eruption from New Zealand. *Nature 319*: 578-582.

Gamble, J.A.; Smith, I.E.M.; Graham, I.J.; Kokelaar, B.P.; Cole, J.W.; Houghton, B.F.; Wilson, C.J.N. 1990: The petrology, phase relations and tectonic setting of basalts from the Taupo Volcanic Zone, New Zealand and the Kermadec Island Arc—Havre Trough, SW Pacific. *Journal of volcanollogy and geothermal research 43*: 235-270.

Goh, K.M. 1972: Amino acid levels as indicators of paleosols in New Zealand soil profiles. *Geoderma 7*: 33-47.

Gibbs, H.S. 1971: Nature of paleosols in New Zealand and their classification. *In* Yaalon, D.H. (ed) Paleopedology — Origin, Nature and Dating of Paleosols. Jerusalem, ISSS & Israel University Press: 229-244.

Gibbs, H.S. 1980: Paleosols. Ch. 8 *in* New Zealand Soils. Wellington, Oxford University Press: 83-90.

Hackwell, K. 1983: The international significance of New Zealand's indigenous forests. *Nature Conservation Council information leaflet* 19. 17p.

Hewitt, A.E. 1992: New Zealand Soil Classification. *DSIR Land Resources scientific report 19.* 133p.

Hodder, A.P.W.; Green, B.E.; Lowe, D.J. 1990: A two-stage model for the formation of clay minerals from tephra-derived volcanic glass. *Clay minerals 25*: 313-327.

Houghton, B.F.; Weaver, S.D.; Wilson, C.J.N.; Lanphere, M.A. 1992: Evolution of a Quaternary peralkaline volcano: Mayor Island, New Zealand. *Journal of volcanology and geothermal research 51:* 217-236.

Houghton, B.F.; Wilson, C.J.N.; McWilliams, M.; Lanphere, M.A.; Weaver, S.D.; Briggs, R.M.; Pringle, M.S. 1994: Volcanic and structural evolution of a large silicic volcanic system: central Taupo Volcanic Zone. Submitted to *Geology.*

Kamp, P.J.J. 1984: Neogene and Quaternary extent and geometry of the subducted Pacific Plate beneath North Island, New Zealand: implications for Kaikoura tectonics. *Tectonophysics 108*: 241-266.

Kamp, P.J.J. 1986: Late Cretaceous-Cenozoic tectonic development of the southwest Pacific region. *Tectonophysics 121*: 225-251.

Kamp, P.J.J. 1992. Tectonic architecture of New Zealand. *In* Soons, J.M.; Selby, M.J. (eds) Landforms of New Zealand 2nd Edition. Longman Paul, Auckland: 1-30.

Kamp, P.J.J.; Green, P.F.; White, S.H. 1989: Fission track analysis reveals character of collisional tectonics in New Zealand. *Tectonics 8*: 169-195.

Kamp, P.J.J.; Tippett, J.M. 1993: Dynamics of Pacific Plate Crust in the South Island (New Zealand) zone of oblique continent-continent convergence. *Journal of geophysical research 98 (B9)*: 16 105-16 118.

Kennedy, N.M. 1988: Late Quaternary loess associated with the Mamaku Plateau, North Island, New Zealand. *In* Eden, D.N.; Furkert, R.J. (eds) Loess: Its Distribution, Geology and Soils A.A. Balkema, Rotterdam: 71-80.

Kennedy, N.M. in press: New Zealand tephrochronology ans a tool in geomorphic history of c. 140 ka Mamaku Ignimbrite Plateau and in relating oxygen isotope stages. *Geomorphology 229*

Kermode, L.O. 1992: Geology of the Auckland urban area. Scale 1: 50 000. "Institute of Geological and Nuclear Sciences Geological Map 2". 1 sheet and notes (63 p.). Institute of Geological and Nuclear Sciences Ltd, Lower Hutt.

Kimber, R.W.L.; Kennedy, N.M.; Milnes, A.R. in press: Amino acid racemization dating of a 140,000 year-old tephra-loess-palaeosol sequence on the Mamaku Plateau near Rotorua, New Zealand. *Australian journal of earth sciences*

Kirkman, J.H. 1976: Clay mineralogy of thirteen paleosols developed in Holocene and late Pleistocene tephras of central North Island, New Zealand. *New Zealand journal of geology and geophysics 19*: 179-187.

Kohn, B.P.; Pillans, B.J.; McGlone, M.S. 1992: Zircon fission track age for middle Pleistocene Rangitawa Tephra, New Zealand: stratigraphic and paleoclimatic significance. *Palaeogeography, palaeoclimatology, palaeoecology 95*: 73-94.

Leamy, M.L. 1975: Paleosol identification and soil stratigraphy in South Island, New Zealand. *Geoderma 13*: 53-60.

Leamy, M.L.; Milne, J.G.G.; Pullar, W.A.; Bruce, J.G. 1973: Paleopedology and soil stratigraphy in the New Zealand Quaternary succession. *New Zealand journal of geology and geophysics 16*: 723-744.

Limmer, A.W.; Wilson, A.T. 1980: Amino acids in buried paleosols. *Journal of soil science 31*: 147-153.

Lowe, D.J. 1986: Controls on the rates of weathering and clay mineral genesis in airfall tephras: a review and New Zealand case study. *In* Colman, S.M.; Dethier, D.P. (eds) Rates of Chemical Weathering of Rocks and Minerals. Academic Press, Orlando: 265-330.

Lowe, D.J. 1988: Stratigraphy, age, composition, and correlation of late Quaternary tephras interbedded with organic sediments in Waikato lakes, North Island, New Zealand. *New Zealand journal of geology and geophysics 31*: 125-165.

Lowe, D.J. 1990: Tephra studies in New Zealand: an historical review. *Journal of the Royal Society of New Zealand 20*: 119-150.

Lowe, D.J.; Hogg, A.G. 1992: Application of new technology liquid scintillation spectrometry to radiocarbon dating of tephra deposits, New Zealand. *Quaternary international 13/14*: 135-142.

Lowe, D.J.; Percival, H.J. 1993: Clay mineralogy of tephras and associated paleosols and soils, and hydrothermal deposits, North Island. *Guide Book for New Zealand Pre-Conference Field Trip F1*, 10th International Clay Conference, Adelaide, Australia. 110p.

McGlone, M.S. 1983: Polynesian deforestation of New Zealand: a preliminary synthesis. *Archaeology in Oceania 18*: 11-25.

McGlone, M.S. 1985: Plant biogeography and the late Cenozoic history of New Zealand. *New Zealand journal of botany 23*: 723-749.

McGlone, M.S. 1988: New Zealand. *In* Huntley, B.; Webb, T.III (eds) Vegetational History. Kluwer Academic Publishers: 557-599.

McGlone, M.S. 1989: The Polynesian settlement of New Zealand in relation to environmental and biotic changes. *New Zealand journal of ecology (supplement) 12*: 115-129.

McSaveney, M.J.; Whitehouse, I.E. 1989: Anthropic erosion of mountain land in Canterbury. *New Zealand journal of ecology (supplement) 12*: 151-163.

Milne, J.D.G.; Smalley, I.J. 1979: Loess deposits in the southern North Island of New Zealand: an outline stratigraphy. *Acta Geologica Academiae Scientiarum Hungaricae 22*: 197-204.

Molloy, L. 1988. Soils in the New Zealand Landscape. New Zealand Society of Soil Science and Mallinson Rendel, Wellington. 239p.

Nairn, I.A.; Wood, C.P.; Bailey, R.A. in press: The Reporoa Caldera, Taupo Volcanic Zone: source of the Kaingaroa Ignimbrites. Submited to ~~*Journal of volcanology and geothermal research*~~ Bull. Volc.

Neall, V.E. 1972: Tephrochronology and tephrostratigraphy of western Taranaki (N108-109), New Zealand. *New Zealand journal of geology and geophysics 15*: 507-557.

Neall, V.E. 1979. Sheets P19, P20, & P21 *New Plymouth, Egmont, and Manaia* (1st ed) "Geological Map of New Zealand 1: 50 000". Three maps and notes (36 p.). New Zealand Department of Scientific and Industrial Research, Wellington.

Neall, V.E.; Stewart, R.B.; Smith, I.E.M. 1986: History and petrology of the Taranaki volcanoes. *The Royal Society of New Zealand bulletin 23*: 251-263.

Nelson, C.S.; Hendy, C.H.; Jarrett, G.R.; Cuthbertson, A.M. 1985a: Near synchroneity of New Zealand alpine glaciations and Northern Hemisphere continental glaciations during the past 750 ka. *Nature 318*: 361-363.

Nelson, C.S.; Froggatt, P.C.; Gosson, G.J. 1985b: Nature, chemistry, and origin of late Cenozoic megascopic tephras in Leg 90 cores from the southwest Pacific. *In* Kennett, J.P.; von der Borch, C.C. et al. (eds) Initial Reports of the Deep Sea Drilling Project 90, Washington: 1161-1173.

Nelson, C.S.; Cooke, P.J.; Hendy, C.H.; Cuthbertson, A.M. 1993: Oceanographic and climatic changes over the past 160,000 years at Deep Sea Drilling Project Site 594 off southeastern New Zealand, southwest Pacific Ocean. *Paleoceanography 8*: 435-458.

Newnham, R.M.; Ogden, J.; Mildenhall, D. 1993: A vegetation history of the Far North of New Zealand during the Late Otira (Last Glaciation). *Quaternary research* 39: 361-372.

Pillans, B.J. 1992: New Zealand Quaternary stratigraphy: an overview. *Quaternary science reviews 10*: 405-418.

Pillans, B.J.; Wright, I. 1992: Late Quaternary tephrostraitgraphy from the southern Havre Trough — Bay of Plenty, northeast New Zealand. *New Zealand journal of geology and geophysics 35*: 129-143.

Pillans, B.J.; Pullar, W.A.; Selby, M.J.; Soons, J.M. 1992: The age and development of the New Zealand landscape. *In* Soons, J.M.; Selby, M.J. (eds) Landforms of New Zealand 2nd Edition. Longman Paul, Auckland: 31-62.

Pillans, B.J.; McGlone, M.S.; Palmer, A.S.; Mildenhall, D.; Alloway, B.V.; Berger, G.W. 1993: The Last Glacial Maximum in central and southern North Island, New Zealand: a paleoenvironmental reconstruction using the Kawakawa Tephra Formation as a chronostratigraphic marker. *Palaeogeography, palaeoclimatology, palaeoecology 101*: 283-304.

Porter, S.C. 1975: Equilibrium line of late Quaternary glaciers in the Southern Alps, New Zealand. *Quaternary research 5*: 27-48.

Pringle, M.S.; McWilliams, M.; Houghton, B.F.; Lanphere, M.A.; Wilson, C.J.N. 1992: $^{40}Ar/^{39}Ar$ dating of Quaternary feldspar: Examples from the Taupo Volcanic Zone, New Zealand. *Geology 20*: 531-534.

Runge, E.C.A.; Walker, T.W.; Howarth, D.T. 1974: A study of late Pleistocene loess deposits, South Canterbury, New Zealand. Part I. Forms and amounts of phosphorus compared with other techniques for identifying paleosols. *Quaternary research 4*: 76-84.

Selby, M.J.; Lowe, D.J. 1992: The middle Waikato Basin and hills. *In* Soons, J.M.; Selby, M.J. (eds) Landforms of New Zealand 2nd Edition. Longman Paul, Auckland: 233-255.

Shane, P.A.R. 1991: Remobilised silicic tuffs in middle Pleistocene fluvial sediments, southern North Island, New Zealand. *New Zealand journal of geology and geophysics 34* 489-499.

Skinner, D.N.B. 1986: Neogene volcanism of the Hauraki Volcanic Region. *Royal Society of New Zealand bulletin 23*: 21-47.

Soengkono, S.; Hochstein, M.P.; Smith, I.E.M.; Itaya, T. 1992: Geophysical evidence for widespread reversely magnetised pyroclastics in the western Taupo Volcanic Zone (New Zealand). *New Zealand journal of geology and geophysics 35*: 47-55.

Soil Bureau Staff 1968. Soils of New Zealand Part 1. *New Zealand Soil Bureau bulletin 26 (1)*. 142 p.

Soil Survey Staff 1992. Keys to Soil Taxonomy (5th edition). *SMSS Technical Monograph 19*. Pocahontas Press, Blacksburg, Virginia. 566 p.

Stern, T. A. 1987: Asymmetric back-arc spreading, heat flux and structure associated with the Central Volcanic region of New Zealand. *Earth and planetary science letters 85*: 265-276.

Stevens, K.F.; Vucetich, C.G. 1985: Weathering of Upper Quaternary tephras in New Zealand, 2. Clay minerals and their climatic interpretation. *Chemical geology 53*: 237-247.

Stokes, S.; Lowe, D.J. 1988: Discriminant function analysis of late Quaternary tephras from five volcanoes in New Zealand using glass shard major element chemistry. *Quaternary research* 30: 270-283.

Stokes, S.; Lowe, D.J.; Froggatt, P.C. 1992: Discriminant function analysis and correlation of late Quaternary rhyolitic tephra deposits from Taupo and Okataina volcanoes, New Zealand, using glass shard major element composition. *Quaternary International 13/14*: 103-117.

Tatsumi, Y.; Tsunakawa, H. 1992: Cenozoic volcanism, stress gradient and back-arc opening in the North Island, New Zealand: Origin of Taupo-Rotorua Depression. *The island arc 1*: 40-50.

Tippett, J.M.; Kamp, P.J.J. 1993: Fission track analysis of the Late Cenozoic vertical kinematics of continental Pacific crust, South Island, New Zealand. *Journal of geophysical research 98 (B9)*: 16 119-16 148.

Tomlinson, A.I. 1975: Climate. *In* Wards, I. (ed) New Zealand Atlas. Government Printer, Wellington: 82-89.

Tonkin, P.J.; Runge, E.C.A.; Ives, D. 1974: A study of late Pleistocene loess deposits, South Canterbury, New Zealand. Part II. Paleosols and their stratigraphic implications. *Quaternary research 4*: 217-231.

Topping, W.W. 1973: Tephrostratigraphy and chronology of late Quaternary eruptives from the Tongariro Volcanic Centre, New Zealand. *New Zealand journal of geology and geophysics 16*: 397-423.

Towns, D.R.; Atkinson, I.A.E. 1991: New Zealand's restoration ecology. *New scientist 1765*: 30-33.

Walker, G.P.L. 1984: Downsag calderas, ring faults, caldera sizes, and incremental caldera growth. *Journal of geophysical research 89(B10)*: 8407-8416.

Williams, P.W. 1991: Tectonic geomorphology, uplift rates and geomorphic response in New Zealand. *Catena 18*: 439-452.

Wilson, C.J.N. 1986: Reconnaissance stratigraphy and volcanology of ignimbrites from Mangakino Volcano. *Royal Society of New Zealand bulletin 23*: 179-193.

Wilson, C.J.N. 1993. Stratigraphy, chronology, styles and dynamics of late Quaternary erptions from Taupo volcano, New Zealand. *Philosophical transactions of the Royal Society, London A343*: 205-306.

Wilson, C.J.N.; Rogan, A.M.; Smith, I.E.M.; Northey, D.J.; Nairn, I.A.; Houghton, B.F. 1984: Caldera volcanoes of the Taupo Volcanic Zone, New Zealand. *Journal of Geophysical Research 89(B10)*: 8463-8484.

Wilson, C.J.N.; Houghton, B.F.; Lloyd, E.F. 1986: Volcanic history and evolution of the Maroa-Taupo area, central North Island. *Royal Society of New Zealand bulletin 23*: 194-223.

Wright, I.; Carter, L.; Lewis, K. 1990: GLORIA survey of the oceanic-continental transition of the Havre-Taupo back-arc basin. *Geo-marine letters 10*: 59-67.

DAY 1: HAMILTON—RAGLAN—HAMILTON

R. M. Briggs & D. J. Lowe
Department of Earth Sciences
University of Waikato, Private Bag 3105
Hamilton, New Zealand

G. G. Goles
Center for Volcanology
University of Oregon
Eugene, Oregon 97403
USA

T. G. Shepherd
Landcare Research
Private Bag 11-052
Palmerston North, New Zealand

Briggs, R.M.; Lowe, D.J.; Goles, G.G.; Shepherd, T.G. 1994. Intra-conference Tour Day 1: Hamilton-Raglan-Hamilton. In: Lowe, D.J. (ed) Conference Tour Guides. Proceedings International Inter-INQUA Field Conference and Workshop on Tephrochronology, Loess, and Paleopedology, University of Waikato, Hamilton, New Zealand, 24-44.

Outline of Day 1 (Wednesday 9 February)

8.30-9.00 am	Depart Bryant Hall, University of Waikato, and travel on SH 23 to Raglan Saddle
9.00-9.15 am	STOP 1 — Overview of Alexandra Volcanics from Raglan Saddle
9.15-9.30 am	Travel to Stop 2
9.30-10.30 am	STOP 2 — Woodstock Section: Kauroa and Hamilton Ash Fm.
10.30-10.35 am	Travel from Stop to Raglan
10.35-10.45 am	STOP 3 — Comfort stop, Raglan
10.45-11.00 am	Travel to Stop 4 on Wainui -Whaanga Roads
11.00-11.15 am	STOP 4 — Bryant Home Section, Manu Bay
11.15-11.30 am	Travel to Stop 5 (Te Toto Gorge)
11.30 am-4.30 pm	STOP 5 — Te Toto Gorge & Amphitheatre, Mt Karioi LUNCH at appropriate place and time
4.30-5.30 pm	Return from Te Toto Gorge to Hamilton Evening: Barbecue at Bryant Hall (all conference participants)

INTRODUCTION

Today's trip to the Raglan district, western North Island, is primarily an introduction to (1) the Alexandra Volcanics, a group of chiefly basaltic deposits of Plio-Pleistocene age, and (2) the Kauroa and Hamilton Ash formations, two groups of weathered, predominantly rhyolitic, tephra beds of Plio-Pleistocene age that, in places, are intercalated with Alexandra Volcanics. Buried paleosols are associated with both the Alexandra and Kauroa/Hamilton deposits. We plan on spending around half the day at one site — Stop 5 — on the Karioi edifice on the west coast, just south of Raglan (Figs. 1.1, 1.5). Here we will examine, in a relaxed and informal manner, outcrops in and near Te Toto amphitheatre and gorge, a critical locality for understanding the stratigraphic succession and petrologic evolution of Karioi (see Fig. 1.9 below).

Our trip westward initally crosses the surface of the Hamilton Basin, esssentially a fault-bounded basement depression of Pliocene and Pleistocene age (Fig. 1.2). Throughout the Quaternary, this basin has been infilling with terrestrial sediments and pyroclastic materials, derived mainly from extrabasinal sources to the southeast (especially the Central Volcanic Region), from Coromandel Volcanic Zone, and from erosion of the bounding ranges (Kear & Schofield 1978; Selby & Lowe 1992). Mesozoic basement is downfaulted ≈200-300 m on the western margins of the basin (Waipa Fault). Much Late Tertiary vertical displacement on the (mainly subsurface) Waipa Fault is inferred from the difference in elevation of basement across the basin, and drilling and gravity data suggests that the Mesozoic basement occurs at variable depth and, in places, up to ≈2000 m below the surface (Kear & Schofield 1978).

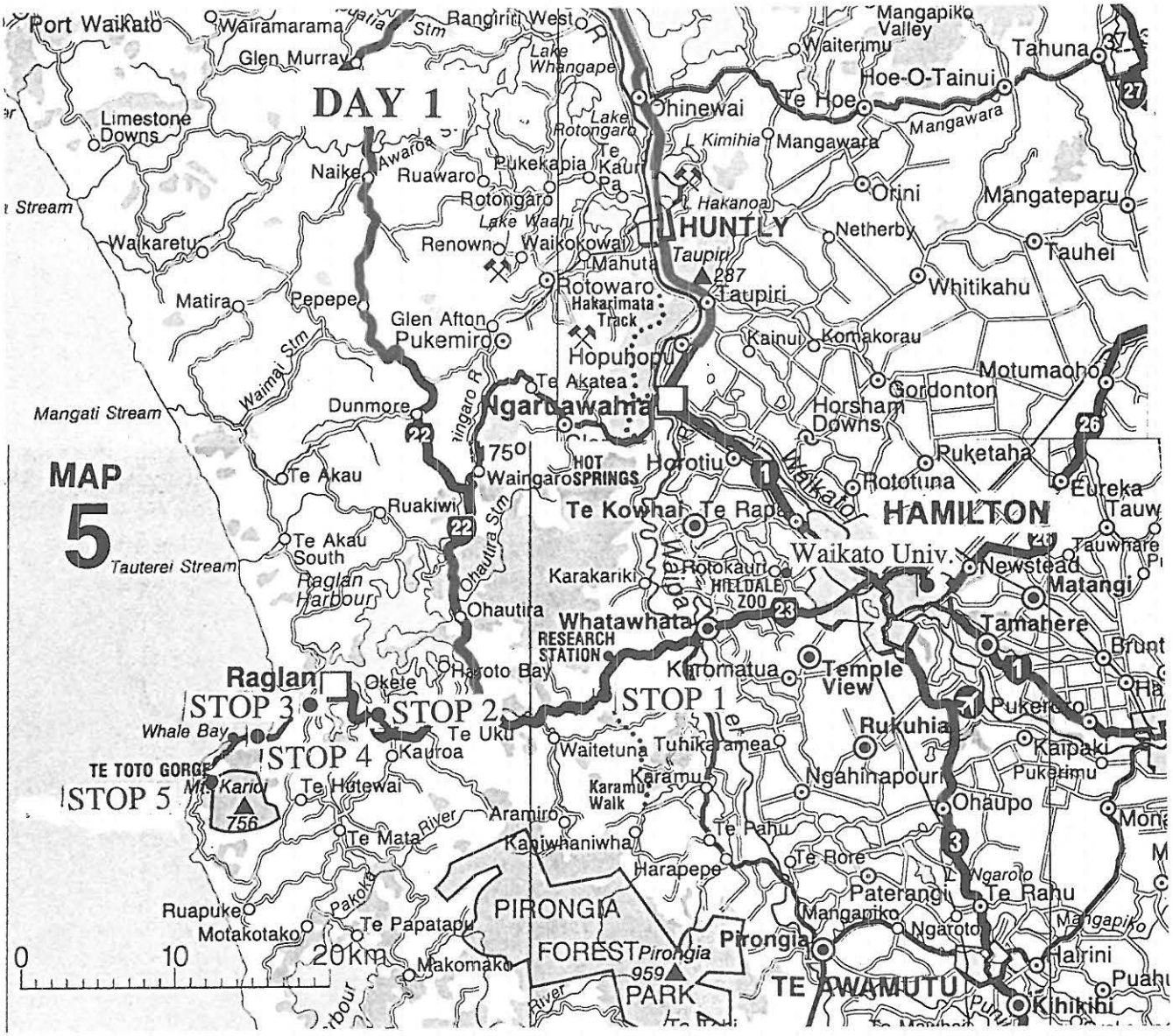

Figure 1.1: Route map for Day 1.

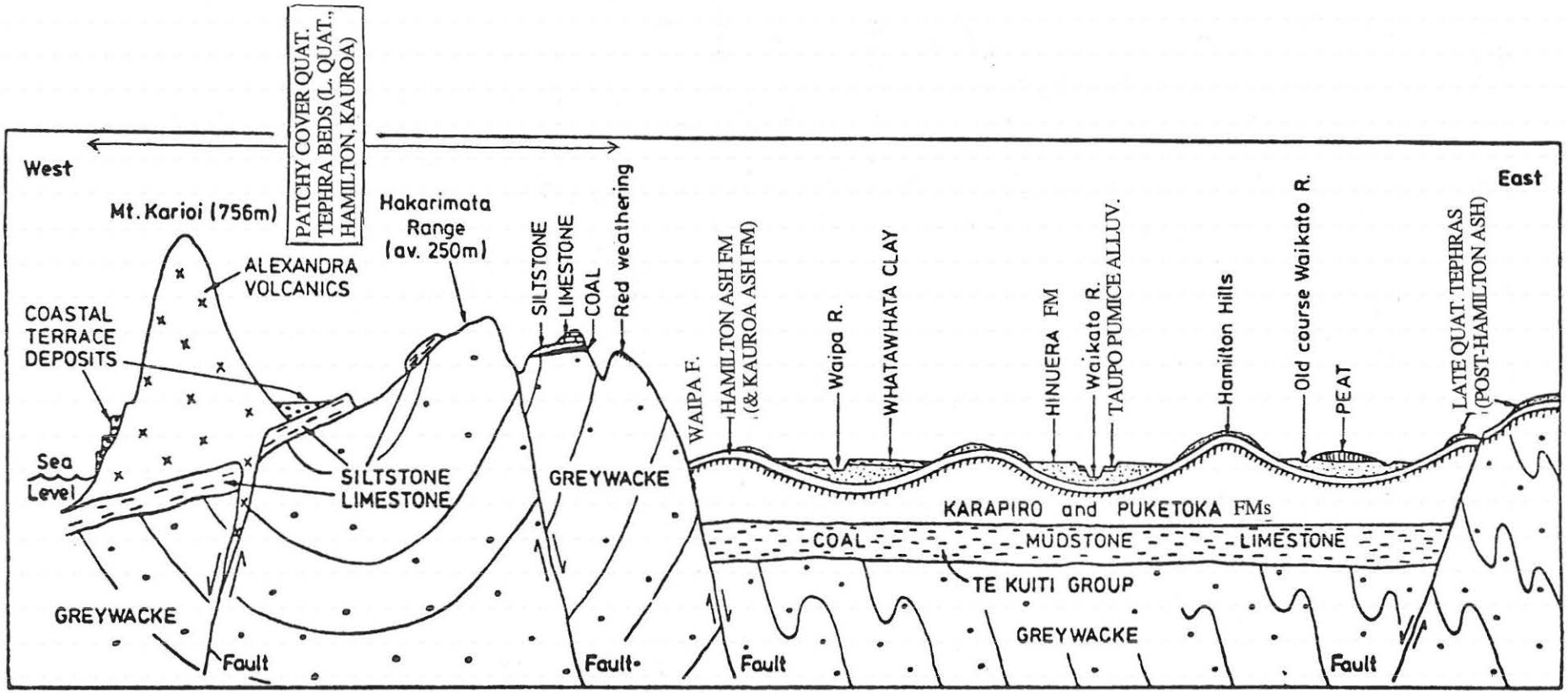

Figure 1.2: Schematic cross section across the Raglan Hills-Hamilton Basin (after Kear & Schofield 1978 and Selby & Lowe 1992).

A simplified stratigraphy of the Quaternary deposits in the basin is summarised in Fig. 1.2, and described in Selby & Lowe (1992). The soil pattern of the Hamilton basin was described by McCraw (1967).

In the Raglan Hills district, the geological pattern provides a basis for the recognition of several physiographic regions, each of which is characterised by an assemblage of distinctive landforms (Bruce 1978; Fig. 1.3). The soil pattern has been described by Bruce (1978).

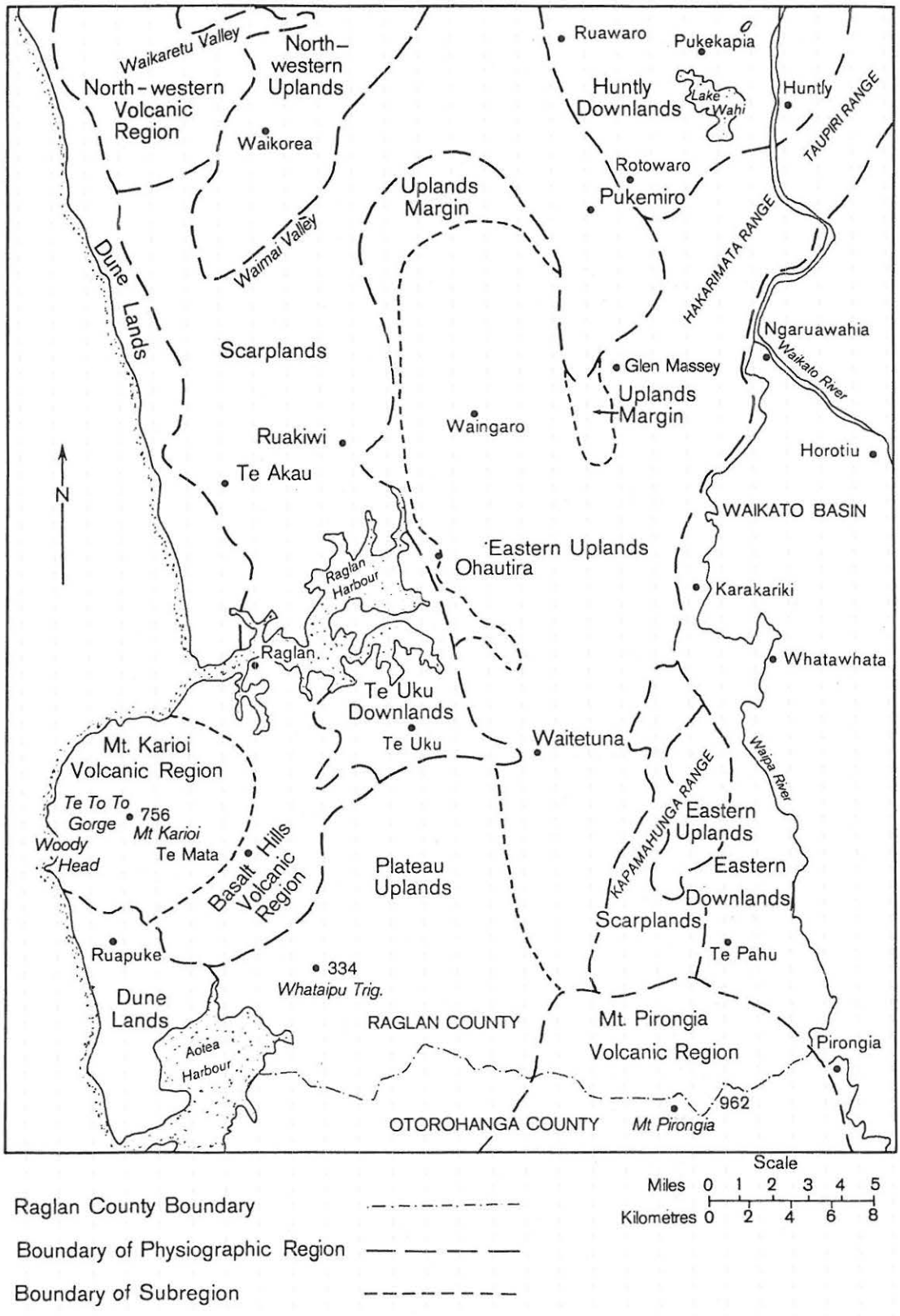

Figure 1.3: Physiographic regions of the Raglan Hills (part Raglan County), western Waikato (from Bruce 1978, p. 12).

ALEXANDRA VOLCANICS

The Alexandra Volcanics Group (AVG) is the southernmost of the Pliocene-Quaternary (2.7 to 1.6 Ma) basalt fields of northern North Island, northwest of the Taupo Volcanic Zone (TVZ) (Briggs et al. 1989; see Fig. 0.2). The most voluminous of the basalt fields (55 km^3), and covering an area of 450 km^2, the AVG forms a 65 km-long volcanic chain with a pronounced northwesterly alignment at right angles to the strike of the TVZ (Briggs 1983; Briggs & Goles 1984; Briggs & McDonough 1990; Fig. 1.4). The AVG has erupted two contrasting magma series: a convergent margin calc-alkalic magma (Pirongia and Karioi Volcanics), and an alkalic intraplate magma (Okete Volcanics), which are both closely spatially and temporally associated (Briggs & McDonough 1990). Field relationships indicate that these diverse magma types were contemporaneous, and thus their mantle source regions coexisted, in a single tectonic environment (Briggs & McDonough 1990).

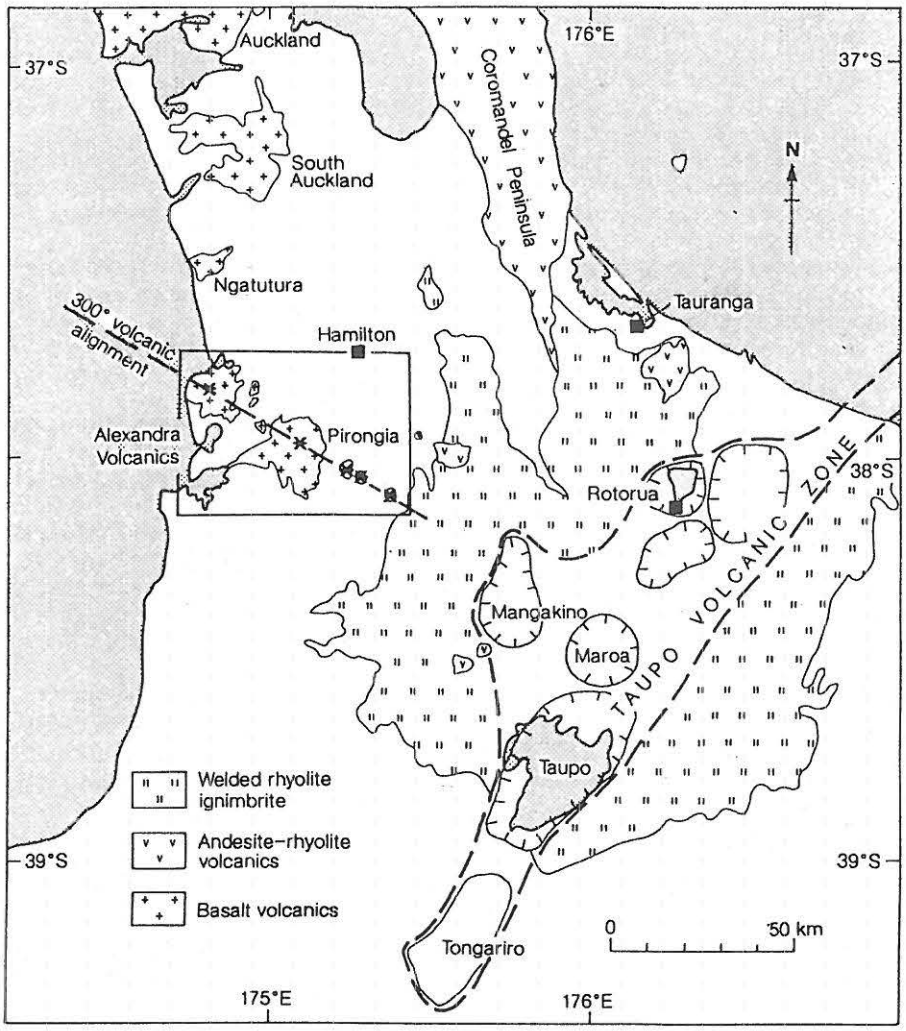

Figure 1.4: Map of the central North Island, New Zealand, showing the tectonic setting and volcanic alignment of the Alexandra Volcanic Group (in box) in relation to the Taupo Volcanic Zone (from Briggs & McDonough 1990). [The locations of recently-identified Whakamaru and Reporoa calderas in the TVZ are shown in Fig. 0.5.]

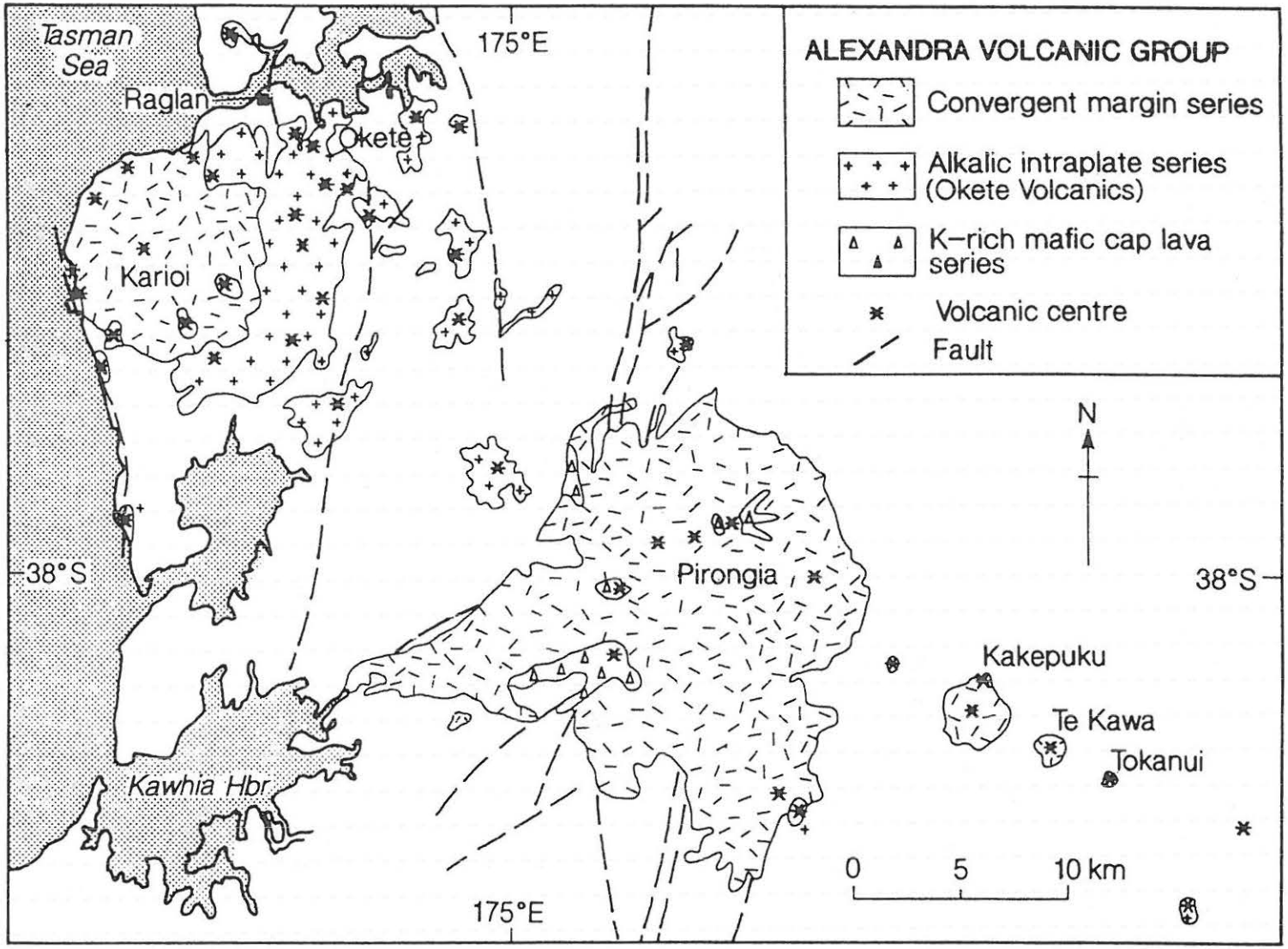

Figure 1.5: Distribution of the calc-alkalic lavas (Karioi, Pirongia, Kakepuku, Te Kawa, Tokanui) and alkalic lavas (Okete) of the Alexandra Volcanic Group (from Briggs & McDonough 1990).

The calc-alkalic convergent margin suite forms low-angle composite cones and shields constructed of lava flows, volcanic breccias, dikes, and minor lapilli tuffs and tuffs (Fig. 1.5). they are predominantly basaltic in composition but include high-K andesites. A K-rich mafic series (basanites and absarokites) form capping lavas on Pirongia, the largest of the stratovolcanoes.

The alkalic intraplate series has produced a volcanic field of monogenetic basaltic volcanoes consisting of lava flows, scoria cones, and tuff rings. Rock types range from basanites to alkali olivine basalts to hawaiites.

In contrast to the convergent margin volcanoes, the alkalic Okete suite shows no northwesterly structural alighnment, but instead is controlled by a system of N-S and NE-SW striking faults, typical of the trends of the extensional back-arc environment of western North Island.

KAUROA AND HAMILTON ASH BEDS

The Kauroa Ash Formation (locally referred to as 'K-beds') comprises a sequence of extremely weathered, clay-rich (av. 85% clay), rhyolitic tephra deposits recognised largely in the Waikato region (Ward 1967; Pain 1975; Davoren 1976; Salter 1979; Kirkman 1980). The beds are quite variable in character, ranging from friable to extremely firm in consistence, and with many colours and structures. Much of the sequence has been removed by erosion — in the Hamilton Basin it is seldom thicker than 1-2 m, but in western Waikato it may be up to 12 m thick — and outcrops are sparse (Selby & Lowe 1992). We will be visiting the type section at Woodstock near Raglan, where Salter (1979) identified 15 units, labelled K1 to K15 from bottom to top, respectively, and numerous associated paleosols (see Stop 2 below).

Stratigraphic interfingering of early Kauroa beds with K-Ar dated basalts of the Alexandra Volcanics enabled K1/2 to be dated at 2.3 Ma (Briggs et al. 1989; Fig. 1.6). New, provisional fission-track dates on zircons from several other beds are reported below. Where preserved, the youngest bed, K15 (also known as Waiterimu Ash), forms an extremely prominent dark reddish brown paleosol with usually a strongly developed blocky or prismatic structure. Not yet dated radiometrically, K15 may have been deposited c. 0.95 Ma (based on stratigraphic work in progress). If so, it represents the tiny remnants of an old land surface that apparently persisted for perhaps half a million years or so (Selby & Lowe 1992). The Kauroa Ash beds evidently represent distal airfall tephra and ignimbrite deposits from early TVZ eruptions, some probably deriving from Mangakino volcano (Fig. 1.4).

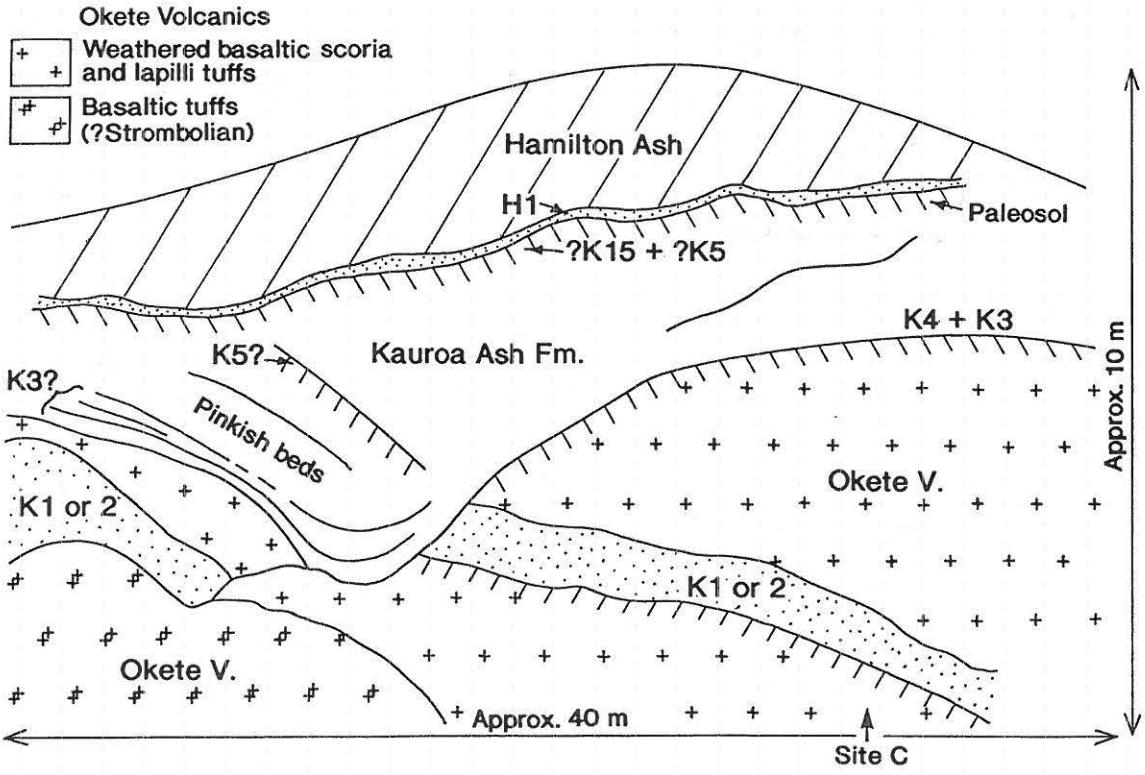

Figure 1.6: Sketch of section on Kauro-Te Mata Road (R14/787722) showing stratigraphic relationships of Okete Volcanics (Ohiapopoko cone, Maungatawhiri centre) and Kauroa and Hamilton Ash beds. 'Site C' is described in Briggs et al. (1989, p. 427).

The Hamilton Ash Formation, separated from the underlying Kauroa beds by a well defined erosional unconformity, comprises a sequence of strongly weathered, clay-textured tephra beds and paleosols well represented in the Waikato-South Auckland regions (Ward 1967; Pain 1975). Usually between 3 and 5 m thick, the beds are sometimes thin and patchy, presumably because of erosion (Selby & Lowe 1992). The sequence has been divided into eight units numbered H1 to H8 from bottom to top, respectively. The oldest bed (H1; also known as Ohinewai Tephra: Vucetich et al. 1978) is typically a pale yellowish brown colour with a sharp lower boundary marked by a coarse yellow, quartz-rich sandy layer forming a prominent marker bed. Based on correlations with other tephra deposits in central and southern North Island, and in deep sea cores, H1 (and perhaps H2) has been identified as the Rangitawa Tephra, which has an age (based on fission track analysis of zircons) of 0.35 ± 0.04 Ma (Nelson 1988; Kohn et al. 1992). Rangitawa Tephra is probably a distal correlative of the biotite and quartz-bearing Whakamaru-group ignimbrites erupted from Whakamaru or Taupo volcanoes (Kohn et al. 1992). The remaining Hamilton beds, all clayey in texture (≈60-85% clay), range from friable to firm in consistence with reddish-yellow to strong brown colours, and may well have originated from these sources too. Their ages are currently unknown, although Shepherd (1994) suggests that H8 was deposited probably during a glacial period at Stage 6 c. 150-120 ka. The presence of up to 7 paleosols in the sequence suggests that there were considerable periods without eruptions.

At some localities, halloysitic clay lobes with associated contorted stratification occur in basal beds; Tonkin (1970) suggested that such lobes were formed by deformation and plastic flowage into more sensitive overlying beds, perhaps during earthquake shocks. Where the Hamilton Ash materials are exposed at or near the surface, well-developed and strongly structured soils occur, usually Humults or Udults

The Hamilton Ash beds are evidently rhyolitic in origin (based on trace element analysis of titanomagnetites; Shepherd 1984). Their clay mineralogy has been documented by Hogg (1974) and Shepherd (1984) (summarised by Lowe & Percival 1993). The clays are dominated by halloysite with three common morphologies: large and small spheroids, long tubes, and short and medium-sized laths and tubes (Shepherd 1984); small amounts of allophane, goethite, gibbsite, and ferrihydrite also occur. In some beds (especially H2) a sand-sized golden platy mineral has been identified as a 2:1:1 partially random interstratified micaceous kaolinite intergrade (Shepherd 1984), probably the result of dissolution of biotite and recrystallisation of kaolinite at linear boundaries (Lowe & Percival 1993).

STOP 1 — Raglan Saddle (S14/920723*)

Here we stop briefly to overview the major composite cones of Pirongia and Karioi of the Alexandra Volcanics. Priongia (959 m a.s.l.) has a long and complex volcanic history with an age of 1.60 Ma at the summit and 2.74 Ma on its southern slopes — i.e. spanning the entire duration of the Alexandra Volcanics (Briggs et al. 1989). Karioi volcano (756 m) also has an involved volcanic history (see Stop 5), with reliable ages ranging from 2.40-2.16 Ma.

Based on the apparent decrease in degree of erosion from Karioi to Kawa (i.e. from NW to SE), it was suggested previously that the stratovolcanoes become progressively younger to the southeast. However, the K-Ar radiometric dates indicate that they have broadly similar ages and do not young in any direction, and, moreover, overlap in age with the Okete Volcanics (Briggs et al. 1989).

STOP 2 — Woodstock Section: Kauroa and Hamilton Ash beds (R14/783734) [Please be especially careful of traffic here]

This is the type section for the Kauroa Ash Formation (the name 'Woodstock' derives from the original name of the adjacent farm), and a reference site for the Hamilton Ash Formation (Ward 1967). Rainfall is ≈1400 mm p.a. (Bruce 1978).

---

* Grid references throughout the guide are based on the 1:50 000 New Zealand Map Series 260 with a 1000 m grid.

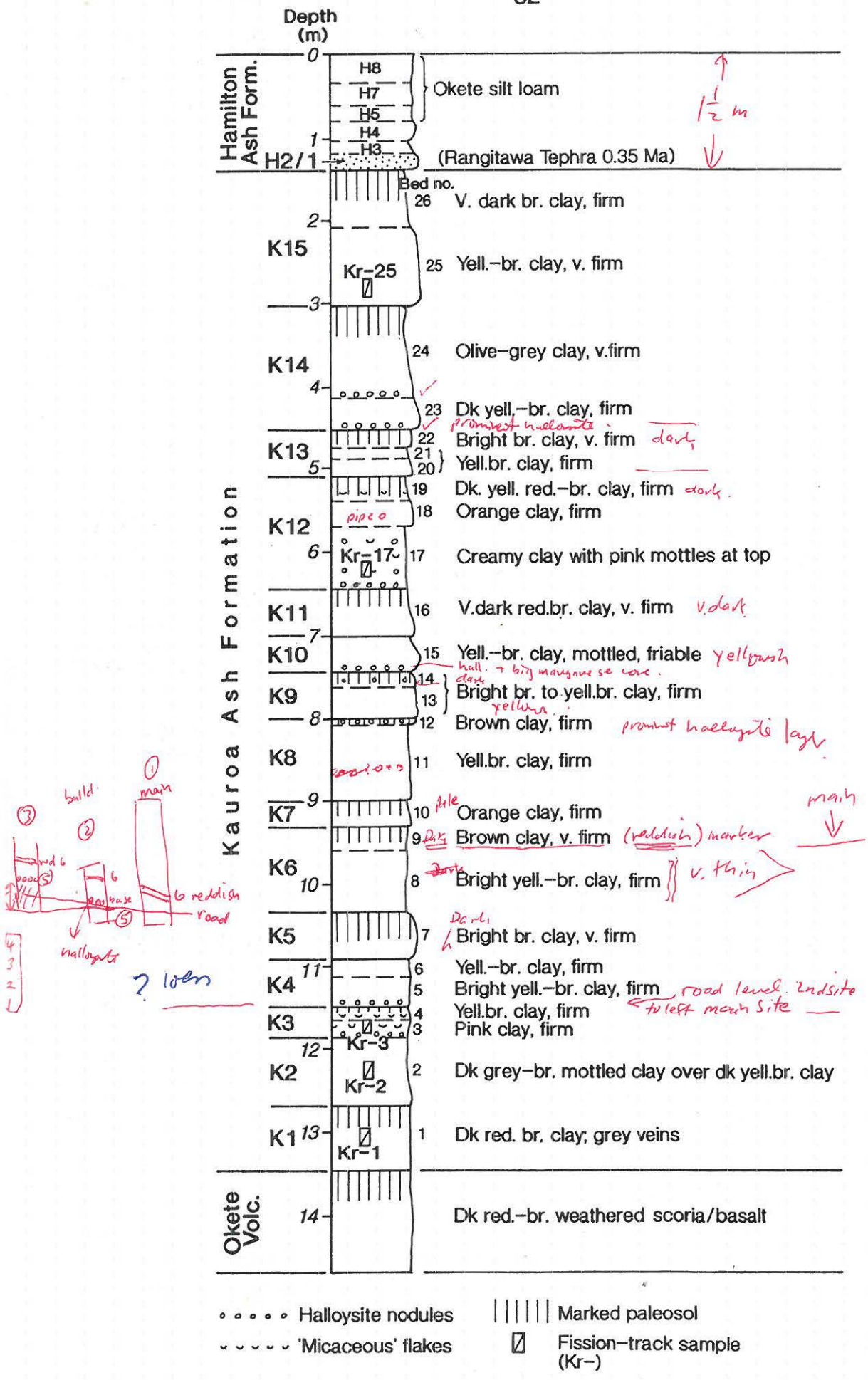

Figure 1.7: Stratigraphy of the Hamilton and Kauroa Ash beds at Woodstock near Raglan (mainly after Salter 1979; Hamilton Ash stratigraphy after Ward 1967).

The stratigraphy of the section is summarised in Fig. 1.7. Salter (1979) identified and analysed 26 beds within the section, enabling the sequence to be classified into 15 members (K1-15). This stratigraphy has been slightly modified by T.G. Shepherd (unpub. data). Provisional fission-track ages (subject to further counting) on zircons extracted from five beds (Fig. 1.7) are as follows (Table 1.1) (J. M. Tippett & P. J. J. Kamp unpub. data):

TABLE 1.1 Provisional fission-track ages, Kauroa Ash Formation, Woodstock

Sample	Member	Age ± 2 S.D. (Ma)
Kr-25	K15	nd (inadequate zircons)
Kr-17	K12	1.41 ± 0.26
Kr-3	K3	1.70 ± 0.32
Kr-2	K2	1.50 ± 0.44
Kr-1	K1	2.30 ± 0.56

The age for K1 (Kr-1) agrees with those obtained by Briggs et al. (1989) for this bed intercalated with two dated basalts at nearby Maungatawhiri volcanic centre (2.26, 2.25 Ma). K12, the prominent whitish marker bed, has been tentatively correlated with Ongatiti Ignimbrite (probably equivalent to Oparau Tephra; Pain 1975; Salter 1979) and the age of 1.41 ± 0.26 Ma (Kr-17), taking errors into account, is consistent with the Ar/Ar age of 1.23 ± 0.02 Ma obtained on Ongatiti Ignimbrite (Briggs et al. 1993). Briggs et al. (1989) demonstrated that K15 must be younger than 1.81 Ma, and the age on K12 supports this contention. As noted above, stratigraphic work suggests a possible age of c. 0.95 Ma(?) for K15; a minimum age is given by H1/2 (Rangitawa Tephra) of the overlying Hamilton Ash sequence (0.35 Ma; Kohn et al. 1992).

The Kauroa beds here have high clay contents, ranging from 69-92% (<2 μm fraction). The small amounts of primary minerals are dominated by quartz, cristobalite, (titano)magnetite, ilmenite, and zircon.

The clays have been analysed by Kirkman (1980), Salter (1979), and Shepherd (1994 and unpub. data). Table 1.2 summarises the latest data: the amounts of kandite (kaolinite plus halloysite) and gibbsite were determined by DTA (Whitton & Churchman 1987); halloysite and kaolinite were estimated by XRD analysis of formamide-treated samples (Churchman et al. 1984); allophane was estimated by the acid oxalate (Al, Si) and pyrophosphate (Al) extractions (Parfitt & Wilson 1985); ferrihydrite and goethite were estimated by oxalate, dithionite, and pyrophosphate (Fe) extractions (Childs 1987) (see Lowe & Percival 1993 for a summary of techniques).

The beds are dominated by kandite (60-95% whole sample basis) with smaller amounts of goethite (2-15%) and minor amounts of allophane (0.5-2%), ferrihydrite (0.1-1%), and gibbsite (<0.1-2%). Halloysite (50-95%) is by far the major component of the kandite mineral group, with kaolinite varying from 0-20% (Table 1.2). Bed K8IV has significantly more goethite than other beds (15%), while K10 has most gibbsite (2%). Salter (1979) additionally identified traces of montmorillonite-vermiculite intergrades in K2 and K4.

The predominance of halloysite throughout the entire Kauroa sequence is possibly a product of its relative stability in the current weathering environment where the ionic concentration of the various reactants for halloysite in solution (especially [Si]) is in equilibrium with its solubility product, a function in part of the age of the beds and their strongly weathered nature. It is possible that allophane would have formed in significant quantities in the past, but has since been 'converted' to halloysite either by the solid state transformation of Si-rich allophane (Al/Si = ≈1), or by the dissolution of Al-rich (proto-imogolite) allophane (Al/Si = ≈2) followed by its reprecipitation as halloysite.

The type of allophane that now remains is primarily of the Al-rich type, likely to be a function of its greater stability (depending on silica activity; Percival 1985). A remnant amount of Si-rich allophane occurs only in K8III and K4I (Table 1.2).

TABLE 1.2. Mineralogical composition[1] of the Kauroa Ash beds at Woodstock

Sample	Thickness cm	Kandite (%)	Halloy. (%)	Kaol. (%)	Alloph. (%)	Alloph. (Al/Si)	Alloph./ Kandite	Ferrihy. (%)	Goeth. (%)	Gibb. (%)
H2	35	85	85	0	1	a	0.01	0.2	4	<0.1
K15 III	38	60	55	5	1	a	0.02	0.5	7	<0.1
K15 II	29	65	60	5	1	a	0.02	0.5	8	0.5
K15 I	33	90	90	0	1	a	0.01	0.5	6	1
K14 VII	32	70	65	5	1	a	0.01	0.1	7	<0.1
K14 VI	29	75	70	5	1	a	0.01	0.5	8	<0.1
K14 V	18	75	70	5	1	a	0.01	0.5	7	0.5
K14 IV	58	85	80	5	1	a	0.01	0.5	6	0.1
K14 III	27	80	80	0	1	a	0.01	0.5	6	0.5
K14 II	14	90	90	0	1	a	0.01	0.5	5	<0.1
K14 I	16	95	95	0	1	a	0.01	0.5	2	0
K13 III	21	80	75	5	1	a	0.01	0.5	4	0.1
K13 II	15	85	80	5	1	a	0.01	0.5	5	0.5
K13 I	27	85	85	0	2	a	0.02	0.5	4	0
K12 IV	20	75	75	0	2	a	0.03	0.5	8	0.5
K12 III	39	75	70	5	0.5	a	0.01	0.5	5	0.1
K12 II	16	90	85	5	1	a	0.01	0.1	3	0
K12 I	57	95	90	5	0.5	3.2	0.01	0.5	2	0
K11	66	65	60	5	0.5	2.2	0.01	0.1	8	0.1
K10	49	75	70	5	0.5	3.3	0.01	0.5	8	2
K9 II	20	95	95	0	2	a	0.02	1	5	0.5
K9 I	38	85	85	0	0.5	2.0	0.01	0.5	6	0.5
K8 IV	6	70	70	0	0.5	2.2	0.01	0.5	15	0.5
K8 III	28	95	95	0	1	1.1	0.01	0.5	5	0.1
K8 II	9	90	75	15	1	3.6	0.01	0.5	5	0.5
K8 I	12	90	90	0	0.5	3.3	0.01	0.1	3	0
K7 II	8	90	80	10	1	a	0.01	0.1	4	0.1
K7 I	19	85	85	0	1	a	0.01	0.1	5	0.1
K6 II	24	75	70	5	1	a	0.01	0.5	5	0.1
K6 I	19	80	80	0	1	2.5	0.01	0.1	7	0.5
K5	70	60	50	10	1	a	0.02	0.5	10	0.5
K4 II	15	70	55	15	1	1.9	0.01	0.5	7	0.5
K4 I	20	80	70	10	1	1.0	0.01	0.5	7	0.5
K3	29	65	60	5	2	2.8	0.01	1	6	0.5
K2 III	16	80	70	10	1	3.6	0.01	0.5	5	0.1
K2 II	6	95	90	5	1	2.3	0.01	0.5	2	0
K2 I	18	85	80	5	1	a	0.01	0.1	5	0.1
Weathered basalt lapilli tuff ?	15	95	85	10	0.5	a	0.01	0.1	7	0.1
K1 III	25	70	60	10	0.5	a	0.01	0.1	6	<0.1
K1 II	30	70	50	20	1	a	0.01	0.1	8	0.1
K1 I	40	85	75	10	0.5	a	0.01	0.1	5	0.1
On weathered basaltic scoria (Alexandra Volcanics)										

[1] Mineralogical composition of the whole soil. oooooo = White halloysite nodules a = insufficient silica present
Halloy. = Halloysite; Kaol. = Kaolinite; Alloph.= Allophane; Ferrihy. = Ferrihydrite; Goeth. = Goethite Gibb. = Gibbsite
Wavy line represents an unconformity. Shading signifies the presence of a paleosol.

An alternative explanation for the predominance of halloysite is that the drainage and leaching conditions at Woodstock have always been such that halloysite formation, rather than (Al-rich) allophane, has been favoured, i.e. the halloysite is relict. This contention requires that silica concentration has been relatively high (hence leaching of Si low, either because of low rainfall or slow drainage, or both) as halloysite is more stable than imogolite and Al-rich allophane only at high silica activities (Lowe & Percival 1993; Lowe 1994); kaolinite is the most stable mineral of those found in the Kauroa beds. The presence of halloysite concretions or nodules in some beds, typically with associated Mn nodules (Table 1.2; Salter 1979), indicates perhaps that silicon enrichment through wetting and drying and perching has occurred (Stevens & Vucetich 1985; Lowe 1986).

Both allophane (Al/Si = ≈2) (up to 60% whole sample) and halloysite (up to 66%) occur in a sequence of strongly weathered tephra beds near Te Kuiti, where Stevens & Vucetich (1985) suggested that the allophane-rich beds weathered under warmer, wetter (interglacial) conditions, and the halloysitic beds under colder, drier (glacial) conditions based on the leaching models of Parfitt et al. (1983) and Singleton et al.(1989). The Te Kuiti sequence probably has an appreciably greater andesitic component than that at Woodstock; if so, this would additionally favour the formation of allophane over halloysite (Lowe 1986).

Sand-sized 'micaceous' or platy minerals found in K3, K4, and K-12 were identified as b-axis disorded kaolinite books and stacks (Salter 1979). Sparse relict pumice fragments, coated with an iron oxide, were also identified in these beds (Salter 1979).

Numerous paleosols occur within the Kauora sequence — Salter (1979) identified around 10 and Shepherd (1994) 14 (Table 1.2). They are identified (not always easy in such strongly weathered materials) on the basis of various field properties including colour (darker and more reddish hue), consistence (very firm), and structure (strongly developed blocky/polyhedral), and occasional root traces or rodlet pseudomorphs.Their occurrence is supported by the distribution of total carbon, and by the increase of halloysite with depth from the top of the paleosol to the base of the tephra bed (T.G. Shepherd unpub. data).

STOP 3 — Toilet stop, Raglan

STOP 4 — Bryant Home Section, Manu Bay (R14/705737)

This section shows some of the TVZ-derived Kauroa Ash beds overlying laharic deposits derived from Mt Karioi (Fig. 1.8). The brief stop here is primarily to illustrate the contemporay activity of Mt Karioi and in TVZ. More sections, predominantly showing laharic material with one or two intercalated older K-beds, and paleosols, occur a little further along the road (around the corner). None of these sections has been studied in detail.

STOP 5 — Te Toto Amphitheatre and Gorge (Car Park at R14/665717)

The Te Toto area is a large scallop-shaped erosional amphitheatre that has formed on the northwestern flank of Karioi volcano (Figs. 1.9-10). The amphitheatre has exposed an Okete tuff ring, surge beds, and pillow lavas just above sea level, which are overlain by a thick sequence of Karioi lavas that form most of the upper cliffs.

The Okete Volcanic Formation has been divided into a stratigraphically lower Pauaeke Member that underlies Karioi lavas, which are exposed here at Te Toto (Figs. 1.11 & 1.13), and a stratigraphically upper Marumaruaitu Member that overlies Karioi lavas. The Karioi Volcanic Formation consists of three members, all of which are exposed in Te Toto amphitheatre and Gorge (Fig. 1.11). The Te Toto Member is stratigraphically lowest and consists of a series of three lava flows, separated from a thick sequence of shield-building Whaanga lavas by the prominent orange main marker horizon. The Whaanga Member consists of at least 15 sheet flows, and in the upper part of the stratigraphic succession exposed in road cuts in Te Toto Gorge, it is overlain in turn by Wairake Member lavas and lahars.

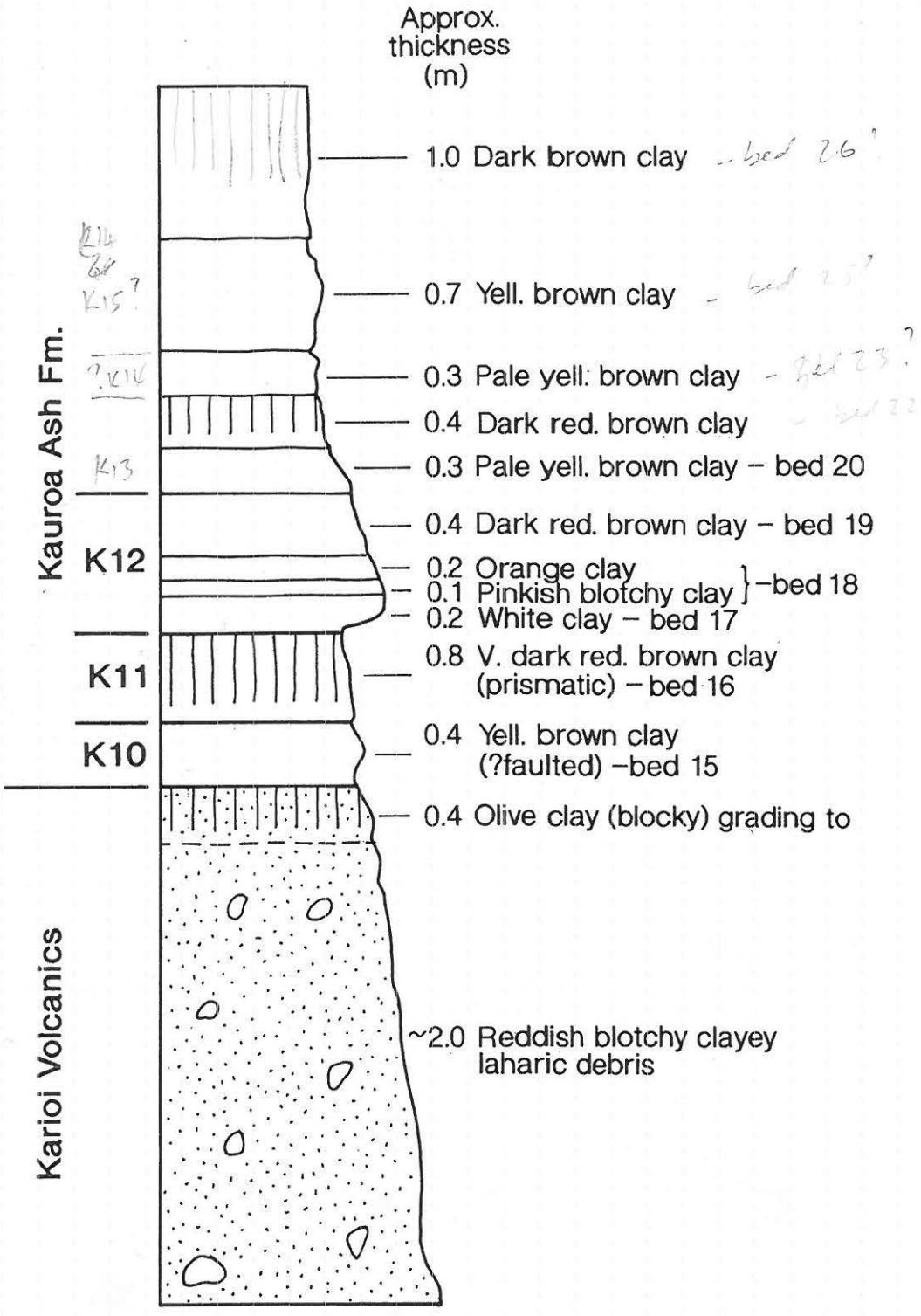

Figure 1.8: Stratigraphy of Kauroa Ash beds and Karioi laharic deposits at the Bryant Home Section, Manu Bay.

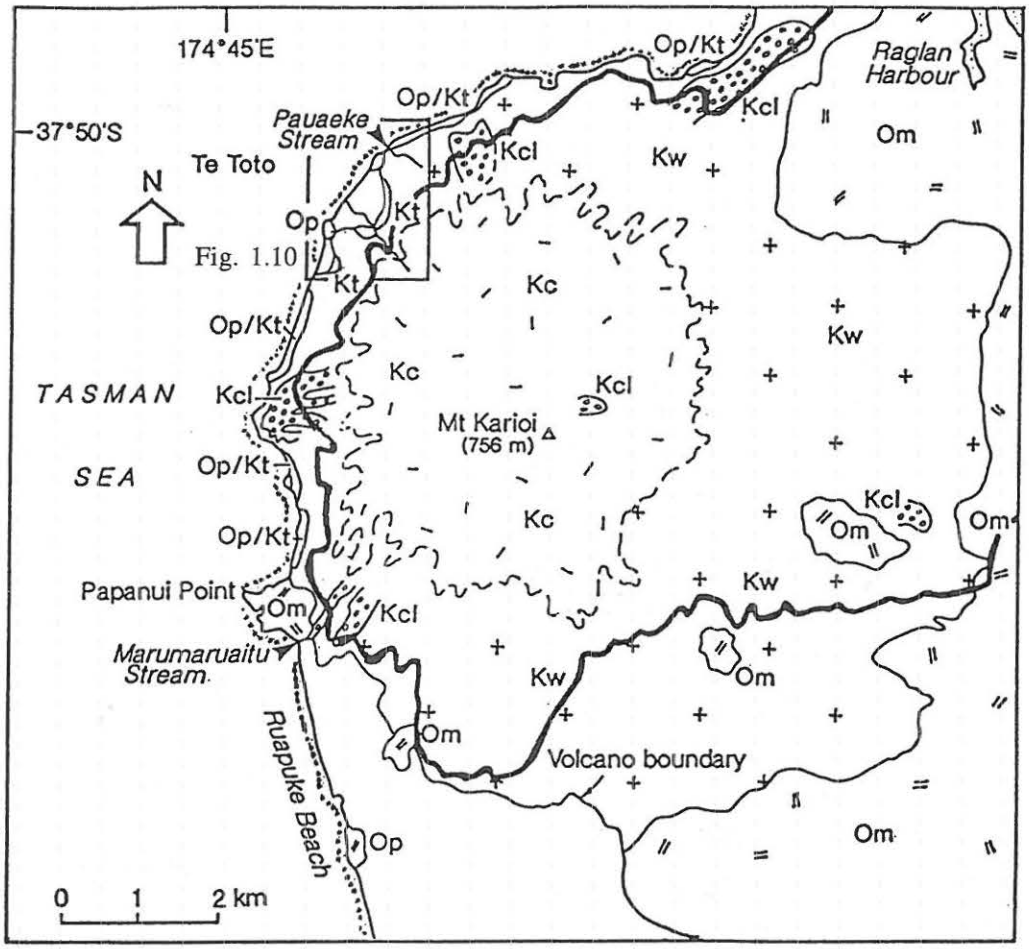

LEGEND

Karioi Volcanic Formation

Kc Wairake Member: Cone-building lavas, tuffs, dikes, volcanic breccias, laharic deposits (Kcl), and valley-filling lavas

Kw Whaanga Member: Sheet lavas, volcanic breccias, minor interbedded tuffs, and rare dikes

Kt Te Toto Member: Lavas, volcanic breccias, interbedded tuffs

Okete Volcanic Formation

Om Marumaruaitu Member: Lavas and interbedded tuffs postdating Karioi volcanics

Op Pauaeke Member: Lavas, lapilli tuffs predating Karioi volcanics

Figure 1.9: Map of Karioi volcano showing the distribution of volcanic formations and members. Some data from Matheson (1981) and Keane (1985).

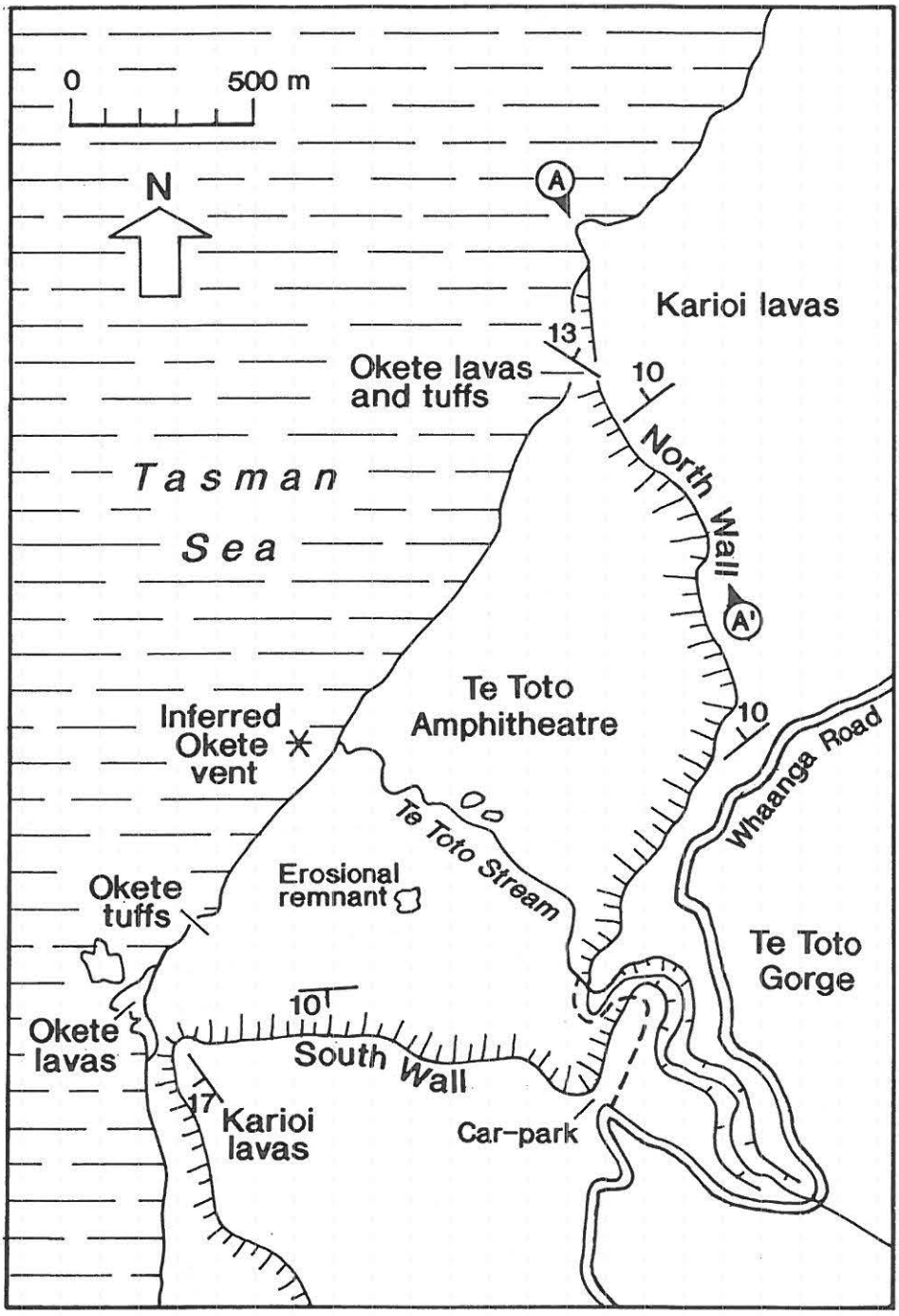

Figure 1.10: Map of Te Toto Gorge and amphitheatre, northwestern flank of Karioi volcano. A-A' is the line of the Pauaeke type section (Fig. 1.13), North Wall of Te Toto amphitheatre.

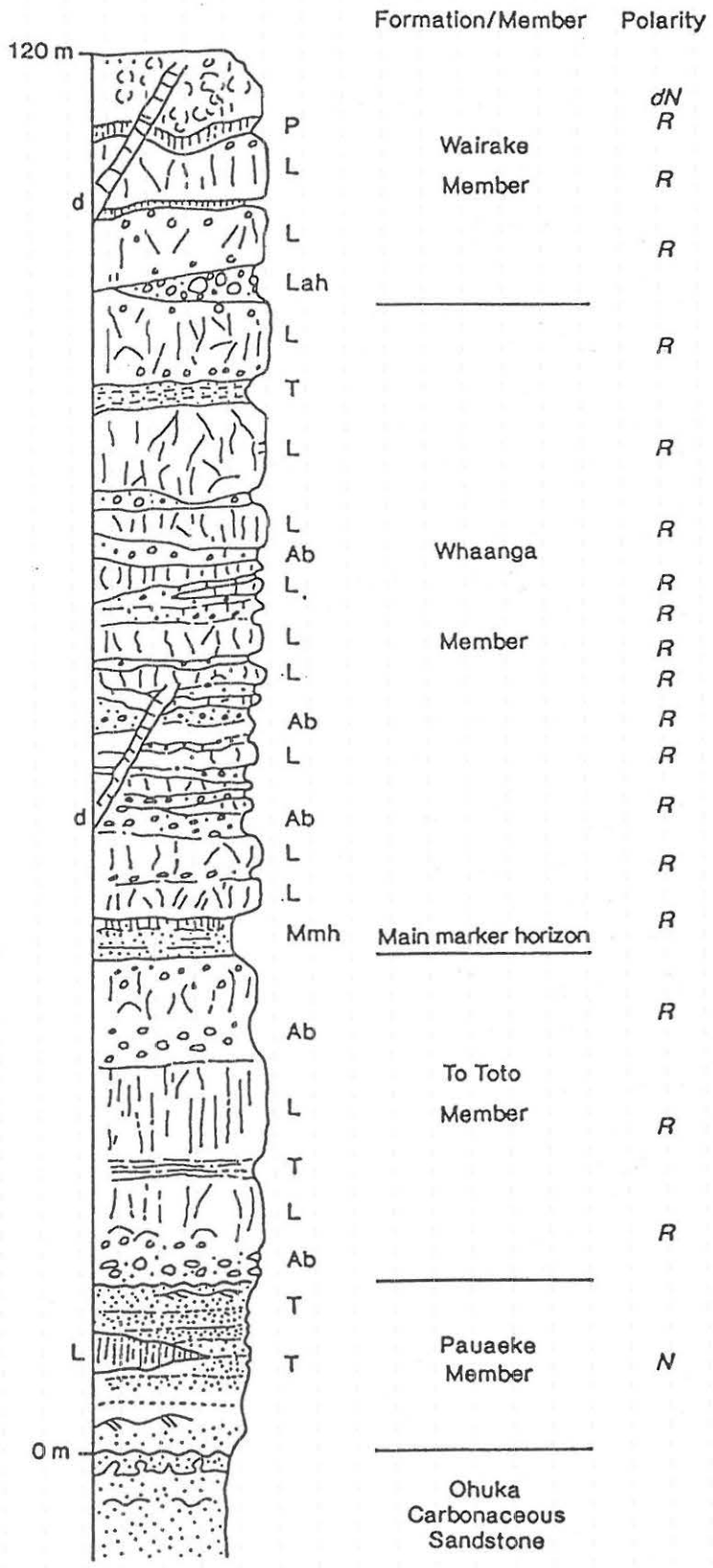

Figure 1.11: Composite stratigraphic section through the Karioi Volcanics exposed in the South Wall of Te Toto amphitheatre and in Te Toto Gorge. L = lava, Ab = autoclastic breccia, T = tuff and lapilli tuff, d = dike, Lah = laharic deposit, Mmh = main marker horizon, P = paleosol.

We shall begin with a general overview of Te Toto amphitheatre from the car park reserve of Whaanga Road. Then we shall examine the roadcut just east of the parking area, where there are exposed uppermost units of the Whaanga Member (including a strikingly plagioclase-phyric lava), the erosional unconformity that caps the Whaanga units, a basal Wairake lahar, and three Wairake lavas above that lahar (Fig. 1.12).

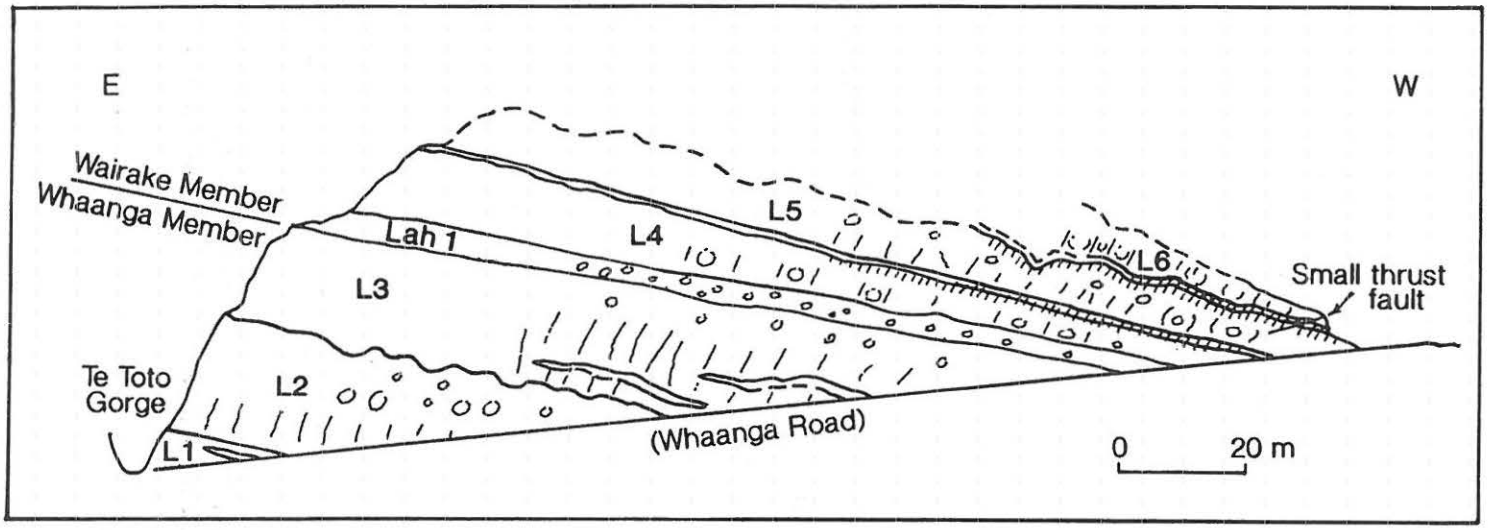

Figure 1.12: Sketch of lava flow sequence (L1-L6), with intercalated laharic deposits marking the local base of the Wairake Member, at the Whaanga Road section in Te Toto Gorge.

We shall then follow the trail down into Te Toto Gorge and amphitheatre, and examine:

(a) the vent-proximal facies of the Te Toto Member of thick calc-alkalic lavas and breccias;
(b) the Pauaeke type section (Fig. 1.13) at the seaward end of the North Wall of the amphitheatre (and archaeological features en route); and
(c) Okete (Pauaeke Member) lavas and enclosed mantle xenoliths, surge beds, and contacts with underlying Ohuka Carbonaceous Sandstone beds, near the end of the South Wall.

While in Te Toto amphitheatre, participants will see some of the indications of a close relationship between the alkalic Okete Volcanic Formation (Pauaeke Member) and the calc-alkalic Karioi Volcanic Formation (Te Toto Member). These indications include suggestions of a relatively short interval between cessation of eruption of Pauaeke magmas and beginning of Te Toto activity, and evidence that both sets of magmas were erupted from small central vent volcanoes under much the same kinds of structural control.

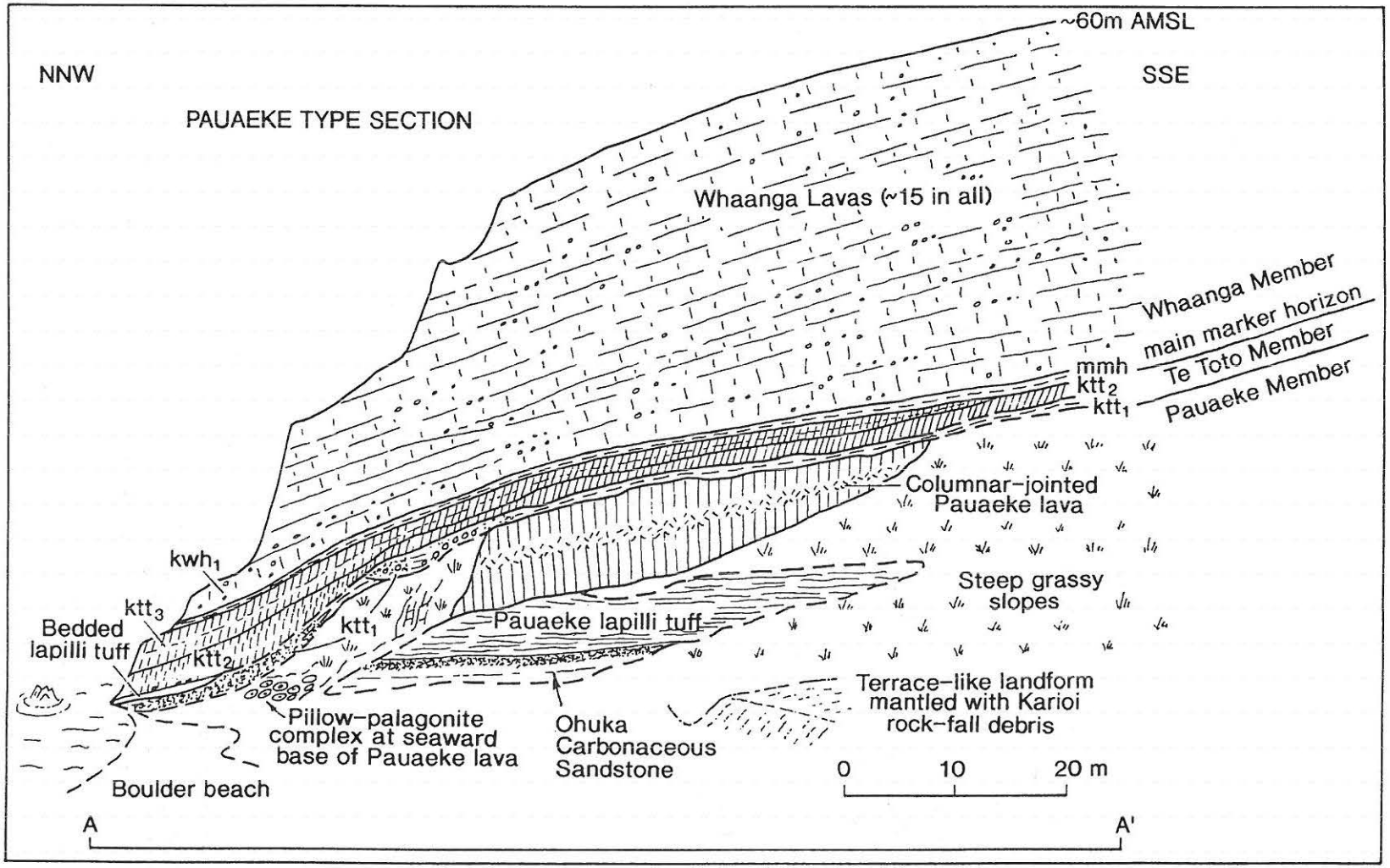

Figure 1.13: Sketch of Pauaeke type section at the North wall of Te Toto amphitheatre (A-A' in Fig. 1.10). Ktt_1-Ktt_3 are Te Toto Member lava flows overlying Pauaeke lava; mmh = main marker horizon; kwh_1 = basal Whaanga lava.

In Fig. 1.14, we show a spidergram for data on rocks from these two units. There is a tendency for some of the Pauaeke lavas to have greater Ba contents than Te Toto lavas, and there is a strong contrast in Nb abundance as commonly observed betwen these magma types. Pauaeke lavas also have greater contents of LREE, Sr, P, Zr, and Ti.

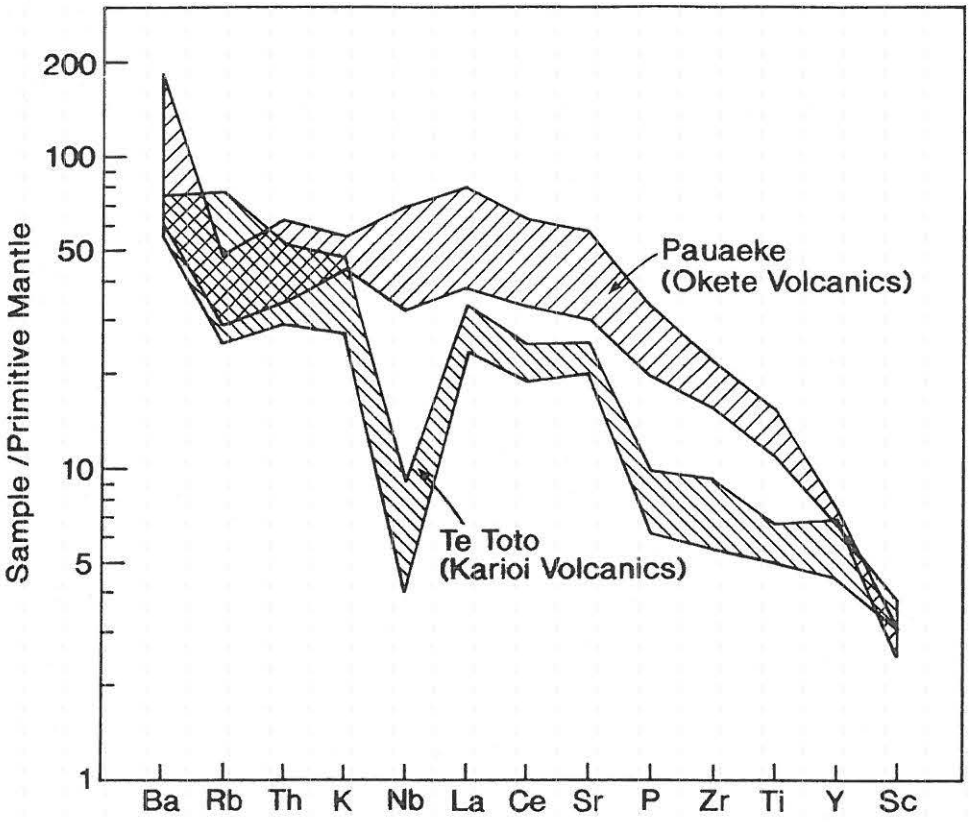

Figure 1.14: Primitive mantle normalized diagram for Pauaeke Member (Okete Volcanics Formation) and Te Toto (Karioi Volcanics Formation) lavas from Te Toto amphitheatre.

The Karioi ediface is only ≈70 km^2 in area, yet shows a remarkable diversity of magma types and physical volcanological processes. Early alkalic magmas brought an extraordinary array of mantle-derived xenoliths to the surface. The Pauaeke lavas and tuffs were succeeded after only a short pause by calc-alkalic augite-phyric Te Toto breccias and lavas. vents for both Pauaeke and Te Toto eruptions built all volcanic centres, with locations apparently controlled by regional-scale fault systems. After an hiatus (marked by the transgressive erosion surface beneath the 'main marker horizon', and by the 'main marker horizon' itself), the Whaanga shield was built by a series of fissure eruptions some of which are represented by dikes visible in the walls of Te Toto amphitheatre. Field evidence suggests that recurrence intervals between Whaanga eruptions initially were short, but became longer (allowing incision of the shield by streams) late in Whaanga times. A proto-Wairake composite cone may have been under construction before Whaanga eruptive activity had completely died away, but the exact temporal relationship between fissure eruptions that built the Whaanga shield and central vent eruptions that built the Wairake cone can only be determined by mapping in detail. The first clear indication of the existence of the Wairake cone in most locations is laharic debris. These same laharic deposits may afford the most complete record of Wairake volcanism, although, because of the alteration of most such deposits, deciphering that record would be difficult. Late in the history of the Wairake composite cone, it was intruded by at least one large hornblende andesite dike (exposed at the summit). That dike may have fed a flow of similar lithologic character, found on the western slopes of the ediface.

A curious feature of the volcanic history outlined here, as we presently know it, is that there seems to be an antithesis between alkalic Okete volcanism and calc-alkalic Karioi volcanism. We have found no instance of an alkalic eruption contemporaneous with, or interdigitating with, products of calc-alkalic eruptions, although more details of these temporal relations are required to confirm this.

REFERENCES

Briggs, R.M. 1983: Distribution, form, and structural control of the Alexandra Volcanic group, North Island, New Zealand. *New Zealand journal of geology and geophysics 26*: 47-55.

Briggs, R.M.; Goles, G.G. 1984: Petrological and trace element geochemical features of the Okete Volcanics, western North Island, New Zealand. *Contributions to mineralogy and petrology 86*: 77-88.

Briggs, R.M.; McDonough, W.F. 1990: Contemporaneous convergent margin and intraplate magmatism, North Island, New Zealand. *Journal of petrology 31*: 813-851.

Briggs, R.M.; Itaya, T.; Lowe, D.J.; Keane, A.J. 1989: Ages of Pliocene-Pleistocene Alexandra and Ngatutura Volcanics, western North Island, New Zealand, and some geological implications. *New Zealand journal of geology and geophysics 32*: 417-427.

Briggs, R.M.; Gifford, M.G.; Moyle, A.R.; Taylor, S.R.; Norman, M.D.; Houghton, B.F.; Wilson, C.J.N. 1993. Geochemical zoning and eruptive mixing in ignimbrites from Mangakino volcano, Taupo Volcanic Zone, New Zealand. *Journal of volcanology and geothermal research 56:* 175-203.

Bruce, J.G. 1978: Soils of part Raglan County South Auckland. *New Zealand Soil Bureau bulletin 41*. 102p.

Childs, C.W. 1987. Weighted mean concentrations of minerals in New Zealand soils. 1. Ferrihydrite. *New Zealand Soil Bureau scientific report 81*. 28p.

Churchman, G.J.; Whitton, J.S.; Claridge, G.G.C.; Theng, B.K.G. 1984: Intercalation method using formamide for differentiating halloysite from kaolinite. *Clays and clay minerals 32*: 241-248.

Davoren, A. 1976: A pedological study of the Kauroa Ash Formation at the University of Waikato. Unpublished MSc thesis, University of Waikato, Hamilton.

Hogg, A.G. 1974: A pedological study of the Hamilton Ash Formation at Te Uku. Unpublished MSc thesis, University of Waikato, Hamilton.

Keane, A.J. 1985: The age, form and volcanic mechanisms of the Okete Volcanics near Raglan. Unpublished MSc thesis, University of Waikato, Hamilton.

Kear, D.S.; Schofield, J.C. 1978: Geology of the Ngaruawahia Subdivision. *New Zealand Geological Survey bulletin 88*. 168p.

Kirkman, J.H. 1980: Mineralogy of the Kauroa Ash Formation of south-west and west Waikato, North Island, New Zealand. *New Zealand journal of geology and geophysics 23*: 113-120.

Kohn, B.P.; Pillans, B.J.; McGlone, M.S. 1992: Zircon fission track age for middle Pleistocene Rangitawa Tephra, New Zealand: stratigraphic and paleoclimatic significance. *Palaeogeography, palaeoclimatology, palaeoecology 95*: 73-94.

Lowe, D.J. 1986: Controls on the rates of weathering and clay mineral genesis in airfall tephras: a review and New Zealand case study. *In* Colman, S.M.; Dethier, D.P. (eds) Rates of Chemical Weathering of Rocks and Minerals. Academic Press, Orlando: 265-330.

Lowe, D.J. 1994: Teaching clays: from ashes to allophane. *Proceedings, 10th International Clay Conference,* Adelaide. CSIRO (in press)

Lowe, D.J.; Percival, H.J. 1993: Clay mineralogy of tephras and associated paleosols and soils, and hydrothermal deposits, North Island. *Guide Book for New Zealand Pre-Conference Field Trip F1*, 10th International Clay Conference, Adelaide, Australia. 110p.

Matheson, S.G. 1981: The volcanic geology of the Mt Karioi region. Unpublished MSc thesis, University of Waikato, Hamilton.

McCraw, J.D. 1967: The surface features and soil pattern of the Hamilton Basin. *Earth Science Journal 1*: 59-74.

Nelson, C.S. 1988: Revised age of a late Quaternary tephra at DSDP Site 594 off eastern South Island and some implications for correlation. *Geological Society of New Zealand newsletter 82*: 35-40.

Pain, C.F. 1975: Some tephra deposits in the south-west Waikato area, North Island, New Zealand. *New Zealand journal of geology and geophysics 18*: 541-550.

Parfitt, R.L.; Wilson, A.D. 1985: Estimation of allophane and halloysite in three sequences of volcanic soils, New Zealand. *Catena supplement 7*: 1-8.

Parfitt, R.L.; Russell, M.; Orbell, G.E.1983: Weathering sequence of soils from volcanic ash involving allophane and halloysite, New Zealand. *Geoderma 29*: 41-57.

Percival, H.J. 1985: Soil solutions, minerals, and equilibria. *New Zealand Soil Bureau scientific report 69*. 21p.

Salter, R.T. 1979: A pedological study of the Kauroa Ash Formation at Woodstock. Unpublished MSc thesis, University of Waikato, Hamilton.

Selby, M.J.; Lowe, D.J. 1992: The middle Waikato Basin and hills. *In* Soons, J.M.; Selby, M.J. (eds) Landforms of New Zealand 2nd Edition. Longman Paul, Auckland: 233-255.

Shepherd, T.G. 1984: A pedological study of the Hamilton Ash Group at Welches Road, Mangawara, North Waikato. Unpublished MSc thesis, University of Waikato, Hamilton.

Shepherd, T.G. 1994: Paleoclimatic implications of clay minerals and paleosols within strongly weathered Plio-Pleistocene tephras of the Waikato region, central North Island, New Zealand. *Programme and Abstracts*, International Inter-INQUA Field Confernce and Workshop on Tephrochronology, Loess, and Paleopedology, Hamilton, New Zealand (in press).

Singleton, P.L.; McLeod, M.; Percival, H.J. 1989: Allophane and halloysite content and soil solution silicon in soils from rhyolitic volcanic material, New Zealand. *Australian journal of soil research 27*: 67-77.

Stevens, K.F.; Vucetich, C.G. 1985: Weathering of Upper Quaternary tephras in New Zealand, 2. Clay minerals and their climatic interpretation. *Chemical geology 53*: 237-247.

Tonkin, P.J. 1970: Contorted stratification with clay lobes in volcanic ash beds, Raglan-Hamilton region, New Zealand. *Earth science journal 4*: 129-140.

Vucetich, C.G.; Birrell, K.S.; Pullar, W.A. 1978: Ohinewai Tephra Formation; a c. 150,000-year-old tephra marker in New Zealand. *New Zealand journal of geology and geophysics 21*: 71-73.

Ward, W.T. 1967: Volcanic ash beds of the lower Waikato Basin, North Island, New Zealand. *New Zealand journal of geology and geophysics 10*: 1109-1135.

Whitton, J.S.; Churchman, G.J. 1987: Standard methods for mineral analysis of soil survey samples for characterisation and classification in New Zealand Soil Bureau. *New Zealand Soil Bureau scientific report 79*.

DAY 2: HAMILTON—ROTORUA—HAMILTON

Lowe, D.J.; Briggs, R.M. 1994. Intra-conference Tour Day 2: Hamilton–Rotorua–Hamilton. In: Lowe, D.J. (ed) Conference Tour Guides, Proceedings International Inter-INQUA Field Conference and Workshop on Tephrochronology, Loess, and Paleopedology, University of Waikato, Hamilton, New Zealand, 45-71.

D. J. Lowe & R. M. Briggs
Department of Earth Sciences
University of Waikato, Private Bag 3105
Hamilton, New Zealand

Outline of Day 2 (Thurdsay 10 February)

8.30-9.10 am	Depart Bryant Hall, University of Waikato, and travel (SH 1) to Hinuera Quarry
9.10-9.50 am	STOP 1 — Ongatiti Ignimbrite, Hinuera Quarry
9.50-10.05 am	Travel to Tirau
10.05-10.15 am	STOP 2 — Comfort stop, Tirau
10.15-10.30 am	Travel from Tirau to Tapapa
10.30-11.15 am	STOP 3 — Tapapa Section, Tapapa
11.15-12.00 pm	Travel to Rainbow Springs, Rotorua
12.00-1.30 pm	STOP 4 — Rainbow Springs LUNCH at Springs Restaurant 12.00-12.45 pm Tour of Springs 12.45-1.30 pm
1.30-2.00 pm	Travel to Te Ngae
2.00-2.45 pm	STOP 5 — Te Ngae Section, Te Ngae
2.45-3.00 pm	Travel to Gisborne Point (Lake Rotoiti) and enter Rotoiti Forest on Rotoiti Rd
3.10-5.00 pm	STOPS 6, 7, & 8 — Three sections on Rotoiti Rd of proximal Holocene eruptives, Haroharo Caldera
5.00-6.00 pm	Travel from Haroharo Caldera to Aorangi Peak Restaurant, Mt Ngongataha (Rotorua)
6.00-6.30 pm	STOP 9 — Overview of Rotorua Caldera and Okataina Volcanic Centre, from Aorangi Peak Restaurant
6.30-8.30 pm	CALDERA DINNER at Aorangi Peak Restaurant (Tarawera Room)
8.30-10.00 pm	Return from Rotorua to Bryant Hall, University of Waikato, Hamilton

INTRODUCTION

We have a reasonably long day ahead of us, but it promises to be both interesting and relaxing. We will be examining a range of distal and proximal pyroclastic deposits including airfall and flow (ignimbrite) units derived from the Mangakino and Okataina Volcanic Centres, Taupo Volcanic Zone (TVZ), tephric loess deposits, and buried paleosols on tephra beds — in other words, something for everyone attending our three-discipline conference. As well, we shall see a variety of volcanic landforms both on our journey from Hamilton and in the Rotorua region itself. We finish the day with a 'Caldera Dinner' overlooking Rotorua and Haroharo calderas, and Mt Tarawera, from the top of Ngongataha rhyolite dome.

From Hamilton (Fig. 2.1) we initially travel SE over the surface of a large, low angle fan of volcaniclastic sediments (the Hinuera Formation) deposited by an ancestral Waikato River system (Hume et al. 1975; Green & Lowe 1985; Selby & Lowe 1992). The age of this surface in the Hamilton Basin is c. 18-15 ka, and is mantled with a thin cover of distal tephra beds from various sources (Lowe 1986, 1988).

Stop 1 (off SH 29) is located in a quarry on cliffed margins in a shallow valley running approximatey N-S. The valley was previously occupied by the Waikato River discharging into the Hauraki Gulf/Firth of Thames (between c. 0.14 Ma and 50 ka, and between c. 24-19 ka; Selby & Lowe 1992).

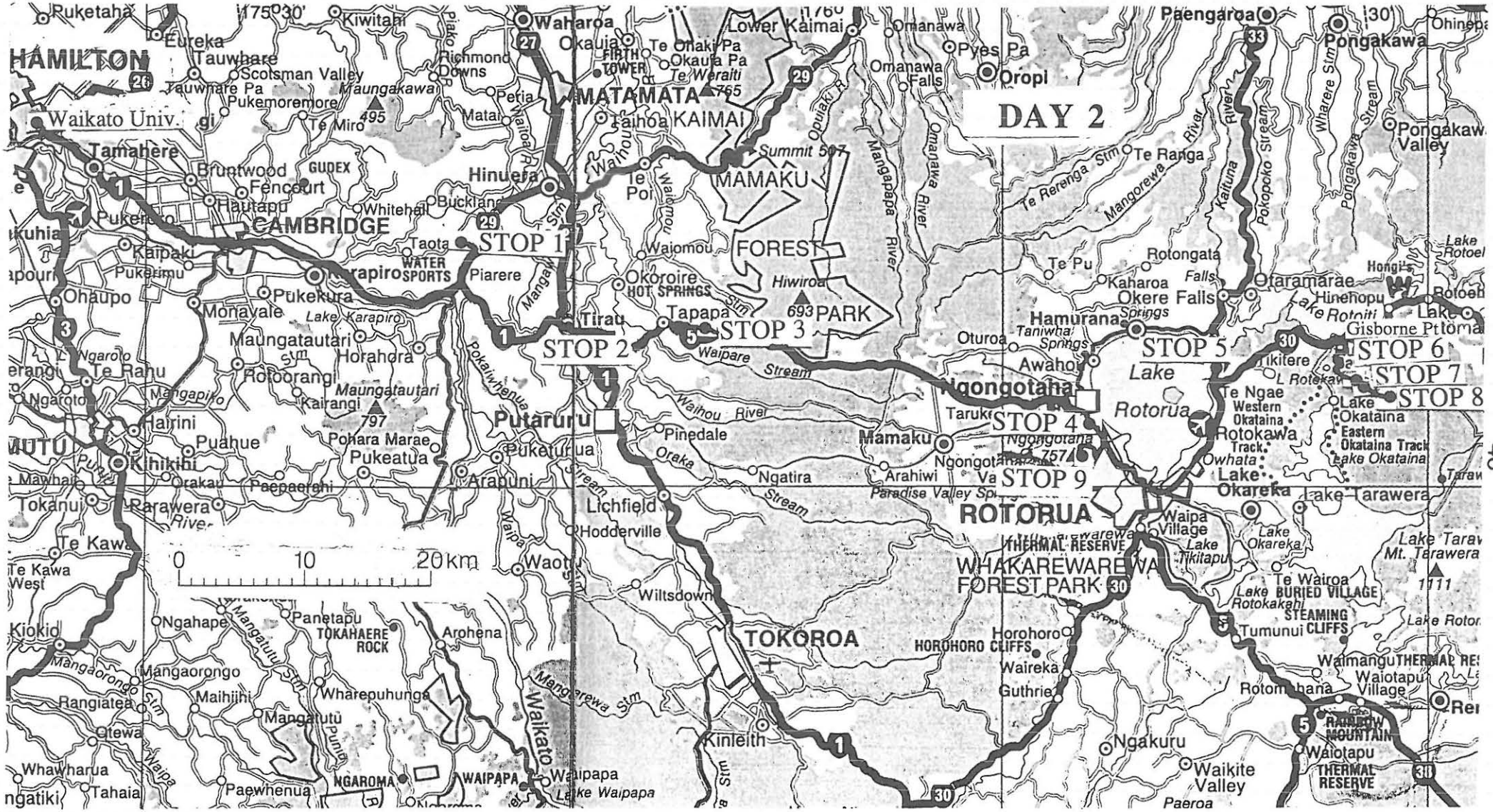

Figure 2.1: Route map for Day 2.

STOP 1 — Ongatiti Ignimbrite, Hinuera Quarry (T15/461614)
[Note: Hard hats must be worn]

The quarry (owned by Firth Industries) is developed in cliffs of Ongatiti Ignimbrite. The ignimbrite here is overlain by a 5+ m thick sequence of tephra beds including Hamilton Ash and younger airfall tephras.

TABLE 2.1. Summary of the stratigraphy, age, and characteristics of eruptives from the Mangakino Volcanic Centre (from Briggs et al. 1993).

Name	Ar/Ar age (Ma)	Volume (km^3)	Composition (SiO_2 wt.%)	Aspect ratio*	Nature
Waioraka Ignimbrite	–	<0.1	–	–	Non-welded, pumice-rich, vapour-phase altered ignimbrite with abundant lithic-rich lenses.
Whakaahu lava dome	0.87±0.08	<1	–	–	
Marshall Ignimbrites	0.91±0.02	>50	71–77	1:700	Marshall A: partially to densely welded ignimbrite, brown pumice, crystal-rich, pale buff-brown matrix. Marshall B: non-welded to partially welded, crystal-poor ignimbrite, with black and orange-brown pumice in a sandy black matrix. (Marshall A and B correlated with Ignimbrite I of Wilson, 1986).
Kaahu Ignimbrite	0.92±0.07	<0.5	74	–	Pumice-rich, crystal-poor ignimbrite, extensively vapour-phase altered. (Correlated with Ignimbrite H of Wilson, 1986).
Rocky Hill Ignimbrite	0.97±0.02	>300	71–76	1:3,200	Partially to densely welded, pumice-rich, crystal-rich ignimbrite with abundant hornblende.
Unit E	1.01±0.06	>300	71–76	–	Poorly exposed phreatomagmatic fall deposits with overlying non-welded ignimbrite.
Ahuroa Ignimbrite	1.19±0.03	>50	65–76	1:6,000	Non-welded to densely welded ignimbrite with an inverse thermal zonation; lower unit is crystal-rich with orange platy rhyolitic pumice and black dacitic pumice in a sandy black matrix, upper unit is strongly lenticular with fiamme.
Unit D	1.18±0.02	>10	67–75	–	Phreatomagmatic fall deposits with overlying non-welded ignimbrite.
Ongatiti Ignimbrite	1.23±0.02	>300	70–75	1:4,000	Pumice-rich, crystal-rich, non-welded to partially non-welded ignimbrite.
Tumai lava dome	1.27±0.05	<0.1	–	–	
Ignimbrite C	1.62±0.11	>10	60	–	Poorly exposed, partially welded andesitic ignimbrite.
Ignimbrite B	1.51±0.02	?	–	–	Poorly exposed, partially welded ignimbrite, extensively vapour-phase altered.
Ngaroma Ignimbrite	1.60±0.03	>50	71	1:3,000	Partially welded, purplish-brown extensively vapour-phase altered ignimbrite. (Correlated with Ignimbrite A of Wilson, 1986).

*Aspect ratio is defined by Walker et al. (1980) and Walker (1983) as V/H, where V is the average thickness, and H is the diameter of a circle covering the same areal extent as the rock unit.

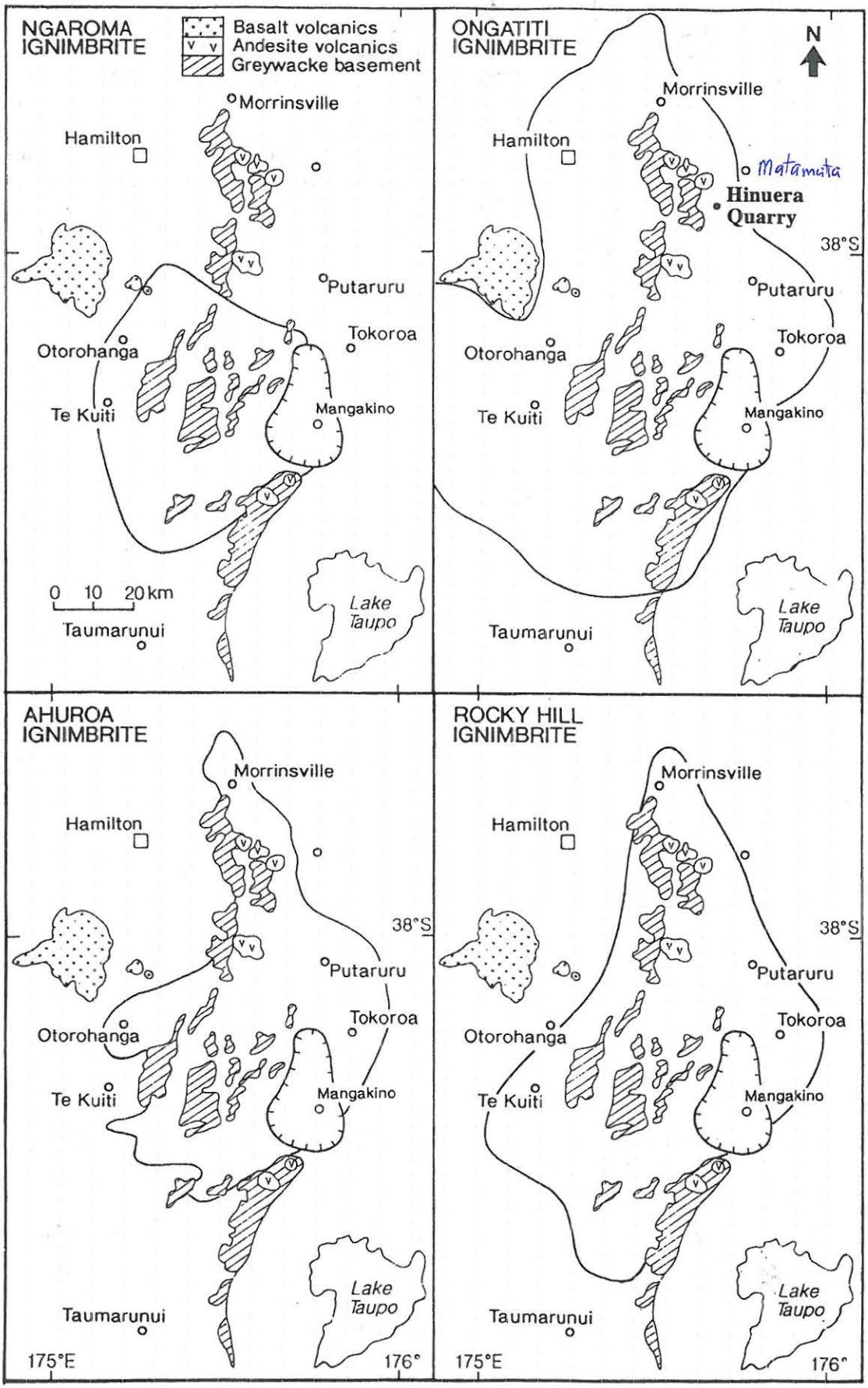

Figure 2.2: Distribution of four major Mangakino-derived ignimbrites, including Ongatiti. Lines represent envelopes around the outermost preserved outcrops and exposures, which are mainly the partially and densely welded portions of the units; hence they represent minmal areas covered by the deposits because of erosion, and the original nonwelded portions were much more widespread (from Briggs et al. 1993). The delineation of the Mangakino caldera is after Wilson et al. (1984).

The Ongatiti Ignimbrite, dated at 1.23 ± 0.02 Ma, is one of at least three ignimbrites derived from Mangakino volcano mapped in this area (Fig.2.2), the others including Ahuroa (1.19 ± 0.03 Ma) and Rocky Hill (0.97 ± 0.02 Ma) ignimbrites that lie above Ongatiti (Table 2.1; Briggs et al. 1993). In this section, the Ongatiti Ignimbrite has prominent but widely-spaced columnar jointing. It comprises a lower pumice-poor, crystal-rich, lithic-poor unit, a middle moderately welded flow unit, and an upper pumice-rich partially welded* unit (Fig. 2.3). The upward coarsening and abundance of pumice is also matched by the lithics, and so is not simply a fluidization-induced grading. These stratigraphic relations imply that the the ignimbrite consists of multiple flows that were erupted in a series of directional lobes. Briggs et al. (1993) suggested that the Ongatiti eruption commenced with highly energetic, violent and relatively cool flows which generated the finer-grained lower pumice-poor flows, and the eruption later escalated into a series of hotter but less energetic, coarser-grained pumice flows.

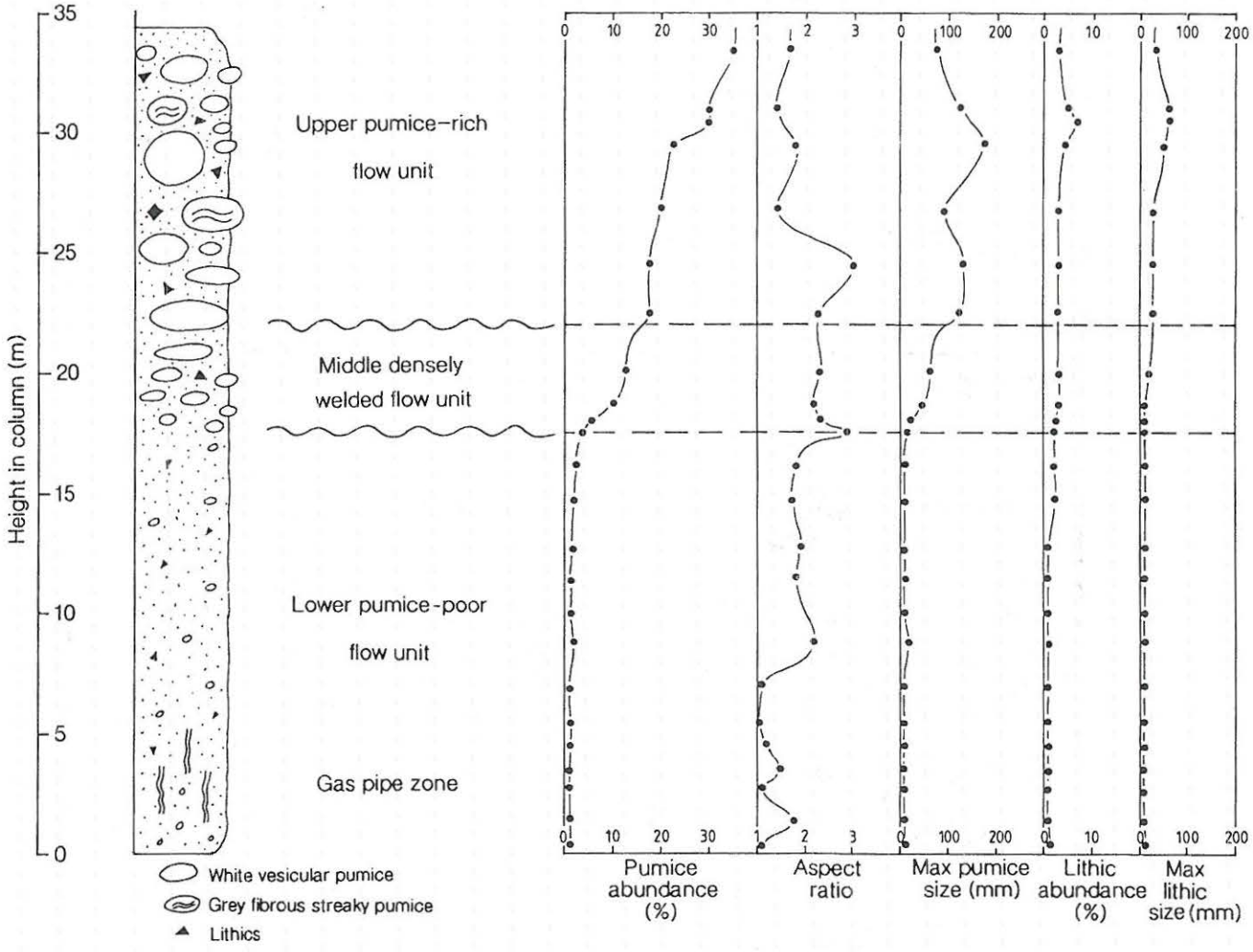

Figure 2.3: Stratigraphic section of Ongatiti Ignimbrite at Hinuera Quarry (from Briggs et al. 1993).

lithics - incl. rhyolite microdiorite gneiss

* Note: Ignimbrite welding (the sintering together of hot pumice fragments and glass shards under a compactional load; Cas & Wright 1987) can be described on a four-point scale: non-welded (can pluck pumicefragments out by hand) — weakly welded — partially welded — densely welded (pumice clasts break when ignimbrite cracked with hammer).

Mineralogically, plagioclase (oligoclase, andesine) is the dominant crystal and phenocryst, together with quartz, orthopyroxene (mainly ferrohypersthene), calcic hornblende, titanomagnetite, ilmenite, zircon, and apatite (Briggs et al. 1983). Glass shard analyses show a noteably homogenous composition (Table 2.2), and hence provide little evidence for mixing, whereas analyses of whole pumice clasts (i.e. glass in pumice + phenocrysts) are heterogeneous and, in contrast, provide evidence for mixing (Briggs et al. 1993). Other major- and trace-element analyses show that pumice in Ongatiti Ignimbrite varies compositionally (from 69.7 to 73.5 wt% SiO_2) but there are no systematic trends with stratigraphic height in the ignimbrite. Rather, pumices adjacent to one another in outcrop have variable composition, and the lack of any systematic trend is consistent for all oxides and trace elements. The compositional variation in pumice fragments demonstrates that the magma chamber was not homogenous but contained a significant range of compositions.

TABLE 2.2. Representative microprobe glass shard compositions in the Ongatiti Ignimbrite, normalised to 100% water free (from Briggs et al. 1993).

Sample	0/18	0/18	0/12	0/12	0/10	0/10	0/17	0/17	0/21	0/20
SiO_2	76.95	77.50	77.51	77.58	77.49	77.39	77.88	76.85	77.08	77.30
TiO_2	0.12	0.12	0.13	0.10	0.13	0.14	0.10	0.17	0.12	0.19
Al_2O_3	12.69	12.40	12.44	12.33	12.29	12.18	12.19	12.70	12.41	12.46
FeO*	1.14	1.42	1.07	1.25	1.32	1.43	1.15	1.21	1.36	1.36
MnO	–	–	–	–	–	–	–	–	–	–
MgO	0.11	0.11	0.07	0.06	0.12	0.08	0.12	0.12	0.11	0.09
CaO	0.87	0.82	0.66	0.77	0.74	0.82	0.61	0.73	0.53	0.86
Na_2O	3.52	3.47	3.32	3.21	3.33	3.33	3.31	3.44	2.47	3.23
K_2O	4.34	3.90	4.46	4.48	4.26	4.36	4.35	4.52	5.60	4.34
Cl	0.26	0.26	0.34	0.22	0.32	0.27	0.29	0.26	0.32	0.17

* Total Fe

Briggs et al. (1993) additionally report REE and Sr and Nd isotope analyses for Ongatiti Ignimbrite, and discuss these with respect to parallel analyses on other Mangakino eruptives and their petrogenesis.

Quarrying operation

The Ongatiti Ignimbrite, known commercially as Hinuera Stone (Hinuera locality is nearby), was first quarried experimentally in 1894 for corners and window surrounds of 'Bishop's Palace' in Ponsonby, Auckland; these are still in good condition. Although the Government Geologist, P. Marshall, suggested in 1923 that Hinuera Stone would be suitable for building purposes (and several houses were built using it in the mid 1930s), it was only in 1954 that the present quarry commenced full commercial operations. This took place because of the development of new techniques in quarrying that reduced costs significantly. The ignimbrite is cut into blocks of various sizes and widely used thoughout the North Island, mostly as a cladding stone for quality houses or decorative stone walls (Hayward 1987). Sometimes the faces of ignimbrite slabs have been heated with oxy-acteylene torches which vitrify the natural glass and result in a sparkling glass surface, occasionally coloured as well, and useful as facing panels in murals. The blocks are extracted using a combination of explosives, giant chain saws, and large air bags to 'lift' blocks from the outcrop face.

STOP 3 — Tapapa Section, Tapapa (T15/635524)

At this site the main focus is on the cover bed stratigraphy, but we will also be able to look at Mamaku Ignimbrite and a classic Andisol. In addition, there are good views from the top of the section of the interfluve surfaces with patches of indigenous forest and, to the N, the low-lying Hauraki Depression, a large continental rift structure (Hochstein & Nixon 1979; Hochstein et al. 1986; de Lange & Lowe 1990).

Andesitic volcanic centres of late Miocene age, the Kiwitahi Volcanics, extend along the western boundary of the Hauraki Rift (Black et al. 1992); Maungatautari volcano, an isolated, bush-covered andesite-dacite composite volcano dated at 1.8 Ma (Briggs 1986), lies to the SW .

The Tapapa Section, on private land owned by B. and J. Goodwin, lies at an elevation of ≈260 m, has an annual rainfall of 1600 mm, and a mean annual temperature of ≈13°C. Native vegetation since c. 15 ka was almost certainly mixed broadleaf-podocarp forest (Newnham et al. 1989). The modern soils (Waiohotu series) are Typic Hapludands (McLeod 1992) (see Table 2.6). The 7 m section exposed here contains a comprehensive stratigraphic record of tephra deposits, tephric loess, and buried paleosols representing alternating periods of deposition and soil formation over the past c. 140 ka on the Mamaku Plateau (Kennedy 1982, 1988, in press). The section is described in Table 2.3 and the stratigraphy summarised in Fig. 2.4.

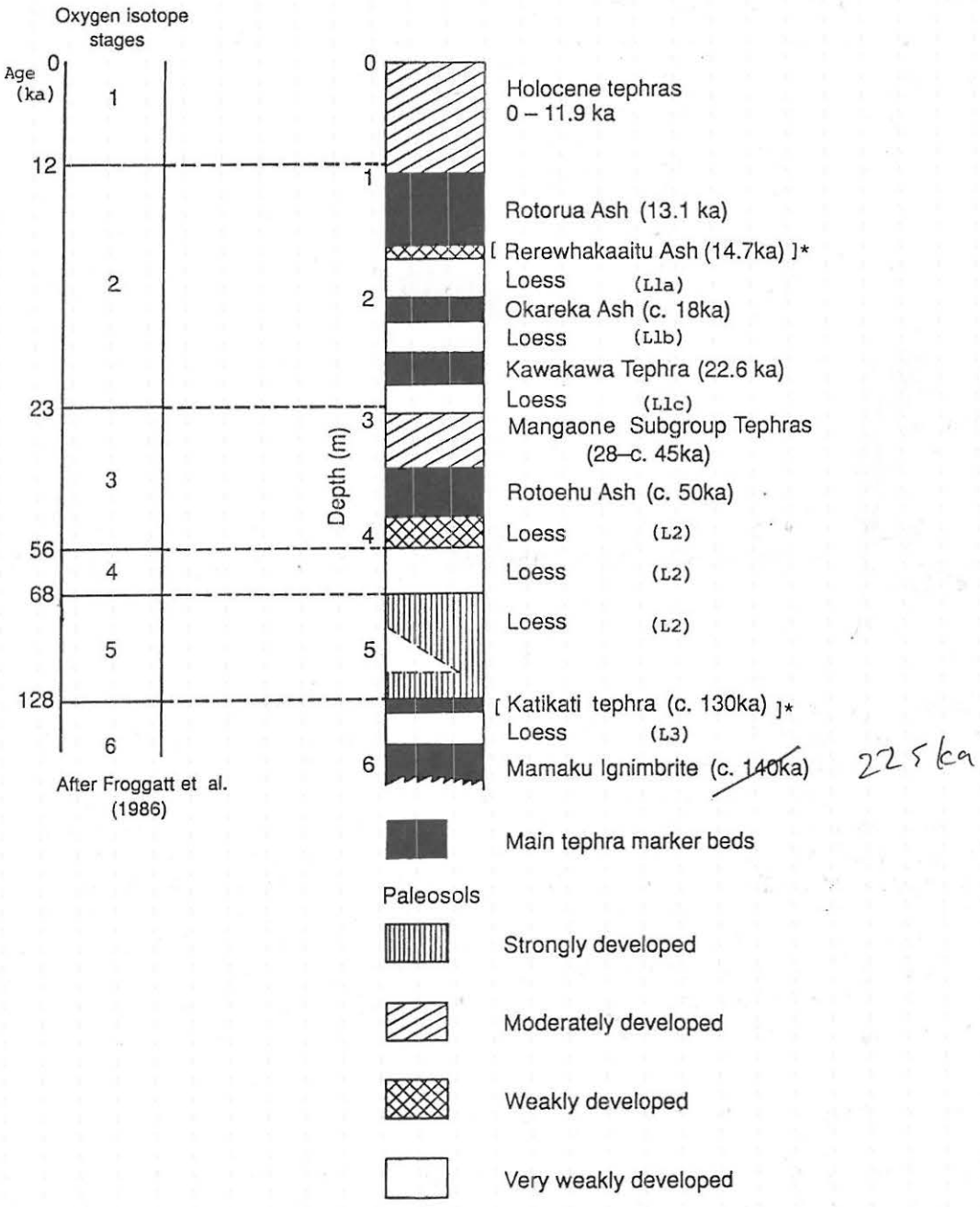

Figure 2.4: Stratigraphy of cover beds on the Mamaku Plateau and correlation with the marine oxygen isotope record (from Kennedy in press). The Tapapa section, on which the diagram is based, provides the best stratigraphic record of the cover bed stratigraphy. * Not present at Tapapa. Loess units from Eden et al. in prep.).

TABLE 2. 3. Description of Tapapa section (from Kimber et al. in press).

Depth (m)	Description	
0.00 - 1.00	Multiple Holocene tephra deposits (not differentiated): dark yellowish brown (10YR 5/6) to yellowish brown silt loam; moderately weak; weakly developed nut and block structure; indistinct boundary,	Waiohotu gritty silt loam
1.00 - 1.15	Rotorua Tephra (c.13.4 ka): brownish yellow (10YR 6/6) coarse sand; moderately weak; massive breaking to single grain structure; indistinct boundary,	Rr
1.15 - 1.45	Loess: yellowish brown (10YR 5/4) silt loam; moderately firm; weakly developed coarse blocky structure; distinct boundary,	Loess 1a*
1.45 - 1.60	Okareka Tephra (c.18 ka): yellowish brown (10YR 5/6) sandy loam; moderately firm; massive structure; distinct boundary,	Ok
1.60 - 2.00	Loess: yellowish brown (10YR 5/4) silt loam; moderately firm; massive structure; distinct boundary,	Loess 1b
2.00 - 2.45	Kawakawa Tephra (c. 22.5 ka): very pale brown (10YR 7/3) and pink banded silt loam, and sandy loam; moderately firm; massive structure; sharp boundary,	Kk
2.45 - 2.65	Loess: light yellowish brown (10YR 6/6) silt loam; moderately firm; massive structure; few Fe/Mn concretions; indistinct boundary,	Loess 1c
2.65 - 3.35	Palaeosol (in tephra): yellowish brown (10YR 5/6) gritty silt loam; moderately firm; weakly developed coarse blocky structure; horizon includes some Mangaone Subgroup tephras (c. 28-45 ka); indistinct boundary,	Pal 2a
3.50 - 3.95	Rotoehu Ash (c. 50 ka): light grey, yellow and very pale brown layered loamy sand to silt loam; moderately firm to very firm; massive structure; indistinct boundary,	Re
3.95 - 4.20	Weak palaeosol (in loess): brown (10YR 5/3) silty clay loam; moderately firm; massive structure; indistinct boundary,	Pal 2b
4.20 - 4.73	Loess: yellowish brown (10YR 5/4) silty clay loam; moderately firm; massive structure; indistinct boundary,	Loess 2
4.73 - 5.63	Strong palaeosol (in loess but includes some andesitic tephra deposits): dark yellowish brown (10YR 4/4) to yellowish brown (10YR 5/6) silty clay loam; very firm; massive breaking to moderately developed coarse blocky structure; indistinct boundary,	Pal 3
5.63 - 5.98	Loess: yellowish brown (10YR 5/4) silty clay loam; moderately firm; massive structure; few small soft black Fe/Mn concretions; indistinct boundary,	Loess 3
5.98 - 6.33	Palaeosol (in loess but includes some andesitic tephra deposits): yellowish brown (10YR 4/4) silty clay loam; moderately firm; massive structure breaking to moderately developed medium nutty structure; few small black Fe/Mn concretions; indistinct boundary,	Pal 4
6.33 - 6.63	Loess: yellowish brown (10YR 5/4) silty clay loam; moderately firm; massive breaking to weakly developed blocky structure; few weakly weathered ignimbrite fragments; indistinct boundary,	Pal?
6.63+ *on*	Pale grey (10YR 7/2) soft Mamaku Ignimbrite (c. ~~140 ka~~).	

* Loess and paleosol units from Eden et al. (in prep)

Note redated to 225 ka after this guide printed

The macroscopic rhyolitic tephra layers, derived from mainly the Okataina and also the Taupo volcanic centres and dated by the radiocarbon method, and the Mamaku Ignimbrite* at the base, provide the main chronology for the section via tephrochronology (Froggatt & Lowe 1990). They range from c. 140 ka* to 1.85 ka in age. Intermixed tephras in addition to those shown in Fig. 2.4, including small additions from andesitic sources, have been identified in parts of the sequence, especially in the periods from c. 130-70 ka and c. 50-20 ka (Lowe 1986; Kennedy in press). The age of the Rotoehu Ash is estimated at c. 50 ka by Froggatt & Lowe (1990); Berryman (1992) determined an age of 52 ± 7 ka based on correlation with marine terrace chronology. Others have suggested ages ranging from c. 45 ka to 64 ka (Buhay et al. 1992; Wilson et al. 1992; Kimber et al. in press). Our current preference is for an age c. 50-60 ka.

The tephric loess layers, dominantly yellowish brown (10YR 5/4-5/6), contrast with the interbedded tephras in that they have finer textures (silt to clay) and no pumice lapilli (Kennedy in press); they also have better sorting (Lowe 1981; Benny et al. 1988). They are evidently derived largely from aeolian reworked rhyolitic tephra materials. Such deposits are widespread on the Mamaku Plateau, having been first recognised by Vucetich & Pullar (1969) (see Fig. 2.6 below). The loess is dominated by subangular volcanic glass but may also contain charcoal and freshwater diatoms, consistent with accumulation during devegetated, drier and windier periods (Barratt 1988a; Kennedy 1988). An exception is the oldest loess-like layer (6.3-6.6 m; Table 2.3), which appears to have formed partly from weathering of the underlying ignimbrite (hence is referred to as a paleosol by Eden et al. in prep.). Textures range from clay in the oldest loesses (pre-140 ka) to clay loams in the younger loesses (c. 140-50 ka, units 2-3) to silt loams and fine sandy loams in the youngest loess (c. 25-15 ka, units 1a-1c). The loess layers have been matched with cold climate intervals in the marine $\partial^{18}O$ record and correlated with quartzo-feldspathic loess sequences in southern North Island (Fig. 2.4; Kennedy 1988, in press). The paleomagnetic properties of the loess were examined by Froggatt (1988), who found peaks in magnetic susceptibility corresponding to paleosols (at $\partial^{18}O$ stages 3, 5a, and 5e). Lower values related to periods of loess deposition, but Froggatt (1988) suggested that some loess (e.g. Loess 3) evidently accumulated during $\partial^{18}O$ stage 5 (the Last Interglacial).

The paleosols, developed on both tephra and loess, reflect periods of non-deposition or slow accretion when soil weathering is active. They are distinguished mainly by their darker colours, more clay, and more strongly developed structures than immediately underlying tephra or loess beds (Kennedy in press). Gradual additions of andesitic tephra appear to have enhanced soil development. The paleosols also show microstructural evidence for greater soil biotic activity under vegetation (Barratt 1988a, b). Organic and weathering processes appear to have reached a maximum in the paleosol (Paleosol 3) corresponding to late $\partial^{18}O$ stage 5 (c. 80-100 ka), where iron-rich pseudomorphs of plant fragments and abundant fine excrements suggest a forest vegetation. This phase was followed by clay mobilisation and redeposition, possibly when conditions became cooler and at least seasonally drier (Barratt 1988a). Weathering and organic activity appear to have been minimal in the loess layer corresponding to the coldest part of $\partial^{18}O$ stage 2 (c. 18-22 ka) when dust accreted rapidly. Micromorphology shows silty concentrations indicating mainly mechanical segregation and turbulence, and some associated gleying, indicating temporary water saturation, both possibly caused by seasonal freezing and thawing. Translocated clay derived from weathered minerals also suggests seasonal wetting and drying (Barratt 1988a).

A core taken adjacent to the section has recently been analysed by Kimber et al. (in press) for amino acid racemisation age determinations. D/L values (the ratio of D-amino acids to L-amino acids) for aspartic acid extracted from organic matter (by HCl and by HF on HCl residues) increased rapidly with depth and age. The HF-treated D/L values probably provide the best means of estimating the mean residence time of organic matter, and calibration against the tephrochronological ages provided a numerical age framework (Fig. 2.5; Kimber et al. in press). The ages determined largely agree with the previous estimates (Table 2.4), and provisionally fill the gaps between the Rotoehu Ash and the Mamaku Ignimbrite.

---

* The Mamaku Ignimbrite is dated at 0.14 ± 0.08 Ma (zircon fission track age) by Murphy & Seward (1981), and this age is used here. However, a new age of 0.22 Ma has recently been reported by Houghton et al. (1994).

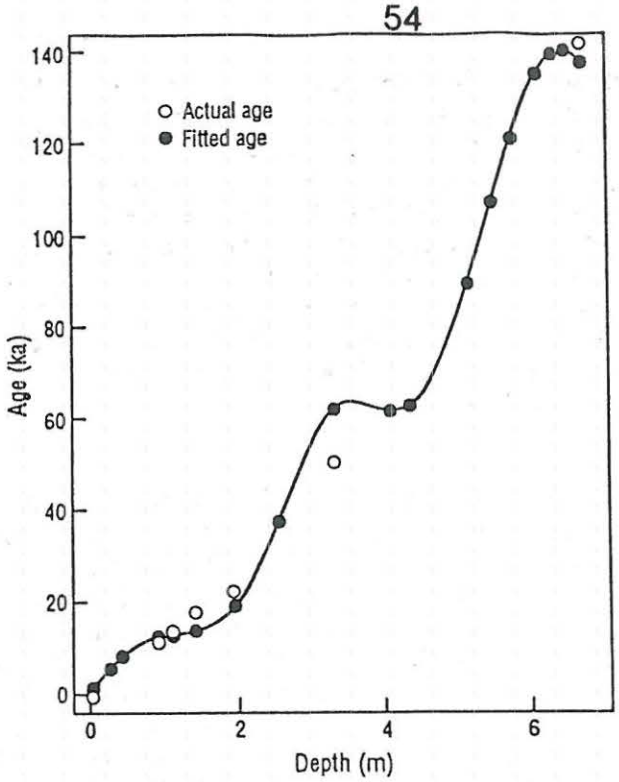

Figure 2.5: Smoothed spline describing the 'best curve' relationship between depth and age based on calibration age and corresponding D/L values at Tapapa (from Kimber et al. in press).

TABLE 2.4. Analysis of racemization data and comparison of age estimates with those from previous work (after Kimber et al. in press).

Sample No.	Deposit/palaeosol	Depth (cm)	I		Age (ka)		Previous age (ka) estimates
			Observed	Smoothed	Observed	Fitted	
0		0	0.1	0.16		1	0
2	Holocene tephra	15 – 31	0.25	0.23		5	
3	Holocene tephra	31 – 58	0.35	0.28		8	
5	Waiohau Tephra	87 – 99	0.35	0.35	11.85	12	11.85
6	Rotorua Tephra	100 – 115	0.36	0.36	13.4	13	13.4
7	Loess 1a	127 – 137	0.41	0.38		14	
9	Okareka Ash	159 – 162	–	–	18		18
12	Loess 1b	185 – 203	0.34	0.46		19	19 – 20
14	Kawakwa Tephra	203 – 248	–	–	22.5		22.5
16	Loess 1c	248 – 261	0.73	0.77		37	22.5 – 24
21	Rotoehu Ash palaeosol 2a	328 – 342	1.42	1.19		61	28 – 45
23	Rotoehu Ash	342 – 397	–	–	50		50
26	Weak Palaeosol 2b	397 – 422	1.15	1.19		61	55 – 60
27	Loess 2	422 – 450	1.07	1.2		62	65 – 75
31	Strong Palaeosol 3	508 – 536	1.59	1.65		88	80 – 110
33	Strong Palaeosol 3	542 – 567	2.07	1.95		105	80 – 110
34	Loess 3	567 – 687	1.99	2.16		117	110
37	Palaeosol 4	610 – 628	2.59	2.43		133	120 – 130
39	Loess	632 – 649	2.34	2.5		137	130 – 137
40	Loess/Pal	649 – 662	3.06	2.52		138	–
41	Ignimbrite	662 – 699	2.09	2.47	140	136	140 Recalculated to 225 ka

The full Tapapa sequence has been analysed by Eden et al. (in prep); Lowe (1986) worked on the post-Rotoehu Ash materials. Eden et al. (in prep) assayed water content, bulk density, particle size distribution, C content, sand, silt, and clay mineralogy, and major and trace elements of whole samples. In summary, the tephra layers are distinguished from one another by stratigraphic position, sand mineralogy, and major and trace element chemistry patterns. The sand mineral assemblages are dominated by glass with lesser amounts of plagioclase and cristobalite, tridymite, quartz, and kaolin subgroup aggregated clays in the felsic fractions (>91% of sand fraction); amphiboles (both calcic hornblende and cummingtonite, the latter characterising the Rotoehu Ash), clinopyroxenes, orthopyroxenes, biotite, and Fe-Ti oxides occur in varying proportions in the mafic fractions (<9% of sand fraction). Paleosols are distinguished from loess layers in being finer textured and having the lowest bulk densities, highest water contents, and highest C contents; major and trace element compositions also differ.

The <2 μm clay fractions, analysed using a combination of XRD, DTA, and acid oxalate extraction (Whitton & Churchman 1987), are dominated by kaolin subgroup minerals, likely to be mostly halloysite, and allophane (Table 2.5). In the modern soil profile, allophane ± imogolite predominate (35-63%) with kaolin minerals (3-40%) and vermiculite (10-15%, derived from biotite in the parent tephras as the vermiculite is trioctahedral; Lowe 1981), also being common. Feldspar, cristobalite, and rare quartz are also present in trace amounts. Below ≈1 m depth, kaolins increase to ≥70% and predominate throughout the rest of the section below ≈1 m, peaking in the Kawakawa and Rotoehu tephra layers (≥95%). Allophane concomitantly diminishes to only a few percent below ≈1 m depth, increasing to around 10% in Paleosol 3, Loess 3, and Paleosol 4 units between ≈4.7 m and 6.5 m (Table 2.5). Small amounts of gibbsite (≤5%) occur in beds below the Rotoehu Ash but attain about 10% in Mamaku Ignimbrite at the base of the section. The predominance of allophane in the modern soil, formed in tephra materials deposited since climatic amelioration about 14 ka, supports the notion of leaching of Si in soil solution from the upper horizons during warm, wet interglacial periods (i.e. $\partial^{18}O$ stage 1). The increase of kaolins with increase in depth suggests an increase of Si from leaching of the overlying beds. The high ratio of rhyolitic to andesitic materials at this site may have enhanced this effect (Lowe 1986). The predominance of kaolins in the section, especially during the known cold and drier periods around the time of deposition of the Kawakawa Tephra (i.e. $\partial^{18}O$ stage 2) and Loess 2 ($\partial^{18}O$ stage 4), supports the model of weak leaching of Si during glacials or stadial periods. In contrast, the increase in allophane in Paleosol 3, Loess 3, and Paleosol 4, corresponds to warmer, wetter conditions (hence promoting Si leaching) associated with the Last Interglacial between c. 90-130 ka ($\partial^{18}O$ stage 5), and matches the micromorphological evidence of Barratt (1988a) described above. Similarly, gibbsite quantities, although always small, are greatest in units of this same period (Paleosol 3, Loess 3) (Lowe & Percival 1993).

TABLE 2.5. Mineralogy (%) of clay fractions of Tapapa materials (after Eden et al. in prep).

Depth (m)	Unit*	Vermic.	Kaolin s'group†	Allophane ± imog.	Feldspar (plag.)	Cristob.	Gibbsite
0-0.15	Ap	15	25	46	7	3	
0.15-0.31	AB	15	15	47	7	3	
0.31-0.55	Bw1	15	2	63	5	2	
0.55-0.80	Bw2	15	12	51	3	1	
0.80-0.84	BC	10	40	35	3	1	
0.95-1.27	Loess 1a		80	7	3	2	<1
1.27-1.59	Rr		70-90	4-5	3	3	<1
1.59-2.03	Loess 1b		85-90	4-5	0-3	1-3	0-<1
2.03-2.48	Kk		94-97	1	0-2	2-3	
2.48-2.61	Loess 1c		90	1	2	4	
2.61-3.42	Pal 2a		85-90	5	0-2	1-4	
3.42-3.97	Re		95	1-3	0-3	0-1	
3.97-4.22	Pal 2b		90	3	3	4	<1
4.22-4.75	Loess 2		85	3-8	2-3	4-5	1-3
4.75-5.67	Pal 3		55-85	6-10	0-2	2	<1-4
5.67-6.10	Loess 3		50-70	8-10	0-2	2-3	1-5
6.10-6.49	Pal 4		55-60	10-12		4	<1-1
6.49-7.05	Mam. Ig		35-50	1-5	6-12	2-4	3-15

* Units and nos. of samples analysed: Loess 1a, 1; Rr, Rotorua Tephra, 2; Loess 1b, 4; Kk, Kawakawa Tephra, 3; Loess 1c, 1; Pal 2a, 5; Re, Rotoehu Ash, 4; Pal 2b, 1; Loess 2, 3; Pal 3, 4; Loess 3, 3; Pal 4, 3 (loess-like); Mam. Ig, Mamaku Ignimbrite, 3.
† Halloysite ± kaolinite

TABLE 2.6. Profile description and chemical data for Waiohotu gritty silt loam in the vicinity of Tapapa (from McLeod 1992).

Classification: Typic Orthic Allophanic Soil (NZSC; Hewitt 1992) (Typic Hapludand)

Profile description:

Ap1 0–12 cm
Black (10YR 2/1) gritty silt loam; non-sticky; non-plastic moderately weak in situ; few fine pores; moderately developed fine nut structure; many fine roots; indistinct wavy boundary.

Ap2 12–22 cm
Dark yellowish brown (10YR 3/4) gritty silt loam; non-sticky; non-plastic; moderately weak; few fine pores; moderately developed fine nut structure; many fine roots; indistinct wavy boundary.

Bw1 22–43 cm
Dark yellowish brown (10YR 4/6) gritty silt loam, non-sticky; non-plastic; moderately weak; abundant pores; weakly developed medium nut structure; few fine roots; diffuse wavy boundary.

Bw2 43–65 cm
Dark yellowish brown (10YR 4/6) gritty silt loam; non-sticky; slightly plastic; moderately weak; abundant pores; weakly developed medium and coarse nut structure; few dark brown (7.5YR 4/4) coatings down old root channels; diffuse boundary.

Bw3 65–90 cm
Yellowish brown (10YR 5/6) gritty silt loam; non-sticky; non-plastic; moderately weak; many pores; massive; few fine roots; indistinct wavy boundary.

2C 90–108 cm
Yellowish brown (10YR 5/8) gritty silt loam; non-sticky; slightly plastic moderately weak (but firmer than above); few coarse pores; few dark brown (7.5YR 3/4) coatings associated with old root channels; no roots; indistinct boundary.

Soil Name: WAIOHOTU GRITTY SILT LOAM — Lab No: SB10119

Horizon	Horizon depth (cm)	Lab letter	Sample depth (cm)	pH H_2O	C (%)	N (%)	C/N	Phosphorus fractions (mg %) 0.5 M H_2SO_4	Inorg.	Organic	Total	P retn (%)
Ap1	0–12	A	0–12	4.5	10.8	0.78	14	21	28	85	113	91
Ap2	12–22	B	12–22	5.4	5.7	0.37	15	14	13	45	58	98
Bw1	22–43	C	22–43	5.6	3.4	0.24	14	17	18	25	43	99
Bw2	43–65	D	43–65	5.8	1.7	0.09	19	13	16	12	28	100
Bw3	65–90	E	65–90	5.9	1.0	0.06	17	10	11	8	19	100
2C1	90–108	F	90–108	5.9	0.88	0.05	18	7	10	7	17	99
2C2	108–120+	G	108–120	5.7	1.5	0.06	25	4	8	11	19	98
Profile sample		Y	0–7.5	4.6	14.4	1.06	14	32	32	104	136	87
Composite cores		Z	0–7.5	4.5	12.3	0.89	14	24	27	90	117	89

Horizon	Horizon depth (cm)	Lab letter	Sample depth (cm)	Cation exchange (NH_4OAc @ pH7 me.%) CEC	Sum bases	%BS	Ca	Mg	K	Na	KCl ext. Al (me.%)	Exchange acidity (me.%)	Reserve Mgr (me.%)	Reserve Kc (me.%)	Phosphate ext. SO_4 (µg/g)
Ap1	0–12	A	0–12	28.2	3.57	13	2.33	0.53	0.42	0.29	1.7	59.2	0.7	0.08	1
Ap2	12–22	B	12–22	15.2	0.68	4	0.31	0.10	0.10	0.17	0.5	40.4			12
Bw1	22–43	C	22–43	9.8	0.37	4	0.16	0.04	0.06	0.11	0.1	36.9	0.6	0.06	151
Bw2	43–65	D	43–65	7.8	0.63	8	0.47	0.10	0.03	0.03	0.1	28.5			461
Bw3	65–90	E	65–90	7.1	1.30	18	0.84	0.35	0.04	0.07	0.1	25.3			568
2C1	90–108	F	90–108	6.1	0.61	10	0.30	0.24	0.03	0.04	0.0	25.4			483
2C2	108–120+	G	108–120	10.2	0.39	4	0.21	0.08	0.05	0.05	0.1	29.9			314
Profile sample		Y	0–7.5	35.2	8.61	24	6.03	1.29	0.72	0.57	1.5	82.9			2
Composite cores		Z	0–7.5	32.1	6.47	20	4.19	1.00	0.84	0.44	1.8	60.2			1

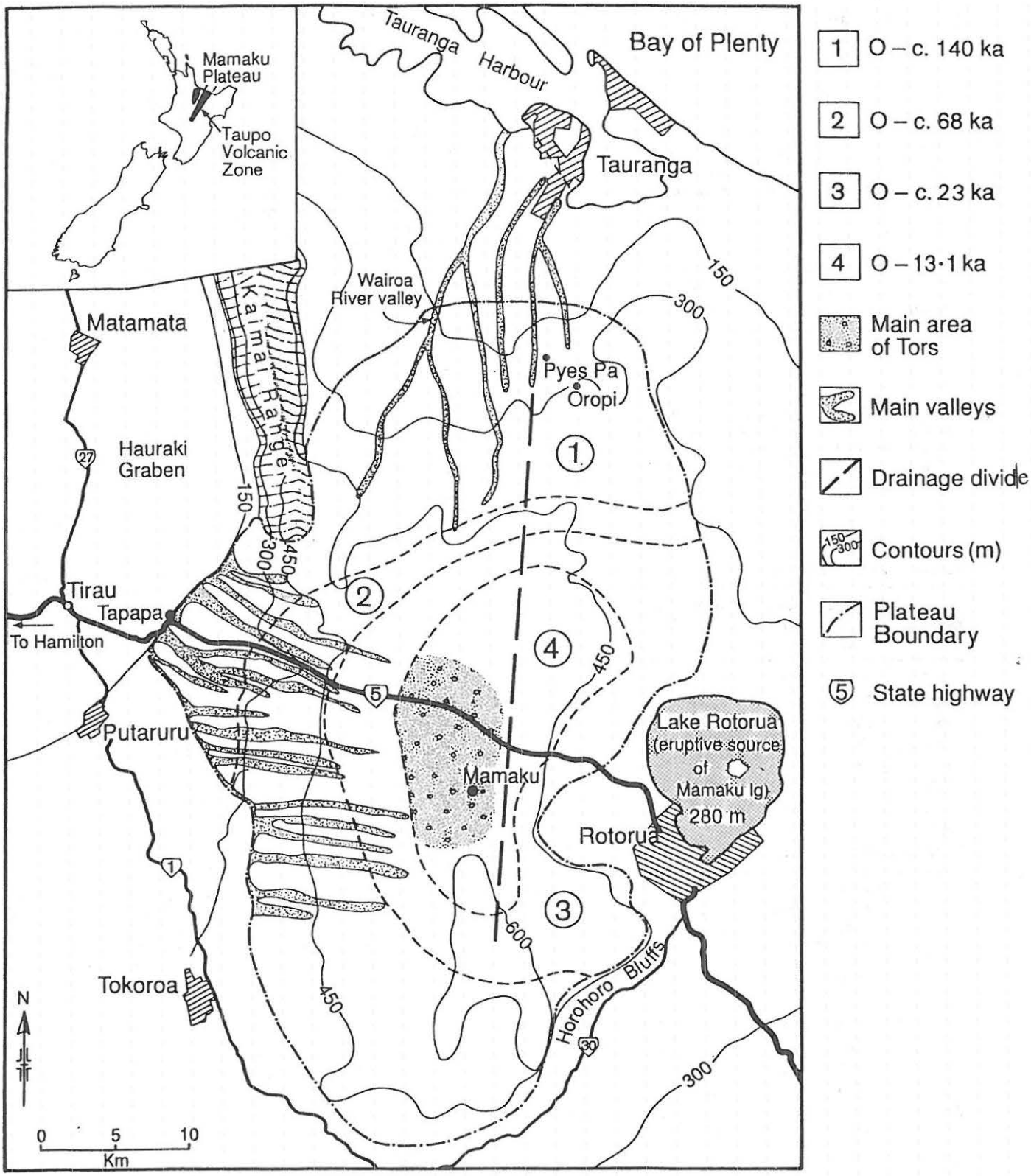

Figure 2.6: Distribution of cover bed sequences and the main geomorphic features on the Mamaku Plateau, c. 140 ka to present. Four main cover bed sequences are identified (nos. 1-4); the maximum age for each sequence is that of the marker bed immediately overlying Mamaku Ignimbrite (areas 1, 2, and 4), or that of oxygen isotope stage 4 (area 3) (from Kennedy ~~et al. in press~~).

GEOMORPHOLOGY OF MAMAKU PLATEAU AND ROTORUA BASIN

Mamaku Plateau

The Mamaku Plateau (Fig. 2.6), ≈1250 km^2 in area, lies between 150 and 650 m elevation to the west of Rotorua, but much is at ≈500 m. It has a shallow domed form, sloping gently to its margins to the west and north, but more abruptly to the east and south east. It is composed largely of densely to partly or non welded, greyish to pinkish, Mamaku Ignimbrite, often with prominent columnar jointing. The ignimbrite covers an area of >3000 km^2 and has a volume >300 km^3 (Wilson et al. 1984). The ignimbrite is up to 180 m thick near the highest part of the Plateau, thinning to <10 m towards the southern and western margins (Kennedy 1988, in press). It often directly overlies Pokai Ignimbrite (B.F. Houghton in Kennedy in press). On the crest of the Plateau (≈500-600 m), the hard ignimbrite is mostly weakly to moderately welded, the softer, less-welded ignimbrite having been eroded away (Kennedy in press). The topography is generally flat to rolling with some deeply dissected valleys and gullies, particulary to the west and north (Fig. 2.6).

The Mamaku Ignimbrite is overlain by a covering of interbedded tephras, loess, and paleosols (as at Stop 3), occasionally with dune sand as well, and these deposits have enabled detailed reconstruction of geomorphic events on the Plateau (Kennedy in press). Major erosion occurred soon after emplacement of the ignimbrite and during two intervals of cold climate: c. 68-56 ka and c. 23-15 ka (oxygen isotope stages 4 and 2, respectively; Fig. 2.4). Cover beds, especially in the southern and central part of the Plateau, were stripped and the underlying ignimbrite exposed. Widespread erosion was triggered at the beginning of these cold intervals by the destruction of the vegetative cover. Stripping of the cover beds was more severe during isotope stage 4 than stage 2, suggesting either a more extreme climate or a more fagile vegetation community during stage 4 than during stage 2, or both (Kennedy in press). The erosion produced deep valleys with cuspoid features on south-facing slopes, the cuspoid features being attributed mainly to the differential effects of cold subpolar air masses which apparently destroyed the vegetation cover on south facing slopes, triggering mass wasting or catastrophic slope failure (Kennedy in press). The main soils on the Plateau are Andic Haplohumods (Mamaku series) under rainfalls of >≈2000 mm per annum (Rijske 1979; Parfitt et al. 1981).

Near the crest of the Plateau, unusual conical hillocks or tor-like features (also referred to as inselbergs; J.D. McCraw pers. comm.) occur above ≈450 m elevation. Up to ≈10 m high, they are formed in Mamaku Ignimbrite. Such features, usually associated with old (peneplain) land surfaces, appear quite bizarre in a youthful, flat-lying volcanic landscape, and are unknown in any other ignimbrite landscapes (Kennedy in press). The tops of the tors are generally concordant. They probably represent scattered remnants of jointed ignimbrite, apparently hardened (silicified) in zones by degassing during cooling (Healy 1992). Gas pipes occur in the upper 1.5 m of soft unwelded ignimbrite forming hardened zones (Kennedy in press). The present height of the tors indicates that the Plateau crest has been reduced in elevation by at least 10 m over an area of ≈100 km^2, amounting to a volume of rock weathered and dispersed estimated at ≈1 km^3. The tors are mantled by a distinctive yellowish-orange lapilli — the Rotorua Tepha, aged c. 13 ka — and younger tephras. The surface of the underlying rock is practically unweathered, forming a smooth hard rock (in places the upper 15 cm is laminated as if shattered by frost, and a thin layer of sand sometimes occurs at the interface; J.D. McCraw pers. comm.). Freeze-thaw, wind, and fluvial processes were likely to have occurred across the ignimbrite plateau surfaces during stage 2 and possibly stage 4, although tors are absent from the latter surface (Fig. 2.6). Tor formation thus occurred during stage 2, ceasing by c. 13 ka, but may have commenced during stage 4 (Kennedy in press).

Rotorua Basin

As we descend into the Rotorua Caldera, we pass the rhyolite domes of Mt Ngongotaha (757 m), around the base of which are remnants of +90 m lake level terraces and associated diatomite that relate to the early history of Lake Rotorua, as discussed below .

Lake Rotorua was evidently formed c. 140 ka following the eruption of the Mamaku Ignimbrite and associated caldera collapse (see Fig. 2.8). The lake has an area of 80 km^2 and a maximum depth of 45 m (Lowe & Green 1992). The highest level, about 90 m above present lake level (280 m), occurred when deposits of the Rotoiti Tephra, erupted from the Okataina volcano c. 50-60 ka, blocked the northward drainage from the lake. This level is marked by extensive terraces around the lake on which part of Rotorua City is built. Tephrochonological studies show that the lake remained high until drastically lowered to near its present level c. 22 ka when the Rotoiti deposits were breached (Fig. 2.7; Kennedy et al. 1978). The lake dropped to below its present level between c. 19 and 9 ka, creating further small terraces in the process. Subsequent changes in depth, including a rise of about +10 m at c. 7 ka after the Mamaku eruption, were caused mainly by growth of the volcanic pile in the adjacent Okataina Volcanic Centre (Nairn 1989). Since then, lake levels have steadily dropped, probably because of downcutting at the Ohau outlet. The higher lake levels between c. 7 and 4 ka may have partly resulted from higher rainfall than at present (McGlone 1983). Mokoia Island in Lake Rotorua is a rhyolite dome.

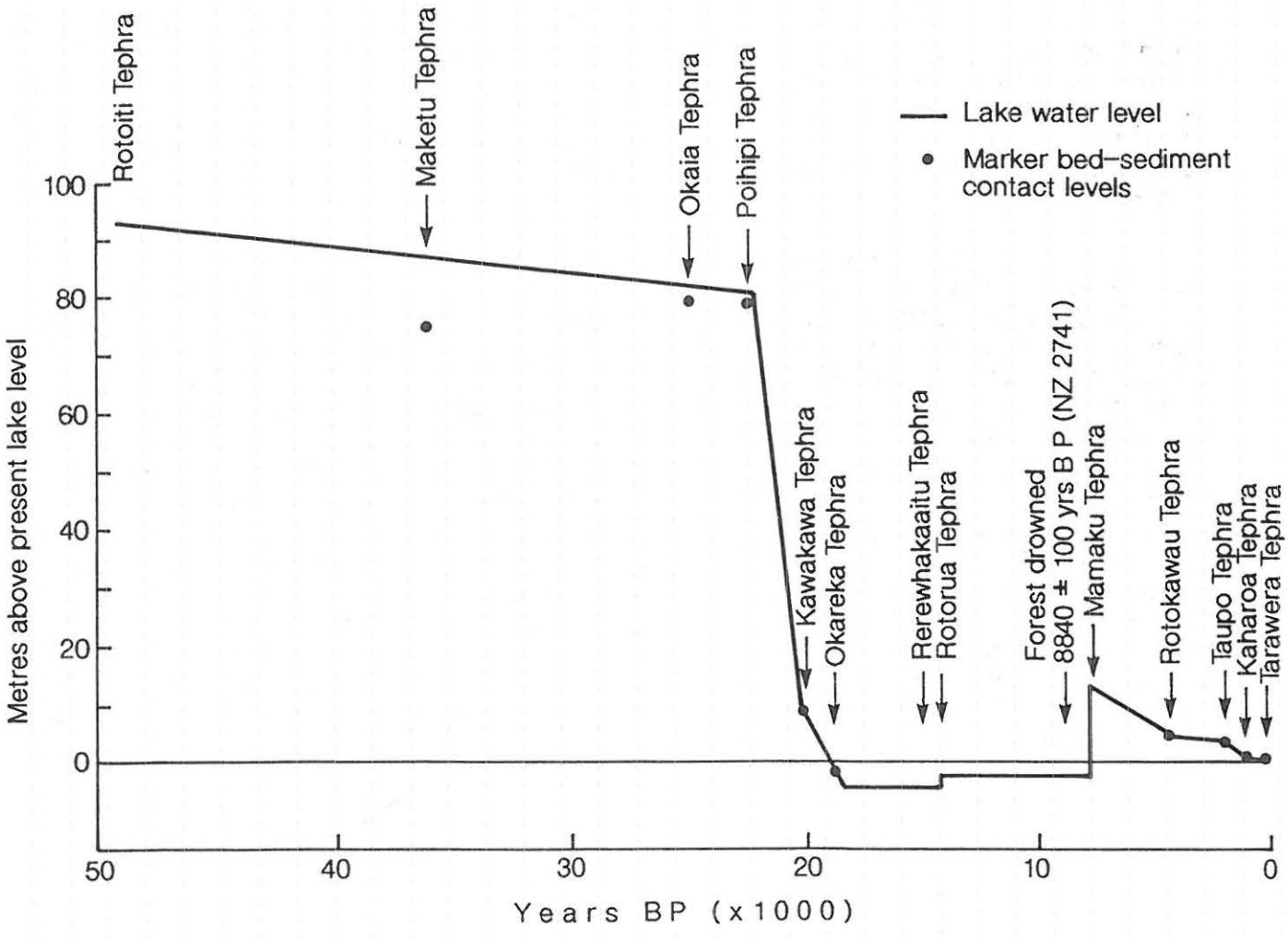

Figure 2.7: Variations in water levels of Lake Rotorua from c. 50-60 ka to the present based on tephrochronology. Present lake level is 280 m a.s.l. From Lowe & Green (1992) based on Kennedy et al. (1978) and Nairn & Wood (1987).

OKATAINA VOLCANIC CENTRE AND LATE QUATERNARY TEPHRAS

The Okataina volcano is the most recently active of the TVZ rhyolitic centres and, with Taupo volcano, one of the two most productive rhyolite volcanoes known (Nairn 1989; Wilson 1993). Lying to the east of Rotorua Caldera (Fig. 2.8), it has been active from c. 380 ka, but since the eruption of the Rotoiti Tephra c. 50 ka, the Haroharo and Tarawera volcanic complexes have grown on the caldera floor, formed by the overlapping of multiple collapse structures associated with a succession of voluminous (>100 km3) pyroclastic eruptions. A clear age distinction exists between the exposed eruptives within the caldera, all <22 ka, and the rocks forming the caldera margins, all >140 ka (Nairn 1989). Nairn (1989) and Nairn & Wood (1987) describe the early deposits in detail.

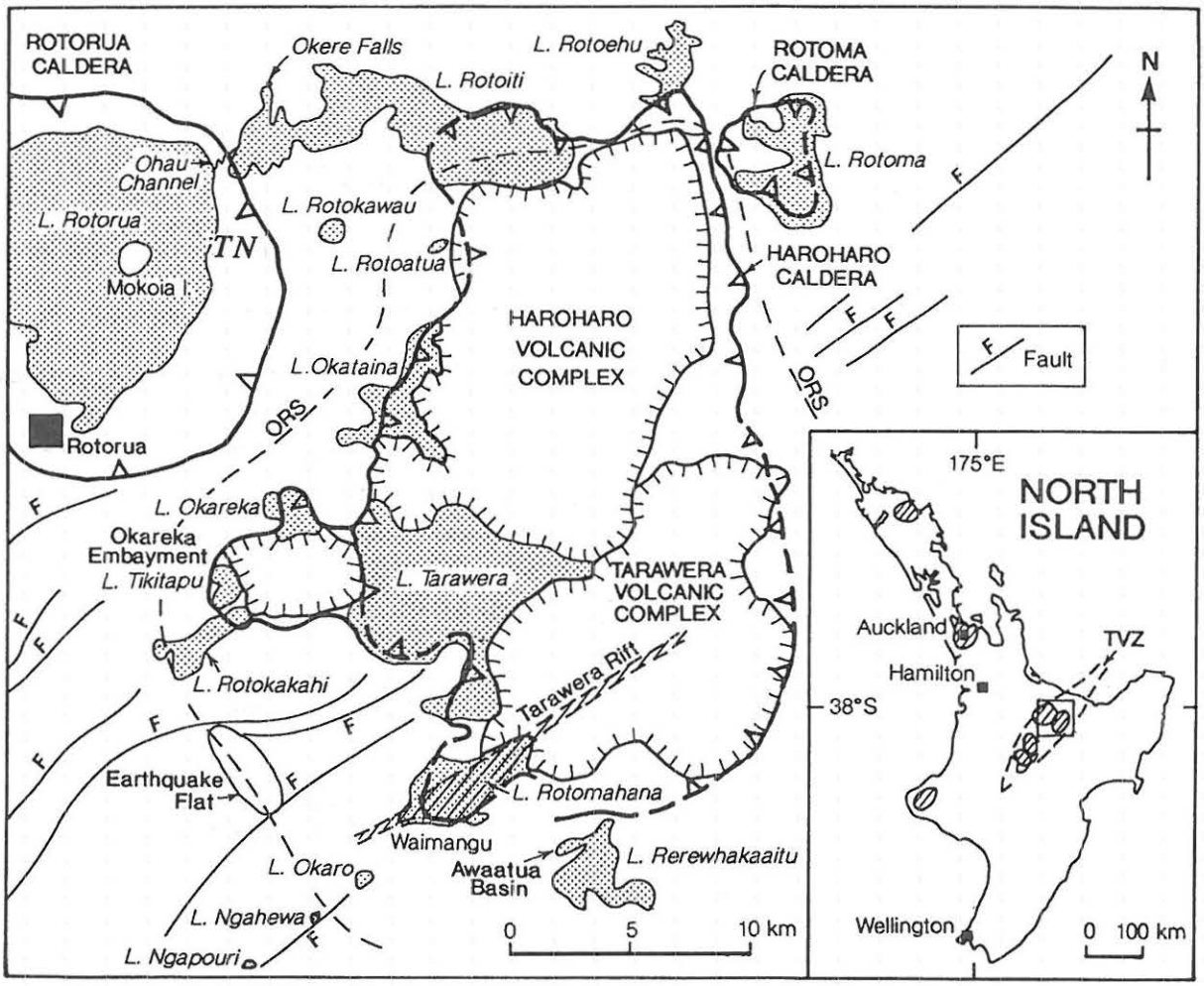

Figure 2.8: Structural and volcanic features of the Rotorua area associated with the Rotorua and Haroharo calderas. The latter lies within the Okataina Volcanic Centre (marked by ORS, the Okataina Ring Structure). After Nairn (1989). TN = Te Ngae site (Stop 5).

There have been 11 eruptive episodes during the past c. 22 ka from vents in the Haroharo and Tarawera complexes, separated by quiescent periods lasting up to a few thousand years (Table 2.7; Nairn 1989, 1992). All were rhyolitic except for several basaltic events, including the most recent (and one of the smallest), the Tarawera-Rotomahana-Waimangu eruption on 10 June 1886 (Walker et al. 1984). The erupted volumes of pyroclastic material are relatively uniform, varying from ≈1 to 15 km^3. A generalised map of the lavas and major pyroclastic deposits of the Haroharo Volcanic Complex is given in Fig. 2.9; the stratigraphy and chronology of these are summarised in Table 2.8.

TABLE 2.7. Sequence of intracaldera eruptions at Okataina (post-22 ka) with estimated volumes. All are rhyolitic apart from the named basalts, although the Okareka and Kaharoa eruptives also contain a basalt component (from Nairn 1989).

Eruptive episode	age (yrs B.P.)	Lava volume (km^3)	Pyroclastics volume (km^3)	Equivalent magma volume (km^3) Haroharo	Tarawera
Tarawera Basalt (1886 A.D.)			2[1]	--	0.7
Kaharoa	c. 800	2.5	5	--	5
Rotokawau Basalt[2]	c. 3500		0.7	0.5	--
Whakatane	c. 5500	9	10	13	--
Mamaku	c. 7500	15	6	17.5	--
Rotoma	c. 9000	2	13	8	--
Waiohau	c. 11000	4	14.5	--	10.5
Rotorua	c. 13500	1	7	4	--
Rerewhakaaitu	c. 15000	2	6	--	5
Okareka	c. 18000?	5	5	--	7
Te Rere	c. 21000	7.5	3	9	--
			Totals	52	28.2
				c. 80	

Notes
1 Walker et al. 1984.
2 Strictly not an intracaldera eruptive.

TABLE 2.8. Stratigraphy and chronology of Haroharo Volcanic Complex lavas and pyroclastics shown on Fig. 2. 9. From Nairn (1989).

Eruptive episode and age (yrs B.P.)	Lavas	Pyroclastics
Whakatane	Tikorangi dome	
c. 5500	Makatiti dome	Minor pyroclastic eruptions
	Haroharo dome	
	Makatiti lava flows	
	Rotokohu dome	
	Okataina lava flow	Rotokohu tuff cone
	Tapahoro dome	Whakatane Ash (plinian)
	Tapahoro lava flows	Whakatane Pyroclastics
	Rotoroniu lava flows	
Mamaku		Te Whekau explosion breccia
c. 7500	Te Horoa dome	Local flow and surge deposits
	Hainini dome	
	Hainini lava flow	
	Te Matae lava flow	
	Parewhaiti dome	
	Ruakokopu lava flow	Hainini Pyroclastics
	?Otangimoana lava flow	
	?Oruaroa lava flow	Mamaku Ash (plinian)
	Waiti lava flow	
	Kaipara lava flow	
Rotoma	Te Pohue lava flows	?Otamuri Pyroclastics
c. 9000		Tuahu Pyroclastics
	Rotoma lava flow[1]	Rotoma Ash (plinian)[1]
Te Rere	Haumingi lava flow	
c. 21000	Te Koutu lava flow	?Tapuaeharuru Pyroclastics
	Tuarae lava flow	?Te Haehaenga Pyroclastics
	?Fenton's Mill lava flow	Te Rere Ash (plinian)

Notes
1 From Rotoma Caldera

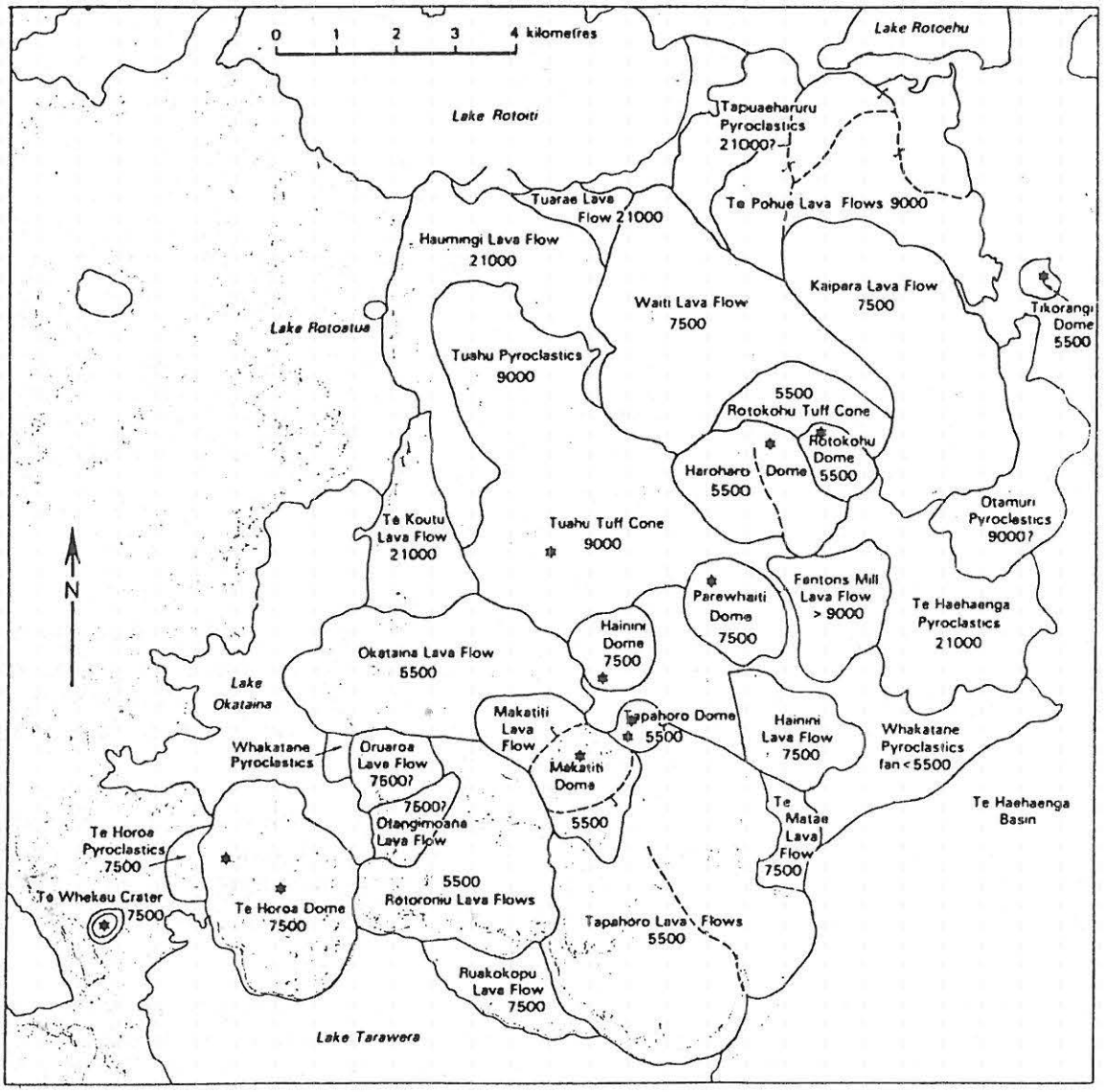

Figure 2.9: Generalised map of Haroharo Volcanic Complex lavas and major pyroclastic deposits. See Table 2.8 for correlation with eruption episodes (from Nairn 1989).

STOP 5 — Te Ngae Section (U15/018418) [Please be especially careful of traffic]

The Te Ngae section occurs alongside Highway 33 near Te Ngae on a sub-vertical terrace cliff face a few hundred metres east of Lake Rotorua. The 6-m high exposure lies at 300 m altitude, and the site has a mean annual rainfall of 1490 mm with a mean annual temperature of 11.9°C. Native vegetation from c. 9 ka to 1 ka was a *Dacrydium cupressinum* (rimu)-dominant podocarp-hardwood forest, with Polynesian fires since c. 1 ka reducing the forest cover to fernland, grass and scrub by 400 years ago (McGlone 1983). The modern soil is formed from multiple tephra layers including Rotomahana Mud, Kaharoa Tephra, Taupo Tephra, and Rotokawau Tephra overlying earlier eruptives (Fig. 2.10). It is mapped as the Rotoiti series (Rijske 1979), an ashy, mesic, Humic Udivitrand.

The section comprises 11 major tephra deposits aged from 1886 A.D. to c. 18 ka, most being derived from either the Haroharo or Tarawera complexes within the Okataina Volcanic Centre (Figs. 2.8, 2.10). 'Dustings' of tephras from other centres are likely to be present but are minor (Birrell & Pullar 1973; Green 1987). The basal tephra exposed is the Okareka Tephra (aged c. 18 ka), which lies interbedded with tephric loess overlying lake sediments. All the tephras have been dated by the radiocarbon method except Okareka, the age of which is well constrained stratigraphically (Froggatt & Lowe 1990; Nairn 1992). The terrace on which the tephras lie relates to higher lake levels, with the highest stand (+ ≈10 m) in recent times occurring c. 7 ka following the Mamaku eruption. This would correspond today to a position at about the foot of the exposure. A brief description of the section is given in Table 2.9. Note that several of the paleosols at the Te Ngae section (e.g. Rotoma, Taupo) are not as well preserved as at other sites in the area.

Analyses of Tephras and Paleosols

The weathering of tephras and associated paleosols at this site, and several other sites in the Rotorua region, have been studied in detail by Green (1987). Part of the study examined the kinetics of glass weathering and implications for the formation of clay minerals, as described in Hodder et al. (1990). Similarly, an associated project for determining volcanic glass content in tephra-derived soils or paleosols using HF dissolution is reported by Lowe & Green (1992a).

The tephra sand and silt fractions are dominated by glass with plagioclase, quartz, and cristobalite making up the remainder of the felsic fractions (≥≈95% of the sand fraction), with ferromagnesian minerals (hypersthene, augite, biotite, calcic hornblende, cummingtonite, apatitie, and zircon) and Fe-Ti oxides (titanomagnetite) dominating the mafic fractions (≤≈5% of the sand fraction). The glass is highly siliceous (74-77% SiO_2 on a hydrous basis; Stokes et al. 1992).

The paleosols, notably the buried Bw horizons, were analysed using a variety of methods, and Green (1987) found that these tend to have lower bulk density, higher organic C%, and generally finer textures and higher clay contents than associated parent tephra materials. Although generally only weakly weathered, the degree of development of the paleosols, as indicated by wt% allophane on a whole sample basis and in the silt fraction, wt% clay, clay:sand ratio, and, to a lesser extent, by bulk density, is significantly correlated with effective time for weathering (i.e. time between successive eruptions). Fig. 2.11 demonstrates the relationship between time for weathering and clay content of buried Bw horizons on tephras in the Rotorua area (Lowe & Percival 1993). The time for weathering is greatest for the paleosol on Waiohau Tephra (c. 3320 years) and least for that on Kaharoa Tephra (c. 670 years) (Hodder et al. 1990). Such a correlation assumes that there is minimal 'contamination' of the paleosols by andesitic components (cf. Stop 10, Post-Conference Tour Day 1).

The secondary mineral assemblages and clay fractions were analysed using oxalate and pyrophosphate extraction techniques together with IR, DTA, and XRD analysis. The allophane and ferihydrite contents on a whole soil basis are given in Table 2.10, allophane and ferrihydrite ranging up to 13.5% and 4.4%, respectively (in the basaltic Rotokawau Tephra paleosol). The whole sample analyses of allophane closely match the sum of analyses on separate fractions (Lowe & Percival 1993). These latter results emphasise the common occurrence of pedogenic aggregated clay in silt- and sand-sized fractions in tephra materials.

TABLE 2.9. Description of the Te Ngae section (after Green 1987).

A_p	0-18 cm	black(7.5YR 2/1)sandy clay, diffuse irregular boundary (Rotomahana Mud)
C	18-20	greyish yellow(2.5Y 6/2)sand, indistinct discontinuous boundary (Rotomahana Mud)
2uA	21-31	black(10YR 2/1)sandy loam, many pumice clasts, distinct irregular boundary (Kaharoa Ash)
2uBw	31-55	brownish black(7.5YR 3/2)loamy sand, abundant pumice, indistinct irregular boundary (Kaharoa Ash)
2uC	55-60	light grey(10YR 8/1)pumice lapilli, distinct discontinuous boundary (Kaharoa Ash)
3uBC	60-70	dark brown(7.5Y 3/4)sandy loam, soft vesicular pumice, diffuse discontinuous boundary (Taupo Pumice)
4uBw	70-80	brown(10YR 4/6)silt loam, few basalt fragments, indistinct irregular boundary (Rotokawau Ash)
4uC	80-100	grey(10YR 5/1)firm basalt, distinct irregular (Rotokawau basalt)
5uBw	100-110	brown(10YR 4/4)sandy loam, distinct irregular boundary (Whakatane Ash)
5uC	110-120	greyish yellow(2.5Y 7/2)coarse sand, indistinct wavy boundary (Whakatane Ash)
6uBw	120-135	yellowish brown(10YR 5/8)sandy loam, diffuse irregular boundary (Mamaku Ash)
6uBC	135-160	bright yellow brown(2.5Y 7/6)loamy sand, diffuse wavy boundary (Mamaku Ash)
6uC	160-183	light yellow(2.5Y 7/4)coarse sand, indistinct irregular boundary (Mamaku Ash)
6uC	183-194	dull yellowish brown(10YR 5/4)fine sand, discontinuous distinct boundary (Mamaku Ash)
6uC	194-220	light grey(2.5Y 7/1)coarse sand, distinct irregular boundary (Mamaku Ash)
6uC	220-230	light yellow(2.5Y 7/4)medium sand, distinct discontinuous boundary (Mamaku Ash)
6uC	230-234	dull yellowish orange(10YR 7/2)very fine sand, distinct discontinuous boundary (Mamaku Ash)
7uBw	234-275	dull yellow(2.5Y 6/4)loamy sand, distinct irregular boundary (Rotoma Ash)
7uBC	275-293	light yellow(2.5Y 7/3)fine loamy sand, distinct regular boundary (Rotoma Ash)
7uC	293-308	light brownish grey(7/2)medium sand, distinct irregular boundary (Rotoma Ash)
7uC	308-310	light yellow(2.5Y 7/3)fine sand, distinct irregular boundary (Rotoma Ash)
8uBw	310-330	dull yellow orange(10YR 6/4)sandy loam, diffuse wavy boundary (Waiohau Ash)
8uBC	330-346	dull yellow orange(10YR 7/3)loamy sand, diffuse wavy boundary (Waiohau Ash)
8uC	346-366	light yellow(2.5Y 7/3)coarse sand, indistinct irregular boundary (Waiohau Ash)
9uBw	366-384	dull yellow orange(10YR 6/3)sandy loam, indistinct wavy boundary (Rotorua Ash)
9uBC	384-395	dull yellow(2.5Y 6/3)fine sand, distinct wavy boundary (Rotorua Ash)
9uC	395-414	light yellow(2.5Y 7/3)showerbedded coarse sand, distinct smooth boundary (Rotorua Ash)
9uC	414-417	light yellow orange(10YR 8/4)fine sand, distinct wavy boundary (Rotorua Ash)
9uC	417-444	light yellow (2.5Y 7/4)showerbedded ash normally grading from fine sand to coarse lapilli, distinct smooth boundary (Rotorua Ash)
10uBw	444-458	dull yellow orange(10YR 6/4)sandy loam, distinct wavy boundary (Rerewhakaaitu Ash)
10uBC	458-468	greyish yellow(2.5Y 7/2)med sand, indistinct diffuse boundary (Rerewhakaaitu Ash)
10uCg	468-476	dull yellow orange(10YR 6/4)fine sand, regular distinct boundary (Rerewhakaaitu Ash)
11uC	476-512	dull yellow orange(10YR 6/3)silt loam, indistinct irregular boundary (tephric loess)
12uBC	512-524	dull yellow orange(10YR 6/4)loamy sand, diffuse wavy boundary (Okareka Ash)
13uC	524-563	dull yellow brown(10YR 5/4)silt loam, diffuse irregular boundary (tephric loess)
14uBw	563-570	dull yellowish brown(10YR 5/4)loamy sand (lake sediments)

Note: Horizon notation 'u' here indicates a buried horizon

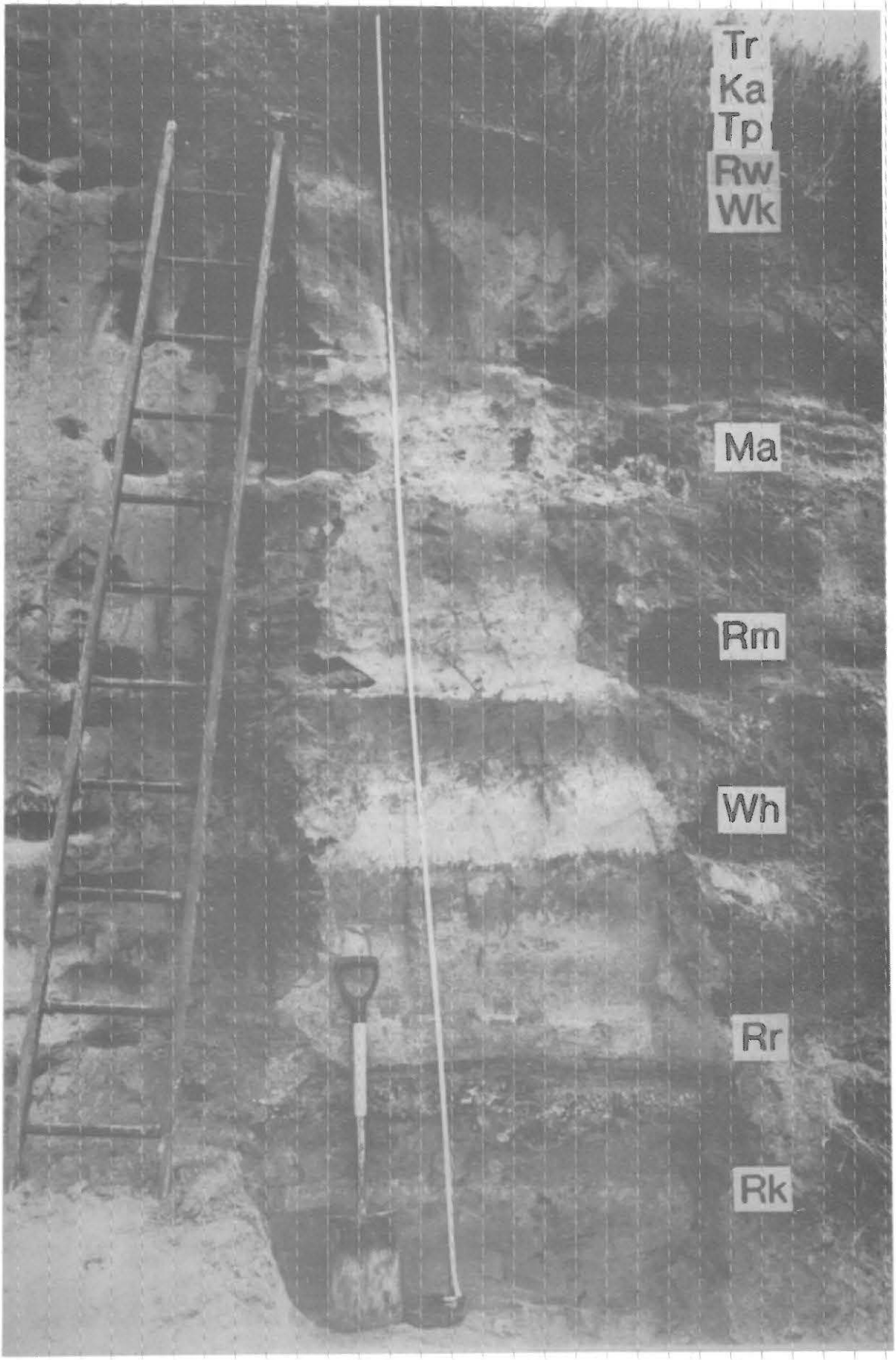

Figure 2.10: Sequence of late Quaternary tephra deposits and paleosols at Te Ngae Road section. Tephra formations and ages (from Froggatt & Lowe 1990) are: Rk, Rerewhakaaitu, 14.7 ka; Rr, Rotorua, 13.1 ka; Wh, Waiohau, 11.9 ka; Rm, Rotoma, 8.5 ka; Ma, Mamaku, 7.3 ka; Wk, Whakatane, 4.8 ka; Rw, Rotokawau, 3.5 ka (basaltic), Tp, Taupo. 1.85 ka; Ka, Kaharoa, 700 yr ago; Tr, Tarawera (Rotomahana Mud), 1886 A.D. Okareka Tephra (c. 18 ka) also occurs in the section in tephric loess below Rk. All the tephras except Tp (from Taupo volcano) are derived from Okataina volcano. Photo: B.E. Green.

TABLE 2.10. Clay content and allophane, ferrihydrite, and halloysite content of whole samples at Te Ngae (after Green 1987).

Tephra#	Hor.	Clay% (<2 μm)	Alloph.* wt%	Ferrih.* wt%	Halloy.† wt%
Tr	Ap	nd	2.0	1.3	
Ka	2A	6.1	2.7	1.3	
	2Bw	6.5	2.6	1.4	
	2Cu	0.9	0.8	neg	
Rw	4Bw	nd	13.5	4.4	
	4Cu	nd	8.9	3.7	
Wk	5Bw	7.1	6.4	1.8	
	5BC	3.8	4.5	1.1	
	5Cu	2.4	2.5	0.2	
Ma	6Bw	8.8	6.7	1.3	
	6BC	4.5	5.5	0.3	
	6Cu1	2.0	1.9	neg	
Rm	7Bw	3.7	3.3	0.2	
	7BC	4.2	5.5	0.2	
Wh	8Bw	13.6	9.2	1.0	4.7
	8BC	7.6	7.4	0.1	nd
	8Cu	3.5	5.3	neg	nd
Rr	9Bw	8.6	6.2	0.2	4.2
	9BC	5.3	5.5	0.1	nd
	9Cu1	2.1	3.7	neg	nd
Rk	10Bw	8.2	1.3	0.7	5.6
	10BC	6.1	1.6	0.5	nd
	10Cg	3.8	1.0	neg	nd
Ok	12BC	nd	1.4	0.1	nd

Abbreviations explained in Fig. 2.10.
* Allophane and ferrihydrite estimated using acid oxalate and pyrophosphate extractions of Al, Si, Fe
† Halloysite estimated using DTA; neg = neglible; nd = not determined

TABLE 2.11. Clay mineral assemblages inferred from IR spectroscopy data for clay fractions in paleosols (Bw horizons) at Te Ngae, Democrat Rd, and Tikitere sections near Rotorua (after Green 1987).

Paleosol	Te Ngae	Democrat Rd Tikitere[T]
Ka	GL ≥Al- & Si-ALL >OM >>H, Q, +	
Tp		Al-ALL >GL > OM >>H, +
Wk	Al-ALL >Si-ALL ≥GL >OM > H, +	[T]Al-ALL >Si-ALL >GL >OM, H, Q, +
Ma	Al-ALL >Si-ALL >GL >OM, FE, H, +	
Rm		Al-ALL >GL > OM >Si-ALL >H, +
Wh	H ≥Si-ALL >GL >>OM, Al-ALL, +	Al-ALL >Si-ALL ≥GL >H >Q, +
Rr	Si-ALL >Al-ALL ≥GL ≥H >>OM, +	H >GL >Si-ALL > OM, +
Rk	H >GL >Si-ALL >OM, Al-ALL, +	

GL, glass; Al- and Si-ALL, Al-rich and Si-rich allophane; H, halloysite; OM, organic matter; FE, iron oxide mineral (e.g. ferrihydrite); Q, quartz; +, other Al and Si phase minerals (e.g. quartz, cristobalite, gibbsite).

The clay fractions may contain a combination of Al-rich and Si-rich allophane, halloysite, volcanic glass, organic matter, oxides and hydroxides of Fe (including ferrihydrite), Al (gibbsite), and Si, and minor crystalline primary (residual) minerals; a summary is given in Table 2.11 (based mainly on IR data and including results of analyses from nearby Tikitere [U15/053436] and Democrat Road [V16/141150] sites). Al-rich allophane predominates in the paleosols on the Te Ngae tephras deposited after Waiohau Tephra in the sequence (i.e. since c. 12 ka). At the same time, halloysite occurs in negligible quantities in these beds, instead occurring in appreciable quantities in paleosols with significant Si-rich allophane structures on the Waiohau, Rotorua, and Rerewhakaaitu tephras. The genesis of these clays essentially accords with the inferred paleoclimatic regime operative during the effective period of weathering at the land surface — climate was windier, drier and colder than present from c. 18 ka to about 12 ka, becoming moister and warmer from c. 12 ka to 8.5 ka or later, then becoming slightly drier and frostier with minor fluctuations in temperature to c. 1850 years ago, and finally attaining present day status (e.g. McGlone 1983, 1988; Newnham et al. 1989; Pillans et al. 1993). Thus conditions for the period from c. 18 ka to about 12 ka were conducive to the formation of halloysite and Si-rich allophane (as in the Rerewhakaaitu paleosol) whereas after about 8.5 ka the conditions favoured stronger leaching and the formation of Al-rich allophane (as in the Rotoma, mamaku, Whakatane, Taupo, and Kaharoa paleosols). However, variations in clay mineral assemblages between the Te Ngae and Democrat Rd sites (Table 2.11) for the Waiohau and Rotorua paleosols suggests that localised microenvironmental variations, such as perching due to textural changes, or some post-burial modification, have affected these (Green 1987).

The micromorphology of the paleosols from Whakatane to Rerewhakaaitu tephras has been studied by Bakker et al. (1994). Sase et al. (1988) studied opal phytoliths in the section.

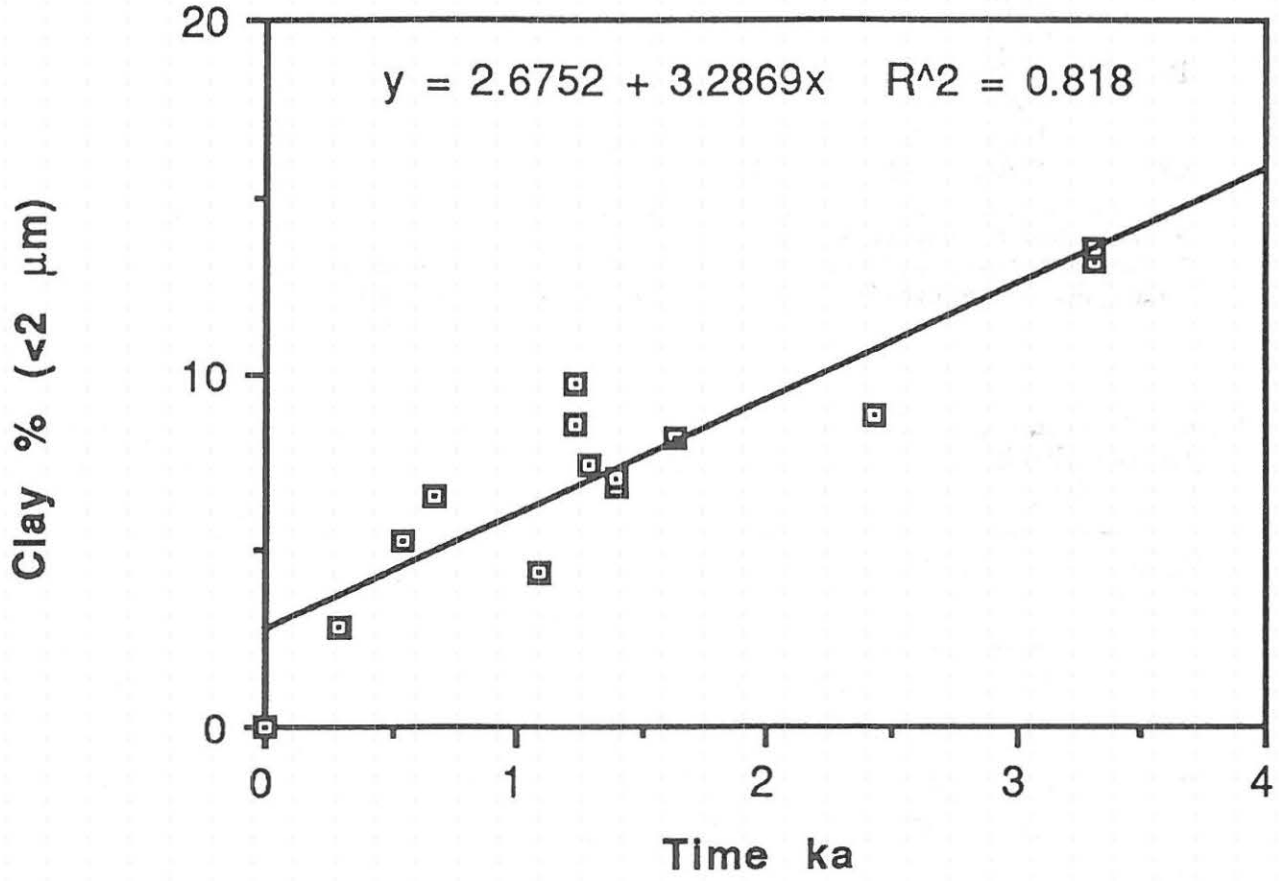

Figure 2.11: Relationship between time for weathering of buried paeosols and clay content (based on data in Green 1987)

The kinetics of clay formation can be described in terms of a combination of parabolic and linear kinetics, reflecting the hydration of glass and the formation of clay minerals, respectively (Hodder et al. 1990). Such a two-stage model is consistent with the formation of clay minerals showing an Arrhenian temperature dependence and suggests, on the basis of calculated activation energies, that the process of formation of Al-rich allophane is diffusion controlled, whereas the rate of formation of Si-rich allophane is controlled by the chemical processes at the site of reaction (Hodder et al. 1990). This model is particularly appropriate for buried paleosols from tephra deposits such as those at Te Ngae where the time for weathering is comparatively short (a few hundred to few thousand years) and contamination is minimal. The rate constant calculated for the weathering of rhyolitic tephras in the Rotorua area is 1.23 ka^{-1}, and the half-life of the glass is c. 18 ka (Green 1987).

STOPS 6,7, & 8 — Holocene Tephra Sections, Haroharo Caldera

Three exposures will be visited along Rototiti Road in the Rotoiti Forest. We have allowed about 40 minutes per stop (including travel in between). After turning off from Gisborne Point, Lake Rotiti (Fig. 2.1), we initially ascend over the toes of the oldest lavas (c. 21 ka) in the Haroharo Caldera (Fig. 2.9, Table 2.8). As the road continues to climb towards the centre of the Haroharo Caldera, the tephras mantling the lavas temd to thicken and coarsen, especially the Rotoma (c. 9 ka), Mamaku (c. 7 ka), and Whakatane (c. 5 ka) eruptives.

STOP 6 — Section A (V15/134046)

This sections shows interbedded fall and (poorly sorted) flow units of the Mamaku Pyroclastics (c. 7 ka) uncomformably overlying strongly eroded Rotoma (= Tuahu; Table 2.8) (c. 9 ka) deposits. The section is located ≈5 km north of the presumed Mamaku vent (Nairn & Wood 1987). Kaharoa deposits (0.7 ka) occur at the top of the section.

STOP 7 — Section B (V15/142044)

This long section shows pyroclastic surge beds, associated co-surge ashes(?), and interbedded fall deposits of the Rotoma-Tuahu (c. 9 ka) eruptive episode from adjacent source vent. Gullies developed in the Rotoma deposits are infilled by Mamaku (c. 7 ka) deposits. Further along the section occasional ballistic blocks, overlying Rotoma surge deposits, mark the base of the Whakatane (c. 5 ka) deposits.

STOP 8 — Section C (V16/173377)

This section is located between the Haroharo Dome (817 m), the source vent for the Whakatane eruptive episode (c. 5 ka), and the 'Ridgetop' domes (651 m). The section exposes essentially planar pyroclastic beds of the Mamaku (c. 7 ka) eruptive episode; these have been eroded and a paleosol has developed on them. Draping the Mamaku deposits are tephra beds of the Whakatane eruptive episode (c. 5 ka). Locally thick Kaharoa (c. 0.7 ka) and Tarawera (AD 1886) basaltic deposits occur at the SE end of the section; both these are derived from Tarawera volcano (1111 m) which is about 12-14 km to the S.

STOP 9 — Overview of Rotorua and Haraoharo calderas, Mt Ngongataha (U16/915381)

Aorangi Peak Restaurant is at 580 m elevation. If the weather is good, we shall have panoramic views of Rotorua City (population ≈55 000), Lake Rotorua, and the rhyolite domes of Mt Tarawera in Haroharo Caldera (Fig. 2.8).

REFERENCES

Bakker, L.; Lowe, D.J.; Jongmans, A.G. 1994: A micromorphological investigation of alteration of tephra material and neoformation of clay minerals in a chronosequence of rhyolitic tephras and buried paleosols, North Island, New Zealand. *Programme and Abstracts*, International Inter-INQUA Field Conference and Workshop on Tephrochronology, Loess, and Paleopedology, Hamilton, New Zealand (in press).

Barratt, B.C. 1988a: Micromorphology and pedogenesis in a Late Pleistocene succession of tephric loesses and paleosols near Tapapa, Mamaku Plateau, North Island, New Zealand (Abstract). *In* Eden, D.N.; Furkert, R.J. (eds) Loess: Its Distribution, Geology and Soils. A.A. Balkema, Rotterdam: 7-8.

Barratt, B.C. 1988b: Micromorphological descriptions of tephric loess and paleosol layers in the Tapapa section, Mamaku Plateau, North Island, New Zealand. *New Zealand Soil Resources report SR16.* 35p.

Benny, L.A.; Kennedy, N.M.; Kirkman, J.H.; Stewart, R.B. 1988: Mineralogical and textural discriminantion of loess derived from a tephra near Rotorua, New Zealand. *Australian journal of soil research 26*: 301-312.

Berryman, K. 1992: A stratigraphic age of Rotoehu Ash and late Pleistocene climate interpretation based on marine terrace chronology, Mahia Peninsula, North Island, New Zealand. *New Zealand journal of geology and geophysics 35*: 1-7.

Birrell, K.S.; Pullar, W.A. 1973: Weathering of paleosols in Holocene and late Pleistocene tephras in central North Island, New Zealand. *New Zealand journal of geology and geophysics 16*: 687-702.

Black, P.M.; Briggs, R.M.; Itaya, T.; Dewes, E.R.; Dunbar, H.M.; Kawasaki, K.; Kuschel, E.; Smith, I.E.M. 1992: K-Ar age data and geochemistry of the Kiwitahi Volcanics, western Hauraki Rift, North Island, New Zealand. *New Zealand journal of geology and geophysics 35*: 403-413.

Briggs, R.M. 1986: Petrology and geochemistry of Maungatautari, a medium-K andesite-dacite volcano. *New Zealand journal of geology and geophysics 29*: 273-289.

Briggs, R.M.; Gifford, M.G.; Moyle, A.R.; Taylor, S.R.; Norman, M.D.; Houghton, B.F.; Wilson, C.J.N. 1993: Geochemical zoning and eruptive mixing in ignimbrites from Mangakino volcano, Taupo Volcanic Zone, New Zealand. *Journal of volcanology and geothermal research 56*: 175-203.

Buhay, W.M.; Clifford, P.M.; Schwarcz, H.P. 1992: ESR dating of the Rotoiti Breccia in the Taupo Volcanic Zone, New Zealand. *Quaternary science reviews 11*: 267-271.

Cas, R.A.F.; Wright, J.V. 1987: Volcanic Successions. Allen & Unwin, London. 528p.

de Lange, P.J.; Lowe, D.J. 1990: History of verical displacement of Kerepehi Fault at Kopouatai bog, Hauraki Lowlands, New Zealand, since c. 10 700 years ago. *New Zealand journal of geology and geophysics 33*: 277-283.

Eden, D.N.; Hunt, J.L.; Whitton, J.S.; Kennedy, N.M.; Lowe, D.J. in prep: Element chemistry, mineralogy, and other properties of a 140 000 year old tephra, loess, and paleosol sequence from Mamaku Plateau, central North Island, New Zealand. Unpublished manuscript.

Froggatt, P.C. 1988: Paleomagnetism of Last Glacial loess from two sections in New Zealand. *In* Eden, D.N.; Furkert, R.J. (eds) Loess: Its Distribution, Geology and Soils. A.A. Balkema, Rotterdam: 59-68.

Froggatt, P.C.; Lowe, D.J. 1990: A review of late Quaternary silicic amd some other tephra formations from New Zealand: their stratigraphy, nomenclature, distribution, volume, and age. *New Zealand journal of geology and geophysics 33*: 89-109.

Froggatt, P.C.; Nelson, C.S.; Carter, L.; Griggs, G.; Black, K.P. 1986: An exceptionally large late Quaternary eruption from New Zealand. *Nature 319*: 578-582.

Green, B.E. 1987: Weathering of buried paleosols on late Quaternary rhyolitic tephras, Rotorua region, New Zealand. Unpublished MSc thesis, University of Waikato, Hamilton.

Green, J.D.; Lowe, D.J. 1985: Stratigraphy and development of c. 17 000 year old Lake Maratoto, North Island, New Zealand, with some inferences about postglacial climatic change. *New Zealand journal of geology and geophysics 28*: 675-699.

Hayward, B.W. 1987: Granite and marble: a guide to building stones in New Zealand. *Geological Society of New Zealand guidebook 8.* 57p.

Healy, J. 1992: Central volcanic region. *In* Soons, J.M.; Selby, M.J. (eds) Landforms of New Zealand 2nd Edition. Longman Paul, Auckland: 256-286.

Hewitt, A.E. 1992: New Zealand Soil Classification. *DSIR Land Resources scientific report 19*. 133p.

Hochstein, M.P.; Nixon, I.M. 1979: geophysical study of the Hauraki Depression, North Island, New Zealand. *New Zealand journal of geology and geophysics 22*: 1-19.

Hochstein, M.P.; Tearney, K.; Rawson, S.; Davidge, S.; Henrys, S.; Backshall, D. 1986: Structure of the Hauraki Rift (New Zealand). *Royal Society of New Zealand bulletin 24*: 333-348.

Hodder, A.P.W.; Green, B.E.; Lowe, D.J. 1990: A two-stage model for the formation of clay minerals from tephra-derived volcanic glass. *Clay minerals 25*: 313-327.

Houghton, B.F.; Wilson, C.J.N.; McWilliams, M.; Lanphere, M.A.; Weaver, S.D.; Briggs, R.M.; Pringle, M.S. 1994: Volcanic and structural evolution of a large silicic volcanic system: central Taupo Volcanic Zone, New Zealand. Submitted to *Geology*.

Hume, T.M.; Sherwood, A.M.; Nelson, C.S. 1975: Alluvial sedimentology of the Upper Pleistocene Hinuera Formation, Hamilton basin, New Zealand. *Journal of the Royal Society of New Zealand 5*: 421-462.

Kennedy, N.M. 1982: Tephric loess in Rotorua-Bay of Plenty region, North Island, New Zealand. *In* Wasson, R.J. (ed) Quaternary Dust Mantles of Australia, New Zealand and China. Australian National University, Canberra: 119-122.

Kennedy, N.M. 1988: Late Quaternary loess associated with the Mamaku Plateau, North Island, New Zealand. *In* Eden, D.N.; Furkert, R.J. (eds) Loess: Its Distribution, Geology and Soils. A.A. Balkema, Rotterdam: 71-80.

Kennedy, N.M. in press: New Zealand tephro-chronology as a tool in geomorphic history of c. 140 ka Mamaku Ignimbrite Plateau and in relating oxygen isotope stages. *Geomorphology 229*

Kennedy, N.M.; Pullar, W.A.; Pain, C.F. 1978: Late Quaternary land surfaces and geomorphic changes in the Rotorua Basin, North Island, New Zealand. *New Zealand journal of science 21*: 249-264.

Kimber, R.W.L.; Kennedy, N.M.; Milnes, A.R. in press: Amino acid racemization dating of a 140,000 year-old tephra-loess-palaeosol sequence on the Mamaku Plateau near Rotorua, New Zealand. *Australian journal of earth sciences*

Lowe, D.J. 1981: Origin and composite nature of late Quaternary air-fall deposits, Hamilton Basin, New Zealand. Unpiblished MSc thesis, University of Waikato, Hamilton.

Lowe, D.J. 1986: Controls on the rates of weathering and clay mineral genesis in airfall tephras: a review and New Zealand case study. *In* Colman, S.M.; Dethier, D.P. (eds) Rates of Chemical Weathering of Rocks and Minerals. Academic Press, Orlando: 265-330.

Lowe, D.J. 1988: Stratigraphy, age, composition, and correlation of late Quaternary tephras interbedded with organic sediments in Waikato lakes, North Island, New Zealand. *New Zealand journal of geology and geophysics 31*: 125-165.

Lowe, D.J.; Green, J.D. 1992: Lakes. *In* Soons, J.M.; Selby, M.J. (eds) Landforms of New Zealand 2nd Edition. Longman Paul, Auckland: 107-143.

Lowe, D.J.; Green, B.E. 1992a: A hydrofluoric acid dissolution method for determining volcanic glass content of tephra-derived soils (Andisols). *Australian journal of soil research 30*: 573-581.

McGlone, M.S. 1983: Holocene pollen diagrams, Lake Rotorua, North Island, New Zealand. *Journal of the Royal Society of New Zealand 13*: 53-65.

McGlone, M.S. 1988: New Zealand. *In* Huntley, B.; Webb, T.III (eds) Vegetational History. Kluwer Academic Publishers: 557-599.

McLeod, M. 1992: Soils of part northern Matamata County, North Island, New Zealand. *DSIR Land Resources scientific report 18*. 96p.

Murphy, R.P.; Seward, D. 1981: Stratigraphy, lithology, paleomagnetism, and fission track ages of some ignimbrite formations in the Matahana Basin, New Zealand. *New Zealand journal of geology and geophysics 24*: 325-331.

Nairn, I.A. 1989: Geological Map of New Zealand 1:50 000. Sheet V16C Mount Tarawera. New Zealand Geological Survey, Department of Scientific and Industrial Research, Wellington.

Nairn, I.A. 1992: The Te Rere and Okareka eruptive episodes — Okataina Volcanic Centre, Taupo Volcanic Zone, New Zealand. *New Zealand journal of geology and geophysics 35*: 93-108.

Nairn, I.A.; Wood, C.P. 1987: Acive volcanoes of Taupo Volcanic Zone. *New Zealand Geological Survey record 22*. 152p.

Newnham, R.M.; Lowe, D.J.; Green, J.D. 1989: Palynology, vegetation and climate of the Waikato lowlands, North Island, New Zealand, since c. 18,000 years ago. *Journal of the Royal Society of New Zealand 19*: 127-150.

Parfitt, R.L.; Pollock, J.A.; Furkert, R.J. (compilers) 1981: Guide book for Tour 1 Pre-conference North Island, New Zealand. *Soils With Variable Charge Conference,* Palmerston North, New Zealand. 153p.

Pillans, B.J.; McGlone, M.S.; Palmer, A.S.; Mildenhall, D.; Alloway, B.V.; Berger, G.W. 1993: The Last Glacial Maximum in central and southern North Island, New Zealand: a paleoenvironmental reconstruction using the Kawakawa Tephra Formation as a chronostratigraphic marker. *Palaeogeography, palaeoclimatology, palaeoecology 101*: 283-304.

Rijkse, W.C. 1979: Soils of Rotorua Lakes district, North Island, New Zealand. *New Zealand Soil survey report 43.* 124p.

Sase, T.; Hosono, M.; Utsugawa, T.; Aoki, K. 1988: Opal phytolith analysis of present and buried volcanic ash soils at Te Ngae Road tephra section, Rotorua Basin, North Island, New Zealand. *Quaternary research (Japan) 27*: 153-163.

Selby, M.J.; Lowe, D.J. 1992: The middle Waikato Basin and hills. *In* Soons, J.M.; Selby, M.J. (eds) Landforms of New Zealand 2nd Edition. Longman Paul, Auckland: 233-255.

Stokes, S.; Lowe, D.J.; Froggatt, P.C. 1992: Discriminant function analysis and correlation of late Quaternary rhyolitic tephra deposits from Taupo and Okataina volcanoes, New Zealand, using glass shard major element composition. *Quaternary international 13/14*: 103-117.

Vucetich, C.G.; Pullar, W.A. 1969: Stratigraphy and chronology of late Pleistocene volcanic ash beds in central North Island, New Zealand. *New Zealand journal of geology and geophysics 12*: 784-837.

Walker, G.P.L. 1983: Ignimbrite types and ignimbrite problems. *Journal of volcanology and geothermal research 17*: 65-88.

Walker, G.P.L.; Self, S.; Wilson, L. 1984: Tarawera 1886, New Zealand — a basaltic plinian fissure eruption. *Journal of volcanology and geothermal research 21*: 61-78.

Whitton, J.S.; Churchman, G.J. 1987: Standard methods for mineral analysis of soil survey samples for characterisation and classification in New Zealand Soil Bureau. *New Zealand Soil Bureau scientific report 79.*

Wilson, C.J.N. 1986. Reconnaissance stratigraphy and volcanology of ignimbrites from Mangakino Volcano. *Royal Society of New Zealand bulletin 23*: 179-193.

Wilson, C.J.N. 1993: Stratigraphy, chronology, styles and dynamics of late Quaternary erptions from Taupo volcano, New Zealand. *Philosophical transactions of the Royal Society, London A343*: 205-306.

Wilson, C.J.N.; Rogan, A.M.; Smith, I.E.M.; Northey, D.J.; Nairn, I.A.; Houghton, B.F. 1984: Caldera volcanoes of the Taupo Volcanic Zone, New Zealand. *Journal of geophysical research 89(B10)*: 8463-8484.

Wilson, C.J.N.; Houghton, B.F.; Lanphere, M.A.; Weaver, S.D. 1992: A new radiometric age estimate for the Rotoehu Ash from Mayor Island volcano, New Zealand. *New Zealand journal of geology and geophysics 35*: 371-374.

DAY 1: HAMILTON—TOKAANU

C. J. N. Wilson
Institute of Geological and Nuclear Sciences
Wairakei Research Centre, Private Bag 2000
Taupo, New Zealand

Wilson, C.J.N. 1994. Post-conference Tour Day 1: Hamilton-Tokaanu. In: Lowe, D.J. (ed) Conference Tour Guides, Proceedings International Inter-INQUA Field Conference and Workshop on Tephrochronology, Loess, and Paleopedology, University of Waikato, Hamilton, New Zealand, 74-100.

Outline of Day 1 (Sunday 13 February)

8.00-10.00 am	Depart Bryant Hall at the University of Waikato and travel to Wairakei (Fig. 1.1)
10.00-10.30 am	STOP 1— upper lookout for Huka Falls
10.30-10.40 am	Travel along old Highway 1 (Huka Falls Road) to lookout
10.40-10.50 am	STOP 2 — Lookout over Taupo volcano
10.50-11.10 am	Travel to Stop 3 on Highways 1 and 5
11.10-11.40 am	STOP 3 — Sequence of fall deposits from the 1.85 ^{14}C ka Taupo (Y) eruption and underlying post-3.3 ^{14}C ka tephra deposits
11.40-11.50 am	Return towards Taupo on Highway 5, to Stop 4
11.50-12.25 pm	STOP 4 — Sequence of post-10 ^{14}C ka tephras at the De Bretts section
12.25-12.45 pm	Return to Taupo then south on Highway 1, enter East Taupo Forest and head SE on Rotopuha Road
12.45-1.10 pm	STOP 5 — LUNCH at overlook above Hinemaiaia River valley
1.10-1.40 pm	Travel to and view STOP 6 — 1.85 ^{14}C ka Taupo ignimbrite veneer and valley pond on Hingapo Extension Road
1.40-2.15 pm	Travel to and view STOP 7 — 22.5 ^{14}C ka Oruanui ignimbrite and post-10 ^{14}C ka tephras on Hingapo Extension Road
2.15-2.45 pm	Travel to and view STOP 8 — Taupo ignimbrite veneer deposit and lee side lenses on Tiraki Road
2.45-3.20 pm	Travel to and view STOP 9 — structures below the Taupo ignimbrite on Kanuka Road
3.20-3.50 pm	Travel to and view STOP 10 — upper parts of Oruanui ignimbrite, post-10 ^{14}C ka tephras and Taupo ignimbrite on Mission Bay Road
3.50-4.40 pm	Travel to and view STOP 11 — multiple eruptive units previously mapped as the Hinemaiaia and Motutere Tephra Formations
4.40-5.10 pm	Travel to and view STOP 12 — floated giant pumice related to youngest eruption (Z) at Taupo, on Highway 1 at Motutere Bay
5.10-5.30 pm	Travel to Tokaanu Hotel, Tokaanu Evening: Dinner; Hot pool

TAUPO VOLCANO AND ITS PRODUCTS

Today's programme is designed as an introduction to and overview of the products of the rhyolitic Taupo caldera volcano. Recently published and continuing studies are showing how what seemed to be a simple, well studied and understood sequence of young tephra deposits has turned out to be far more complex (and rewarding) than previously supposed.

Taupo volcano is part of the Taupo Volcanic Zone (TVZ), the locus of most of the Quaternary volcanism in New Zealand and related to subduction of the Pacific plate under the North Island. The central segment of the TVZ is one of the most frequently active and productive areas of Quaternary rhyolitic volcanism on Earth, being of a similar size but higher productivity than the better-known Yellowstone system (Houghton et al. 1994). Rhyolitic activity commenced at c. 1.6 Ma, and at least 30 caldera-forming eruptions have occurred, which are presently sourced to 8 calderas, some simple (e.g. Rotorua) and others compound (e.g. Mangakino; Fig. 1.2). Taupo and Okataina volcanoes are the two currently active rhyolite caldera centres; Okataina last erupted in AD 1886 and Taupo about 1850 radiocarbon (c. 1740 calibrated) years ago.

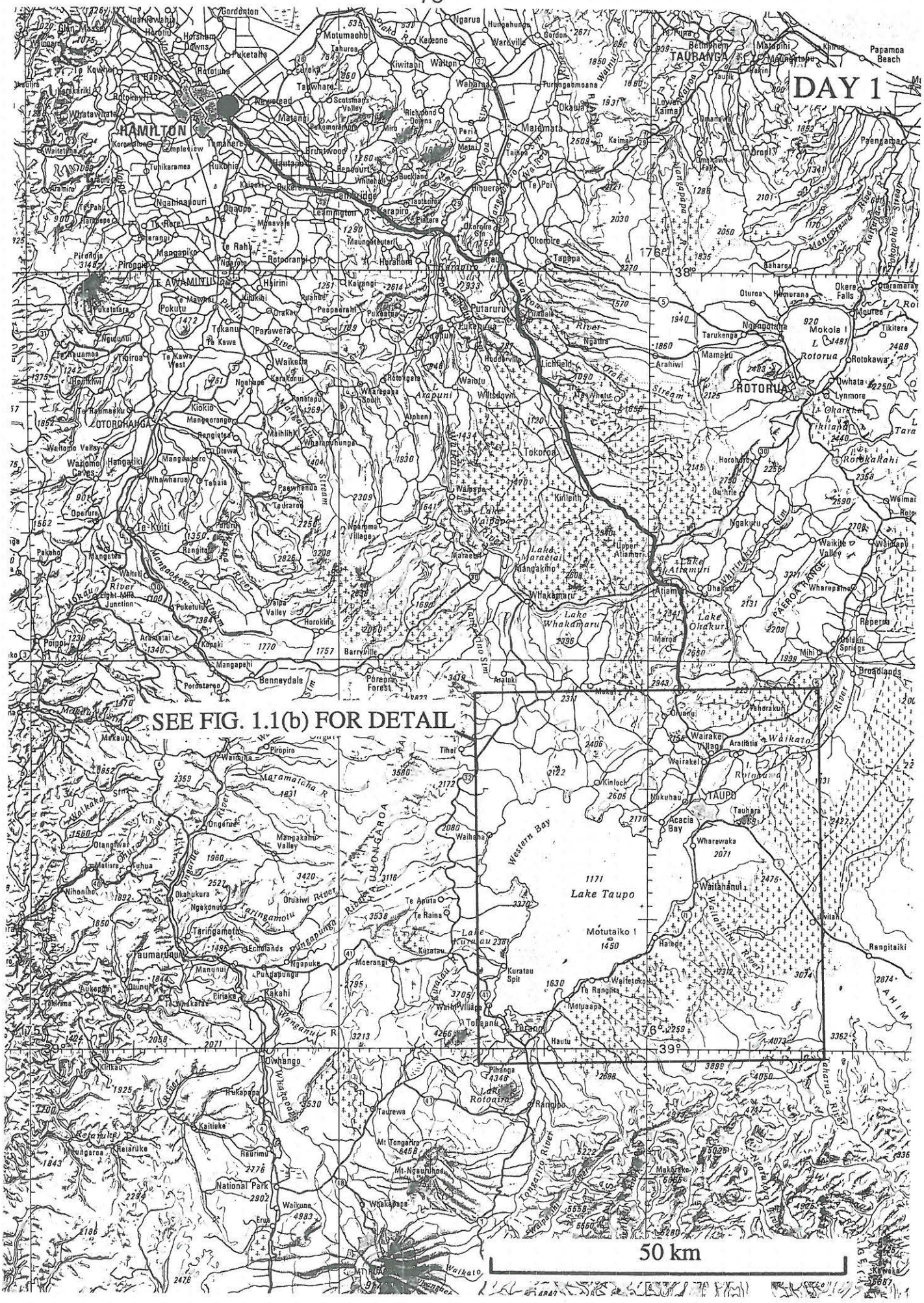

Figure 1.1(a): Map of the route from Hamilton to the Taupo area, Day 1.

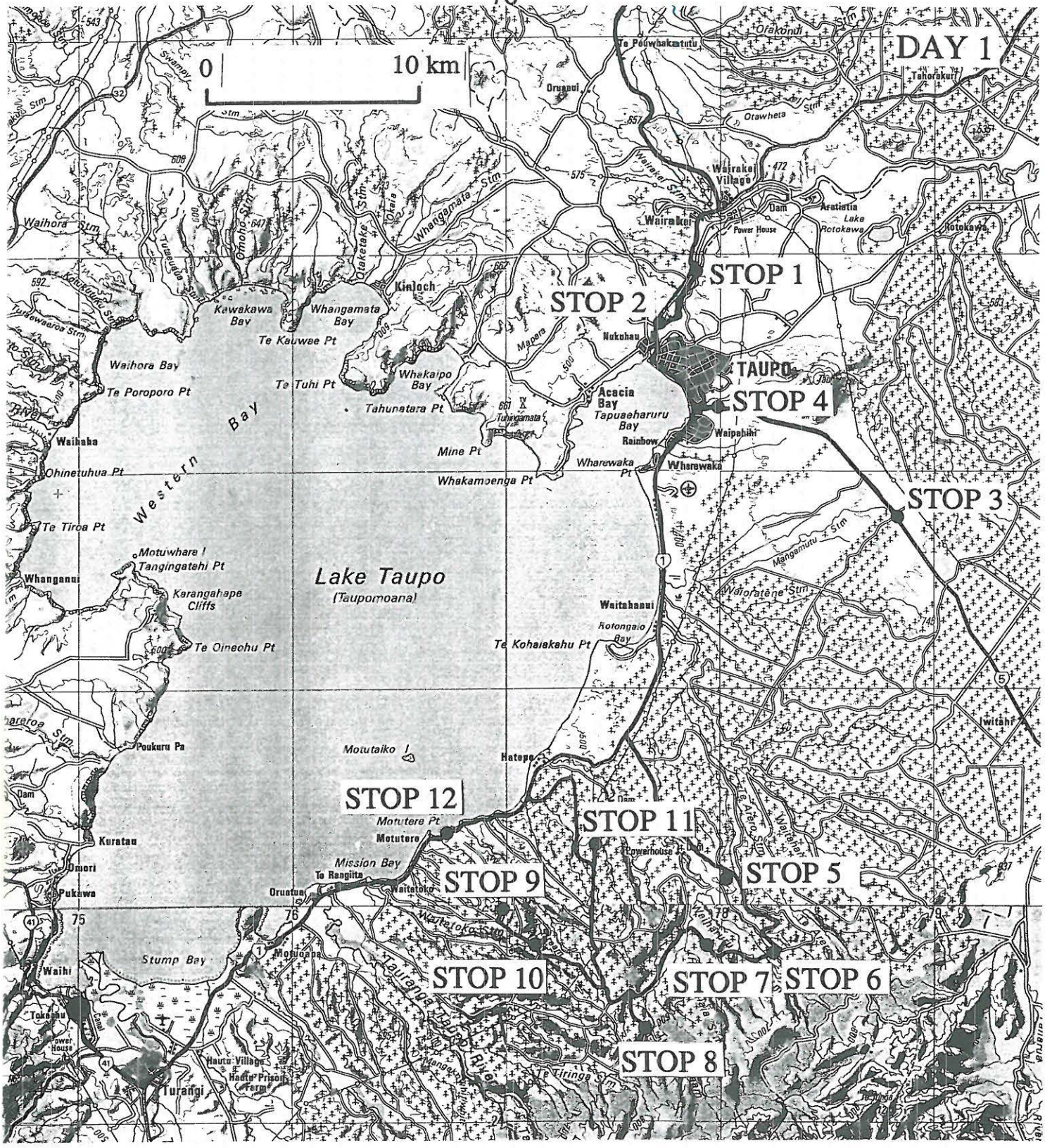

Figure 1.1(b): Tour route and stops around the Taupo area.

Taupo volcano is the single most frequently active and productive rhyolite volcano on Earth. Its activity, together with that of Maroa, its immediate neighbour to the north, commenced after the eruption of the widespread and voluminous Whakamaru group ignimbrites and associated fall deposit(s) dated at 320-350 ka (Wilson et al. 1986; Pringle et al. 1992). Most of the eruptive history of Taupo has yet to be pinned down, but it included production of two modest volume welded ignimbrites, and formation of lava domes and associated pyroclastics SW, SE, and particularly N of the modern lake. The history of Taupo eruptions becomes clearer from about 65 ka onwards as larger, regionally extensive pyroclastic units began to be produced instead of more-locally dispersed deposits accompanying lava extrusions. Several of these have been described (Vucetich & Howorth 1976). At localities between Taupo and Maroa, the tephra stratigraphy implies that as Taupo began to change from mixed lava- and pyroclastic-forming eruptions prior to c. 65 ka to its 'modern', overwhelmingly pyroclastic activity, Maroa volcano underwent a decline in activity, until only one eruption is known in the last 25 ka, that of Puketarata at 14 ^{14}C ka (Brooker et al. 1993). This suggests that there may be some kind of linkage between the two systems, but petrological studies imply this does not involve a shared magma chamber.

From c. 65 ka onwards, Taupo began to stoke up its activity in earnest, culminating at 22.5 ^{14}C ka in a major caldera-forming eruption that shaped much of the volcano as we see it today (Fig. 1.3). The products of this eruption have been mapped under numerous formal and informal names (e.g. see Self & Healy 1987 for a review, and Froggatt & Lowe 1990); I use the term 'Oruanui' to refer to this event, on the basis that this was the first name applied to these deposits that correctly recognised their essential nature, *viz.* a large fall deposit and accompanying large ignimbrite which were erupted from Taupo volcano. The conventional ^{14}C age is well established at 22,590 ± 230 yr B.P. from charcoal in the ignimbrite (Wilson et al. 1988), and this is equivalent to about 26.5 ka (calibrated) from a third-order polynomial curve fitted to the radiocarbon versus U/Th age data presented by Bard et al. (1990), or 24-25 ka (calibrated) from geomagnetic field estimates of ^{14}C production (Mazaud et al. 1991). The Oruanui eruption was phreatomagmatic, and generated a fall deposit of the order 500 km^3, together with a 300 km^3 non-welded ignimbrite (Fig. 1.4; Self 1983; Wilson 1991). The fall deposit is one of the most widespread tephras in the New Zealand region and is widely utilised as a time-plane marker in numerous palaeoenvironmental studies (e.g. Eden et al. 1992; Pillans et al. 1993). Caldera collapse associated with this eruption generated much of the modern outline of the basin now partly filled by Lake Taupo.

After the Oruanui event, previous studies had inferred there was a prolonged hiatus, represented by a substantial erosion surface, until the current sequence of eruptions began at 10.1 ^{14}C ka, and a sequence of 9 tephra formations has been described (Vucetich & Pullar 1973; Froggatt 1981; Froggatt & Lowe 1990). In New Zealand tephrochronological studies, the term 'tephra formation' is used in the sense of '[containing] all the primary pyroclastic products of one eruptive episode, each separated by significant time intervals that are often marked by paleosols' (Froggatt & Lowe 1990, p.91). In practise, previous workers had defined tephra formations as the material from the top of one paleosol to the top of the next paleosol (e.g. Vucetich & Pullar 1973). However, this approach has proved problematic when applied to volcanological studies at Taupo. The simple picture of 9 tephra formations has now been extensively modified by Wilson (1993) who recognised the products of 28 eruptions in the post-Oruanui time period. In order to distinguish between what are now recognised as the deposits of individual eruptions and the old tephra formations, each eruption is designated by a letter; Ψ (the oldest), Ω, A, ..., Z. For volcanological purposes this labelling scheme minimises the number of polysyllabic tephra formation names to be mastered, and allows maximum flexibility in terminology as numerical or alphabetical suffixes can be used to label successively finer details of individual eruptive units (Wilson 1993).

A summary of the ages and volumes of the post-Oruanui tephras or eruptions is given in Table 1.1. Isopach and isopleth data have been used where available to infer vent positions (Fig. 1.5); most of these are in a linear zone which runs NNE-SSW parallel to the overall trend of the TVZ. The wide ranges in repose periods and eruption sizes at Taupo present new challenges in trying to understand the dynamics of the volcano and hence its potential for future activity. When plotted separately, both the repose periods and eruptive volumes apparently show self-similar properties (Wilson 1993: Figs. 51-52). However, when the eruption volumes are plotted against the repose periods (Fig. 1.6), either before or after the relevant eruption, there is what I interpret as a chaotic pattern.

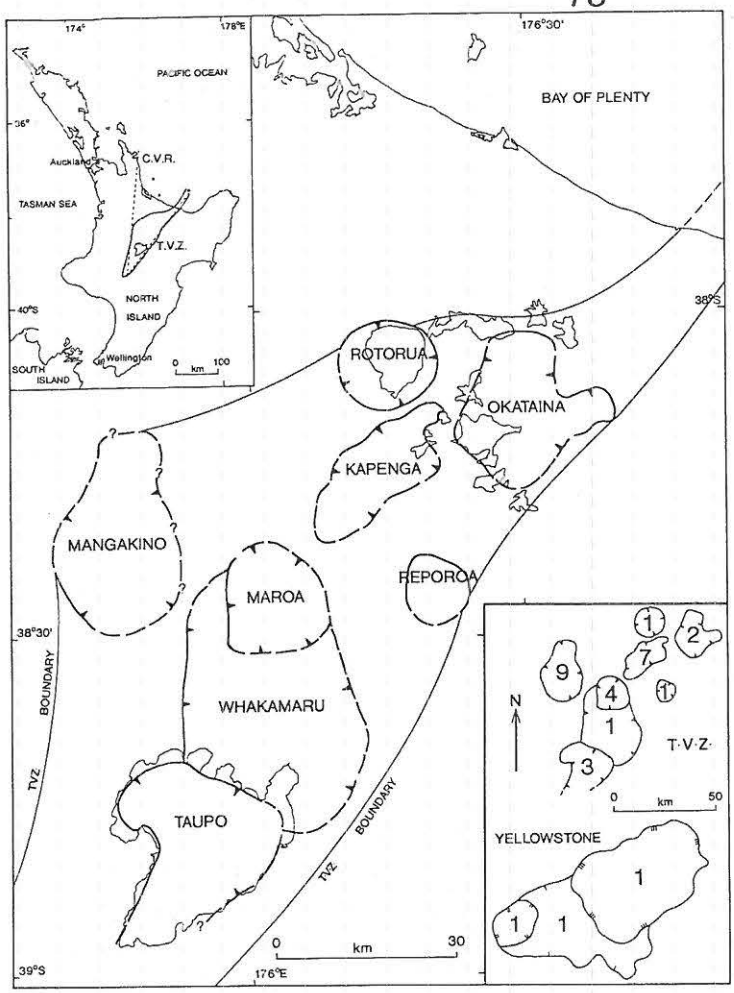

Figure 1.2: Map of the central TVZ to show the caldera volcanoes so far identified as active during the last 1.6 Ma (from Houghton et al. 1994). The insets show (top left) the position of the TVZ in the North Island of New Zealand, and (bottom right) a comparison of the caldera areas and number of identified caldera-forming events between the central TVZ and another major Quaternary rhyolitic system, Yellowstone, USA.

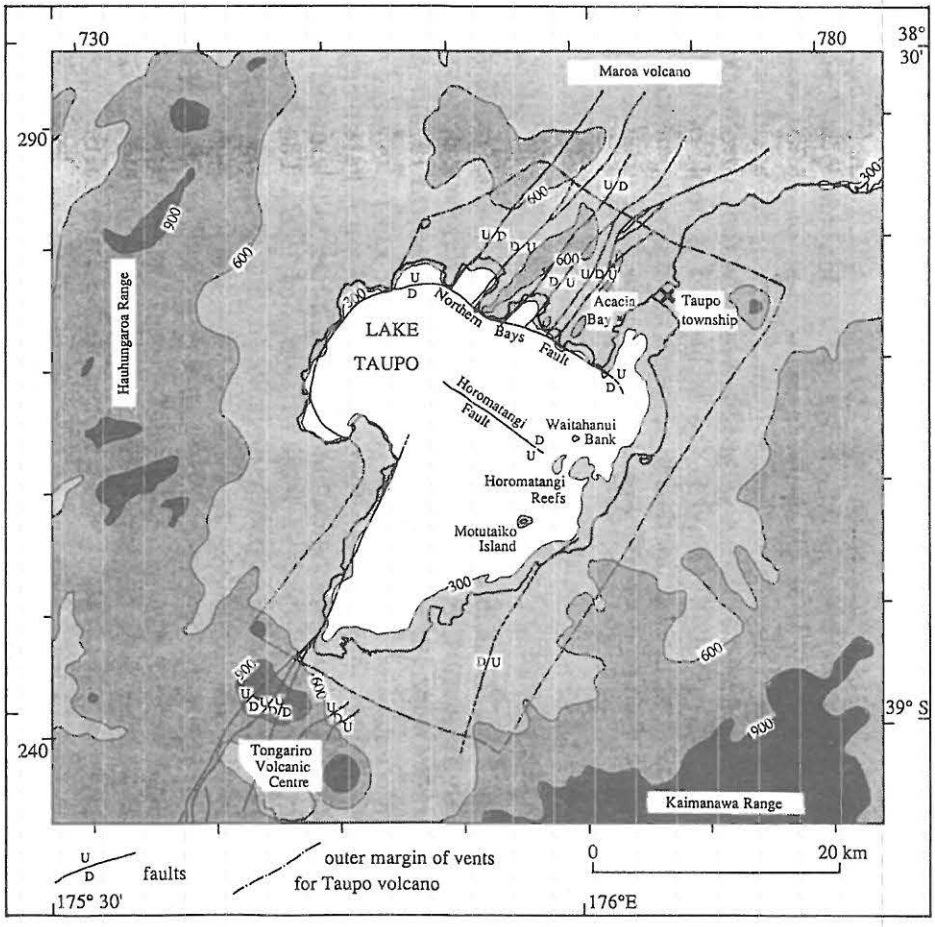

Figure 1.3: Topographic map of Taupo volcano to show its inverse nature. Contours are at 300 m intervals. From Wilson & Walker (1985).

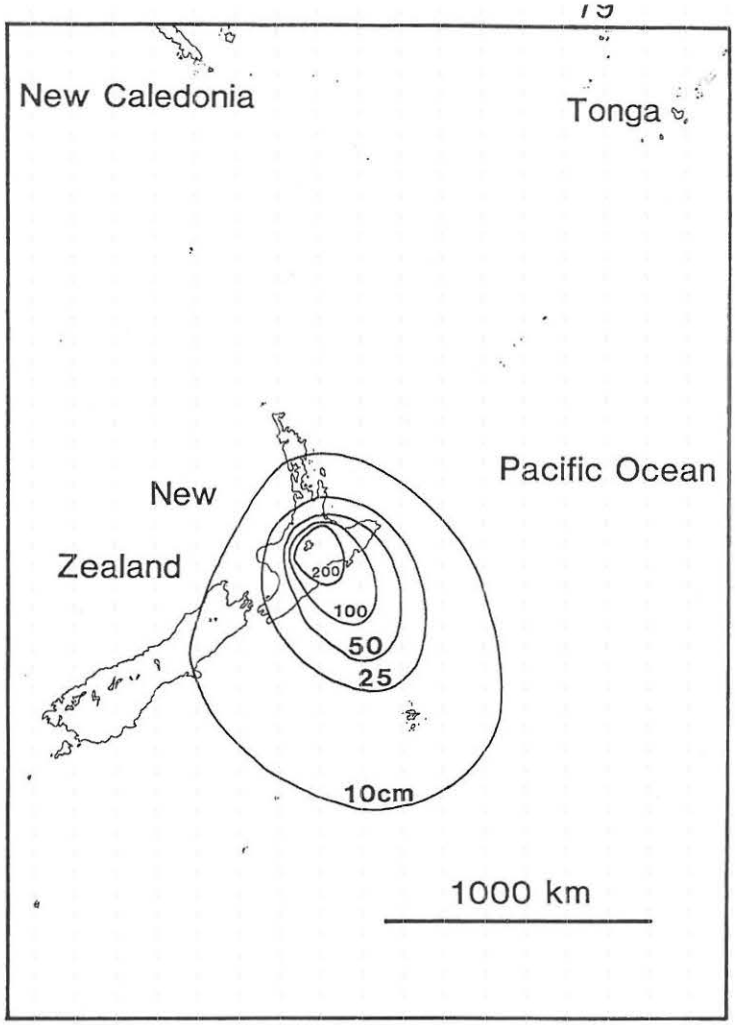

Figure 1.4: (a) Isopach map, showing the inferred original thicknesses of the Oruanui fall deposit, after compaction to present-day bulk densities (from C.J.N. Wilson, unpub. data).

Figure 1.4: (b) Isopach map showing the inferred original thicknesses and extent of the Oruanui ignimbrite (from Wilson 1991). Topographic contours at 500 m intervals.

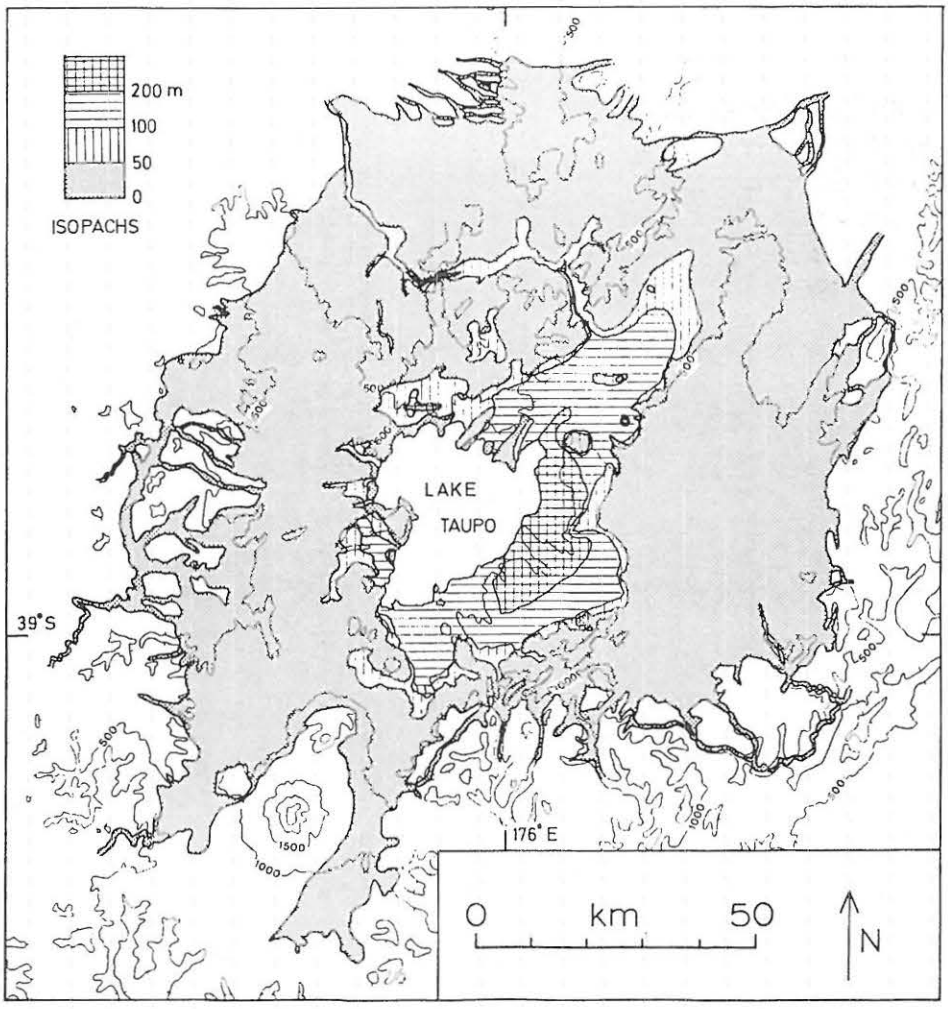

TABLE 1.1: Summary of the tephra formation names, new volcanological names, adopted ^{14}C and calibrated ages, bulk volumes of eruption products, previous estimates of bulk volumes of eruptive products, and the presence (yes), absence (-) or (possible) presence of four major styles of eruptive activity during each eruption. These data are simplified from Wilson (1993: tables 1, 2, 4, and 5; which see for more information on the assumptions behind the data).

Previous published tephra formation name	Volcanological name	Adopted age (years BP) ^{14}C time scale	Adopted age (years BP) calibrated timescale	Bulk volume in km^3 as used by Wilson (1993)	Other volume estimates, in km^3	Eruptive activity 'dry' fall	'wet' fall	Pyroclastic flow(s)	Lava extrusion
(not defined)	Eruption Z	-	1740	0.28	-	-	-	-	yes
Taupo Tephra	Unit Y	1850	1770	44.75	65, 105	yes	yes	yes	-
Mapara Tephra	Unit X	2150	2150	0.8	0.65, 2, 6	yes	yes	-	(possible)
(not recorded)	Unit W	(2650)	2750	0.023	-	-	yes	-	yes
Whakaipo	Unit V	2700	2800	0.8	0.8, 1.5, 2, 6	yes	yes	-	(possible)
Tephra	Unit U	(2750)	2850	0.2		-	yes	-	
(not recorded)	Unit T	(3000)	3200	0.08	-	-	yes	-	(possible)
Waimihia Tephra	Unit S	3300	3550	16.9	15, 17, 19, 29	yes	-	yes	-
	Unit R	3950	4450	0.05		yes	yes	-	-
	Unit Q	(4050)	4550	0.15		-	yes	-	(possible)
	Unit P	(4100)	4750	0.05		yes	yes	-	(possible)
	Unit O	(4150)	4800	0.05		yes	yes	-	(possible)
Hinemaiaia	Unit N	4200	4850	0.15	(3)	yes	yes	-	(possible)
Tephra	Unit M	(4500)	5250	0.2		yes	(possible)	-	(possible)
	Unit L	4550	5300	0.07		-	yes	-	yes
	Unit K	(4600)	5350	0.35		yes	yes	-	(possible)
	Unit J	(4620)	5370	0.015		-	yes	-	(possible)
	Unit I	(5200)	5950	0.02		-	yes	-	(possible)
Motutere	Unit H	(5300)	6050	0.2	(0.5, 1)	yes	yes	-	(possible)
Tephra	Unit G	(5800)	6650	0.5		yes	yes	-	(possible)
(not recorded)	Unit F	(6150)	7050	0.12	-	-	yes	-	yes
Opepe Tephra	Unit E	(9050)	9950	4.8	4, 5, 12	yes	yes	yes	-
Poronui	Unit D	(9780)	11 380	0.2	(3, 3.5, 7)	-	yes	-	yes
Tephra	Unit C	(9800)	11 400	0.75		yes	yes	-	(possible)
Karapiti Tephra	Unit B	10 100	11 800	1.4	2, 5, 6	yes	yes	-	-
(not recorded)	Unit A	(c. 14 200)	(c. 17 000)	(0.01)	-	-	yes	-	(possible)
(not recorded)	Unit Ω	(c. 15 600)	(c. 18 800)	0.1	-	yes	yes	-	-
(not recorded)	Unit Ψ	(c. 17 200)	(c. 20 500)	(0.05)	-	yes	yes	-	(possible)
Kawakawa	Oruanui ignimbrite	22 600	24 000-	300				yes	-
Tephra	Oruanui fall deposit		26 500	c. 500		-	yes	-	-

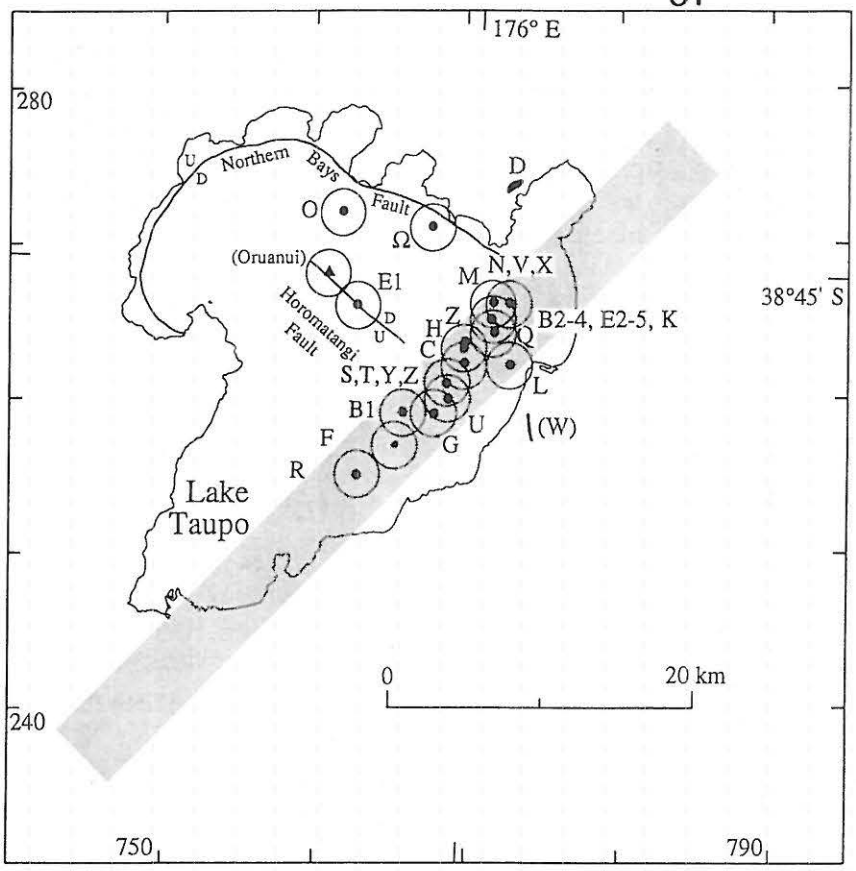

Figure 1.5: Compilation map of vent positions for all post-Oruanui eruptions at Taupo, except those of Units Ψ, A, I, J and P where the vent cannot be located. The stippled NNE-SSW band is a zone proposed as a deep-seated lineament controlling vent positions along the eastern side of Lake Taupo (from Wilson 1993).

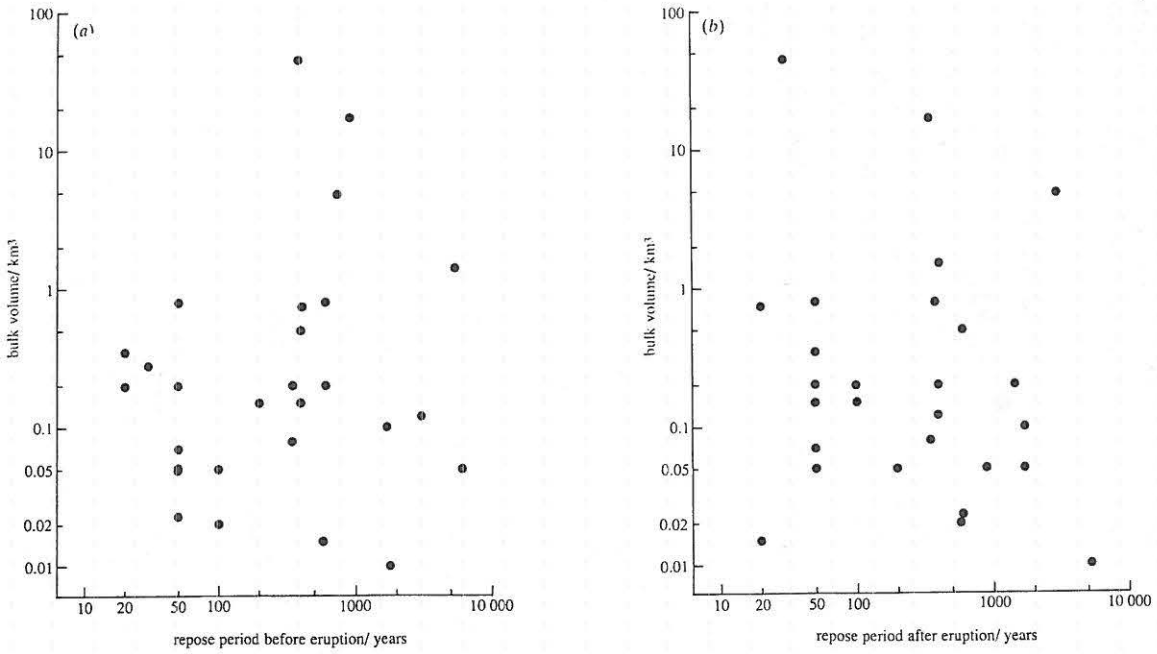

Figure 1.6: Plots of the volumes of the post-Oruanui eruptions at Taupo against the repose periods (calendar-year time scale), (a) prior to the eruption concerned, and (b) following the eruption concerned (from Wilson 1993).

Thus, whilst probabilities can be assigned today to the time period before and the volume of the next eruption, there is absolutely no way these factors can be *predicted* (cf. Froggatt 1982).

Geochemical studies in progress by A. Sutton (The Open University, UK) have shown that the magmatic history of Taupo volcano matches that of the eruptive history in its complexity, with the Oruanui eruption marking the most substantial change in the magmatic system. Pre-65 ka rhyolitic lavas and associated pyroclastics show a wide range of chemical and isotopic values (e.g. SiO_2 = 69-76%, $^{87/86}Sr$ = 0.70519-0.70725) and have ferromagnesian phenocryst assemblages of orthopyroxene + hornblende ± biotite. Spatially related domes often have geochemical and isotopic affinities that allow identification of distinct magma batches which tapped discrete sources. In contrast, rhyolite lavas and pyroclastics from c. 55 ka to 22.5 ^{14}C ka record the growth of an isotopically homogeneous ($^{87/86}Sr$ = 0.70560) magma chamber that finally emptied catastrophically during the Oruanui eruption. The Oruanui deposits themselves show the greatest chemical heterogeneity in the early stages of the eruption (first c. 10% of magma erupted) with SiO_2 = 71-77%, with the bulk of the deposits showing little variation about a c. 76% SiO_2 rhyolite at 770°C. Sparse amounts of juvenile mafic (broadly 'andesitic') material occur in the Oruanui deposits, reflecting the presence of a mafic floor to the magma chamber. The post-Oruanui sequence represents a new magma type, defined by its trace-element contents, higher Fe-Ti oxide temperatures (790-850°C), lack of biotite and scarcity of amphiboles, and higher $^{87/86}Sr$ ratios (0.70598-0.70622). The first three small volume eruptions (Ψ, Ω, A) at c. 17-14 ^{14}C ka are dacitic (66% SiO_2), with c. 20% crystals; $^{87/86}Sr$ ratios of 0.70600 link these magmas to the younger activity and rule against them being dregs from the Oruanui magma chamber. The remaining 25 eruptions from 10.1 to 1.85 ^{14}C ka are crystal poor rhyolite (3-8 % crystals), with very similar major element contents, although earlier and later groups can be distinguished using Y, Zn, and HREE contents. Only one of the post Oruanui eruptions shows evidence for magma mixing or zonation, that of Unit S (Waimihia Tephra) at 3.3 ^{14}C ka (Blake et al. 1992). In contrast to the timescales of (O) 10^5-10^6 years inferred for the development of other comparably-sized rhyolitic systems (e.g. Long Valley caldera, Valles caldera, and individual Yellowstone magmatic cycles), at Taupo magma batches persist for shorter time periods ((O) 10^4 years) and have stepwise, not gradational, changes between them. It is thought that the intensity of faulting associated with regional extension in the Taupo area precludes the existence of longer lived, large, high-level magma chambers considered the 'norm' elsewhere for large-scale silicic volcanism (e.g. Smith 1979; Halliday et al. 1989).

HAMILTON TO WAIRAKEI (FIG. 1.1)

Between Hamilton and Cambridge, the route heads up a large, low angle fan of volcaniclastic sediments, collectively known as the Hinuera Formation (Schofield 1965; Hume et al. 1975), which were brought down by the Waikato River and deposited in the Hamilton Basin. Much of the modern surface of this fan was formed by sedimentation occurred during the last glacial period, following on from the devastation caused by the Oruanui eruption. Beyond Cambridge, the route enters a confined valley, now occupied by the artificial Lake Karapiro (for hydroelectric generation), with numerous terraces as evidence for multiple episodes of infilling by ignimbrites from the TVZ and both alluviation and downcutting by the Waikato River.

At Piarere, a shallow valley, bordered by cliffs of the 1.23 Ma Ongatiti Ignimbrite, heads NE towards the Hauraki Graben; this valley has served on previous occasions as an alternative route for the Waikato River to the Hauraki Gulf. The prominent mountain to the SW is Maungatautari (797 m), an andesite-dacite composite volcano K/Ar dated at 1.8 Ma (Briggs 1986). From Piarere onwards through Tirau, Putaruru, and to S of Tokoroa, the route climbs up the dissected surface of a compound fan of welded ignimbrites, the youngest of these being the Mamaku Ignimbrite (0.22 Ma; Houghton et al. 1994) from Rotorua caldera. Thinner non-welded ignimbrites from Taupo (22.5 and 1.85 ^{14}C ka) mantle this fan from Litchfield southwards and the younger of these two ignimbrites becomes increasingly prominent as the uppermost tephra visible in roadcut exposures.

About 8 km SE of Tokoroa the route reaches a local summit at Tar Hill. This point marks the border between the ignimbrite fan extending NW beyond the TVZ, and the TVZ itself. From here S to Atiamuri, we descend into the graben structure of the TVZ, cross the Waikato River again, then climb up through the dome complex forming the modern topographic expression of Maroa volcano. The route then descends gradually to Wairakei as we enter the topographic low of the Taupo-Reporoa Basin, which is a major zone of young rifting and subsidence. At Wairakei, we cross the line of the steam pipelines from the borefield right (NW) of the road leading down to the power station alongside the Waikato River. Just S of Wairakei we leave the modern Highway 1 and join the old route between Wairakei and Taupo, turning off at the loop road for the upper level viewing platform for the Huka Falls.

STOP 1 — Upper lookout for Huka Falls (U18/789794)

Looking E across the Waikato River from the viewing platform, we can see several features of the local geology. Mount Tauhara (1088 m), a 191 ka (B.F. Houghton et al., unpublished data) dacitic dome complex, is prominent in the middle distance, while the high plateau across and slightly downstream is the accumulation surface of the 22.5 ^{14}C ka Oruanui ignimbrite which is there at least 150 m thick. The lower, rolling surface between us and Tauhara is a post-Oruanui pre-10 ^{14}C ka fluvial erosion surface which, alongside the river itself, is flanked by a 40 m-thick terrace of valley-ponded 1.85 ^{14}C ka Taupo ignimbrite.

The Waikato River at this point flows over largely-volcaniclastic lacustrine and fluvial sediments (Huka Falls Formation) which are pre-22.5 ^{14}C ka in age and represent deposits of a large lake that probably varied widely and rapidly in extent in response to tectonic and volcanic influences. The Huka Falls themselves are incised in these pre-Oruanui sediments which have been locally indurated by cementation associated with warm groundwater around the margins of the Wairakei geothermal system. The present river flows in a narrow slot which is incised into the wider valley floor, and it appears that during early post-1.85 ^{14}C ka drainage of the newly reformed Lake Taupo the Waikato River occupied the full width of the valley floor.

The road cutting at this point is the best section for seeing three of the newly described late Pleistocene fall tephras (Units Ψ, Ω,and A; Wilson 1993) from Taupo volcano and for showing the timing and thickness of loess deposition at this point. Post-Oruanui erosion is inferred to have been extremely rapid; the lower part of the cut exposes a rhyolitic tephra inferred to be distal Okareka Tephra from Okataina volcano (Nairn 1992) and its presence here implies >100 m of ignimbrite was removed at this point between 22.5 and c.18 ^{14}C ka. About 5 m of loess is preserved, with the Okareka Tephra towards the base and the sequence of post-10.1 ^{14}C ka tephras and paleosols above (Fig. 1.7). The loess here, and elsewhere in the Taupo area, is characteristically pinkish brown, vitric ash-grade material derived by wind deflation of the Oruanui ignimbrite. Tephra Units Ψ, Ω, and A from Taupo volcano are sandwiched in with the loess with no signs of significant time breaks (e.g. soils, erosion intervals), suggesting fairly even loess accumulation rates, which have thus been used in conjunction with bracketing age estimates to give approximate ages for these units (Table 1).

From the lookout, continue S on Huka Falls Road (old Highway 1), with an optional brief stop to view the Huka Falls from close at hand. Road cuts opposite the entrance to the lower Huka Falls parking area expose the Huka Falls Formation lake sediments.

STOP 2 — Lookout over Taupo volcano (Highway 1 and Huka Falls Road; U18/773767)

The lookout here gives an overview of the eastern half of Taupo volcano and underlines the contrast in morphologies and eruptive styles between Taupo and the more conventional composite cones to the S. Taupo is the archetypal 'inverse volcano' (Walker 1984; Fig. 1.3); in general, eruptions have been so explosive and dispersed material so widely that the accumulation of material around the vents has not compensated for collapse associated with caldera formation and regional extension. As a result,

the lake bed near Horomatangi Reefs (Fig. 1.3), site of the youngest eruptions, is the lowest point for over 40 km in any direction. In contrast, the andesitic composite cones to the SSW have produced numerous relatively small and weakly- to non-explosive eruptions that have piled up material about the vents to produce high cones that have not been affected by caldera collapse.

To the SE, Mount Tauhara is prominently visible, while behind and to the right of Tauhara the ground slopes gently at 1-2° from the Kaingaroa Plateau (700 m) down to Lake Taupo at 357 m asl, forming the eastern side of Taupo volcano. To the S, the surface of the 150-240 m thick Oruanui ignimbrite similarly slopes down to the lake edge from the feet of the 1400-1700 m high greywacke Kaimanawa Ranges. To the SSW beyond Lake Taupo several andesite composite cones are visible; in the foreground are the Pihanga-Kakaramea chain of late Pleistocene centres, then behind them, increasing in height and distance from us from R to L, are the active centres of Tongariro (1967 m), Ngauruhoe (2287 m), and Ruapehu (2797 m). To place the andesitic composite cones and Taupo in perspective, the total dense-rock equivalent volume of the 22.5 ^{14}C ka Oruanui event (≥300 km^3; a medium-sized example of the 30 or more caldera-forming events in the history of the TVZ) is roughly equal to the combined volumes of all the andesitic edifices visible at the S end of the lake.

From the lookout, travel S on Highway 1 through Taupo township, then SE on Highway 5 to Stop 3.

STOP 3 — Highway 5 near 'Highway 1' crossing (U18/881680)

Cuttings on both sides of the road just SE of where 'Highway 1' (a private forestry road) crosses Highway 5 expose the complete sequence of fall deposits from the latest major pyroclastic eruption at Taupo (eruption Y of Wilson 1993) and some earlier tephra units. This site is roughly 20 km from the vent site at Horomatangi Reefs proposed by Walker (1980).

Eruption Y (which, together with a subsequent lava-producing event [eruption Z], is known as the Taupo eruption) was the latest and largest of the post-Oruanui eruptions at Taupo. It is dated at 1.85 ^{14}C ka from multiple radiocarbon dates, while calendar age estimates have been made of:

- AD 177 (1 s.d. range of AD 166-195) from curve matching of a sequence of ^{14}C ages on a floating tree-ring sequence from logs buried by ignimbrite from this eruption (analyses by J.G. Palmer, quoted in Froggatt & Lowe 1990);
- AD 181 from Greenland ice-core acidity measurements (G. A. Zielinski, University of New Hampshire, oral comm., September 1993, and Zielinski et al. 1993); and
- c. AD 186 from interpretations of Ancient Chinese and Roman records (Wilson et al. 1980) (disputed by Stothers & Rampino 1983).

These estimates are consistent with a new ^{14}C error-weighted age of 1,854 ± 21 yr BP (n = 5), on leaves and seeds buried and preserved by the Taupo ignimbrite at Pureora and Bennydale, calibrated with 82% probability (at 1 SD) to a calendar range of AD 168—256 (after first subtracting 40 years for the S Hemisphere offset). This calibration shows a 34% probability that the eruption was between AD 168—200, and a 48% probability of AD 216—256 (Lowe 1993). Studies of the palaeo-environment of the forest buried by ignimbrite at Pureora imply the eruption occurred in late summer to early autumn (Clarkson et al. 1988), say late March to early April in a typical year. Total eruptive bulk volume estimates range between 45 and 105 km^3, depending on how much intracaldera material is now concealed beneath Lake Taupo and how the volumes of the fall deposits are calculated. The eruption was complex, generating 3 phreatomagmatic ('wet') and 2 plinian ('dry') fall units, a multi-flow unit intraplinian ignimbrite and, at the eruption climax, the extremely violently emplaced, single flow unit Taupo ignimbrite (Fig. 1.8; Walker 1980, 1981a,b; Wilson & Walker 1985; Wilson 1985). The wide variation in eruption styles and dynamics are due to variations in discharge rate and the degree of interaction between the magma and water in the proto-Lake Taupo; the chemistry of the eruption products is a uniform 73.3-74.3% SiO_2 rhyolite (A. Sutton et al., unpubl. data).

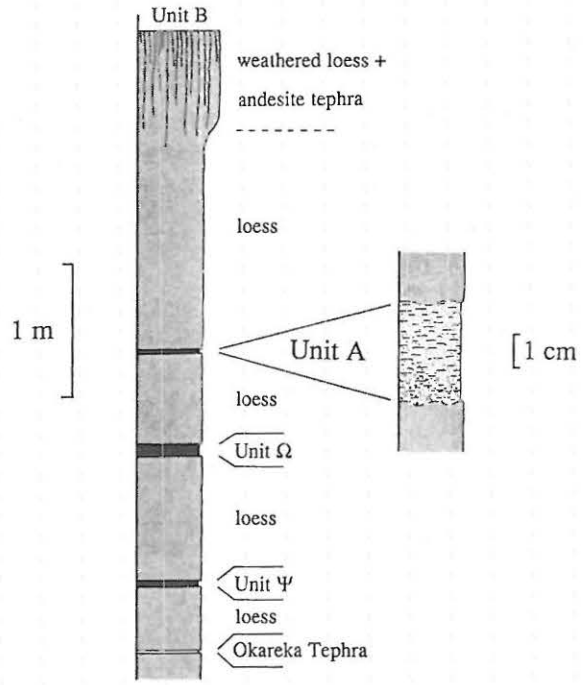

Figure 1.7: Stratigraphic section of Late Pleistocene tephra falls from Okataina (Okareka Tephra) and Taupo (Ψ, Ω and A), and loess at upper Huka Falls lookout, Stop 1 (from Wilson 1993).

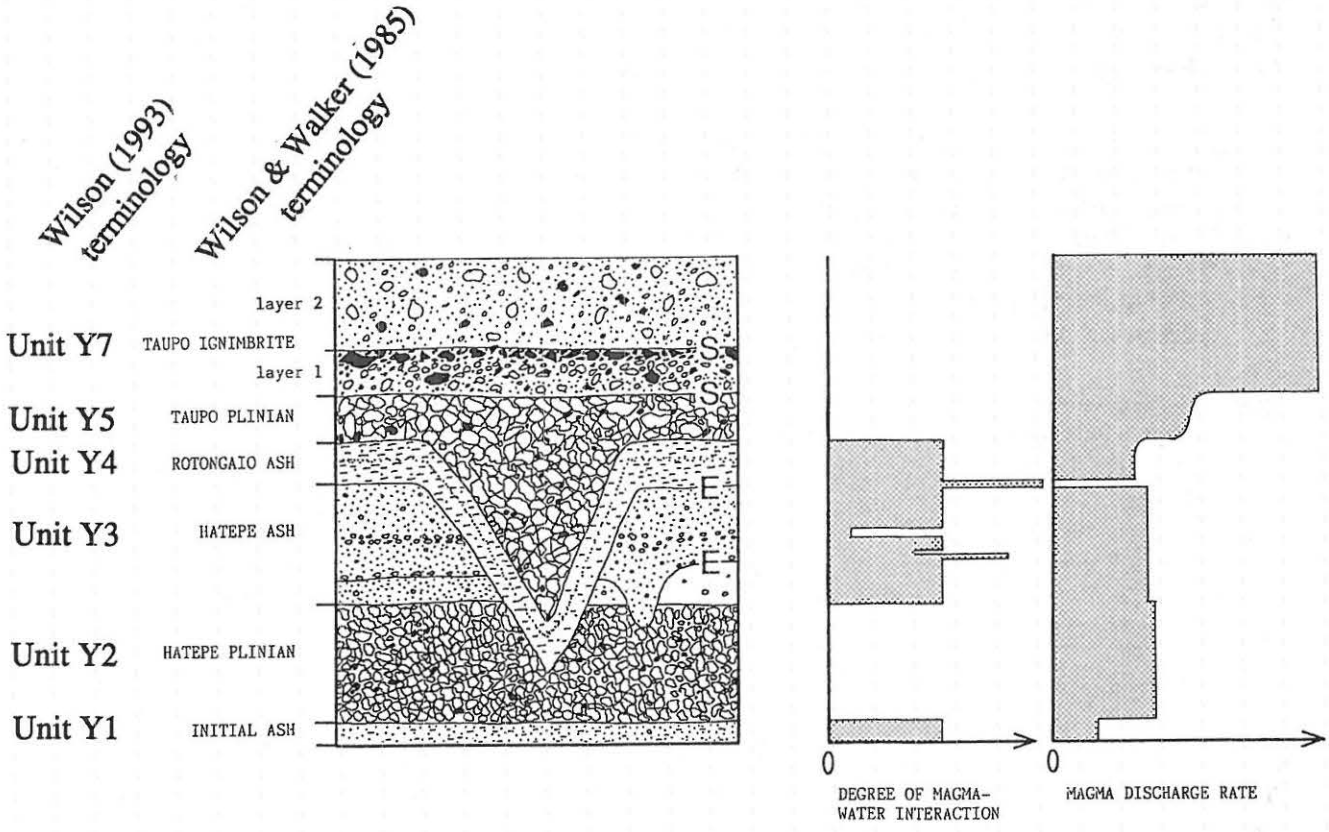

Figure 1.8: Diagram summarising the stratigraphy of pyroclastic deposits of the Taupo eruption (eruption Y of Wilson 1993) as seen at Stop 3. The right-hand parts show qualitatively changes in the inferred degree of magma-water interaction and the magma discharge rate during the eruption. 'E' donotes erosion horizons formed by running water, and 'S' erosion horizons due to shearing beneath the moving pyroclastic flow that deposited the Taupo ignimbrite. (After Wilson & Walker 1985).

At Stop 3 all the fall units of eruption Y are represented, though Unit Y1 (the Initial ash of Wilson & Walker 1985) is very thin (<1 cm). Note in particular the following contrasts:

1. Between the 'dry' plinian fall units (Y2/Hatepe plinian and Y5/Taupo plinian) which are typical fines-free pumice fall deposits and the 'wet' phreatomagmatic units (Y3/Hatepe ash and Y4/Rotongaio ash) which are poorly sorted, and rich in fine ash. This is largely attributed to the premature flushing out of fine ash by water raining out of the eruption plume rather than to any greatly increased abundance of ash-grade material in the eruption plume (Walker 1981b).

2. Between the 'typical' plinian Unit Y3 and the unusually powerful Unit Y5, as evidenced by the much coarser sizes of pumice and lithic fragments in the latter; Unit Y5 is the most powerfully dispersed 'dry' fall unit yet documented.

3. Between the 'wet' Units Y3 and Y4; the former is rich in pumice and is inferred to represent activity when the preceding Y2 plinian column mixed with abundant lake water, whereas the latter represents magma that was poorly vesiculated and would probably have generated a lava dome in the absence of interaction with water (Houghton & Wilson 1989).

Other unusual features here include the detailed patterns of deposition and erosion between Units Y3 and Y4, and during Y4 itself; both are made more complex by effects caused by wet cohesive tephra draping vegetation. The Taupo ignimbrite (Unit Y7) is represented by a stratified veneer deposit (layer 2; see Stop 6).

Below the eruption Y deposits, there is a sequence of thin fall deposits and soils, with the top of the 3.3 ^{14}C ka Unit S (Waimihia Tephra) exposed at road level. Previous studies had defined two tephra formations (Mapara and Whakaipo) in the intervening time interval, but I have recognised the products of 5 eruptions, 4 of which are discernible here.

From this locality, return on Highway 5 NE towards Taupo.

STOP 4 — Highway 5 at the De Bretts Section (U18/797729)

The long road cut opposite the De Bretts Hotel is a classic locality in New Zealand tephra studies. The W end of the cut exposes part of the Oruanui ignimbrite, eroded, then overlain by fluvial and lacustrine sediments and loess, then by the 'Holocene' sequence illustrated by Vucetich & Pullar (1973: Fig. 3). Seven of the 9 tephra formations inferred to be from Taupo are exposed here, including and together with several of the newly described eruption units from Wilson (1993; Fig. 1.9). Features to notice here (and also at a nearby section at U18/789729) are:

1. The yellow to orange colours of the lower deposits (Units B to E), attributed to staining from trace amounts of interbedded andesitic tephras from Tongariro and Ruapehu (Vucetich & Pullar 1973).

2. The generally poor development of paleosols, which are sandy and lack an abundant clay component (compare with Stops 7 and 10 later). The soils include a component of loessic material, identified from its pinkish-brown colour, as late as the time break between Units D and E (9.78 to 9.05 ^{14}C ka).

3. The poorly sorted materials forming the upper parts of Units S (Waimihia Tephra) and E (Opepe Tephra). In Unit S these are interpreted, from the low-angle cross-bedding and presence of carbonised vegetation fragments not in a position of growth, to be deposits of dilute, turbulent volcaniclastic density currents (surges) which were deposited as the outermost fringes of a more-proximal pond of ignimbrite. Evidence for the genesis of the upper part of Unit E is equivocal, but the same stratigraphic level is occupied by probable ignimbrite closer to source and definite fall material further from vent.

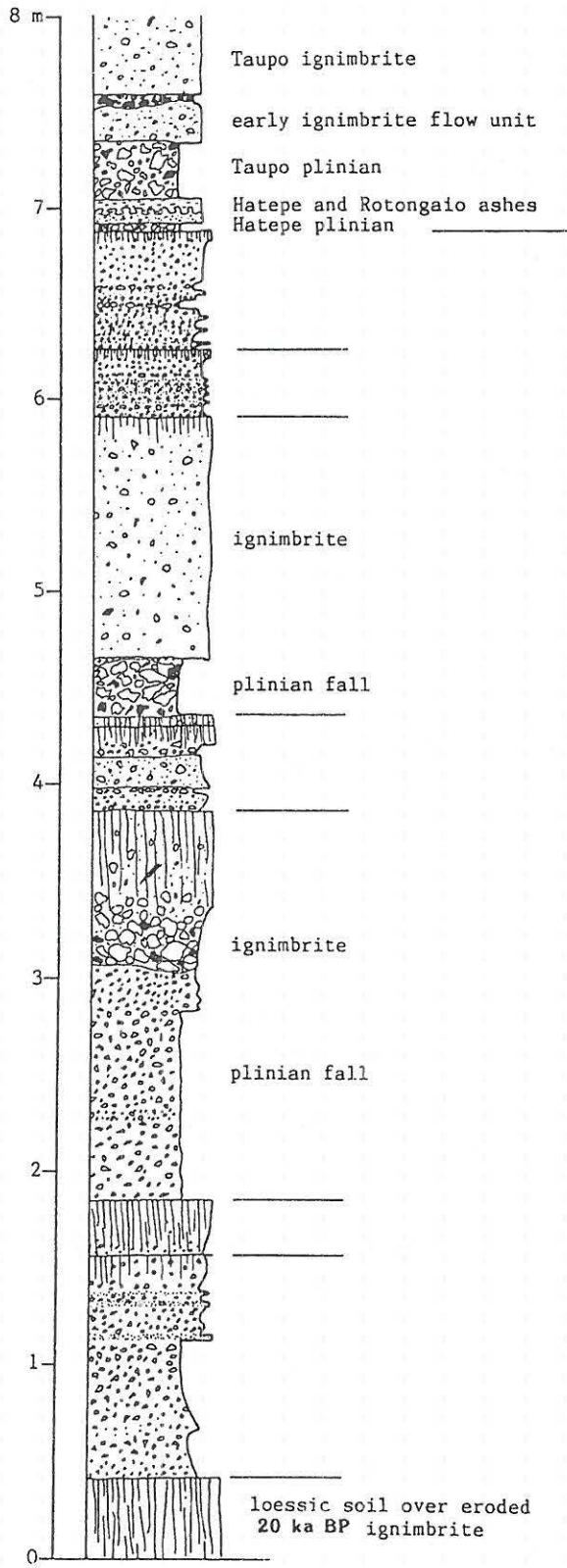

previously named tephra formations and ^{14}C ages (Froggatt & Lowe 1990)	Wilson (1993) terminology and ^{14}C ages
Taupo (1.85 ka)	Unit Y (1.85 ka)
Mapara (2.16 ka)	Unit X (2.15 ka)
Whakaipo (2.69 ka)	Units U (2.75 ka) and V (2.7 ka)
Waimihia (3.28 ka)	Unit S (3.3 ka)
Hinemaiaia (4.51 ka)	Units I (5.2 ka), K (4.6 ka), M (4.5 ka) and N (4.2 ka)
Opepe (9.05 ka)	Unit E (9.05 ka)
Poronui (9.81 ka)	Units C (9.8 ka) and D (9.78 ka)
Karapiti (9.82 ka)	Unit B (10.1 ka)

Figure 1.9: Composite section of the tephras visible at Stop 4 (De Bretts section of Vucetich & Pullar 1973), showing the comparison between the pre-existing tephra formations (Vucetich & Pullar 1973; Froggatt & Lowe 1990) and the newly proposed volcanic nomenclature of Wilson (1993).

4. The presence of evidence for time breaks between layers within the previously defined tephra formations. This is particularly evident here (and also at U18/789729) between the two deposits labelled Units C and D by Wilson (1993: Fig. 11) which were previously termed the Poronui Tephra.

The weak paleosols here on Units V (Whakaipo Tephra) and X (Mapara Tephra) were analysed using acid oxalate and pyrophosphate dissolution techniques, together with IR spectroscopy and DTA (Lowe & Percival 1993). The oxalate analyses on whole samples indicate that allophane (Al/Si ≈2.0) predominates (0.2% in Unit X, 1.0% in Unit V). However, Green (1987) interpreted from all the analyses that the clay fractions in both paleosols are dominated by glass followed by Si-rich allophane, organic matter, Al-rich allophane, ferrihydrite, and traces of halloysite and quartz. The apparent co-existence of both Si- and Al-rich allophane, and traces of halloysite, suggests that Si in soil solution may be near 10 g/m^3 and perhaps fluctuates with seasons or vegetational effects, or varies between weathering microsites (Lowe & Percival 1993).

Continue NE down Highway 5 (with an optional stop at U18/789729), then turn left (S) on to Highway 1. Drive S along the eastern side of Lake Taupo, through Waitahanui then up on to the plateau between Waitahanui and Hatepe. Turn left (SE) on Rotopuha Road and enter Lake Taupo Forest. Drive along Rotopuha Road, then R on to Maungatera Road, through an area of remnant native bush on the summit of Maungatera hill (705 m), begin to descend to the SE then turn R along a short (c. 100 m) pumice road to the reservoir at U18/809506 for Stop 5.

STOP 5 — Viewpoint off Maungatera Road, overlooking Hinemaiaia valley (U18/809506)

This point gives a good view over the Hinemaiaia River valley (at least until the trees grow higher). From here, you can see the following features:

1. The pine tree-covered ridge on the opposite side of the valley is carved out of 150-200 m of non-welded Oruanui ignimbrite. Note how, despite severe erosion, the form and slope of the Oruanui ignimbrite constructional surface can still be seen.

2. The Hinemaiaia River itself flows on one of the welded units of the Whakamaru-group ignimbrites, dated at 0.32 Ma (Wilson et al. 1986; Pringle et al. 1992); the stripped surface of this welded ignimbrite forms the local basement below the Oruanui deposits.

3. The c. 20 m terraces bordering the Hinemaiaia River are not simply the results of dissection of fluvial deposits, but are the remains of a valley pond of the 1.85 ^{14}C ka Taupo ignimbrite.

To the SE, the North Island axial ranges, composed of Permian to Jurassic indurated, partly volcaniclastic sediments ('greywacke'), are prominent and to the SSW the andesitic composite cones of Tongariro, Ngauruhoe, and Ruapehu rise beyond the Oruanui ignimbrite surface.

From here, return to Maungatera Road, then continue SE. At the next junction turn R on to Link Road, and follow this as it descends into the Hinemaiaia valley. At the 'T' intersection turn L on Waiwhiowhio Road, then right at the next 'T' intersection on to Hingapo Extension Road. Stop 6 is the first cut on the left (SE) side of the road, about 100 m from the 'T' intersection.

STOP 6 — 1.85 ^{14}C ka Taupo ignimbrite veneer and valley ponded ignimbrite on Hingapo Extension Road (U19/828478)

The Taupo, like many other ignimbrites, is inferred to have been deposited from a dense, concentrated pyroclastic density current (pyroclastic flow *sensu stricto*). Heights of mountains crossed by the Taupo flow imply it was emplaced at velocities exceeding 200 m s^{-1} (Wilson 1985). The Taupo ignimbrite is composed of several layers, termed 1 to 3, the first two of which can be divided into various facies, and with origins thus (Wilson & Walker 1982; Wilson 1985):

Layer 1. Deposits generated by processes operating at and in the head of the flow, where it interacted with the atmosphere and the ground surface, including vegetation. Facies include the pumice and fines-rich *jetted deposits* which represent material jetted ahead of the flow by violent expansion of ingested air, including the extreme end-member pumice rich, *fines-depleted ignimbrite* (Walker et al. 1980a), formed where the jetted material interacted turbulently with the abundant vegetation, and the lithic rich, fines-poor ground layer *ground layer* (Walker et al. 1981a) formed by sedimentation of segregation bodies in the head of the flow (see Stop 10).

Layer 2. Deposits laid down by the main bulk of the flow. As the flow travelled across the landscape, it left behind a 'tail' of material, slowed primarily by friction against the ground. As this 'tail' slowed, it began to be increasingly influenced by the local ground slope and to drain into topographic lows. This draining was promoted by steeper slopes and inhibited by the loss of mobility of the material as it gradually degassed. Material which clung to and mantled slopes is now seen as a *veneer deposit*, while the material that drained into and accumulated in valleys is now seen as the *valley-ponded ignimbrite* (Walker et al. 1981b). The relative thicknesses and proportions of veneer versus valley ponded facies in the Taupo ignimbrite vary widely, but the best developed valley ponds are seen in areas of steep relief where obstructions occurred on the valley floor and prevented the valley-ponded ignimbrite from draining further down valley.

Layer 3. Deposits from the dilute ash cloud overlying the concentrated pyroclastic flow. The most common facies, and the only one seen in the Taupo ignimbrite, is the *co-ignimbrite ash-fall deposit* (Sparks & Walker 1977) but this is almost everywhere eroded.

At this stop, a c. 2 m high ridge in the pre-ignimbrite topography is mantled by the veneer deposit which passes gradually to the west into a valley pond (Wilson 1985: Fig. 34a). Note that in the veneer the upper surface of the ignimbrite roughly parallels the pre-ignimbrite topography, whereas in the pond the top surface is sub-horizontal. Note that the only significant difference in grain size or composition between the veneer and adjacent valley-ponded ignimbrite is the absence or presence of abundant coarse pumice, respectively. The upper part of the valley-pond shows a pronounced enrichment in coarse pumice, caused by buoyancy induced flotation during emplacement (see Sparks 1976).

From this stop, continue westward on Hingapo Extension Road to Stop 7.

STOP 7 — Oruanui deposits cut by a clastic dike, and post-Oruanui tephras (U19/795479).

At this stop, part of the near-basal succession of the Oruanui deposits can be seen (Fig. 1.10), which should be contrasted with typical later ignimbrite material at Stop 10. In this area, the ignimbrite is >150 m thick and forms the whole of the high ridge visible to the NW. Several features can be seen in the deposits:

1. The presence of multiple, thin flow units, interpreted to reflect the emplacement of several small-volume flows at this time. Evidence for time breaks (between some flow units) are the presence of discrete fall layers, as well as the presence of concentrations of accretionary lapilli towards the tops of some flow units. In contrast, the later portions of the Oruanui ignimbrite in this area accumulated so rapidly that flow unit boundaries are not discernible (e.g. Stop 10).

2. The contrast between the earlier, lithic-poorer material and later, lithic-richer material (Fig. 1.10). (Lithics are defined as fragments of pre-existing country rocks incorporated into the deposit by processes such as vent erosion, or surface scouring by pyroclastic flows, during eruption and emplacement.) The nature of the lithics changes also, from mostly fresh lava (early) to dominantly hydrothermally altered (later). These changes are matched elsewhere in the Oruanui deposits and are inferred to result from a period of rapid vent enlargement, accompanying (and due to?) the rupture of a hydrothermal system.

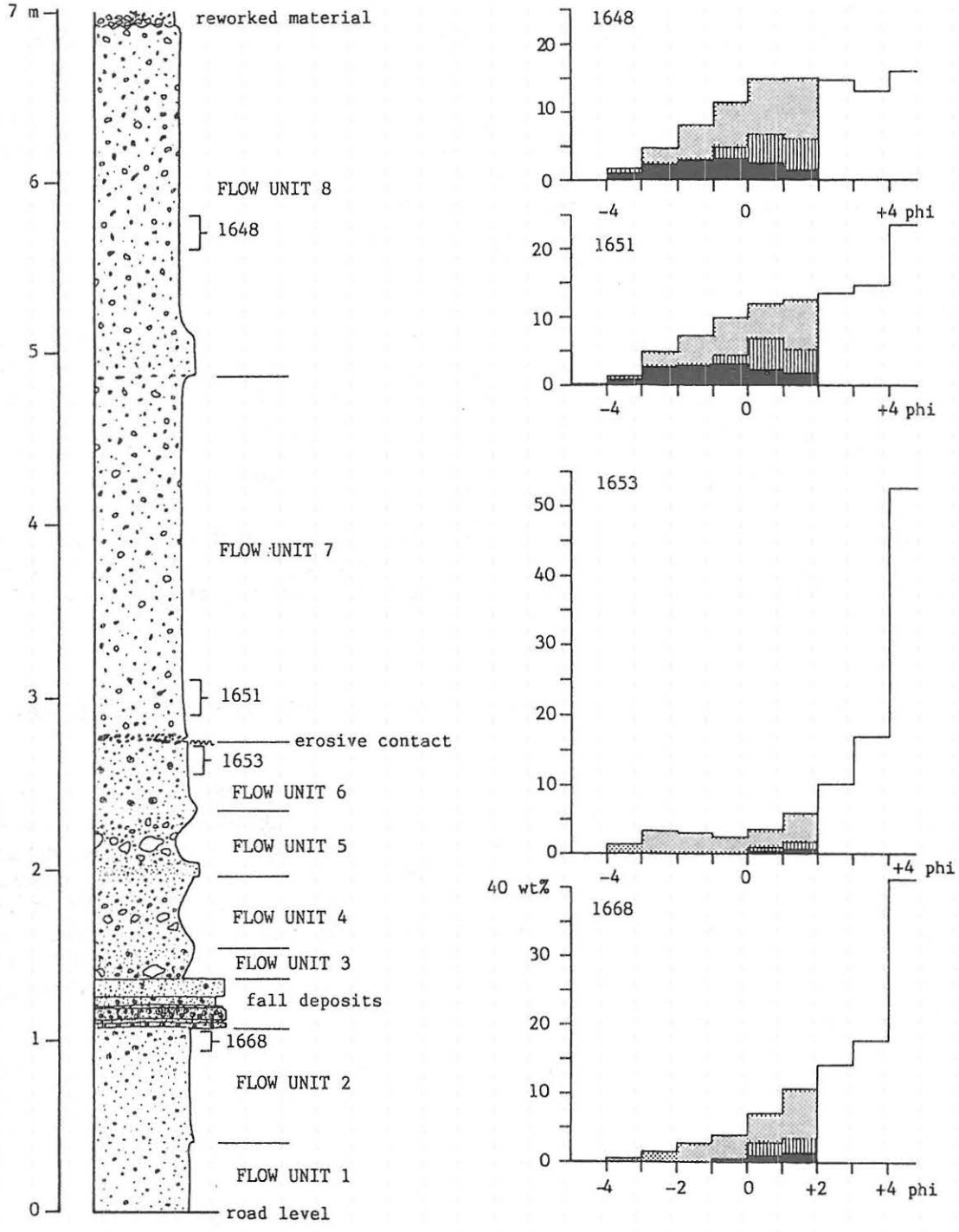

Figure 1.10: Stratigraphy of the Oruanui ignimbrite at Stop 7, with grain size and componentry data for selected samples (C.J.N. Wilson data). In the histograms, the coarser than +2 phi fraction is divided into its three components: pumice (plus minor accretionary lapilli) - stippling; crystals - vertical hatching; lithics - black.

3. Note that the maximum sizes of lithic fragments is a few mm in the lower flow units and a few cm in the upper two flow units. This upward coarsening is characteristic of the Oruanui ignimbrite in this area (Fig. 1.11) and reflects the increasing coarseness of successively erupted batches of material as 150-200 m of ignimbrite accumulated around the developing vent area now concealed beneath Lake Taupo. In contrast, the Taupo ignimbrite shows such variations *laterally* from proximal to distal areas of deposition of a single pyroclastic flow (Fig. 1.11).

4. An 80 cm wide clastic dike, which cuts the Oruanui deposits and is in turn truncated by the post-Oruanui erosion surface. Note the absence of any vertical displacement across the dike, the presence of an ultra-fine ash margin, and the vertical stratification of the infill. Comparisons with similar features developed after emplacement of the Taupo ignimbrite (Wilson & Walker 1985) lead me to conclude that these dikes are filled by material falling into open fissures developed by severe ground shaking (accompanying caldera collapse?) which occurred shortly after the eruption.

The Oruanui deposits are truncated by an erosion surface, overlain by steeply dipping, bedded ?aeolian reworked sediments and loess, then by the 'Holocene' succession of tephras and paleosols. The main deposits visible here are Units B (Karapiti), C (Poronui), E (Opepe), G plus H ('Motutere'; see Stop 11), S (Waimihia) and Y (Taupo). Compared with Stop 4, note how much better developed the intervening paleosols are; in this area minor amounts of andesitic tephras fall much more frequently and these have broken down much more readily than the rhyolitic material.

Continue NW on Hingapo Extension Road, cross the Hinemaiaia River (note the 0.32 Ma welded ignimbrite forming the stream bed) and shortly afterwards turn left (SW) on to Hingapo Road. At U19/759459 turn left again (S) on to Tiraki Road and travel S for approximately 2 km to where the road crests a low rise. This is Stop 8.

STOP 8 — 1.85 ^{14}C ka Taupo ignimbrite veneer deposit with lee-side lenses, on Tiraki Road (U19/828478)

The Taupo ignimbrite was emplaced at high speeds over an often-rugged terrain, and in many places there is evidence to suggest the flow locally left the ground and free-flighted on the downflow side of obstacles. This evidence is well displayed at this locality, where the stratified veneer deposit seen on the N (up-flow) side of a ridge in the pre-ignimbrite landscape thickens and coarsens on the down-flow side and includes the structures termed lee-side lenses (Walker et al. 1981b). These lee-side lenses are broadly interpreted to represent fossil vortices developed where the flow left the ground in the lee of the ridge. Note also the development of layer 1 deposits on the up-flow side of the ridge and their paucity on the down-flow side; it is thought that the head of the flow could not deposit material in this relatively sheltered lee-side situation.

Turn here, and return N on Tiraki Road, then turn left (W) up Hingapo Road, right (N) at the next junction on to Opawa Road, then after about 800 m left (W) on Mission Bay Road. Continue along Mission Bay Road for some kilometres, climbing a ridge, then down a gentle slope towards Lake Taupo. Where the road bends at a 4-way junction at T19/695491, turn right (NE) on to Kanuka Road, and Stop 9 is after 500 m.

STOP 9 — The 'Taupo Orogeny' on Kanuka Road; the impact of the Taupo ignimbrite (T19/698496)

This locality gives a graphic picture of the violent emplacement of the Taupo ignimbrite flow. The flow collided with a small ridge or possibly a gully wall developed in post-Oruanui tephras and paleosols, with spectacular results. On the NW side of the road, it can be seen that the flow scoured down into and caused multiple reverse faulting in the 'basement' lithologies. On the SE side, there is developed scouring, reverse faulting, and a nappe structure where a sequence of tephras and paleosols has been flipped over by the flow. An inverted section from Unit S (Waimihia) to Unit Y4 (Rotongaio ash) can be recognised in the overturned limb.

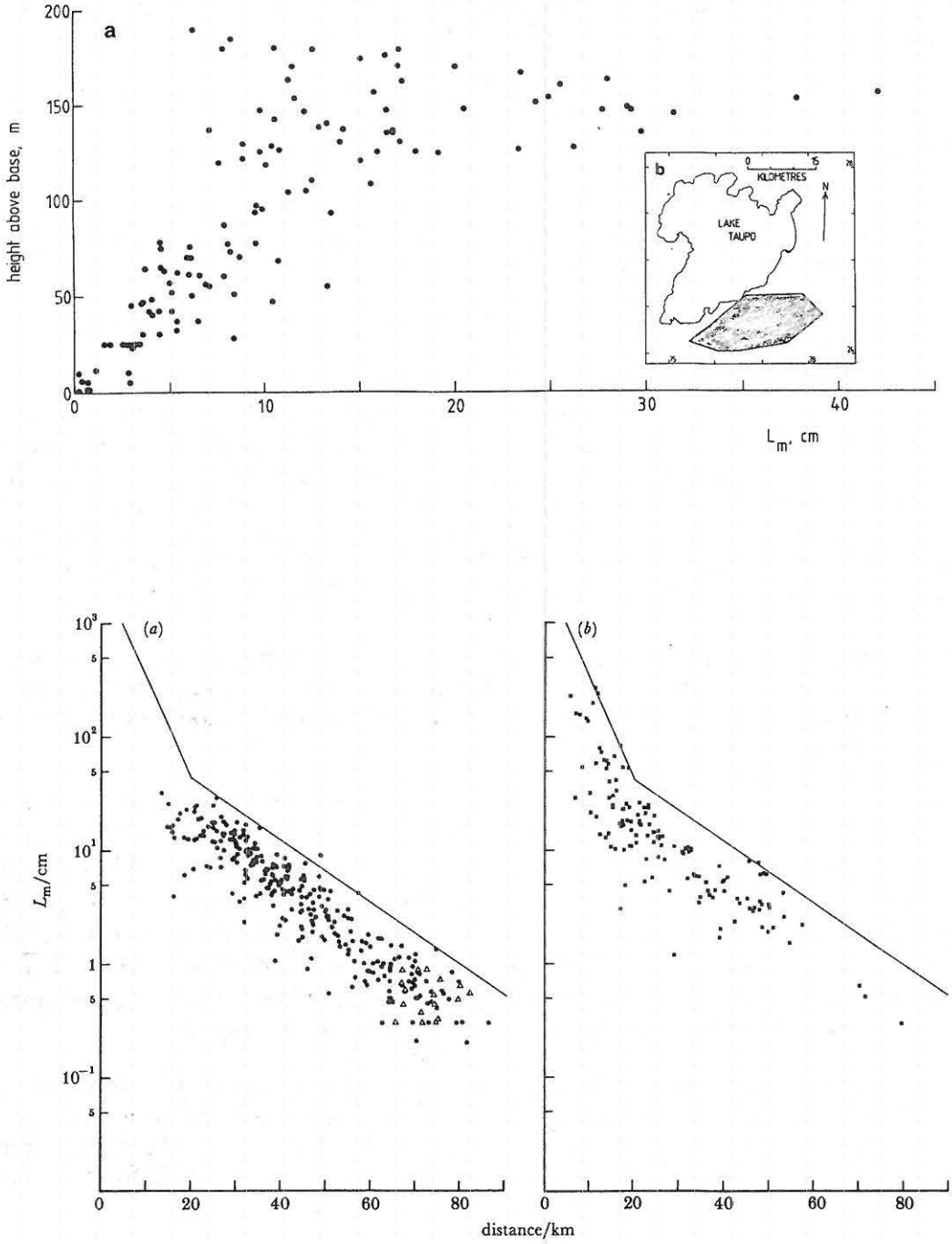

Figure 1.11: Summary diagram to contrast the vertical lithic size variations in the Oruanui ignimbrite (Wilson et al., 1986) with lateral variations in the Taupo ignimbrite (Wilson 1985). The top diagram shows the variations in the average length of the 5 largest lithic fragments (L_m, cm) versus the *vertical* height above base in the Oruanui ignimbrite. The data were collected from the area shaded in the inset map. The bottom pair of diagrams plot the same parameter (L_m) from (a) pumice-rich layer 1 deposits, and (b) lithic- and crystal-rich layer 1 deposits in the Taupo ignimbrite, versus the *lateral* distance from vent.

The presence of a discontinuous layer 1 deposit (ground layer) along the suture between upright and inverted material implies that the flip-over took place beneath the moving flow.

Turn here, return to Mission Bay Road, turn left (SE) and continue along straight road until it bends and cuts through local high point of the ridge; the road cuts here and SE to the junction with Halfway Road Extension are Stop 10.

STOP 10 — Oruanui ignimbrite and post-Oruanui tephras on Mission Bay Road (U19/714479 -715476)

Walking SE from the summit of the hill on Mission Bay Road, we can see several features in turn.

1. The Taupo ignimbrite veneer deposit (layer 2), which forms a gently curved 1-1.5 m thick drape over the ridge; flow direction was obliquely from the NNW, so the lee-side structures lie out of the plane of the road cut. The underlying layer 1 deposits are more irregular in thickness as they infill hollows on the underlying palaeosurface and were then shaved off by the later stages of the flow. Two facies are displayed in layer 1, the lithic-rich ground layer and pumice-rich fines-depleted ignimbrite. The latter is rare closer to vent than this, and this is interpreted to mean that the velocity of the flow was so high that material in the flow head could not be jetted in advance of the flow proper (Wilson 1985: Fig. 4 a).

2. The 'Holocene' (pre 1.85 ^{14}C ka) succession (Fig. 1.12) shows rhyolitic tephra units generally thinning (as we are now S of most of their axes of dispersal), but the intervening paleosols and occasional discrete andesitic fall units increasing in importance as we are now closer to the andesitic volcanoes.

3. The Oruanui ignimbrite is exposed at probably the highest stratigraphic level in this area. Compared with Stop 7, note the absence of flow unit boundaries in a c. 25 m thick continuous exposure. Notice also that the ignimbrite here continues the upwards trend of coarser and more abundant lithic fragments; component analyses for the ≥0.25 mm fractions give figures of 24.0 wt% lithics for material from this upper part of the ignimbrite, versus 3.1 (Sample 1668, Fig. 1.10) and 14.1 (Sample 1648, Fig. 1.10) wt % for typical early material. The total volume of lithics ejected in this event probably exceeds 40 km^3 and it would appear that substantial amounts of vent widening were a major feature of the eruption.

From here, continue SE on Mission Bay Road, then turn left (N) at the 'T' junction with Opawa Road. Continue N for 6 km, past the junction with Pahikohuru Road and following the line of the HV power lines until the main road bends left (and becomes Te Heu Heu Road). At this point turn right and continue going N for 1 km along the continuation of Opawa Road. Stop 11 is in the northernmost road cuts as Opawa Road descends on to a lower surface.

STOP 11 — The 'Hinemaiaia' and 'Motutere Tephras' on Opawa Road; tephra formations versus volcanic eruptive units (U18/742529)

Vucetich & Pullar (1973) originally defined a single 'Hinemaiaia Tephra' with its type locality at the De Bretts section (Stop 4), and this was split by Froggatt (1981) into two formally defined units, the 'Motutere' and 'Hinemaiaia' Tephra Formations, with a type locality at this section. Subsequent usage of these terms has equated them with single eruptive events (e.g. Lowe 1986), as with the other formally defined tephra formations at Taupo (e.g. Froggatt 1982; Latter 1985; Froggatt & Lowe 1990). However, at this locality there is evidence to show that these tephra formations represent multiple events.

The 'Motutere Tephra' here consists of 2 pumice fall deposits (Units G and H of Wilson 1993; cf. Fig. 1.13a) separated by a paleosol interpreted, from ^{14}C age determinations, to represent c. 500 ^{14}C years. Each deposit is a completely separate eruptive event, from different vent positions (Fig. 1.5).

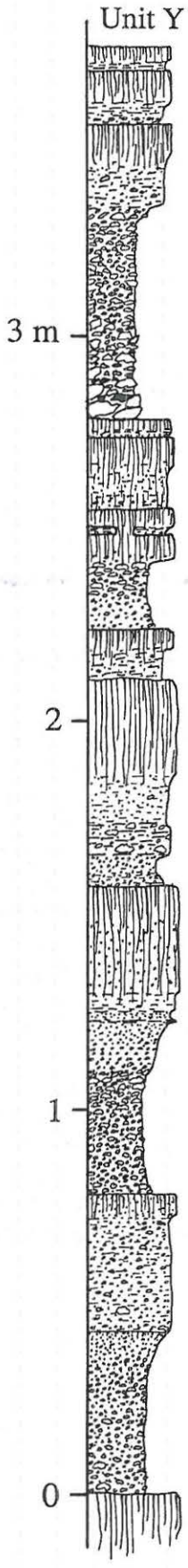

tephra formation name	volcanological term
	Unit Y
Mapara Tephra	Unit X
Whakaipo Tephra	Unit V
Waimihia Tephra	Unit S
Hinemaiaia Tephra	Unit R (Unit L) (Unit K)
Motutere Tephra	Unit H Unit G
	Unit F
Opepe Tephra	Unit E
(weathered andesite fall deposit)	
Poronui Tephra	Unit C
(weathered andesite fall deposit)	
Karapiti Tephra	Unit B
loessic soil with weathered andesitic fall deposits over Oruanui ignimbrite	

Figure 1.12: Stratigraphic section of the post-Oruanui, pre-Y (1.85 ^{14}C ka) rhyolitic tephras visible at Stop 10. Note the presence of interbedded macroscopic andesitic tephras, derived from Tongariro volcano to the S, and the relatively greater importance of palaeosols (vertical lining) relative to tephras.

The 'Hinemaiaia Tephra' here consists of 6 tephra units (J, K, L, N, Q, and R of Wilson 1993; Fig. 1.13b), separated by either paleosols or other evidence for a significant time break (≥10-20 years). In total, field stratigraphy and ^{14}C age determinations have been used by Wilson (1993) to interpret the 'Hinemaiaia Tephra' as a sequence of 10 fall deposits (Units I to R, Fig. 1.14; Stop 11 is locality 2380 in that figure). As a mapping term for a definable time-stratigraphic unit the term 'Hinemaiaia Tephra' remains valid, but as a volcanological term it is very misleading. The style of activity represented by the 'Hinemaiaia Tephra' differs markedly from that considered archetypal for large rhyolitic caldera volcanoes; instead of fewer but larger catastrophic eruptions at intervals of hundreds to thousands of years, there were more numerous but smaller events at intervals of tens to hundreds of years. The effects of the individual 'Hinemaiaia' eruptions were such that the local ecosystems were often merely interrupted (rather than wiped out, as with the larger events at Taupo) and hence vegetation could continue to grow almost immediately after each event. Thus what is seen as the 'Hinemaiaia Tephra' at anyone locality represents a balance between the accumulation of deposits, and their mixing by bioturbation. Where the deposit of an individual eruption was thicker (typically >20-30 cm), or the succeeding inferred repose period only decades or so, clearly definable separate deposits are found. Where thinner deposits were separated by longer inferred repose periods accumulated, the distinction between individual eruption units is lost.

From this stop, return to the junction with Te Heu Heu Road and turn right (NW). After 7.5 km Te Heu Heu Road meets Highway 1. Turn left (SW) and travel 4.5 km on Highway 1, then 250 m SW of Bulli Point pull off the road into a parking area on the LHS. Stop 12 is on the SE side of the road, about 80 m back towards Taupo township.

STOP 12 — Evidence for eruption Z: the floated giant pumice at Motutere (T18/673535)

Although previously included in the events termed the 'Taupo eruption' by Wilson & Walker (1985), the feature seen here is now interpreted to represent a separate event (eruption Z; Wilson 1993). Exposed in this road cut (Wilson & Walker 1985: Fig. 8) is a c. 6 m block of prismatic jointed, pumiceous rhyolite which rests within a sequence of stratified pumiceous lacustrine sediments that elsewhere are seen to be eroded from pyroclastic products of eruption Y. At its base the rhyolite block has slightly compacted the sediments and a water-escape structure is visible, implying that the block came to rest here very gently, and was not ejected in a pyroclastic explosion. The block (and numerous other examples down the E side of Lake Taupo) is interpreted as a fragment which spalled off the pumiceous carapace of a dome which was being extruded under the lake. The fragment is inferred to have floated and been driven ashore by the prevailing westerly winds to strand on a shoreline that is no more than 10 m above the modern lake level. It seems reasonable to suppose that during eruption Y much of the lake had been destroyed by incorporation in phreatomagmatic activity or drainage down the Waikato River. After that event the lake re-formed, rose to an average level of +34 m, then fell back episodically to essentially its modern level, cutting shoreline terraces in the process. The critical question is: how long did this take? Consideration of the water balance for the lake following the eruption suggests this process must have occupied roughly 20-30 years. Thus the lava-producing event of eruption Z post-dated the pyroclastic phases of eruption Y by that order of time, and hence (for consistency with the approach adopted to subdivide the 'Hinemaiaia Tephra') is considered to be a separate eruptive event. Waitahanui Bank and the Horomatangi Reefs (Fig. 1.3) are interpreted to be the remnants of this episode of dome-building activity.

Note that no accompanying pyroclastic material is known; the evidence for this event is solely from these giant pumice blocks. It is thus not known how many other times purely effusive activity like this might have occurred at Taupo. The danger from this is apparent when you consider that people's expectations of the eruptive power of the volcano are highly coloured by the devastating events of eruption Y, yet the next eruption at Taupo might well be a small effusive event that poses minimal threat to life or property. It is this degree of unpredictability that makes Taupo volcano such a great challenge to study and understand.

From this point continue SW on Highway 1 to Turangi, then turn right (W) on Highway 41 to Tokaanu and the Tokaanu Hotel.

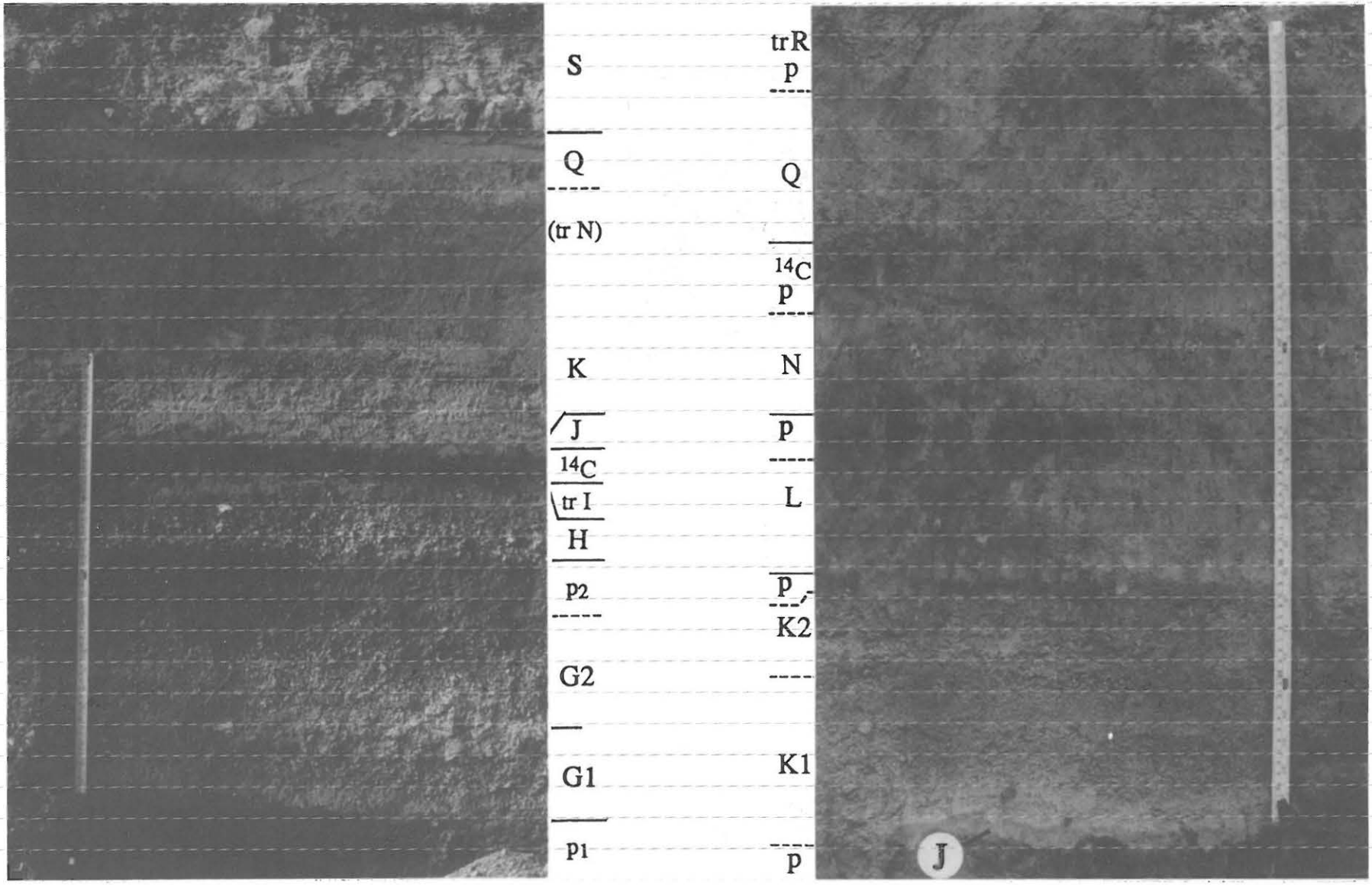

Figure 1.13: (Left) photograph of a section at U18/739518 close to Stop 11, showing the material previously described as the 'Motutere Tephra' (Base of G1 to top of H) and 'Hinemaiaia Tephra' (Units I to Q). Eruption units of Wilson (1993) are labelled in capitals, tr = trace, p_1 = pre-G palaeosol with traces of Unit F, p_2 = palaeosol separating Units G and H, and ^{14}C = palaeosol where a radiocarbon age determination was made (see Figure 1.14, section 2379).

(Right) photograph of the section at Stop 11, to show the subdivisions of the 'Hinemamaia Tephra' there. Lettering as in the left-hand photo (this is locality 2380 in Figure 1.14). Both photographs from Wilson (1993).

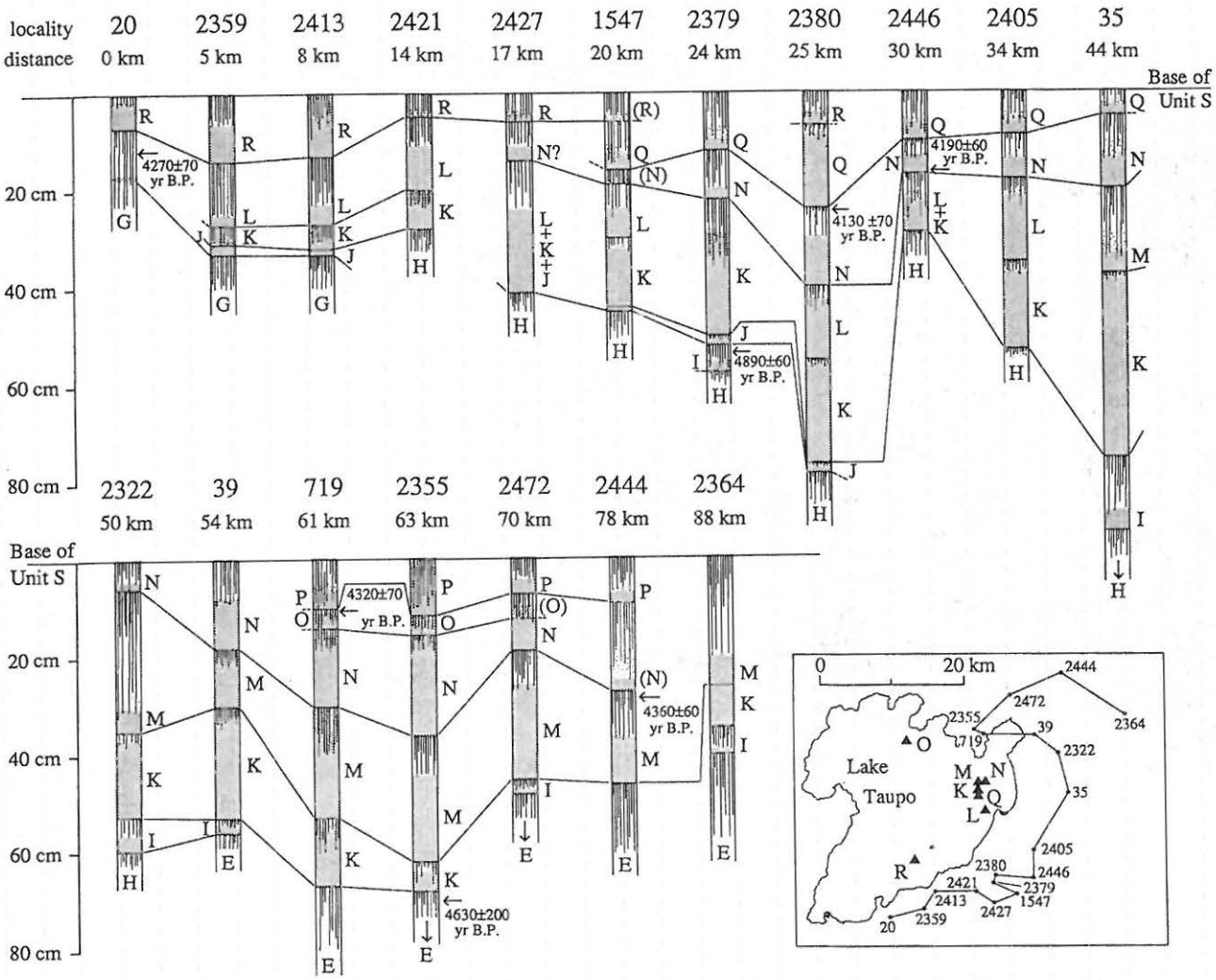

Figure 1.14: Schematic scaled stratigraphic columns to show lateral correlations between Units I to R previously mapped as the 'Hinemaiaia Tephra'. Fresh tephra is represented by stippling, soilified ash and palaeosols by vertical lining. The inset map shows the inferred vent positions for those units where adequate isopach and isopleth data are available. (From Wilson 1993.)

REFERENCES

Bard, E.; Hamelin, B.; Fairbanks, R.G.; Zindler, A. 1990: Calibration of the ^{14}C time scale over the past 30,000 years using mass spectrometric U-Th ages from Barbados corals. *Nature, London 345*: 405-410.

Blake, S.; Wilson, C.J.N.; Smith, I.E.M.; Walker, G.P.L. 1992: Petrology and dynamics of the Waimihia mixed magma eruption, Taupo volcano, New Zealand. *Geological Society of London journal 149*: 193-207.

Briggs, R.M. 1986: Petrology and geochemistry of Maungatautari, a medium-K andesite-dacite volcano. *New Zealand journal of geology and geophysics 29*: 273-289.

Brooker, M.R.; Houghton, B.F.; Wilson, C.J.N.; Gamble, J.A. 1993: Pyroclastic phases of a rhyolitic dome-building eruption: Puketarata tuff ring, Taupo Volcanic Zone, New Zealand. *Bulletin of volcanology 55*: 395-406.

Clarkson, B.R.; Patel, R.N.; Clarkson, B.D. 1988: Composition and structure of the forest overwhelmed at Pureora, central North Island, New Zealand, during the Taupo eruption (c. AD 130). *Journal of the Royal Society of New Zealand 18*: 417-436.

Eden, D.N.; Froggatt, P.C.; McIntosh, P.D. 1992: The distribution and composition of volcanic glass in late Quaternary loess deposits of southern South Island, New Zealand, and some possible correlations. *New Zealand journal of geology and geophysics 35*: 69-79.

Froggatt, P.C. 1981: Motutere Tephra Formation and redefinition of Hinemaiaia Tephra Formation, Taupo Volcanic Centre, New Zealand. *New Zealand journal of geology and geophysics 24*: 99-105.

Froggatt, P.C. 1982: Review of methods of estimating rhyolitic tephra volumes: applications to the Taupo Volcanic Zone, New Zealand. *Journal of volcanology and geothermal research 14*: 301-318.

Froggatt, P.C.; Lowe, D.J. 1990: A review of late Quaternary silicic and some other tephra formations from New Zealand: their stratigraphy, nomenclature, distribution, volume, and age. *New Zealand journal of geology and geophysics 33*: 89-109.

Green, B.E. 1987: Weathering of buried paleosols on late Quaternary rhyolitic tephras, Rotorua region, New Zealand. Unpublished MSc thesis, University of Waikato, Hamilton.

Halliday, A.; Mahood, G.A.; Holden, P.; Metz, J.M.; Dempster, T.J.; Davidson, J.P. 1989: Evidence for long residence times of rhyolitic magma in the Long Valley magmatic system: the isotopic record in precaldera lavas of Glass Mountain. *Earth and planetary science letters 94*: 274-290.

Houghton, B.F.; Wilson, C.J.N. 1989: A vesicularity index for pyroclastic deposits. *Bulletin of volcanology 51*: 451-462.

Houghton, B.F.; Wilson, C.J.N.; McWilliams, M.; Lanphere, M.A.; Weaver, S.D.; Briggs, R.M.; Pringle, M.S. 1994: Volcanic and structural evolution of a large silicic volcanic system: central Taupo Volcanic Zone, New Zealand. Submitted to *Geology*.

Hume, T.M.; Sherwood, A.M.; Nelson, C.S. 1975: Alluvial sedimentology of the Upper Pleistocene Hinuera Formation, Hamilton Basin, New Zealand. *Journal of the Royal Society of New Zealand 5*: 421-462.

Latter, J.H. 1985: Frequency of eruption at New Zealand volcanoes. *Bulletin of the New Zealand national society for earthquake engineering 18*: 55-110.

Lowe, D.J. 1986: Revision of the age and stratigraphic relationships of Hinemaiaia Tephra and Whakatane Ash, North Island, New Zealand, using distal occurrences in organic deposits. *New Zealand journal of geology and geophysics 29*: 61-73.

Lowe, D.J. 1993: Explosive volcanism and climatic change — a New Zealand perspective. *Abstracts*, IGBP PAGES - INQUA COT Meeting "Climatic Impact of Explosive Volcanism", Tokyo: 24-25.

Lowe, D.J.; Percival, H.J. 1993: Clay mineralogy of tephras and associated paleosols and soils, and hydrothermal deposits, North Island. *Guide Book for New Zealand Pre-Conference Field Trip F1,* 10th International Clay Conference, Adelaide, Australia. 110 p.

Mazaud, A.; Laj, C.; Bard, E.; Arnold, M; Tric, E. 1991: Geomagnetic field control of ^{14}C production over the last 80 ky: implications for the radiocarbon time-scale. *Geophysical research letters 18*: 1885-1888.

Nairn, I.A. 1992: The Te Rere and Okareka eruptive episodes - Okataina Volcanic Centre, Taupo Volcanic Zone, New Zealand. *New Zealand journal of geology and geophysics 35*: 93-108.

Pillans, B.J.; McGlone, M.S.; Palmer, A.S.; Mildenhall, D.C.; Alloway, B.V.; Berger, G.W. 1993: The Last Glacial Maximum in central and southern North Island, New Zealand: a paleoenvironmental reconstruction using the Kawakawa Tephra Formation as a chronostratigraphic marker. *Palaeogeography, palaeoclimatology, palaeoecology 101*: 283-304.

Pringle, M.S.; McWilliams, M.; Houghton, B.F.; Lanphere, M.A.; Wilson, C.J.N. 1992: $^{40}Ar/^{39}Ar$ dating of Quaternary feldspar: examples from the Taupo Volcanic Zone, New Zealand. *Geology 20*: 531-534.

Schofield, J.C. 1965: The Hinuera Formation and associated Quaternary events. *New Zealand journal of geology and geophysics 8*: 772-791.

Self, S. 1983: Large scale phreatomagmatic silicic volcanism: a case study from New Zealand. *Journal of volcanology and geothermal research 17*: 433-469.

Self, S.; Healy, J. 1987: Wairakei Formation, New Zealand: stratigraphy and correlation. *New Zealand journal of geology and geophysics 30*: 73-86.

Smith, R.L. 1979: Ash-flow magmatism. *Geological Society of America Special Paper 180*: 5-27.

Sparks, R.S.J. 1976: Grain size variations in ignimbrites and implications for the transport of pyroclastic flows. *Sedimentology 23*: 147-188.

Sparks, R.S.J.; Walker, G.P.L. 1977: The significance of vitric-enriched air-fall ashes associated with crystal-enriched ignimbrites. *Journal of volcanology and geothermal research 2*: 329-341.

Stothers, R.B.; Rampino, M.R. 1983: Volcanic eruptions in the Mediterranean before A.D. 630 from written and archaeological sources. *Journal of geophysical research 88*: 6357-6371.

Vucetich, C.G.; Howorth, R. 1976: Late Pleistocene tephrostratigraphy in the Taupo district, New Zealand. *New Zealand journal of geology and geophysics 19*: 51-69.

Vucetich, C.G.; Pullar, W.A. 1973: Holocene tephra formations erupted in the Taupo area and interbedded tephras from other volcanic sources. *New Zealand journal of geology and geophysics 16*: 745-780.

Walker, G.P.L. 1980: The Taupo pumice: product of the most powerful known (ultraplinian) eruption? *Journal of volcanology and geothermal research 8*: 69-94.

Walker, G.P.L. 1981a: The Waimihia and Hatepe plinian deposits from the rhyolitic Taupo Volcanic Centre. *New Zealand journal of geology and geophysics 24*: 305-324.

Walker, G.P.L. 1981b: Characteristics of two phreatoplinian ashes and their water-flushed origin. *Journal of volcanology and geothermal research 9*: 395-407.

Walker, G.P.L. 1984: Downsag calderas, ring faults, caldera sizes, and incremental caldera growth. *Journal of geophysical research 89*: 8407-8416.

Walker, G.P.L.; Wilson, C.J.N.; Froggatt, P.C. 1980a: Fines-depleted ignimbrite in New Zealand: product of a turbulent pyroclastic flow? *Geology 8*: 245-249.

Walker, G.P.L.; Self, S.; Froggatt, P.C. 1981a: The ground layer of the Taupo ignimbrite: a striking example of sedimentation from a pyroclastic flow. *Journal of volcanology and geothermal research 10*: 1-11.

Walker, G.P.L.; Wilson, C.J.N.; Froggatt, P.C. 1981b: An ignimbrite veneer deposit: the trail marker of a pyroclastic flow. *Journal of volcanology and geothermal research 9*: 409-421.

Wilson, C.J.N. 1985: The Taupo eruption, New Zealand. II. The Taupo ignimbrite. *Philosophical transactions of the Royal Society of London A314*: 229-310.

Wilson, C.J.N. 1991: Ignimbrite morphology and the effects of erosion: a New Zealand case study. *Bulletin of volcanology 53*: 635-644.

Wilson, C.J.N. 1993: Stratigraphy, chronology, styles and dynamics of late Quaternary eruptions from Taupo volcano, New Zealand. *Philosophical transactions of the Royal Society of London A343*: 205-306.

Wilson, C.J.N.; Walker, G.P.L. 1982: Ignimbrite depositional facies: the anatomy of a pyroclastic flow. *Geological Society of London journal 139*: 581-592.

Wilson, C.J.N.; Walker, G.P.L. 1985: The Taupo eruption, New Zealand. I. General aspects. *Philosophical transactions of the Royal Society of London A314*: 199-228.

Wilson, C.J.N.; Ambraseys, N.N.; Bradley, J.; Walker, G.P.L. 1980: A new date for the Taupo eruption, New Zealand. *Nature, London 288*: 252-253.

Wilson, C.J.N.; Houghton, B.F.; Lloyd, E.F. 1986: Volcanic history and evolution of the Maroa - Taupo area, central North Island. *Royal Society of New Zealand bulletin 23*: 194-223.

Wilson, C.J.N.; Switsur, V.R.; Ward, A.P. 1988: A new ^{14}C age for the Oruanui (Wairakei) eruption, New Zealand. *Geological magazine 125*: 297-300.

Zielinski, G.A.; Germani, M.S.; Mayewski, P.A.; Meeker, L.D.; Fiacco, R.J.; Whitlow, S.; Twickler, M.; Morrisin, M. 1993: Tephra and sulfate records from the GISP 2 ice core: high-resolution dating and evaluation of past volcanic eruptions. *Abstracts*, IGBP PAGES - INQUA COT Meeting "Climatic Impact of Explosive Volcanism", Tokyo: 4-5.

DAY 2: TRAVERSE OF TONGARIRO VOLCANO (OPTION A)

R. M. Briggs
Department of Earth Sciences
University of Waikato, Private Bag 3105
Hamilton, New Zealand

Briggs, R.M. 1994. Post-conference Tour Day 2A: Traverse of Tongariro Volcano. In: Lowe, D.J. (ed) Conference Tour Guides, Proceedings International Inter-INQUA Field Conference and Workshop on Tephrochronology, Loess, and Paleopedology, University of Waikato, Hamilton, New Zealand, 101-110.

Outline of Day 2, Option A (Monday 14 February)

8.00-8.45 am	Depart Tokaanu Hotel and travel via SH 47 to Mangatepopo Rd
8.45-9.00 am	Check of field gear
9.00 am-5.00 pm	Traverse of Tongariro volcano (Mangatepopo-Ketetahi Track)
5.00-5.45 pm	Travel from Okahukura Bush Car Park to Tokaanu Hotel, Tokaanu
	Evening: Dinner; Hot pools

Introductory note

The traverse will involve a moderately strenuous ≈8 hour hike and a 750 m climb, mainly in exposed alpine conditions to an altitude of ≈1860 m. It is essential that all participants carry warm clothing, waterproof anoraks or coats, woollen gloves and hat, and wear stout boots. New Zealand weather in summer, especially in these alpine areas, can be very uncertain and changeable, and the traverse is subject to fine weather. Please note that the trip will be entirely within Tongariro National Park, and collection of samples or use of geological hammers is not permitted.

The three peaks of Tongariro, Ngauruhoe, and Ruapehu were gifted to the Crown by Chief Te Heuheu Tukino of the Ngati Tuwharetoa people in 1887 'for the purposes of a National Park'. Parliament formally constituted Tongariro National Park in 1894, the first such park in New Zealand. Initially comprising only 2630 ha, the park now covers 75 260 ha and was accorded World Heritage status in January this year. The name 'Tongariro' derives from 'Tonga' *south wind* and 'riro' *carried away* and originally applied to all three volcanoes.

TONGARIRO VOLCANIC CENTRE

The Tongariro Volcanic Centre lies at the southwestern end of the Taupo Volcanic Zone, and is a NE-aligned belt of young (<260 ka) andesitic stratovolcanoes. The most prominent volcanoes are Ruapehu (2797 m), Ngauruhoe (2287 m), and Tongariro (1967 m), although Ngauruhoe is regarded as a parasitic volcano on the flank of Tongariro. Two smaller andesitic massifs, Kakaramea and Pihanga, occur to the northeast between Tongariro and Lake Taupo, and the cones and flows of Maungakatote, Pukeonake, Hauhungatahi, and Ohakune lie on the western side (Fig. 2A.1) (Cole 1978).

The oldest radiometric age of volcanism in the Tongariro Volcanic Centre is 260 ka (K-Ar age, Stipp 1968), but andesitic pebbles, presumably derived from Tongariro, occur in Lower Pleistocene conglomerates in the Wanganui district to the south (Fleming 1953). The Tongariro Volcanic Centre is presently active from vents on Ruapehu, Ngauruhoe, and Tongariro (Red Crater, Te Mari Crater), all of which have known eruptions of different types and styles over the last 150 years (Fig. 2A.2).

A major lava and ash eruption on Ruapehu occurred in 1945 but there have been small magnitude phreatomagmatic and magmatic eruptions over the 125-year historical record (Houghton et al. 1987). The most recent recorded lava flows of Ngauruhoe occurred in 1870, 1949, and 1954-55 (Gregg 1960), and there were major vulcanian eruptions in 1974 and 1975 (Nairn & Self 1978). Ngauruhoe, like Ruapehu, is a very active volcano and has had phreatomagmatic and magmatic eruptive episodes every 1-7 years, but it has been dormant since 1975. The times of historic activity from Red Crater are uncertain, but there may have been eruptions in 1855, the early 1890s, and possibly in 1926 (Gregg 1960). Eruptions from Te Mari Craters on the northern slopes of Tongariro occurred in 1869 and 1892-96 (Gregg 1960).

Volcanic activity from the Tongariro centre volcanoes has produced proximal cone-forming lava flows, autoclastic breccias, welded agglomerates and welded airfall tuffs, dikes, block- and ash-flows, or pyroclastic avalanches, tephras, and lahars. Distal ring plain deposits include lahars, debris avalanche deposits, fluvial beds, and intercalated andesitic and rhyolitic tephra deposits (Topping 1973; Topping & Kohn 1973; Hackett & Houghton 1986; Donoghue 1991; Donoghue et al. 1991, 1994) (see notes for Day 2, Option B trip).

Tongariro Volcanic Centre lavas are calc-alkaline, medium-K basaltic andesites to andesites with minor basalts and dacites (Graham & Hackett 1987; Hobden 1993). They are strongly porphyritic with phenocrysts of plagioclase, orthopyroxene, clinopyroxene, ± olivine (in basalts and basaltic andesites), ± hornblende (in andesites), ± titanomagnetite, ± ilmenite. The more primitive basaltic magmas are asthenospheric melts associated with active subduction of the Pacific plate beneath the Australian plate (Gamble et al. 1990, 1993). The andesitic rocks show abundant evidence in their petrography, presence of xenoliths, and their geochemical and isotopic compositions for crustal contamination and assimilation, and a complex variety of magmatic processes like fractional crystallization, mixing and hybridisation, and source heterogeneity (Graham & Hackett 1987; Smith & Gamble 1993). Representative chemical analyses of Tongariro Volcanic Centre lavas are given in Table 2A.1.

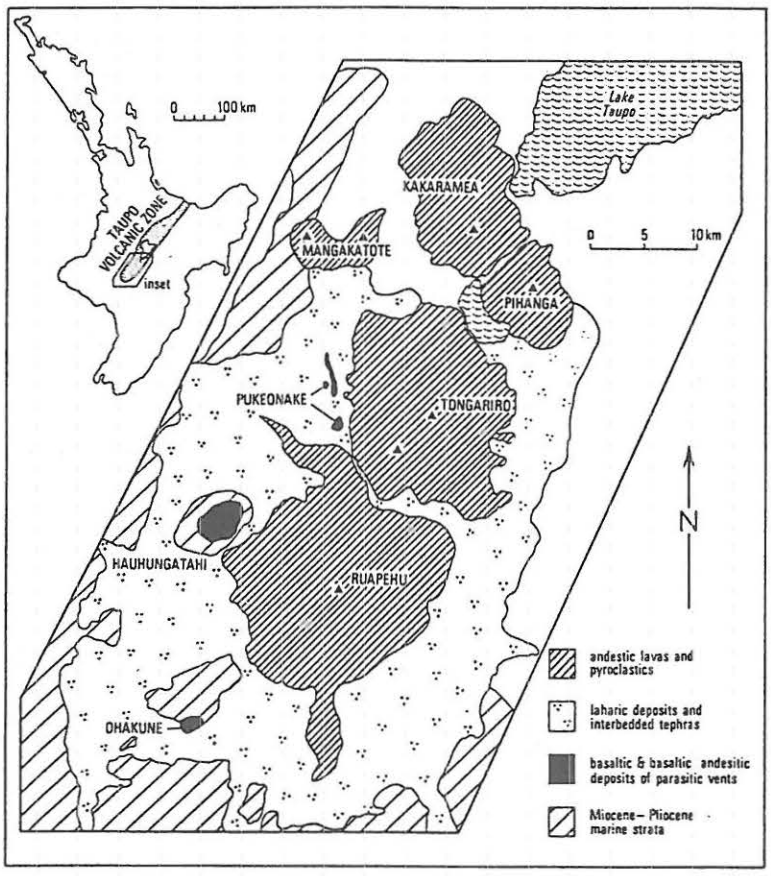

Figure 2A.1: General geology of the Tongariro Volcanic Centre (from Houghton & Hackett 1984).

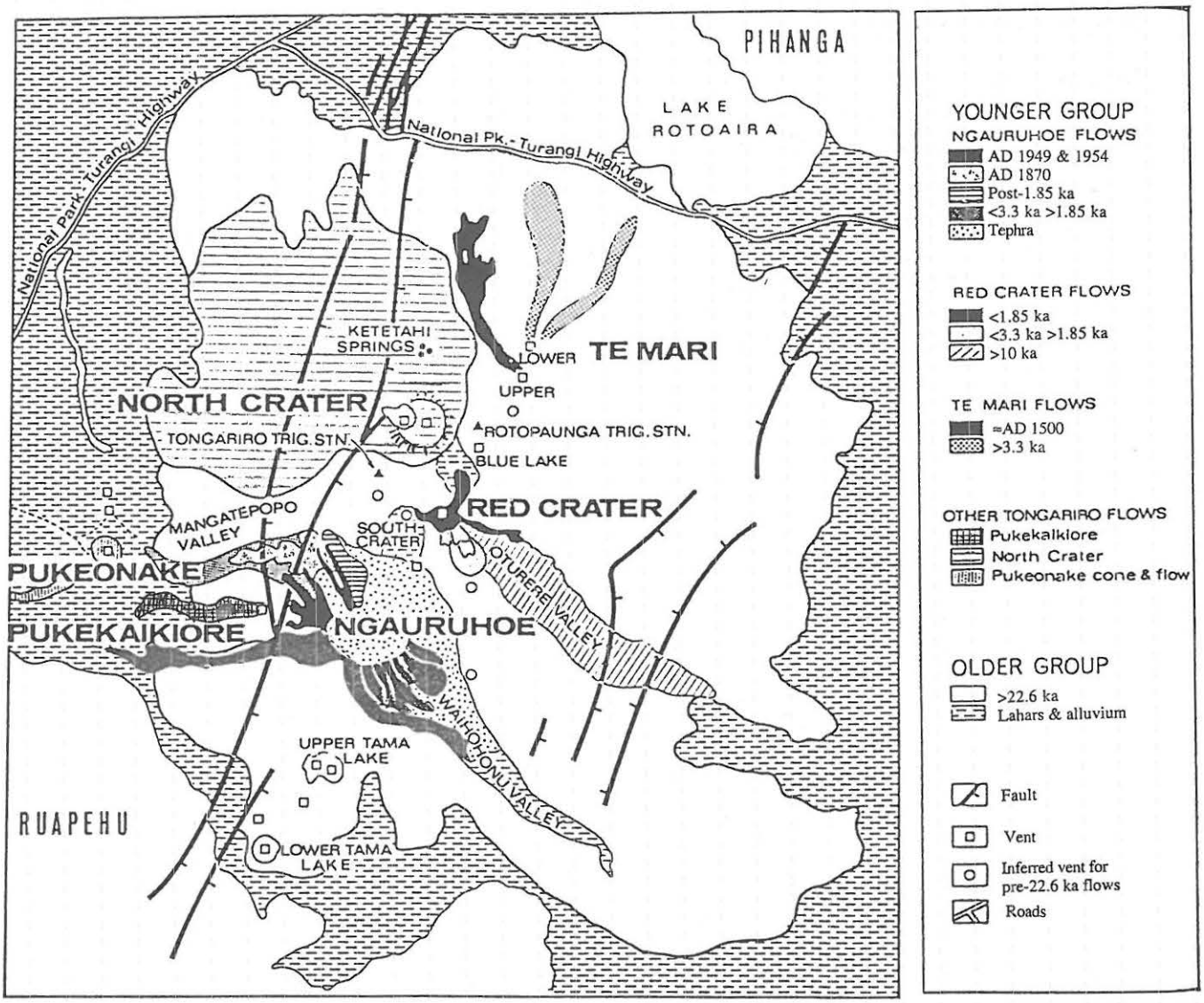

Figure 2A.2: Geological map of Tongariro volcano, showing the location of vents, lava flows and faults (from Cole 1978).

TABLE 2A.1. Representative chemical analyses of basalts, basaltic andesites, andesites, and dacites from Tongariro Volcanic Centre.

No	1	2	3	4	5	6	7
SiO_2	51.94	52.27	55.56	56.22	57.01	59.99	63.62
TiO_2	0.72	0.64	0.77	0.76	0.69	0.73	0.84
Al_2O_3	15.14	15.34	17.40	16.63	14.29	16.67	15.38
Fe_2O_3	9.82*	1.12	2.31	2.37	1.68	1.38	2.06
FeO	nd	7.45	5.52	6.14	5.54	4.95	3.20
MnO	0.17	0.16	0.12	0.15	0.15	0.09	0.04
MgO	7.60	9.15	5.00	5.24	8.64	3.80	3.12
CaO	10.19	9.61	8.11	8.31	7.26	6.49	4.76
Na_2O	2.39	2.76	2.93	3.14	2.75	3.27	3.03
K_2O	0.66	0.58	1.11	1.14	1.45	1.82	3.02
P_2O_5	0.08	0.08	0.12	0.17	0.11	0.17	0.15
LOI	0.08	0.00	1.09	0.19	0.83	0.83	0.97
Total	98.79	99.93	100.04	100.46	100.40	100.19	100.19
Ba	137	182	313	214	355	413	535
Rb	20	12	34	38	49	73	132
Sr	278	199	251	247	277	293	215
Pb	2	5	8	8	8	15	17
Th	< 2	1.09	4	4	6	10	13
Zr	68	48	84	95	115	139	226
Nb	< 2	1	2	2	5	6	6
Hf	-	1.48	-	-	-	-	-
Ta	-	0.36	-	-	-	-	-
La	6	4.64	8	10	15	17	21
Ce	12	10.7	20	29	29	33	34
Y	21	-	21	24	18	23	24
Sc	36	35	26	26	21	19	18
V	271	256	216	220	181	164	151
Cr	281	375	132	100	507	53	113
Ni	63	139	49	29	237	24	48
Cu	73	78	54	41	96	22	44
Zn	84	88	74	89	71	67	54
Ga	15	15	19	20	16	19	19
$^{87}Sr/^{86}Sr$	0.70482	-	0.70529	0.70551	0.70480	0.70584	0.70545
$^{143}Nd/^{144}Nd$	0.51280	-	-	0.51273	0.51275	-	-

1. Red Crater basalt, Tongariro (from Graham & Hackett 1987)
2. Ruapehu basalt (Gamble et al. 1993)
3. Ruapehu basaltic andesite (Graham & Hackett 1987)
4. Ngauruhoe andesite, 1954 lava flow (Graham & Hackett 1987)
5. Pukeonake andesite, hybrid lava (Graham & Hackett 1987)
6. Ruapehu andesite (Graham & Hackett 1987)
7. Ruapehu dacite (Graham & Hackett 1987)

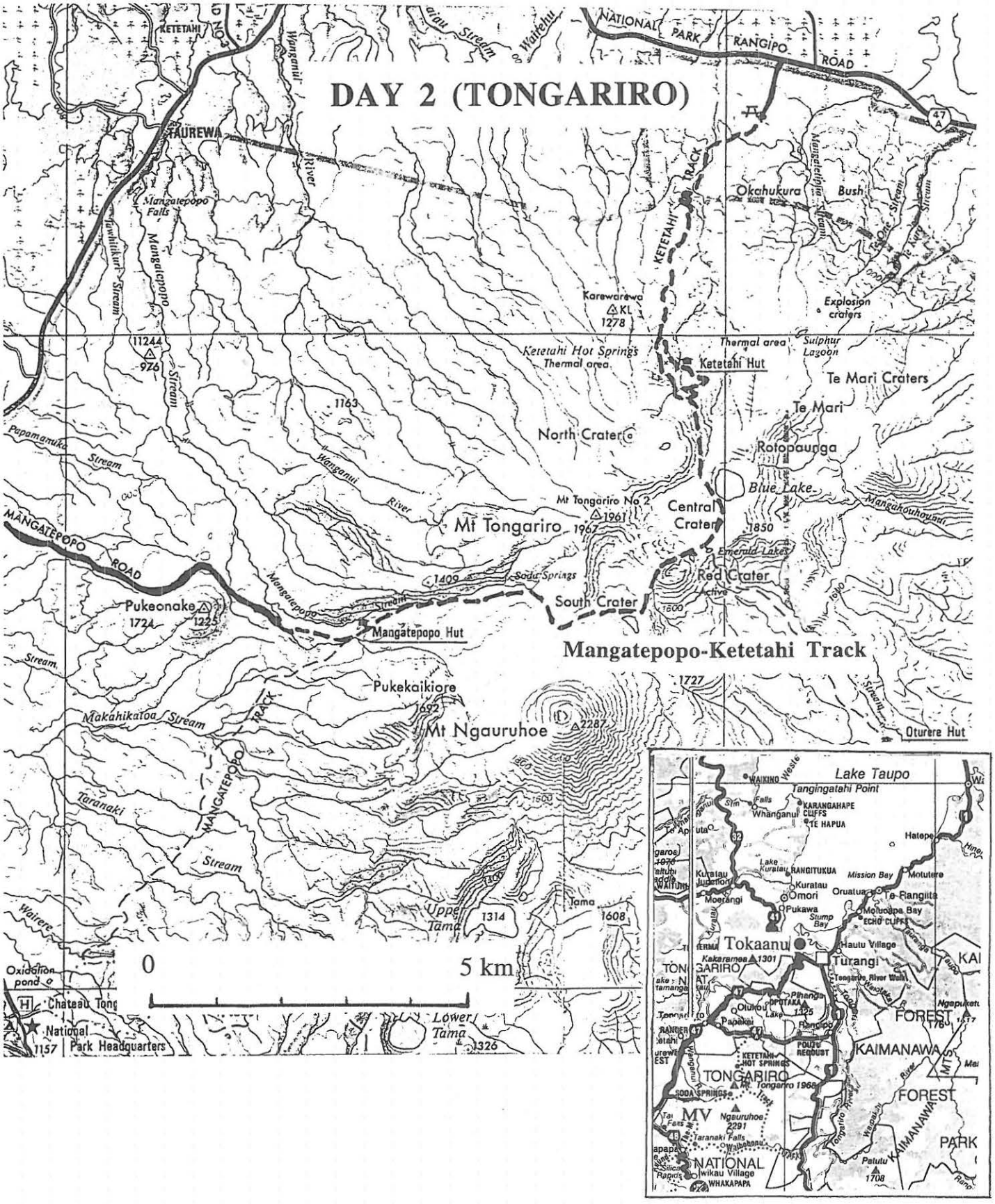

Figure 2A.3: Route map for traverse of Tongariro. Inset shows route from Tokaanu to Mangatepopo Valley (MV).

TRAVERSE OF TONGARIRO VOLCANO

Tongariro is a large (c. 80 km^3) complex stratovolcano built up by andesitic eruptions from at least 12 vents, and was probably constructed during the past 0.5 Ma (Cole 1978; Hobden 1993). It has been constructed from a number of cone-building episodes, evidenced from sequences of lavas and pyroclastics, separated by pronounced angular unconformities. The older volcanic features are modified by glacial and subaerial erosion and are dominated by sequences of lava flows, thick welded scoria cone and airfall tephra deposits, pyroclastic flows and surges, and laharic-fluvial deposits (Hobden 1993).

The traverse of Tongariro will start from the end of Mangatepopo Road, and then follow the walking track (marked with poles) towards Tongariro (Fig. 2A.3). The route passes up a broad glacial valley flanked by moraines and floored by Ngauruhoe lavas.

Pukeonake is the young (>22.6 ka) basaltic andesite scoria cone on the ring plain near the end of Mangatepopo Road. It consists of well-exposed strombolian and phreatomagmatic cone deposits, and a partly eroded summit crater which contains 22.6 ka Kawakawa Tephra (= Oruanui) deposits derived from Taupo Volcanic Centre. The lava at Pukeonake is a distinctive olivine-bearing basaltic andesite with a complex mineralogy, considered to have originated by mixing between high-magnesian basaltic andesitic and dacitic liquids (Graham & Hackett 1987).

The track passes Pukekaikiore (to the south), an eroded older massif consisting of several thick columnar-jointed lava flows, with a young vent near its summit. Lavas from Ngauruhoe have flowed up against its eastern side.

Just after the turnoff to Mangatepopo Hut, the track reaches the edge of a young pre-European lava flow with its typical rough, clinkery, aa surface. Note the contrasting growth of vegetation between this lava and the younger 1949 and 1954 lavas higher up on the northwestern flanks of Ngauruhoe. The main pioneering plants are *Dracophyllum recurvum* and *Notodanthonia setifolia.*

Ngauruhoe

Ngauruhoe is a spectacular 900 m andesitic cone (c. 2 km^3) with a 33° slope, which commenced activity about 2500 years ago. It has a recorded history of strombolian eruptions and lava flows (1954-55), and vulcanian eruptions with large ballistic ejecta, small pyroclastic flows and debris avalanches, and tephra falls (1974-75).

Ngauruhoe eruption 1954-55

About 10 million cubic metres of lava were extruded from Ngauruhoe as 10 lava flows over a four month interval between June and September 1954 (Gregg 1960). The eruption began in May 1954 with 2 weeks of weak explosive activity followed by lava extrusion, accompanied by lava fountaining to 800 m in height above the crater. The blocky lava flows were channelled by topography onto the northwestern flank of the cone. Airfall tephra (ash) was dispersed up to 70 km downwind at the height of the eruption. Minor explosive activity continued until March 1955 and lava remained in the vent until June 1955.

Ngauruhoe eruption 1974-75

A series of vulcanian eruptions took place from Ngauruhoe in 1974 and 1975 which generated avalanches of hot pyroclastic debris (Fig. 2A.4). The pyroclastic avalanches were generated by eruptions consisting of near continuous gas streaming and periodic sequences of violent discrete cannon-like explosions (Nairn & Self 1978). Blocks up to a metre across were ejected 2.8 km from the vent, with airfall tephra dispersed tens of kilometres downwind (strong southerlies carried the ash erupted on 20 February 1975 as far north as Hamilton City). Parts of the eruption column collapsed, generating hot pyroclastic avalanches, or block- and ash-flows, which funnelled down the northern flank of the volcano in a series of paler grey chutes. Nairn & Self (1978) suggested that the explosions were caused by magmatic intrusions rapidly heating confined meteoric water, and were probably largely driven by phreatic steam rather than magmatic gases.

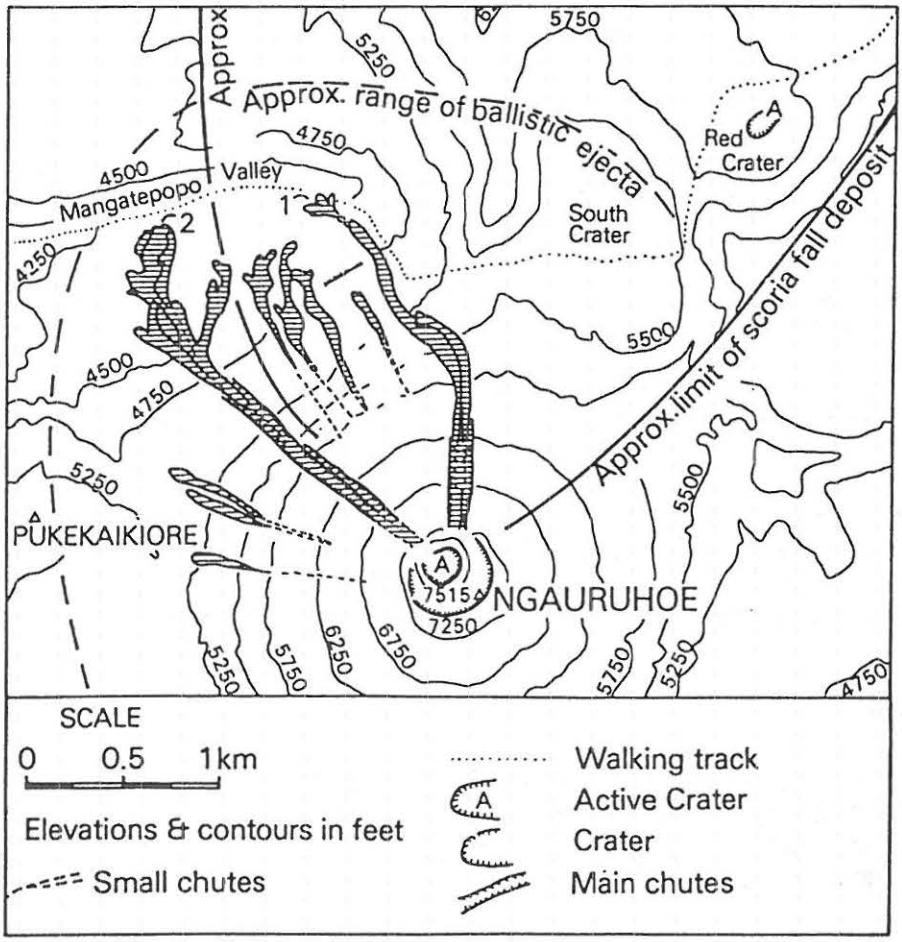

Figure 2A.4: Map of Ngauruhoe volcano, showing the location of avalanche deposits and approximate range of ballistic ejecta from the 1975 eruption (from Nairn & Self 1978).

The best examples of the pyroclastic avalanche deposits can be observed at the head of the Mangatepopo Valley. The chutes have distinct flow channels flanked on either side by levees. The temperatures of the blocks and bombs in the avalanches varies from incandescent (>900°C) to cold. The ejecta include juvenile slaggy scoriaceous andesitic bombs, some with breadcrusted and cauliflower textures indicating that they must have been hot, and have cracked and contracted on cooling. There are also accessory orange-red blocks derived from hydrothermally altered andesite on the vent rim.

Ngauruhoe lavas contain a variety of xenoliths including metaquartzites and buchitic metagreywackes. The buchites are typified by layered and lensoidal structures of alternating light coloured quartz-rich layers and darker quartz-poor layers, and are comprised of up to 80% glass and a mineral assemblage of cordierite-orthopyroxene-spinel-ilmenite-rutile-pyrrhotite (Graham et al. 1988). Tongariro eruptives elsewhere commonly contain schists and granulites (Graham & Hackett 1987).

Tongariro volcano

Good views of older Tongariro lavas can be seen at the head of Mangatepopo Valley, and the dip on these lava sections indicate that Ngauruhoe eruptives have been emplaced over the top of them and they must predate the age of Ngauruhoe volcano.

At the head of the Mangatepopo Valley, the track then climbs steeply up a pre-Taupo Tephra (= Unit Y of Wilson 1993; 1850 yr BP) Ngauruhoe flow to the Saddle. On the northern wall of the Valley, two NE-striking faults can be observed which downthrow the Tongariro lavas to the southeast.

South Crater

The route then traverses South Crater, which in fact shows little evidence of a crater origin, and may be a cirque or an older crater modified by glacial erosion. A recent pit has been blasted through its southeastern floor, and a small lava flow (post-1850 yr BP) from Red Crater descends its northern wall. The track then climbs to the lip of Red Crater (1860 m, the highest point of the traverse), and passes outcrops of welded agglomerate or spatter on the ridge between South Crater and Oturere Valley. Both pre- and post-1850 yr BP. lavas from Red Crater form the floor of the Oturere Valley where their form is well preserved.

Red Crater

Red Crater is the source of some of the most recent lava flows from Tongariro (1855, early 1890s, 1926). The crater is set in a small scoria cone, and the cone is intruded by dikes which fed lava flows from the vent. The most spectacular dike is exposed in the scoria walls of Red Crater which fed a flow into Oturere Valley. The dike has been evacuated to form a lava tube selvedged by solidified basalt.

The earlier pre-1850 yr BP lavas from Red Crater were olivine two-pyroxene andesites but all the younger flows are olivine basalts (Table 2A.1).

The most recent explosive eruptions at Red Crater were phreatic, which punched a line of explosion craters occupied by the Emerald Lakes. Topping (1974) considered that the Emerald Lakes may have formed about 1250 years ago. The lakes have pH values of 3-4. Their bright green colour is probably due to the luxuriant growth of the filamentous chlorophyte (microalgae) *Zygogonium* as green felts across the lake bottom (Vincent & Forsyth 1987). Steam vents occur in the vicinity of Red Crater and solfataric activity has been continuous during historical times.

Blue Lake Crater

The track then crosses the southern part of Central Crater and leads to the crater occupied by Blue Lake (1686 m). Blue Lake Crater is a circular crater 400 m in diameter, occupied by a 16 m deep lake. The slopes above the lake are mantled by welded airfall agglomerates and tuffs that mantle the topography, and occur in numerous distinct beds. Excellent sections of welded airfall tuffs can be observed around the crater walls and particularly on the northern Ketetahi side of North Crater. The welded airfall agglomerates and tuffs superficially resemble lava flows, and sometimes exhibit well-developed vertical cooling joints, but they show mantle bedding, internal stratification, and drape over the pre-existing topography. They were probably produced by vigorous and high fire fountaining, with high discharge and accumulation rates of ejecta (Cas & Wright 1987).

Isopachs for the 9.7 ka Poutu Lapilli, a widespread, conspicuous, strong yellowish brown tephra distributed mainly to the north and east of Tongariro, suggest that Blue Lake Crater was its source (Topping 1973) and is the distal equivalent of these welded airfall deposits.

North Crater

If time permits, we will leave the track and climb the cone of North Crater (1830 m). North Crater is a flat-topped cone with a 1100 m wide crater infilled by a cooled lava lake. In places, the lava lake overtopped the crater rim and lavas flowed down the flanks of the cone (Hackett & Houghton 1986). Welded airfall agglomerates and tuffs occur on the crater rim. A 300 m wide, 60 m deep explosion crater was excavated in the lava lake at a late stage of cooling, evidenced from radial contraction fractures in ejected blocks of the lake lavas, indicating they were erupted while still hot. The pit predates 1850 yr BP, and most of the cone predates the Te Rato Lapilli (9.7 ka), a greenish-grey tephra distributed to the northeast of Tongariro, which was probably erupted from North Crater (Topping 1973).

The Te Mari Craters on the northern slopes of Tongariro can be observed from the northern rim of North Crater. Activity at Te Mari probably commenced about 14 ka ago and has continued through to the present (Hackett & Houghton 1986). The poorly vegetated lava flows were erupted about 400-500 years ago from Te Mari and the most recent eruptions were in 1869 and 1892-96 (Gregg 1960).

Excellent views of Pihanga and Lake Rotoaira can also be seen to the north, and south of Lake Taupo, as the track descends from the summit. Note also the welded airfall tuffs mantling the upper slopes of North Crater cone. The tuffs display a decreasing degree of welding and thinning with increasing distance from source.

Ketetahi Springs

The route then descends down the northern side of Tongariro to Ketetahi, an area of hot springs (recorded up to 91°C) and fumaroles (up to 132°C).

N.B. Please take care here because some of the ground is unstable. Keep to the track.

Hot springs at Ketetahi discharge acid-sulphate water, high in boric acid and in some springs ammonia. Some pools are near neutral due to reaction of sulphate water with ammonia. The stream discharging from the springs has pH values in the range 2-5. Ketetahi may be the surface expression of a dry steam field, dominated by vapour rather than water. The area around the hot springs is extensively hydrothermally altered, and a lahar, presumably initiated by a slip in the hydrothermal area, descended from Ketetahi in historic times. The yellow, clayey lahar deposit is visible in several places near the track below Ketetahi. The microalga *Zygogonium* occasionally forms purple-coloured mats on the warm, highly acid soils around the springs (Vincent & Forsyth 1987).

The track descends below Ketetahi through subalpine tussock into Okahukura Bush, and then to the carpark adjacent to the main road. We will meet the bus at the carpark and return to Tokaanu.

REFERENCES

Cas, R.A.F.; Wright, J.V. 1987: *Volcanic successions, modern and ancient.* London, Allen and Unwin. 528p.

Cole, J.W. 1978: Andesites of the Tongariro Volcanic Centre, North Island, New Zealand. *Journal of volcanology and geothermal research 3:* 121-153.

Donoghue, S.L. 1991: Late Quaternary volcanic stratigraphy of the southeastern sector of Mount Ruapehu ring plain, New Zealand. Unpublished PhD thesis, Massey University, Palmerston North.

Donoghue, S.L.; Hodgson, K.A.; Neall, V.E.; Palmer, A.S. 1991: Volcanic hazards — southwestern ring plain of Ruapehu volcano. *Geological Society of New Zealand miscellaneous publication 59B*: 56-88.

Donoghue, S.L.; Neall, V.E.; Palmer, A.S. 1994: Late Quaternary andesitic tephrostratigraphy and chronology, Tongariro Volcanic Centre, New Zealand. *Journal of the Royal Society of New Zealand* (in press).

Fleming, C.A. 1953: The geology of Wanganui Subdivision. *New Zealand Geological Survey bulletin 52.*

Gamble, J.A.; Smith, I.E.M.; Graham, I.J.; Kokelaar, B.P.; Cole, J.W.; Houghton, B.F.; Wilson, C.J.N.1990: The petrology, phase relations and tectonic setting of basalts from the Taupo Volcanic Zone, New Zealand, and Kermadec Island Arc - Havre Trough, SW Pacific. *Journal of volcanology and geothermal research 43*: 235-270.

Gamble, J.A.; Smith, I.E.M; McCullouch, M.T.; Graham, I.J.; Kokelaar, B.P. 1993: The geochemistry and petrogenesis of basalts from the Taupo Volcanic Zone and Kermadec Island Arc, SW Pacific. *Journal of volcanology and geothermal research 54*: 265-290.

Graham, I.J.; Hackett, W.R. 1987: Petrology of calc-alkaline lavas from Ruapehu volcano and related vents, Taupo Volcanic Zone, New Zealand. *Journal of petrology 28*: 531-567.

Graham, I.J.; Grapes, R.H.; Kifle, K. 1988: Buchitic metagreywacke xenoliths from Mount Ngauruhoe, Taupo Volcanic Zone, New Zealand. *Journal of volcanology and geothermal research 35*: 205-216.

Gregg, D.R. 1960: Volcanoes of Tongariro National Park. *New Zealand Department of Scientific and Industrial Research information series 28.*

Hackett, W.R.; Houghton, B.F. 1986: Active composite volcanoes of Taupo Volcanic Zone. *New Zealand Geological Survey record 11*: 61-114.

Hobden, B.J. 1993: Volcanology and petrology of Tongariro volcano, Taupo Volcanic Zone, New Zealand. *Abstracts*, IAVCEI, Canberra: 48.

Houghton, B.F.; Hackett, W.R. 1984: Strombolian and phreatomagmatic deposits of Ohakune Craters, Ruapehu, New Zealand: a complex interaction between external water and rising basaltic magma. *Journal of volcanology and geothermal research 21*: 207-231.

Nairn, I.A.; Self, S. 1978: Explosive eruptions and pyroclastic avalanches from Ngauruhoe in February 1975. *Journal of volcanology and geothermal research 3*: 39-60.

Smith, I.E.M.; Gamble, J.A. 1993: Northland and Taupo Zone volcanism, North Island, New Zealand. *Australian Geological Survey Organisation record 1993/65.*

Stipp, J.J. 1968: The geochronology and petrogenesis of the Cenozoic volcanics of the North Island, New Zealand. Unpublished PhD thesis, Australian National University, Canberra.

Topping, W.W. 1973: Tephrostratigraphy and chronology of Late Quaternary eruptives from the Tongariro Volcanic Centre, New Zealand. *New Zealand journal of geology and geophysics 16:* 397-423.

Topping, W.W. 1974: Some aspects of Quaternary history of Tongariro Volcanic Centre. Unpublished PhD thesis, Victoria University of Wellington, Wellington.

Topping, W.W.; Kohn, B.P. 1973: Rhyolitic tephra marker beds in the Tongariro area, North Island, New Zealand. *New Zealand journal of geology and geophysics 16:* 375-395.

Vincent, W.J.; Forsyth, D.J. 1987: Geothermally influenced waters. *In* Viner, A.B. (ed) Inland Waters of New Zealand. *New Zealand Department of Scientific and Industrial Research bulletin 241*: 349-377.

DAY 2: RANGIPO 'DESERT' (OPTION B)

A. S. Palmer
Department of Soil Science
Massey University, Private Bag 11-222
Palmerston North, New Zealand

S. M. Donoghue
Department of Geography & Geology
University of Hong Kong
Pokfulam Road, Hong Kong

S. J. Cronin
Department of Soil Science
Massey University, Private Bag 11-222
Palmerston North, New Zealand

Palmer, A.S., Donoghue, A.M., Cronin, S.J. 1994. Post-conference Tour Day 2B: Rangipo 'Desert'. In: Lowe, D.J. (ed) Conference Tour Guides, Proceedings International Inter-INQUA Field Conference and Workshop on Tephrochronology, Loess, and Paleopedology, University of Waikato, Hamilton, New Zealand, 111-138.

Outline of Day 2, Option B (Monday 14 February)

8.00-8.20 am	Depart Tokaanu Hotel and travel to Poutu
8.20-8.50 am	STOP 1 — Poutu tephra section
8.50-9.20 am	Travel to Desert Rd Section 15.
9.20-9.50 am	STOP 2 — DR15. Mangamate Formation (9.95-8.7 ka)
9.50-10.10 am	Travel to Bullot Track
10.10-11.10 am	STOP 3 — Bullot Track. Bullot Formation (22.6-9.95 ka)
11.10-11.30 am	Travel to Whangaehu Cliffs
11.30-1.15 am	STOP 4 — Whangaehu Cliffs (LUNCH if fine). Tephras 0-15 ka over lahars
1.15-1.30 pm	Travel to Waiouru
1.30-1.45 pm	Waiouru comfort stop (and lunch if windy or wet)
1.45-2.00 pm	Travel to Tangiwai Bridge
2.00-2.10 pm	Tangiwai Bridge: photo opportunity (site of 1953 rail disaster)
2.10-2.20 pm	Travel to Tirorangi Marae
2.20-2.50 pm	STOP 5 — Tirorangi Marae. Holocene lahars
2.50-3.30 pm	Travel to Waikato Stream
3.30-5.00 pm	STOP 6 — Waikato Stream (a) Late Holocene tephras (b) Papakai Formation c. 9.7-3.4 ka (c) Mangamate Formation c. 9.95-9.7 ka (d) Bullot Formation c. 22.6-9.95 ka (e) Oruanui Ignimbrite c. 22.6 ka (f) Pre 22.6 ka tephras and lahars
5.00-5.30 pm	Travel to Tokaanu Hotel, Tokaanu Evening: Dinner; Hot pools

LATE QUATERNARY DEPOSITS, EASTERN TONGARIRO VOLCANIC CENTRE

Today we travel south across the 'Desert Road' east of the volcanoes of the andesitic Tongariro Volcanic Centre. (see notes for Day 2, Option A) (Fig. 2B.1) The term 'desert' is a misnomer as the area receives more than 1200 mm rainfall per annum. The devegetated landscape is due to a combination of factors including:

1. Devastation following the Taupo Ignimbrite eruption 1.85 ka.

2. Active aggradation of debris flows, hyperconcentrated flows, and fluvial deposits on the Whangaehu fan. The Whangaehu Fan and River has been the main conduit of debris flows, hyperconcentrated flows, and stream flow from the eastern side of the mountains.

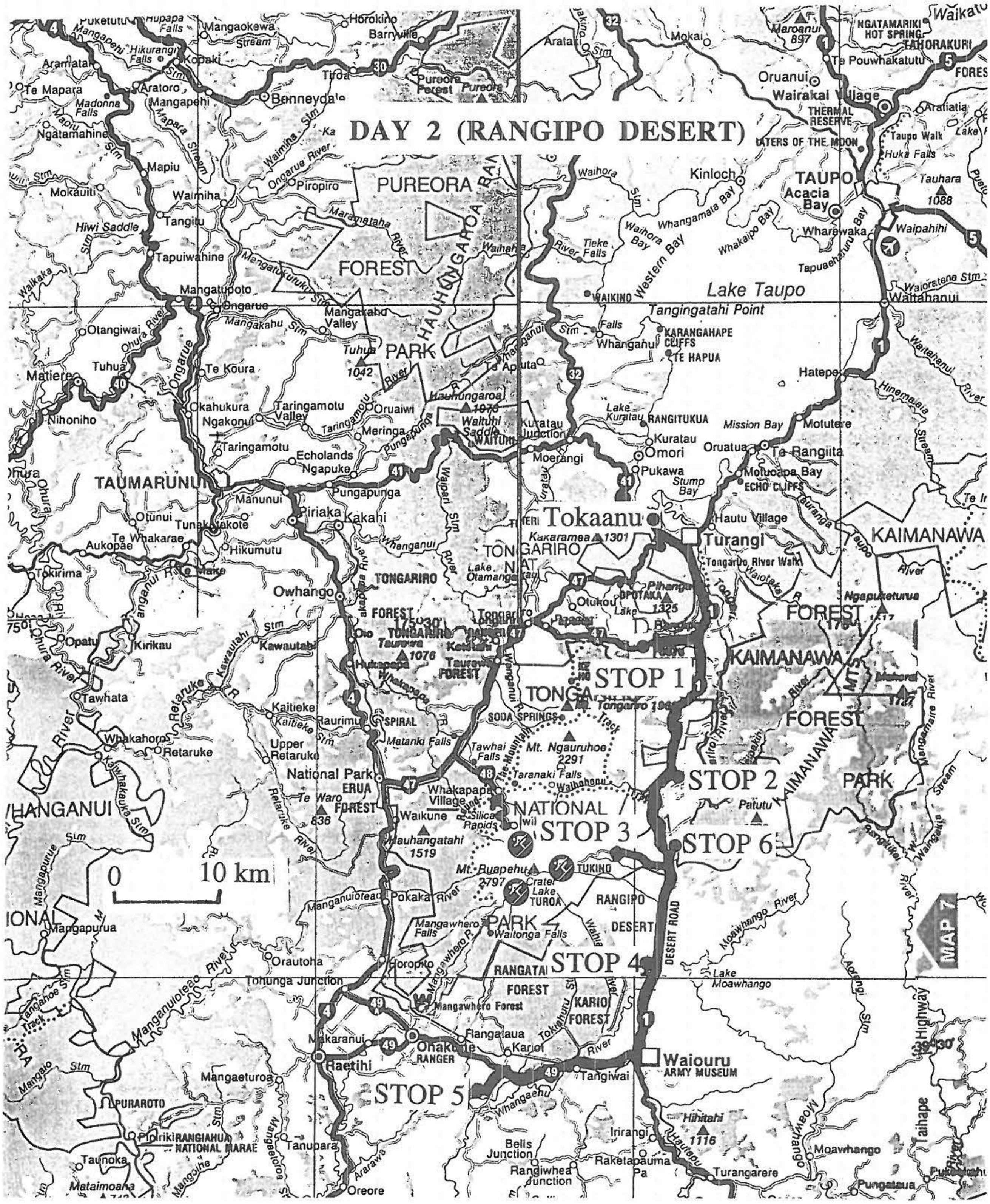

Figure 2B.1: Route map for Day 2 (Option B): eastern Tongariro Volcanic Centre.

3. The prevailing westerly winds blow tephra towards the east, thus tephra deposits (albeit relatively minor in the Holocene) are thicker on the eastern side.

4. Fires have been an important factor in at least the last 1000 years, and late last century when attempts were made to farm the area.

5. Aeolian and fluvial erosion are features of this area.

Mt Ruapehu was particularly active c. 22.6—10 ka with the eruption of a series of sub-plinian pumiceous andesitic tephras (the Bullot Formation). A period of quiescence followed, but there was renewed activity at Tongariro in a spectacular burst of pumiceous and lithic tephra between c. 9.95 and 9.7 ka (the Mangamate Formation). It may or may not be coincidental that a series of significant rhyolitic eruptions occurred at Taupo at around this time (Wilson 1993). Holocene eruptive activity at both Ruapehu and Tongariro has been relatively minor. The last c. 2.5 ka has seen spectacular growth of Ngauruhoe cone on Tongariro and a number of minor phreatomagmatic eruptions through the crater lakes on Mt Ruapehu. Since the formation of the Crater Lake, Ruapehu has been the source of frequent lahars.

The stops for today should provide some feel for the eruptive and other activity on the eastern side of Tongariro Volcanic Centre. Information for each site is drawn from PhD theses of Sue Donoghue (1991), Katy Hodgson (1993), and Shane Cronin (in progress), all supervised by Drs Vince Neall, Alan Palmer, and Bob Stewart at Massey University. Note that because this work was completed prior to Wilson's (1993) revision of the stratigraphy and chronology of late Quaternary eruptives from Taupo volcano, then names and ages used for Taupo-derived tephra deposits essentially follow those of Topping & Kohn (1973) and Froggatt & Lowe (1990). [A summary of Wilson's (1993) revision is given in Table 1.1.]

A complex stratigraphy has been erected (Fig. 2B.2). At each stop it will be easiest to refer to this summary figure first to establish the time-frame and formation names. A more detailed list of the interdigitating rhyolitic and andesitic tephra beds is given in Table 2B.1.

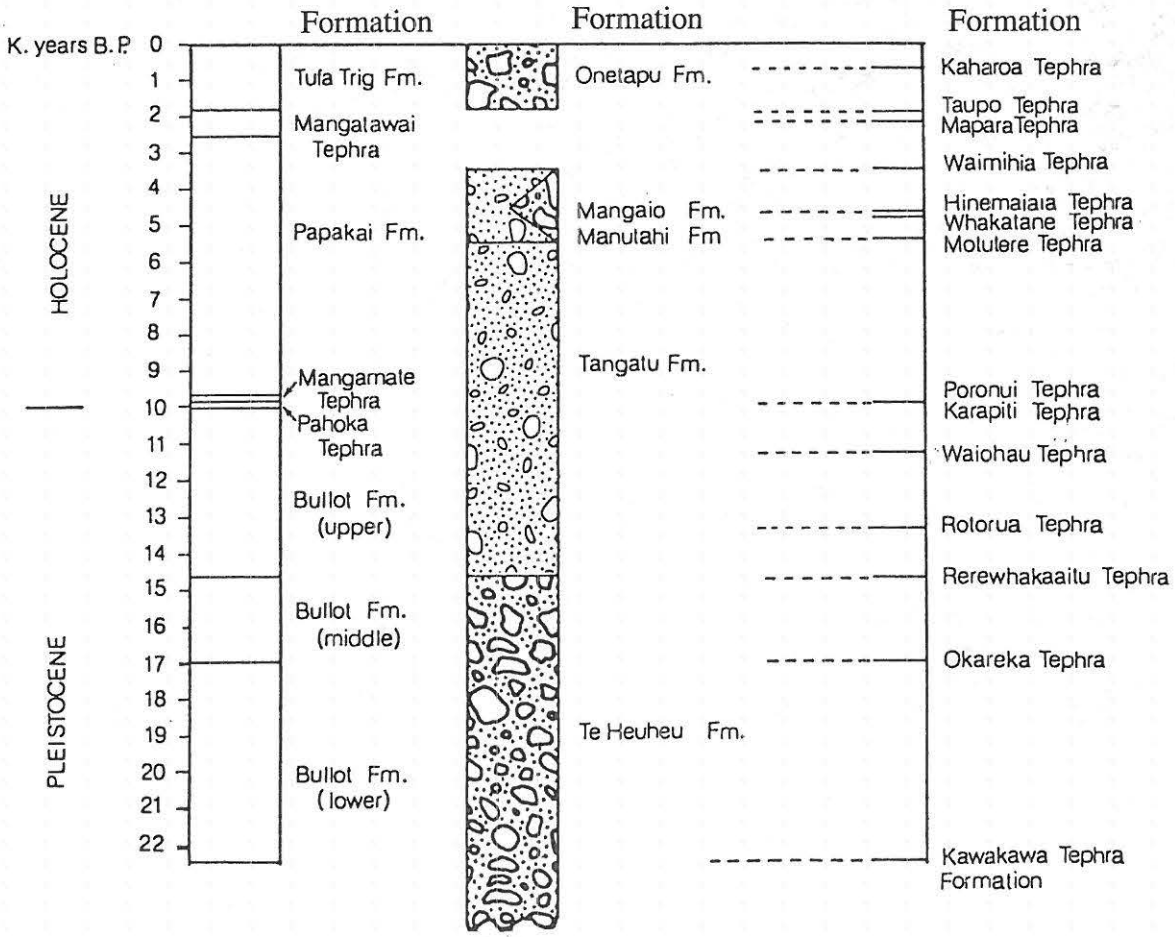

Figure 2B.2: Summary of the stratigraphy and chronology (22.6-0 ka) of Tongariro Volcanic Centre-derived andesitic tephras, distal rhyolitic tephras from Taupo and Okataina volcanoes, and laharic deposits preserved on the SE Mt Ruapehu ring plain (Donoghue 1991).

TABLE 2B.1. Stratigraphy and chronology of andesitic and rhyolitic (italicised) tephras preserved on the southeastern Mt Ruapehu ring plain (from Donoghue 1991; Donoghue et al. 1991a, 1994).

Formation	Member		Source [§]	Age [*] (years B.P.)	^{14}C No.	Reference to Age
Tufa Trig Formation & Ngauruhoe Formation	Tf18 – Tf8 [a]	Tf Ng	Mt Ruapehu TgVC	*c.* 1800 to present		Defined this study Redefined this study
Kaharoa Tephra		*Ka*	*OVC*	*665 ± 58*		
Tufa Trig Formation & Ngauruhoe Formation	Tf7 – Tf1	Tf Ng	Mt Ruapehu TgVC			Defined this paper Redefined this paper
Taupo Pumice	*Taupo Ignimbrite*	*Tp*	*TVC*	*c. 1819 ± 17* [†]		
Mangatawai Tephra		Mg	Mt Ngauruhoe			Redefined this paper
Mapara Tephra		*Mp*	*TVC*	*c. 2100*		
Mangatawai Tephra		Mg	Mt Ngauruhoe	2500 ± 200	NZ188	Fergusson & Rafter (1959)
Papakai Formation		Pp	TgVC			
Waimihia Tephra		*Wm*	*TVC*	*c. 3400*		
Papakai Formation	black ash-2	ba-2	Mt Ruapehu			
Hinemaiaia Tephra		*Hm*	*TVC*	*4650 ± 80*		
Papakai Formation	black ash-1 orange lapilli-2 orange lapilli-1	ba-1 or-2 or-1	Mt Ruapehu Mt Ruapehu Mt Ruapehu			
Whakatane Tephra		*Wk*	*OVC*	*4770 ± 170* [†]		
Papakai Formation		Pp	TgVC			
Motutere Tephra		*Mt*	*TVC*	*5370 ± 90*		
Papakai Formation		Pp	TgVC			
Mangamate Formation		Mm	Mt Tongariro			
	Poutu Lapilli Wharepu Tephra	Pt Wp	Mt Tongariro Mt Tongariro	*c.* 9700		Topping (1973)
Poronui Tephra		*Po*	*TVC*	*c. 9900* [†]		
Mangamate Formation	Ohinepango Tephra Waihohonu Lapilli unnamed tephra Otutere Lapilli Te Rato Lapilli	Oh Wa ut' Ot Tt	Mt Tongariro Mt Tongariro - Mt Tongariro Mt Tongariro	9780 ± 170	NZ1372	Topping (1973)
unnamed	unnamed tephra		-			
Karapiti Tephra		*Kp*	*TVC*	*9910 ± 130*		
unnamed tephra			-			
Pahoka Tephra		Pa	Mt Tongariro	*c.* 10 000 – 9800		Topping (1974)
Bullot Formation (upper)		Bt	Mt Ruapehu	*c.* 10 000		
	Ngamatea lapilli-2 Ngamatea lapilli-1 Pourahu Member L18 – L17 Shawcroft Tephra L16	Nt-2 Nt-1 Ph Sh 	Mt Ruapehu Mt Ruapehu Mt Ruapehu Mt Ruapehu Mt Ruapehu Mt Ruapehu			Defined this paper
Waiohau Tephra		*Wh*	*OVC*	*11 250 ± 200*		
Bullot Formation (upper)	L15 – L8	Bt	Mt Ruapehu			
?Rotorua Tephra [b]		*Rr*	*OVC*	*13 450 ± 250*		
Bullot Formation (upper)		Bt	Mt Ruapehu			
Rotoaira Lapilli [b]		Rt	Mt Tongariro	13 800 ± 200	NZ1559	Topping (1973)
Bullot Formation (upper)	L15 – L8	Bt	Mt Ruapehu			
Rerewhakaaitu Tephra		*Rk*	*OVC*	*14 700 ± 200*		
Bullot Formation (middle)	L7b – L4	Bt	Mt Ruapehu			
Okareka Tephra		*Ok*	*OVC*	*c. 17 000* [‡]		
Bullot Formation (lower)	L3 – L1	Bt	Mt Ruapehu			
Kawakawa Tephra Fm.		*Kk*	*TVC*	*22 590 ± 230* [†]		

[*] All ^{14}C ages discussed are conventional ages in radiocarbon years B.P. based on the old (Libby) half life of 5568 years.

[†] Average or combined radiocarbon age.

[‡] Estimated age.

[§] TVC = Taupo Volcanic Centre; OVC = Okataina Volcanic Centre; TgVC = Tongariro Volcanic Centre.

[a] Exact stratigraphic position of Kaharoa Tephra relative to Tufa Trig Formation members is unknown.

[b] Exact stratigraphic position of these tephras relative to Bullot Formation members is unknown.

STOP 1 — Poutu Tephra Section (PT)

This roadcut is representative of sections on the northern slopes of Tongariro. Late Pleistocene and Holocene rhyolite tephras from Taupo and Okataina volcanic centres are well represented. Once identified and correlated they are valuable chronostratigraphic marker beds. All the andesitic tephra formations recognised (Mangatawai, Papakai, Mangamate, Pahoka, and Bullot) are thin because this section is well north of the dominant dispersal axis and NW prevailing wind direction for deposition of tephra from the volcanoes of the Tongariro Volcanic Centre.

Poutu Description

Section Name and Map Code: Poutu [PT]

Grid Reference: T19/481325 [N112/239901]

Locality: A large cutting on the National Park–Taupo Road, 5.7 km west of Rangipo. Description taken from Topping (1973), with modifications (this study) given in italics

Formation	*Member*	*Unit Depth (mm)*	*Cum. Depth (m)*	*Description*
Taupo Pumice		400	0.400	Pale yellow rhyolitic ash, lapilli and blocks
Mangatawai Tephra		420	0.820	Dark yellowish brown and dark grey ash
Papakai Formation & Waimihia Tephra & Hinemaiaia Tephra		300	1.120	Yellowish brown andesitic ash, with interbedded pale brown fine ash (Waimihia Tephra) and white coarse pumiceous ash (Hinemaiaia Tephra)
Papakai Formation		200	1.320	Strong brown ash with grey lithic lapilli dispersed throughout; paleosol
Papakai Formation & Motutere Tephra		200	1.520	Strong brown ash with interbedded pale brown fine and coarse ash 'cream cakes' (Motutere Tephra)
Mangamate Tephra	Poutu Lapilli	900	2.420	Brownish yellow weakly bedded lapilli
	Wharepu Tephra	60	2.480	Very dark greyish brown to dark olive grey ash
Poronui Tephra		30	2.510	Pale yellow fine rhyolitic ash
Mangamate Tephra	Ohinepango Tephra	60	2.570	30 mm Strong brown medium ash 30 mm Very dark grey medium ash
	Waihohonu lapilli	30	2.600	Yellowish red medium and coarse ash and fine lapilli
	unnamed tephra	30	2.630	Brown ash
	Oturere Lapilli	10	2.640	Yellowish brown medium lapilli
	Te Rato Lapilli	160	2.800	Very dark grey coarse ash and lapilli and pale yellow lapilli
***	***	*90*	2.890	*Dark brown sandy clay loam textured ash, greasy*
Pahoka Tephra		*20*	2.910	*Dark grey fine pumiceous lapilli and fine angular, platy pumiceous fragments; indistinct tephra*
?Bullot Formation (upper)	*unnamed*	530	3.440	*Greyish brown sandy clay loam textured ash, and interbedded yellowish brown fine lapilli; discrete lapilli beds*
?Waiohau Tephra		20	3.460	Yellow fine rhyolitic ash; discontinuous tephra
?Bullot Formation (upper)	*unnamed*	710	4.170	*Greyish brown andesitic ash; prominent; sharp lower contact*
Rotoaira Lapilli		380	4.550	160 mm Yellowish red coarse ash and lapilli 20 mm Black ash 20 mm Shower bedded brownish lapilli and coarse ash; erosion break
?Bullot Formation (upper)	*unnamed*	120	4.670	Yellowish brown ash with scattered strong brown lapilli
Rerewhakaaitu Tephra		80	4.750	Light olive brown ash with sparse strong brown lapilli; a few angular cobbles throughout these two units which may be water-laid; in places up to 50 mm white rhyolitic ash present (may not be primary)
?Bullot Formation	*unnamed*	380	5.130	Shower bedded strong brown and brownish yellow ash and lapilli
Hinuera Formation		820	5.950	Current bedded gravelly sands; erosion break
Oruanui Formation *(Kawakawa Tephra Formation)*	Oruanui Breccia *(Oruanui Ignimbrite)*	390	6.340	Pale brownish grey massive ash with scattered pumice lapilli
	Oruanui Ash *(Aokautere Ash)*	570	6.910	310 mm Very pale brown ash, shower bedded and studded with chalazoidites up to 30 mm across 100 mm Very pale brown shower bedded ash 40 mm Pale yellow shower bedded ash 120 mm Pale yellow shower bedded fine and coarse ash; sharp contact with
		2000+	8.910	Tuff, lapilli tuff and alluvium

STOP 2 — Desert Road Section 15 (DR15)

Our objective here is to examine the Mangamate Formation — six andesitic tephras erupted c. 9.9-9.7 ka from various craters on Mt Tongariro (Topping 1973; Donoghue 1991). These tephras are unusual for the dense nature of their pumice and high proportion of lithics, which often include schist xenoliths. Some tephras contain forsteritic olivine with two crystals habits: (a) granular or polyhedral, and (b) skeletal euhedral hopper and H-chain morphologies (Donoghue et al. 1991b).

There are six tephra members to the formation (i.e. overlying Karapiti Tephra):

Andesitic tephra	Rhyolite tephra	
Poutu Lapilli Wharepu Tephra		
	Poronui Tephra	9740 yr BP
Ohinepango Tephra Waihohonu Lapilli Oturere Lapilli Te Rato Lapilli		
	Karapiti Tephra	9910 ± 130 yr BP
Pahoka Tephra		

In this section we can also examine the Papakai Formation — a series of younger, fine-grained andesitic tephra beds containing rhyolite marker beds (Table 2B.1). The base of the section is marked by the uppermost part of the Bullot Formation.

STOP 3 — Bullot Track Section 1 (BT1)

Bullot Track is an unsurfaced road into Mt Ruapheu's third and least development skifield at Tukino. The landscape is typical of the northern Rangipo Desert.

As we leave State Highway 1, the track soon passes from a surface that has not been invaded by lahars for c. 22 500 years to the actively-aggrading Whangaehu Fan. The pattern of soils and vegetation on the fan, together with tephra and aeolian sand cover, can be used to establish the ages of different parts of the fan. Whangaehu Fan is the most actively aggrading lahar suface on the Ruapehu ring plain.

The type section for tephra beds of the Bullot Formation is located near the terminus of lava flows where slopes steepen on the lower flanks of the mountain. Our objective here is to examine andesitic tephras of the Bullot Formation. Oruanui Ignimbrite (c. 22.6 ka) has been located at the base of the section and members of the Mangamate Formation overlie the Bullot Formation. Thus the tephras we will examine were deposited between c. 22.6 and c. 9.95 ka, i.e. during the last cold period followed by warming towards the Holocene. The section is remarkable for its lack of paleosols and evidence of time between eruptions. Nineteen major sub-phinian andesitic lapilli units and a number of minor lapilli and ashes are present in the formation.

Correlation of Bullot Formation members to other sections (e.g. Waikato Stream, Stop 6) has proven difficult, because of variable distribution of the various members and hydrological conditions at each site altering their appearance. Donoghue (1991) employed a variety of techniques both in the field and in the laboratory to characterise the major units (Fig. 2B.3).

Correlation and recognition of the andesitic tephras of the Bullot Formation, and interbedded rhyolitic tephras, is important because it allows the dating and mapping of major laharic surfaces constructed in the region during their deposition. Laharic deposits that correspond to the lower and middle Bullot Formation tephras are Te Heuheu Formation, while those deposited during the time of the upper Bullot Formation tephras are included in Tangatu Formation (Fig 2B.2) (Donoghue 1991).

Desert Road Description

Section Name and Map Code: Desert Road Section 15 [DR15]

Grid Reference: T20/462135

Locality: A large cutting on the eastern side of the Desert Road, immediately south of a crossing over a tributary of Te Piripiri Stream

Formation	*Member*	*Unit Depth (mm)*	*Cum. Depth (m)*	*Description*
Ngauruhoe Formation		160	0.160	Dark brown sandy loam textured unit; with an iron-stained basal contact
Tufa Trig Formation	member Tf5	10	0.170	Black coarse ash
***	***	30	0.200	Dark brown sandy loam textured ash; paleosol developed in Taupo Ignimbrite
Taupo Pumice	Taupo Ignimbrite	520	0.720	White poorly sorted coarse ash and lapilli; average depth 260 mm
Mangatawai Tephra		470	1.190	250 mm Very dark greyish brown (2.5Y3/2) fine sandy loam textured ash, greasy, with two interbedded black medium ash beds; with dark brown coated root channels; paleosol 220 mm Alternately bedded black coarse ash and greyish brown (2.5Y3/2) greasy fine sandy loam textured ash beds
Papakai Formation		180	1.370	Dark yellowish brown (10YR4/4) coarse sandy loam textured ash, greasy; with distinct root channels, and occasional scattered lapilli
Waimihia Tephra		20	1.390	Pale brown to white fine ash 'cream cakes', and intermixed brown fine andesitic ash; distinct tephra
Papakai Formation		270	1.660	Dark yellowish brown (10YR4/4) medium sandy clay loam textured ash, very greasy, with many distinct dark brown coated root channels; indistinct contacts
Hinemaiaia Tephra		90	1.750	Olive yellow (2.5Y6/6) and white coarse pumiceous ash dispersed throughout dark yellowish brown (10YR4/4) greasy sandy clay loam textured Papakai Formation; indistinct boundaries
Papakai Formation		410	2.160	Dark yellowish brown (10YR4/4) and dark brown (7.5YR4/4) sandy clay loam textured ash, very greasy, with moderately well developed nut structure, and cracked exterior; with many scattered bluish grey lithic lapilli interbedded nears base; distinct dark coated root channels; paleosol
Motutere Tephra		25	2.185	Pale pinkish brown coarse and fine ash 'cream cakes', grading laterally to scattered fine pumice fragments; indistinct lower contact
Papakai Formation		270	2.455	Dark yellowish brown (10YR4/4) and dark brown (7.5YR4/4) sandy clay loam, very greasy, with cracked exterior; some interbedded white pumice fragments; dark greyish brown coated root channels; paleosol
Mangamate Tephra	Poutu Lapilli	330	2.785	320 mm Strong brown (7.5YR5/6) iron-stained dominantly fine, and very fine lapilli, with dark greyish brown (2.5Y4/2) and strong brown (7.5YR5/6) interiors; firm, angular, non- and poorly vesicular lapilli; lithic lapilli dominant; weakly cemented at surface of outcrop; normally graded tephra
		10	2.795	Black coarse ash, firm; sharp distinct basal contact

DR15 contd

Formation	Member	Unit Depth (mm)	Cum. Depth (m)	Description	
Mangamate Tephra	Wharepu Tephra	770	3.565	480 mm	Grey and strong brown (7.5YR5/6) non- and poorly vesicular lapilli; loose, angular lapilli; normally graded bed, grading upwards from fine and medium lapilli (<20 mm) to fine lapilli (<10 mm) and very fine lapilli; coarsest of the three beds; sharp grain size contrast at contact with overlying Poutu Lapilli
				210 mm	Olive, and strong brown non- and poorly vesicular lapilli; normally graded bed, grading upwards from fine and very fine lapilli to granule dominant top 80 mm
				2 mm	Brown fine ash, firm, distinct; sharp contacts
				110 mm	Strong brown (7.5YR5/6) non- and poorly vesicular lapilli, weakly cemented at surface of outcrop; reversely graded bed, grading upwards from very fine and fine lapilli to dominantly fine lapilli
				30 mm	Brown fine silty textured ash with some scattered lapilli; sharp basal contact
Poronui Tephra		15	3.580	White fine rhyolitic ash, pocketing, discontinuous in outcrop	
Mangamate Tephra	Ohinepango Tephra	390	3.970	Colour-banded tephra comprising alternating 30 mm beds of strong brown (7.5YR5/8) very fine pumice lapilli and coarse ash dominant beds, and black (2.5Y2/0) very fine lithic lapilli dominant and coarse ash beds; sharp contacts	
	Waihohonu Lapilli	340	4.310	110 mm	Grey and strong brown lapilli; reversely graded bed, grading upwards from dominantly fine to dominantly medium lapilli; loose, with 5 mm fine ash base
				130 mm	Dominantly fine grading upwards to dominantly medium lapilli; reversely graded bed
				100 mm	Well sorted very fine lapilli dominant bed; with two distinct 20 mm thick strong brown (7.5YR5/8) pumice dominant beds near base
				20 mm	Black lithic-rich coarse ash and very fine lapilli
	unnamed tephra	180	4.490	20 mm	Greyish brown very fine lapilli and minor coarse ash contact;
				10 mm	Grey coarse ash
				20 mm	Black coarse ash, well sorted; with occasional lithic lapilli
				60 mm	Alternating 10–15 mm beds of fine and very fine lithic dominant lapilli and ash
				10 mm	Brown greasy coarse sandy loam textured ash
				60 mm	Dark grey (2.5Y4/0) coarse ash
	Oturere Lapilli	390	4.880	Very dark grey (5Y3/1) and very dark greyish brown (2.5Y3/2) fine lithic lapilli, and minor light yellowish brown (2.5Y6/4) fine pumice lapilli; angular, loose lithic and pumice lapilli; weakly bedded unit with coarser central 60 mm comprising dominantly medium lapilli	
***	***	210	5.090	70 mm	Light grey (2.5Y7/0 to 2.5Y7/2) gleyed greasy sandy clay textured ash, sticky; with scattered fine and very fine pumice lapilli; with yellowish red iron-stained lower contact
				30 mm	Strong brown very fine pumice lapilli and black very fine lithic lapilli; compacted
				70 mm	Alternating beds of greasy coarse sandy clay loam textured ash, and very fine lithic and pumice lapilli; strong iron-stained lower contact
				40 mm	Olive sandy clay textured ash, sticky; with scattered fine brown pumice lapilli; iron-stained basal contact.
Pahoka Tephra		190	5.280	170 mm	Grey (2.5Y5/0 to 2.5Y6/0) and pale yellow colour-banded fine and very fine pumiceous lapilli, with very fine angular, platy pumiceous fragments concentrated in top 70 mm; normally graded lapilli unit;
				20 mm	Pale yellow pumiceous and black coarse lithic ash
Bullot Formation (upper)	unnamed	190	5.470	90 mm	Very fine pumice and lithic lapilli in brown coarse ash
				100 mm	Dark yellowish brown (10YR4/4) greasy, sticky sandy clay textured ash
	Pourahu Member [tephra unit]	160+	5.630	Pale brown (10YR6/3) and yellowish brown (10YR5/6) very fine and fine pumice and lithic lapilli and coarse ash	

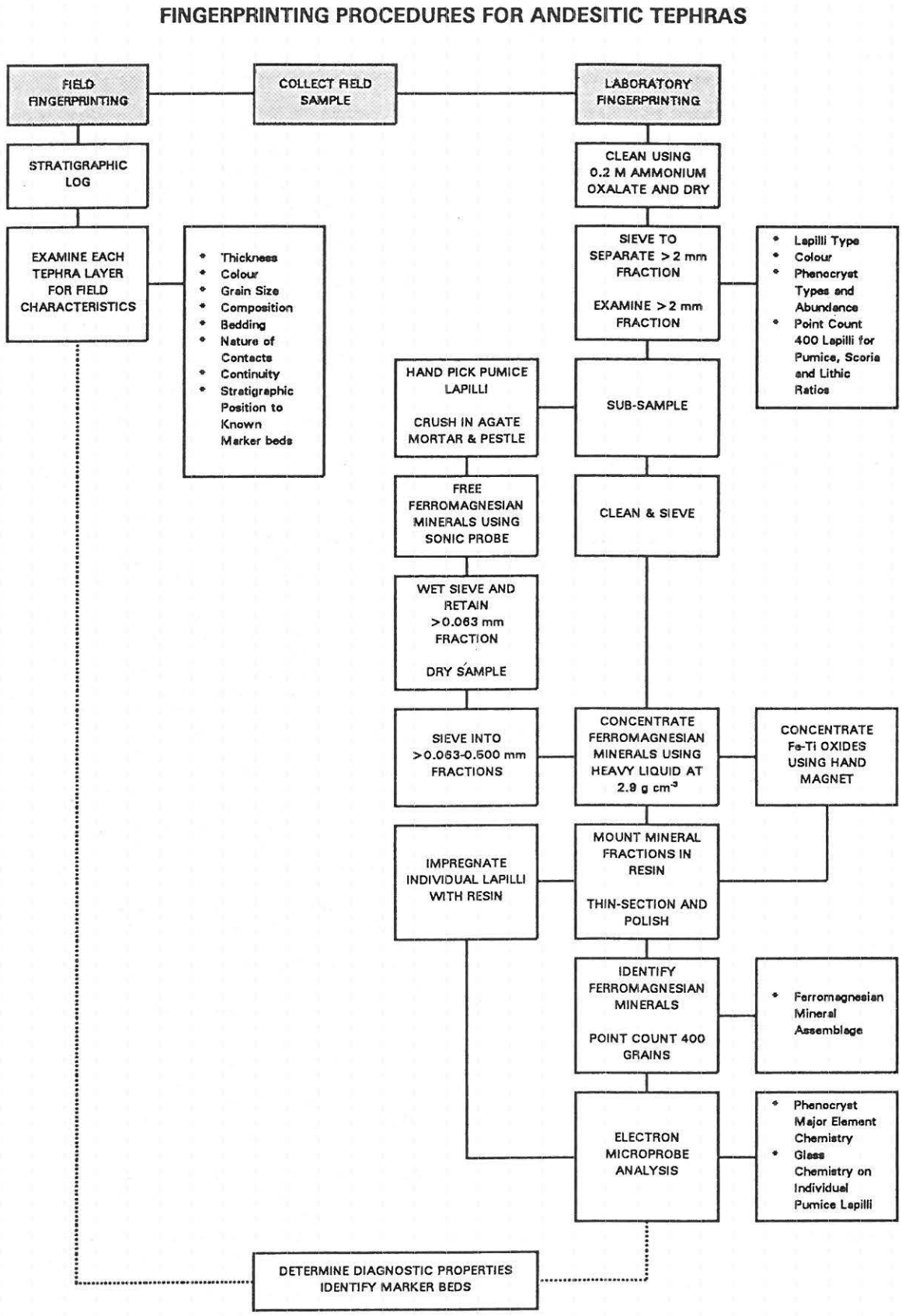

Figure 2B.3: Flow diagram illustrating field and laboratory based fingerprinting for Tongariro Volcanic Centre andesitic tephras (Donoghue 1991).

Bullot Track Description

Section Name and Map Code: Bullot Track Section 1 [BT1]

Grid Reference: T20/412108

Locality: An exposure within an ephemeral stream channel, approx. 200 m south of Bullot Track; the stratigraphy of deposits found overlying a 2 m thick fluvial deposit at 5.26 m is taken from an adjacent gully where the Holocene tephra stratigraphy is preserved

Formation	*Member*	*Unit Depth (mm)*	*Cum. Depth (m)*	*Description*
Onetapu Formation	unnamed	100	0.100	Bedded pebbles and sand, with sandy loam textured interbeds; rounded pumice and lithic pebbles; sharp wavy boundary
***	***	240	0.340	Dark greyish brown (10YR4/2) grading down to dark greyish brown (2.5Y4/2) medium sandy loam textured unit, greasy, with common brown coated root channels; sharp iron-stained lower contact; paleosol developed in Taupo Ignimbrite
Taupo Pumice	Taupo Ignimbrite	670	1.010	White fine to coarse pumice lapilli over poorly sorted ash and lapilli, with charcoalised branches
Mangatawai Tephra		480	1.490	250 mm Dark greyish brown (10YR4/2) fine sandy clay loam textured ash, slightly greasy; with many root channels; sharp contacts; paleosol 40 mm Very dark grey medium ash, firm, pocketing 80 mm Light olive brown to olive brown (2.5Y5/4 – 4/4) fine sandy loam textured ash, with iron-stained root channels; paleosol 110 mm Purplish black bedded fine sandy ash; discontinuous beds with wavy distinct contacts
Papakai Formation		90	1.580	Light olive brown (2.5Y5/4) fine sandy clay loam textured ash, greasy; with many brown coated root channels
Waimihia Tephra		30	1.610	Very pale brown (10YR7/3) fine ash 'cream cakes'
Papakai Formation		170	1.780	Light olive brown (2.5Y5/4) fine sandy loam textured ash, greasy; with many dark brown coated root channels; paleosol
	black ash-2	10	1.790	Very dark grey (5Y3/1) fine ash, pocketing, with interbedded beech leaves
		300	2.090	Yellowish brown (10YR5/6) fine sandy clay loam textured ash, greasy; with many dark brown coated root channels; paleosol; with indistinct lower contact, and a central 40 mm thick bed of brown and grey bedded coarse ash, pocketing;
Hinemaiaia Tephra		60	2.150	White and yellow coarse pumiceous ash interbedded within yellowish brown, greasy sandy loam textured Papakai Formation
Papakai Formation		170	2.320	Yellowish brown (10YR5/6) medium sandy loam textured ash, with many dark brown coated root channels
	orange lapilli-2?	40	2.360	Yellow (10YR7/6) fine pumice lapilli and grey fine lithic lapilli, with sandy loam textured ash matrix; discontinuous unit
		190	2.550	Yellowish brown (10YR5/6) fine sandy loam textured ash, with cracked exterior and many dark coated root channels; with scattered fine lithic lapilli
reworked Mangamate Tephra		80	2.630	Bedded very fine and fine brown and grey lithic lapilli
Mangamate Tephra	unnamed	180	2.810	Grey and brown very fine and fine lithic lapilli, non-vesicular and clast-supported lapilli; weakly bedded at top
Tangatu Formation	unnamed	70	2.880	Grey laminae of fine to coarse sand; ?fluvial sands
***	***	120	3.000	Pale brown fine and medium pumice lapilli, with pale yellow interiors

BT1 contd

Formation	*Member*	*Unit Depth (mm)*	*Cum. Depth (m)*	*Description*
Pahoka Tephra		60	3.060	20 mm Grey very fine angular, platy pumiceous fragments 40 mm Grey fine lapilli with matrix of grey and brown very fine angular, platy pumice fragments
***	***	200	3.260	Brown silty loam to silty clay loam textured medial unit, showing paleosol development; with cracked exterior and scattered fine pumice and lithic lapilli
***	***	2000	5.260	Weakly bedded pale yellow, pale brown, and grey pumice lapilli, and lithic lapilli with very fine sand and silt interbeds; fluvial deposit
		1000	6.260	Alternating beds of very fine compacted sand, and reverse graded pebble-rich beds with cobbles; fluvial deposit
Bullot Formation (upper)	unnamed	50	6.310	Pale orange and brown fine and medium pumice lapilli, angular, with few black fine lithic lapilli and sandy loam textured ash matrix
***	***	110	6.420	Light olive brown (2.5Y5/4) sandy loam textured ash, with interbedded laminae of coarse ash; common coated root channels; paleosol
	unnamed	30	6.450	Black coarse ash with very fine pumice and lithic lapilli
***	***	100	6.550	Dark yellowish brown to yellowish brown (10YR4/4 – 5/4) sandy clay loam textured medial unit, showing paleosol development, with many very fine lithic lapilli; few root channels
	Pourahu member [tephra unit]	140	6.690	White (10YR8/2) and pink (5YR7/3), with pale yellow medium and coarse pumice lapilli, firm, and few lithic lapilli; with coarse ash matrix; reversely graded unit, grading from a very fine lapilli and coarse ash base, to a dominantly medium lapilli top
	M_1	40	6.730	20 mm Grey ash, firm and prominent, with scattered fine strong yellow lapilli 20 mm Yellow ash, firm and prominent
	unnamed	90	6.820	Black fine lithic lapilli and fewer white and very pale yellow fine pumice lapilli
	member L18	90	6.910	Black, and some red angular lithic lapilli, and dark brown to dark yellowish brown (10YR4/3 – 4/4) dominantly fine pumice lapilli; ungraded unit
	unnamed	130	7.040	40 mm Purplish black coarse ash 30 mm Brown very fine angular, platy pumice fragments 60 mm Black coarse ash with many scattered fine lithic lapilli and pale yellow fine and medium pumice lapilli, soft
	member L17	250	7.290	Black fine lithic lapilli, angular, and dark brown (10YR3/3) fine and some medium pumice lapilli; ungraded unit
	M_2	130	7.420	40 mm Brownish grey pumice lapilli and coarse ash 10 mm Brown fine ash 20 mm Black and brown coarse ash 30 mm Yellow to olive coarse ash 30 mm Black coarse ash
	member L16	140	7.560	Strong brown (7.5YR5/8) medium and fine, with few coarse pumice lapilli, with olive brown (2.5Y4/4) interiors, and dark grey with few red fine to coarse lithic lapilli; angular pumice and lithic lapilli; coarse ash matrix; weak normal grading
	M_3	70	7.630	30 mm Grey loamy textured ash with scattered lapilli 20 mm Yellow loamy textured ash with very fine pumice lapilli and very fine angular, platy, pumice fragments 20 mm Dark grey coarse loamy textured ash with scattered lapilli
	member L15	250	7.880	Strong brown (7.5YR5/8) and very dark greyish brown (10YR3/2) very fine and fine pumice lapilli, with olive interiors; angular, hard pumice; and grey, very dark grey and occasional red lithic lapilli; minor coarse ash matrix; normally graded unit
	unnamed	80	7.960	Greyish brown medium ash with dark greyish brown lithic lapilli

BT1 contd

Formation	*Member*	*Unit Depth (mm)*	*Cum. Depth (m)*	*Description*
Bullot Formation (upper)	member L14	90	8.050	Black fine and very fine lithic lapilli, and strong brown fine and very fine pumice lapilli; ungraded unit
	unnamed	30	8.080	Yellowish brown sandy loam textured ash with scattered lapilli
		70	8.150	Purplish black ash with many black very fine lithic lapilli
	member L13	190	8.340	Black, and occasional red, fine lithic lapilli, and strong brown fine and common medium pumice lapilli, with olive brown interiors
	unnamed	50	8.390	Purplish black medium ash with few fine lithic lapilli
	member L12	90	8.480	Black fine lithic lapilli and very dark greyish brown (10YR3/2) fine pumice lapilli, with black interiors; minor black coarse ash matrix
	unnamed	80	8.560	Brown coarse ash
		30	8.590	Pale grey medium ash with fine lapilli
		30	8.620	Brown sandy loam textured ash
		110	8.730	Brown fine pumice lapilli
		190	8.920	Black lithic lapilli in black coarse ash; with interbedded thin greyish brown ash laminae, and a purplish black coarse lithic-rich ash
		180	9.100	Black, and fewer grey and red very fine and fine lithic lapilli, and brown pumice lapilli; normally graded from very fine and fine lapilli base to a coarse ash top
		20	9.120	Purplish black fine sandy loam textured ash, with many very fine black lithic lapilli
		50	9.170	Dark olive grey coarse ash with yellow very fine pumice lapilli and black very fine lithic lapilli
		20	9.190	Purplish black coarse sandy ash with few black fine lithic lapilli
	member L11	110	9.300	Very dark greyish brown (10YR3/2) fine and medium pumice lapilli, with very dark greyish brown (2.5Y3/2) interiors, and black and common red fine and very fine lithic lapilli; hard subangular pumice, and lithic lapilli; with grey coarse ash matrix, grading up to a black coarse ash matrix near top of unit
	unnamed	120	9.420	Greyish brown coarse loamy textured ash, with many fine lithic lapilli
	member L10	120	9.540	Light olive brown (2.5Y5/4) dominantly fine pumice lapilli and black lithic lapilli, with a coarse ash matrix; hard subrounded pumice, and angular lithic lapilli; ungraded unit, with indistinct lower contact
	member L9	180	9.720	Light olive brown (2.5Y5/4) coarse pumiceous ash, fine pumice lapilli, and fewer black fine and very fine lithic lapilli; indistinct contacts
	member L8	180	9.900	Light olive brown (2.5Y5/4) fine and few medium-coarse pumice lapilli, and black dominantly fine lithic lapilli; subangular, soft pumice; distinct lower contact
	unnamed	200	10.100	Greyish brown loamy textured ash, and very fine to fine lithic lapilli
		40	10.140	Brown pumice lapilli and some black coarse lithic lapilli
		40	10.180	Light brownish yellow sandy loam textured ash, with fine pumice and lithic lapilli
		120	10.300	Black and brown coarse loam textured ash, with many fine lithic lapilli
		110	10.410	Brown fine and medium pumice lapilli with a central bed of yellow very fine, angular, platy pumice fragments; distinctive unit
		50	10.460	Black coarse sandy ash
Bullot Formation and Rerewhakaaitu Tephra		30	10.490	Pale brown ash with interbedded white very fine white rhyolitic ash
Bullot Formation (middle)	unnamed	170	10.660	Very dark grey coarse ash and very fine lithic lapilli; gravelly texture
		50	10.710	Yellow medium and fine pumice lapilli, and black medium and fine lithic lapilli

BT1 contd

Formation	*Member*	*Unit Depth (mm)*	*Cum. Depth (m)*	*Description*
Bullot Formation (middle)	unnamed	40	10.750	Brown coarse ash and medium pumice lapilli, with some black lithic lapilli
		30	10.780	Brown coarse loamy sand textured ash
		30	10.810	Black sandy ash
		20	10.830	Grey fine ash and very fine lithic lapilli
		270	11.100	Alternating beds of brown, and very dark grey, loamy textured ash and fine to very fine lapilli
	member L7	180	11.280	Black lithic lapilli, and light yellowish brown (10YR6/4) fine and very fine pumice lapilli, with yellowish brown (10YR5/4) interiors; angular lithics and pumice; normally graded unit
	unnamed	10	11.290	Black to dark grey coarse ash
	member L6 (pink lapilli)	140	11.430	60 mm Pale brown (10YR6/3) to pinkish grey (7.5YR6/2) fine and very fine pumice lapilli, with same coloured interiors, and sandy loam textured ash matrix 80 mm Pale yellow fine pumice lapilli and coarse ash; with bed of black very fine lithic lapilli at base
	unnamed	150	11.580	Very fine pumice and lithic lapilli, and coarse ash
		50	11.630	Black lithic lapilli and yellowish brown pumice lapilli
		20	11.650	Dark greyish brown fine pumice lapilli and black fine lithic lapilli
		90	11.740	20 mm Pinkish brown sandy loam textured ash with scattered fine lithic lapilli 70 mm Brownish yellow to yellow (10YR6/6–7/6) and dark yellowish brown (10YR4/4) pumice lapilli, with olive brown interiors, and black with occasional red lithic lapilli, angular; some ash matrix
		40	11.780	Loamy textured ash
	member L5	100	11.880	Brown (10YR5/3) to dark brown (10YR4/3) fine pumice lapilli, with same coloured interiors, and black fine and medium lithic lapilli and scoria; some sandy loam textured ash matrix
	unnamed	130	12.010	Pale yellow and pink very fine pumice lapilli, with grey interiors, and black very fine lithic lapilli; with brown coarse ash matrix; normally graded unit
	member L4	290	12.300	Pale brown (10YR6/3) and light yellowish brown (2.5Y6/4) dominantly fine pumice lapilli, with light grey to light yellowish brown interiors; some medium and coarse pumice lapilli and occasional pumice bombs; very vesicular, hard pumice; and black and grey very fine lithic lapilli and some scoria; weak normal grading; sharp contacts
	unnamed	230	12.530	Greyish brown to olive brown coarse ash and fine lapilli beds
		150	12.680	Brown very fine and fine pumice lapilli, and black, red and grey lithic lapilli, with a sandy loam textured ash matrix; normally graded and prominent unit
***	***	1800	14.480	Strongly bedded unit comprising poorly sorted dominantly sand-rich, and granule-rich and pebble-rich beds, mostly <50 mm depth; with interbedded silt laminae and pockets of pumice, and lithic lapilli; with scattered very coarse pebbles, cobbles and boulders; weak cross bedding; unit wedges and pinches out at southern end of exposure; fluvial deposit
	unnamed	40	14.520	Brown medium ash and scattered fine pumice and lithic lapilli; sharp contacts
Okareka Tephra		10	14.530	White very fine ash, pocketing, with intermixed very fine black and brown andesitic ash
Bullot Formation (lower)	unnamed	20	14.550	Olive brown fine sandy loam textured ash; distinct contacts
		70	14.620	Black coarse ash; distinct contacts

BT1 contd

Formation	*Member*	*Unit Depth (mm)*	*Cum. Depth (m)*	*Description*
Bullot Formation (lower)	member L3 (hokey pokey lapilli)	230	14.850	Yellowish brown (10YR5/8–5/6), yellowish red (5YR5/8) and few very dark greyish brown (2.5Y3/2–2/2) medium, and some coarse pumice lapilli, and some olive grey pumice blocks with dark greyish brown interiors; very vesicular pumice lapilli; some black fine and medium scoria, angular and very few fine hydrothermally altered lithic clasts; ungraded unit
***	***	330	15.180	?Reworked andesitic pumice lapilli and ash; comprising alternating dark grey poorly sorted coarse sandy ash beds with fine lithic lapilli, and pale yellow dominantly fine pumice lapilli beds; sharp contacts
***	***	630	15.810	?Reworked andesitic lapilli and ash; comprising alternating poorly sorted grey sandy ash beds, and pebble-rich beds comprising pale brown to brown (10YR6/3–5/3) fine pumice and black and red fine lithic pebbles
	unnamed	30	15.840	Black fine sandy ash
	member L2	270	16.110	Light olive brown (2.5Y5/4) to brown (7.5YR5/4, moist colour) and pale yellow (dry colour)dominantly fine pumice lapilli, very vesicular and hard; and few black blocky-shaped lithic lapilli; some coarse ash matrix; reversely graded unit, grading from a dominantly fine lapilli base to a medium, with some coarse lapilli top
	member L1 (green ash)	220	16.330	Well bedded and well sorted, thin (<10 mm) coarse pumiceous ash beds, and pale yellow very fine pumice and greenish grey lithic lapilli beds; distinctive colouring
	unnamed	50	16.380	Coarse ash and fine lapilli
		70	16.450	5 mm Coarse ash 65 mm Olive grey to brownish grey medium and fine lapilli, hard angular lapilli; normally graded
		10	16.460	Purplish grey medium ash
		150	16.610	Bedded lapilli and ash, comprising alternating fine and very fine lithic dominant lapilli beds, and poorly sorted coarse ash beds; beds 30–40 mm thick with distinct contacts; sharp upper and lower contacts
		20	16.630	Brown fine sandy loam textured ash; sharp contacts
		180	16.810	Bedded ash and lapilli, comprising alternating dark olive grey moderately well sorted coarse lithic and pumiceous ash beds, and pale brown (10YR6/3) to light yellowish brown (2.5Y6/4) fine pumice lapilli and black medium lithic lapilli beds; angular lithics and soft pumice; distinctly bedded unit
Kawakawa Tephra Formation	Oruanui Ignimbrite	40	16.850	30 mm Pinkish grey (7.5YR7/2) ash, firm, and fine pumice lapilli
	?Aokautere Ash			10 mm White fine ash
***	***	40	16.890	Brown sandy loam textured ash
Te Heuheu Formation	unnamed	110	17.000	Strong brown (7.5YR5/8) sandy clay loam textured matrix, with brown very fine and fine pumice pebbles and grey andesitic pebbles; ungraded; debris flow deposit
***	***	30	17.030	Greyish brown sand with scattered pebbles; moderately well sorted sand
***	***	100	17.130	Yellowish red (5YR5/8) fine and medium pumice lapilli, with same coloured interiors, soft and firm pumice; and fewer dark grey fine lithic lapilli, angular; some ash matrix; weak normal grading
***	***	520	17.650	150 mm Weakly bedded yellowish red (5YR5/6) very fine and some fine pumice lapilli, with olive brown interiors; angular, hard pumice lapilli; and grey very fine lithic lapilli; prominent unit; indistinct contacts 370 mm As above but dominantly fine pumice lapilli
		140	17.790	Coarse sandy loam textured matrix, poorly sorted, with fine andesitic pebbles and reddish yellow fine pumice pebbles, soft, and scattered andesitic cobbles at upper contact

STOP 4 — Whangaehu Cliffs

Our objective here is to gain a view across Whangaehu River and Fan to Mt Ruapehu (and to have lunch!).

Our vantage point is a late Holocene dune of the Makahikatou Formation (Purves 1990), and it contains tephra deposits from the latest phase of eruptive activity from Mt Ruapehu. The Tufa Trig Formation tephras are small-volume, phreatomagmatic events that show signs of eruption through the crater lake near the summit of the mountain (Donoghue 1991). This site is south of the main dispersal axis of most Tongariro Volcanic Centre tephras and thus most units are now thin.

Although tephras of the Bullot Formation were deposited over a c. 12 500 year period, most activity occurred between c. 14.7 and c. 10 ka. (The upper Bullot Formation.) Near this site the Rerewhakaaitu Tephra (14.7 ka) is the first conformable rhyolitic tephra found overlying indurated lahars. Therefore this constructional surface has an age of c. 15 ka. It is extensive in the region, extending south to Waiouru, and occupying much of the Karioi Forest to the west.

We are standing on a major fault trace. This fault now diverts the Whangaehu River to the south; prior to 15 ka lahars flowed through Waiouru and down Hautapu River to the southeast.

In the foreground is Rangipo Desert and the Whangaehu Fan. Patterns of vegetation clearly show aggradating, eroding, and stable areas. On the apex of the fan one of the youngest lava flows on Ruapehu is visible. The lower part rests on Mangaio Formation lahar that is aged between 4.65 and 3.4 ka and is overlain by 1.85 ka Taupo Tephra (Donoghue 1991). This lava flow may be implicated in the formation of Crater Lake, Mt Ruapehu.

STOP 5 — Tirorangi Marae

The objective of this stop is to examine the deposits from prehistoric lahars in the Whangaehu Valley — the Onetapu Formation (Table 2B.2).

Prehistoric lahars include all those deposits which lie between the Taupo Tephra Formation (dated at 1.85 ka) and the first historically-recorded lahar of February 10, 1861. Deposits of these lahars are confined within the valley of the Whangaehu River, and a number of units have formed aggradational terraces on the valley sites. Historic lahars have left few deposits, and it is supposed that the deposits that are preserved in the geological record represent lahars that were much larger. Hodgson (1993) has calculated velocities and discharge rates for historic and prehistoric lahars to support this hypothesis.

Both debris flows and hyperconcentrated flows are represented in the laharic deposits that we will be examining. Debris flows and hyperconcentrated flows are distinguished according to certain sedimentological principles which relate to the dominant support and transport mechanisms operating during flow. These are a function of the sediment concentration and nature of the matrix of the lahar and are reflected in the field characteristics of each deposit (Fig. 2B.4).

Both sedimentological evidence and observation show that these flow types may be intimately associated. Debris flows may transform to hyperconcentrated flows, or vice-versa, under certain conditions.

Here, post-Taupo Tephra lahar deposits are exposed in the road cutting on the north side of the bridge, and in a metal (gravel) pit on the north bank of the river.

The Taupo Tephra is not found but reworked pumice lapilli lying between deposits in the exposure attest to its presence further upstream. Its lowermost occurrence is in a buried soil which has developed in Holocene ash and hyperconcentrated flows.

Velocity and discharge calculation for lahars Onh, Ong, and Onf have been made at this site; two methods have been used (Table 2B.3).

Whangaehu River Description

Section Name and Map Code: Whangaehu River Section 5 [WR5]

Grid Reference: T20/443045

Locality: A large exposure on the Whangaehu escarpment, approx. 300 m south of an unnamed vehicle track which joins the Desert Road

Formation	*Member*	*Unit Depth (mm)*	*Cum. Depth (m)*	*Description*
Makahikatoa Sands		600	0.600	Grey loamy sand textured unit and overlying present-day soil surface
		40	0.640	Very dark brown (10YR2/2) loamy sand textured unit, with charcoal fragments; weakly developed paleosol
Tufa Trig Formation	?member Tf14	10	0.650	Dark grey coarse sandy ash, pocketing
Makahikatoa Sands		40	0.690	Dark brown (10YR3/3) fine sandy loam textured unit
Tufa Trig Formation	?member Tf13	10	0.700	Dark grey coarse sandy ash, pocketing
Makahikatoa Sands		30	0.730	Dark brown (10YR3/3) fine sandy loam textured unit
Tufa Trig Formation	?member Tf10	10	0.740	Black pocketing coarse ash
Makahikatoa Sands		20	0.760	Dark brown medium sandy loam textured unit, slightly greasy; weakly developed paleosol
Tufa Trig Formation	?member Tf8	45	0.805	10 mm Pale grey fine ash 10 mm Black coarse ash 15 mm Black coarse ash and very fine lithic and pumice lapilli 10 mm Black fine ash base
Makahikatoa Sands		30	0.835	Medium sandy loam textured unit, slightly greasy
Tufa Trig Formation	unnamed	10	0.845	7 mm Dark grey to black coarse ash 3 mm Pale grey fine ash base
Makahikatoa Sands		45	0.890	Medium sandy loam textured unit, slightly greasy
Tufa Trig Formation	unnamed	20	0.910	10 mm Black coarse ash 10 mm Pale grey fine ash base
Makahikatoa Sands		10	0.920	Medium sandy loam textured unit, slightly greasy
Tufa Trig Formation	member Tf6	40	0.960	30 mm Black coarse ash 10 mm Pale grey fine ash base
Makahikatoa Sands		40	1.000	Medium sandy loam textured unit, slightly greasy
Tufa Trig Formation	member Tf5	50	1.050	45 mm Black coarse ash 5 mm Paler grey ash base
Makahikatoa Sands		50	1.100	Sandy loam textured unit, greasy
Tufa Trig Formation	member Tf4	30	1.130	Black coarse ash
Makahikatoa Sands		190	1.320	Fine sandy loam textured unit, greasy; with scattered Taupo Pumice and charcoal fragments; paleosol
Tufa Trig Formation	member Tf2	40	1.360	Dark grey medium scoriaceous lapilli interbedded in sandy loam textured ash
***	***	300	1.660	Yellowish brown slightly greasy sandy loam textured unit; paleosol
Taupo Pumice	Taupo Ignimbrite	240	1.900	White poorly sorted coarse ash and lapilli, with charcoal
Mangatawai Tephra		410	2.310	170 mm Dark brown (10YR3/3) fine sandy clay loam textured ash, greasy; with distinct dark coated root channels 20 mm Black coarse ash, pocketing 70 mm Olive brown (2.5Y4/4) fine sandy loam textured ash 150 mm Alternately bedded black coarse ash and brown fine sandy loam textured ash beds; discontinuous beds
Papakai Formation		140	2.450	Yellowish brown (10YR5/4) fine sandy loam textured ash; paleosol
Waimihia Tephra		30	2.480	Very pale brown (10YR8/3) fine ash 'cream cakes'
Papakai Formation		250	2.730	Light olive brown (2.5Y5/4) fine sandy loam textured ash, with scattered lapilli
	black ash-2	20	2.750	Black coarse ash, pocketing; distinct tephra

WR5 contd

Formation	*Member*	*Unit Depth (mm)*	*Cum. Depth (m)*	*Description*
Papakai Formation & Hinemaiaia Tephra		180	2.930	Light olive brown (2.5Y5/4) fine sandy loam, slightly greasy, with interspersed white and yellowish brown (10YR5/5) coarse pumiceous ash
Papakai Formation	unnamed	?50	2.980	Fine and medium pale pumice lapilli, firm pumice; with light olive brown sandy loam textured ash matrix
		100	3.080	Yellowish brown (10YR5/6) medium sandy loam textured ash, slightly greasy
	unnamed	90	3.170	Medium and fine pumice lapilli; olive interiors, firm pumice
		320	3.490	Yellowish brown (10YR5/6) medium sandy loam textured ash, slightly greasy; with many scattered bluish grey lithic lapilli especially at base
reworked Mangamate Tephra		330	3.820	Weakly bedded olive, grey, and strong brown fine and very fine dominantly lithic lapilli, and very fine angular platy fragments; sharp contacts
Mangamate Tephra	?Poutu Lapilli	50	3.870	Grey, and strong brown iron-stained medium and fine lithic lapilli and few poorly vesicular pumice lapilli
	?Wharepu Tephra	420	4.290	Weakly bedded olive grey fine and very fine dominantly lithic lapilli, and few pumice lapilli; loose sharp angular lapilli; normally graded
		170	4.460	Dark greyish brown (10YR4/2) to dark brown (10YR4/3) coarse lithic ash and fine lapilli, with few strong brown iron-stained very fine pumice lapilli
		30	4.490	Dark grey (10YR4/1) to purplish grey coarse loamy ash
		150	4.640	Very dark grey (10YR3/1) and dark brown (7.5YR4/4) fine and very fine lapilli; angular, non- and poorly vesicular lapilli
		70	4.710	Very dark grey (10YR3/1) fine lithic lapilli, and fewer strong brown pumiceous lapilli; normally graded tephra, grading upwards to coarse ash
Poronui Tephra		30	4.740	White very fine ash, pocketing, interbedded with yellowish brown (10YR5/5) coarse andesitic ash
Mangamate Tephra	Ohinepango Tephra	90	4.830	Colour-banded tephra comprising alternating black lithic dominant, and strong brown pumice dominant coarse ash beds
Bullot Formation (upper)	unnamed	30	4.860	Very pale brown (10YR7/3) medium and fine pumice lapilli, and black lithic lapilli; very vesicular pumice; angular lithics
		5	4.865	Black coarse sandy ash
		30	4.895	Strong brown fine and medium pumice lapilli with sandy loam textured ash matrix
		20	4.915	Yellowish brown coarse sandy loam textured ash, greasy
		20	4.935	Pumice and lithic lapilli, and greasy coarse sandy loam textured ash matrix
***	***	50	4.985	Yellowish brown (10YR5/6) and greyish brown (2.5Y5/2) coarse sandy loam to sandy clay loam textured medial unit, showing paleosol development; with yellowish red iron-stained contacts and mottles
	unnamed	50	5.035	Yellowish brown (10YR5/6) coarse sandy loam textured ash and fine and very fine strong brown pumice lapilli and grey lithic lapilli
		50	5.085	Brownish yellow (10YR6/6) fine and medium pumice lapilli, with light grey (10YR7/2) interiors, and a coarse ash matrix
		90	5.175	Grey (2.5Y5/2) loamy sand
***	***	130	5.305	Yellowish brown (10YR5/4) sandy loam textured medial unit, greasy; with scattered lapilli
	unnamed	80	5.385	Yellowish brown fine and fewer medium pumice lapilli and very fine angular, platy pumice fragments, and a variety of lithic lapilli; loose lapilli, gravelly texture
***	***	280	5.665	Coarse sandy loam textured medial unit, slightly greasy; with many interspersed fine lithic and pumice lapilli, increasing in concentration toward base of unit
***	***	70	5.735	Greyish brown (2.5Y5/2) gleyed sandy loam textured medial unit, showing paleosol development, greasy, with interspersed medium pumice and lithic lapilli, and distinct dark coated root channels; with yellowish brown (10YR5/6) iron-stained contacts;

WR5 contd

Formation	*Member*	*Unit Depth (mm)*	*Cum. Depth (m)*	*Description*
Bullot Formation (upper)	unnamed	40	5.775	Dark yellowish brown (10YR4/4) medium and fine pumice lapilli; with pale yellow ?imogolite coatings on lapilli faces; some coarse sandy loam textured ash matrix
		50	5.825	Coarse sandy loam textured medial unit, with dark coated root channels, and some pumice and lithic lapilli
		30	5.855	Purplish grey coarse ash and scattered lapilli
		80	5.935	Strong brown (7.5YR5/6) medium and fine pumice lapilli, with yellowish brown interiors, and black lithic lapilli; ?imogolite coatings on pumice faces
		50	5.985	Yellowish brown (10YR5/4) coarse sandy ash and lapilli
		50	6.035	Light olive brown (2.5Y5/4) coarse sandy ash; with lapilli at base
		50	6.085	Dark grey (2.5Y4/0) to purplish grey coarse sandy ash
		20	6.105	Grey ash and fine lapilli
		20	6.125	Yellow medium pumice lapilli; some ash matrix
		30	6.155	Black coarse sandy ash
	member L17	50	6.205	Dark greyish brown (2.5Y4/2) medium and coarse pumice lapilli, and few lithic lapilli; very vesicular, brittle pumice; loose lapilli
	unnamed	40	6.245	Yellowish brown loamy ash
		60	6.305	Pumice lapilli and coarse ash
		20	6.325	Yellowish brown greasy sandy loam
	M_2	90	6.415	10 mm Black coarse ash 30 mm Brownish grey loamy ash 20 mm Fine lapilli and coarse ash 30 mm Brownish grey greasy sandy loam textured ash
	member L16	80	6.495	Olive brown (2.5Y4/4) and yellow (10YR7/6) fine, medium, and few coarse pumice lapilli, with yellow and very pale brown (10YR7/3–8/3) interiors, and with black lithic lapilli
	unnamed	50	6.545	Dark yellowish brown (10YR4/4) fine sandy loam textured ash, greasy
		60	6.605	Yellowish brown medium pumice lapilli and sandy loam textured ash
		40	6.645	Yellowish brown medium sandy loam textured ash, slightly greasy
		30	6.675	Medium pumice lapilli in brown sandy loam textured ash
		60	6.735	Brown sandy loam textured ash
		50	6.785	Strong brown pumice and black lithic lapilli; discontinuous tephra
		60	6.845	Grey fine sandy loam textured ash, slightly greasy
Waiohau Tephra		40	6.885	White (10YR8/2) very fine ash; discontinuous tephra; with intermixed black fine andesitic lapilli in base
Bullot Formation (upper)	unnamed	20	6.905	Brownish grey sandy loam textured ash
		20	6.925	Dark purplish black coarse ash
		20	6.945	Purplish grey sandy ash
		60	7.005	Dark purple sandy ash
***	***	110	7.115	Grey gleyed sandy loam textured medial unit, showing paleosol development; very greasy, with scattered lapilli and coated root channels; with dark brown (7.5YR4/4) and dark grey (10YR4/1) contacts
	unnamed	70	7.185	Grey coarse sandy loam textured ash and scattered fine pumice and lithic lapilli; gravelly texture
		60	7.245	Yellowish brown medium and few coarse pumice lapilli, and grey lithic lapilli
		10	7.255	Dark purplish black coarse ash
***	***	60	7.315	Yellowish brown fine sandy loam textured medial unit
	unnamed	20	7.335	Yellow soft pumice lapilli interbedded in a grey sandy ash matrix
		40	7.375	Dark purplish black ash and basal very fine lithic lapilli
		50	7.425	Yellowish brown fine sandy loam textured ash

WR5 contd

Formation	*Member*	*Unit Depth (mm)*	*Cum. Depth (m)*	*Description*
Bullot Formation (upper)	unnamed	90	7.515	Olive brown (2.5Y4/4) fine and medium pumice lapilli, with very dark greyish brown (2.5Y3/2) interiors, and very fine angular, platy pumice fragments and few lithic lapilli; very vesicular pumice
***	***	110	7.625	Olive brown (2.5Y4/4) fine sandy loam textured medial unit, showing paleosol development, slightly greasy; with dark coated root channels and interbedded medium lapilli
Bullot Formation (upper)	?member L8	120	7.745	Light yellowish brown (10YR6/4) to light olive brown (2.5Y5/4) medium to very fine pumice lapilli, and pumiceous coarse ash; very soft pumice; reversely graded tephra, grading upwards from dominantly coarse ash, to dominantly medium lapilli
	unnamed	60	7.805	Dark greyish brown (10YR4/2) fine and medium pumice lapilli
		50	7.855	Lithic lapilli with fewer dark greyish brown (10YR4/2) fine pumice lapilli
***	***	60	7.915	Dark greyish brown medium sandy loam textured medial unit, with interspersed scattered fine lapilli
Rerewhakaaitu Tephra		40	7.955	Light grey (10YR7/1) fine ash interbedded within dark grey coarse andesitic ash and very fine lithic lapilli; discontinuous tephra
Bullot Formation (middle)	unnamed	40	7.995	Greyish brown loamy ash and fine lithic and fewer pumice lapilli
		40	8.035	Greyish brown coarse ash
	member L7	100	8.135	Brownish yellow (10YR6/6) and yellowish brown (10YR5/4) fine, medium and few coarse pumice lapilli, with olive grey (5Y5/2) interiors, and few black and brownish red lithic lapilli concentrated in basal 20 mm; some grey sandy ash matrix
	unnamed	120	8.255	Dark brown (10YR4/3) grey and brown coarse loamy ash
	member L5	220	8.475	Olive (5YR5/6) fine and medium pumice lapilli, with same coloured interiors, and black and olive grey lithic lapilli; with a coarse ash matrix
Te Heuheu Formation	unnamed	8000	16.475	Iron-stained coarse sand and granule matrix, lithified; with matrix-supported dominantly medium purple, red, black and grey andesitic pebbles, and brownish yellow and multicoloured fine and medium pumice pebbles; some cobbles and boulders; angular and subrounded clasts; poorly bedded deposit; debris flow deposit
		5000	21.475	Brown sand and granule matrix; with matrix and pockets of clast-supported andesitic pebbles, cobbles and boulders; maximum clast 2 m (boulder); lower 1 m finer grade with overall smaller clasts; debris flow deposit
		1400	22.875	Bedded coarse and fine sand with pebbles; beds thicknesses generally 50–100 mm; some cross-beds; fluvial deposit
		700	23.575	Dark brown (10YR3/3) centimetre- and millimetre-bedded sand and granule matrix, lithified, with andesitic and pumice pebbles; deposit shows characteristics transitional between fluvial and hyperconcentrated flood flow deposits
Bullot Formation (middle)	unnamed	100	23.675	Strong brown fine airfall pumice lapilli, angular; with a sandy loam textured ash matrix
Te Heuheu Formation	unnamed	1200	24.875	Light brown coarse sand and granule matrix, lithified, and bedded at base; with abundant multicolored fine andesitic pebbles and pale yellow pumice pebbles concentrated in base of deposit; hyperconcentrated flood flow deposit
		2000	26.875	Coarse sand and granule matrix, lithified; upper 400 mm poorly bedded; with many fine and coarse andesitic pebbles; prominent, bluff-forming unit; hyperconcentrated flood flow deposit
		3400	30.275	Pink laminated clay with pocketing olive grey sand interbeds
		100	30.375	Olive grey greasy sandy loam textured medial unit
Bullot Formation (middle)	unnamed	80	30.455	Grey and strong brown pumice lapilli, strongly weathered pumice; with a sandy loam textured ash matrix

TABLE 2B.2. Extent, mean depth, volume and estimated age of Onetapu Formation informal members. The timing of most prehistoric events has been established through radiocarbon dating (Hodgson 1993).

Member name	Extent (m^2)	Mean depth (m)	Volume (m^3)	Age range years B.P. (calendar years)	Estimated age years B.P. (calendar years)
Ono	3×10^3	0.8	$^P9 \times 10^4$ $^H2.4 \times 10^3$ $^T9.24 \times 10^4$	(< 1928)	(1975)
Onn	3×10^3	0.24	7.2×10^2	(< 1750)	(1953)
Onm	3×10^3	0.53	1.6×10^3	(1750 - 1950)	(1861)
Onl	3×10^3	0.22	6.6×10^2	505 - 335	400
Onk	7.5×10^3	0.48	3.6×10^3	505 - 335	400
Onj	6.55×10^6	0.61	$^P4.4 \times 10^6$ $^H4.0 \times 10^6$ $^T8.4 \times 10^6$	477 - 395	450
Oni	3.6×10^6	0.4	$^P3.4 \times 10^6$ $^H1.4 \times 10^5$ $^T4.8 \times 10^6$	615 - 337	550
Onh	6.41×10^6	0.87	$^P1.2 \times 10^7$ $^H5.6 \times 10^6$ $^T1.8 \times 10^7$	615 - 337	600
Ong	3.24×10^6	1.08	3.5×10^6	930 - 700	800 - 600
Onf	2.87×10^6	0.83	$^P0.8 \times 10^6$ $^H2.4 \times 10^6$ $^T3.2 \times 10^6$	930 - 700	850
One	1.5×10^3	1.05	$^P1.8 \times 10^6$ $^H1.6 \times 10^3$ $^T1.8 \times 10^6$	930 - 700	900
Ond	9×10^3	0.3	2.7×10^3	1860 - 850	1200
Onc	4.5×10^3	0.4	1.8×10^3	1860 - 850	1650
Onb	3×10^3	0.2	6×10^2	1860 - 850	1750
Ona	5.9×10^5	0.27	$^P2.8 \times 10^6$ $^H1.6 \times 10^5$ $^T3.0 \times 10^6$	1860 - 850	1800

[P] Total volume estimated for deposits on the Rangipo Desert by Purves (1990).

[H] Total volume estimated for deposits below Tangiwai by Hodgson (this study).

[T] Total combined volume for deposits.

TABLE 2B.3 Calculations of velocity and discharge rates for lahars, Tirorangi Marae (Hodgson 1993).

	Velocity (km/hr)		Discharge (m^3/sec)	
	V1	V2		
Onh	19	15	3474	2746
Ong	21	16	3448	2726
Onf	21	17	2757	2180

For comparison, in 1975 an eruption through Crater Lake on Mount Ruapehu caused the most recent historical lahar in the Whangaehu River which, just upstream, was travelling at c. 16 km/hr with an estimated discharge of 566 m^3/sec.

Ong (a complex of up to three hyperconcentrated flows) and Onf are well exposed to the gravel pit. It would appear that the deposits from Onf occupy what previously formed the channel of the Whangaehu River.

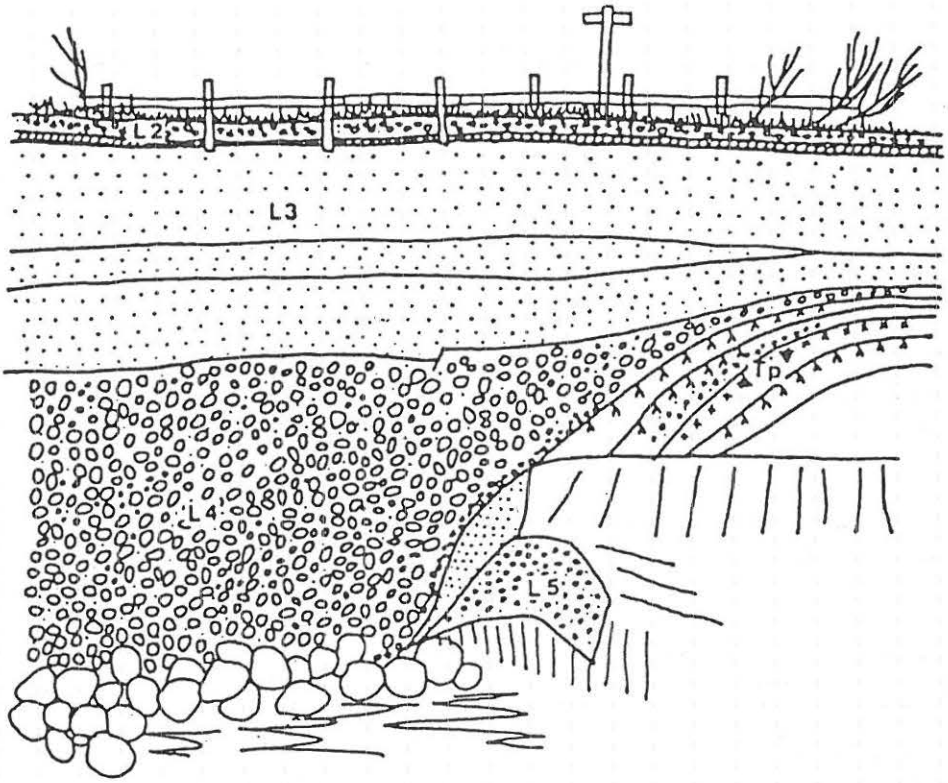

Figure 2B.4: Exposure of post-Taupo Tephra lahar deposits in the gravel pit at Tirorangi Marae. L2 = Onetapu Formation (On), L3 = Ong, L4 = Onf, L5 = Ona, Tp = Taupo Tephra (Donoghue et al. 1991a; Hodgson 1993).

Tirorangi Marae Description

Section Name: Tirorangi Marae
Grid reference: S21/233869

Onetapu Formation and Tangatu Formation are exposed in a metal pit on the west bank of the Whangaehu River, immediately upstream of Tirorangi Marae.

Formation	Member	Unit thickness (mm)	Cumulative thickness (m)	Description
Onetapu Formation	Onh	0.5	1.00	Matrix supported gravel; very poorly soiled; ungraded; massive, clasts subangular to angular; common grey and few red and black lithic clasts; matrix colour dark brown; few pumices granules.
				Distinct non erosional contact
"	"	0.30	1.3	Clast supported, very well sorted, well rounded reworked Taupo lignibrite pumice pebbles with some mud and charcoal.
				District non-erosional contact.
Onetapu Formation	Ong 3	3.60	4.80	Clast-supported sand and granules; normally graded; weak mm thick laminae; dish and pillar structures in upper 1.5 m and few water escape pipe extending from top of unit to about 2m depth; clasts subrounded to rounded; few of these pipes lead directly to a sand volcano, common black and grey and few red lithic clasts; common grey pumice clasts; overall colour olive brown.
				Distinct non-erosional contact.
"	"	0.05	4.85	Clast-supported very well sorted, reworked Taupo lignimibrite pumice pebbles.
				Graded contact.
Onetapu Formation	Ong 2	0.60	5.45	Clast supported sand and granules normally graded to centre then inversely graded; massive; poorly sorted; clasts subangular to angular; common grey, black and few red lithic clasts; common grey pumice clasts; overall colour dark brown.
				Distinct non-erosional contact.
"	"	0.03	5.48	Clast-supported very well sorted, well rounded reworked Taupo lgnimbrite granules and pebbles.
				Distict non-erosional contact.
Onetapu Formation	Ong 1	1.20	6.68	Clast-supported sand and granules; faint mm thick laminae, poorly sorted; inversely graded from bottom to middle then normal graded; common black and grey and few red lithic casts; common grey pumice clasts; few rip up clasts of Tertiary siltstone; overall colour, dark brown.
				Distinct non-erosional contact.

Tirorangi Marae contd

Onetapu Formation	Onf	3.00	11.18	Muddy matrix-supported gravel; very poorly sorted; normally graded; maximum clast size 0.5 m; clasts rounded to subrounded; common grey and few red and black lithic casts; common clasts with orange-red staining, fine=grained pebbly base; matrix colour, grey with orange-red and olive mottles.
				Distict non-erosional contact.
Onetapu Formation	Ond	0.30	11.48	Clast-supported sands with few granules; ungraded; mm thick laminae; poorly soiled; largest clast 0.03 m; clasts subangular to subrounded.
				Distict erosional contact.
Onetapu Formation	One	0.40	11.88	Muddy matrix-supported granules; inversely graded; very poorly sorted; largest clast 0.1 m; clasts subrounded to rounded; common grey and black and few red lithic clasts; matrix colour yellowish brown to olive brown, mottled orange red and grey; contains common orange stained Taupo pumice clasts in upper 0.15 m with charcoal.
				Distict non-erosional contact.
"	"	0.30	12.18	Clast-supported, well sorted, well rounded re-worked Taupo Ignimbrite pebbles and granules.
"	"	0.50	12.48	Very gritty sandy clay loam (10 yr 6/8); contains lenses of rounded lithic granules and pebbles; common soft white pumice.

STOP 6 — Waikato Stream (Please be careful of traffic)

This stop comprises a series of sections that total c. 50 m of stratigraphy. Beds above the Oruanui Ignimbrite member of Kawakawa Tephra (c. 22,6 ka) have been described by Donoghue (1991), while those below are currently under study by Shane Cronin.

The first site we will examine is a good exposure of Bullot Formation tephras. At its base, and overlying diamictons, is Oruanui Ignimbrite. This site, and the Bullot Track site, are the most southward known occurrences of the ignimbrite. A characteristic feature of the Oruanui deposit is the presence of volcanic hailstones (chalazoidites) preserved near the top. We may be able to demonstrate further rhyolite markers, namely the Rerewhakaaitu (c. 14.7 ka) and Waiohau (c. 11.85 ka) tephras, within the Bullot Formation sequence.

Nearby we will see the Oruanui Ignimbrite remarkably preserved in a vertical crack. Could this crack have opened just prior to the eruption due to either doming caused by rising magma or rapid rifting?

Below the Oruanui Ignimbrite is a thick sequence of Bullot Formation-like weathered pumiceous tephras interbedded with fluvial, lahar, and hyperconcentrated flow deposits. Near stream level (c. 46 m) is a layer of lignite over a basal lahar that forms the stream bed. The lignite may be interpreted to date from either the last Interglacial or a warm period c. 60 ka. If this is so, then Ruapehu maintained an extremely active phase from either c. 125 ka or c. 60 ka to c. 10 ka.

Desert Road Description (Section 10)

Section Name and Map Code: Desert Road Section 10 [DR10]

Grid Reference: T20/464091

Locality: A large cutting on the western side of the Desert Road, approx. 100 m north of the junction with Tukino Skifield Road (Bullot Track), and immediately south of Desert Road S.11

Formation	*Member*	*Unit Depth (mm)*	*Cum. Depth (m)*	*Description*
Taupo Pumice	Taupo Ignimbrite	700	0.700	Pink and grey poorly sorted coarse ash and lapilli
Mangamate Tephra, Pahoka Tephra, Bullot Formation (upper)	unnamed	1300	2.000	Undescribed andesitic tephras, occurring between Taupo Pumice and Bullot Formation member L16
Bullot Formation (upper)	member L16	160	2.160	Yellowish red (5YR4/6 – 4/8) dominantly fine, and many medium and few coarse pumice lapilli, with strong brown (7.5YR5/8) interiors, and grey lithic lapilli; vesicular, blocky, angular, firm pumice lapilli and angular lithic lapilli
	$?M_3$	110	2.270	40 mm Olive coarse lithic and pumiceous ash; sharp upper contact 20 mm Pale brown coarse loamy textured ash, firm; with many fine lithic lapilli; discontinuous tephra, with wavy contacts 50 mm Dark purplish black coarse ash and fine lithic lapilli; loose; wavy contacts; distinctive tephra
	unnamed	20	2.290	Brownish yellow coarse ash and fine pumice lapilli; distinct contacts
		70	2.360	Dark grey coarse ash and very fine lithic lapilli; distinct upper contact
		30	2.390	Brown very fine pumice lapilli and grey lithic lapilli with some coarse ash matrix; distinct lower contact
		10	2.400	Brown coarse ash, firm
		60	2.460	Bedded dark purplish black coarse ash and very fine lithic lapilli
		40	2.500	Olive coarse ash and very fine lithic and pumice lapilli; wavy gradational contacts
		30	2.530	Pale grey coarse ash and dark brown (7.5YR4/4) pumice lapilli
	member L15	170	2.700	Dark brown (7.5YR4/4) and reddish yellow (7.5YR6/6) very fine and fine with fewer medium pumice lapilli; loose, gravelly texture; distinctive colouring
	unnamed	30	2.730	Grey coarse ash and very fine lithic lapilli
	member L14	60	2.790	Strong brown fine pumice lapilli with pale yellow interiors, few lithic lapilli, and black coarse ash matrix; vesicular, angular, hard pumice; ungraded unit
***	***	50	2.840	Pale purplish grey medium sandy loam textured medial unit, slightly greasy; with some scattered medium pumice lapilli; distinct contacts
	unnamed	40	2.880	20 mm Coarse ash 20 mm Strong brown fine and some medium pumice lapilli and some grey lithic lapilli; very vesicular pumice
		70	2.950	Black very fine lithic lapilli and coarse ash; loose, gravelly texture; with few fine pumice lapilli; distinct contacts
		10	2.960	Black coarse ash
		10	2.970	Pale brown coarse ash, firm; with scattered yellow fine pumice lapilli
		10	2.980	Brownish yellow very fine, angular, platy pumice fragments; loose, distinct contacts; strong colouring
		70	3.050	Black coarse ash
		70	3.120	Dark purplish black coarse ash and very fine and fine lithic, scoria and few pumice lapilli
		30	3.150	Olive grey coarse ash

DR10 contd

Formation	*Member*	*Unit Depth (mm)*	*Cum. Depth (m)*	*Description*
Bullot Formation (upper)	unnamed	70	3.220	20 mm Black coarse ash and lithic lapilli 50 mm Brown medium and fine pumice lapilli and coarse ash; with imogolite on lapilli faces; ungraded tephra
		50	3.270	Grey coarse lithic lapilli and few pumice lapilli
		40	3.310	Brown coarse sandy ash with few lapilli
		30	3.340	Grey sandy ash with scattered lapilli
		120	3.460	80 mm Coarse lithic ash with fine pale brown pumice lapilli 40 mm Coarse ash with yellow fine and few medium pumice lapilli, with olive to light grey interiors, and fine lithic lapilli
Rerewhakaaitu Tephra		100	3.560	Olive grey coarse ash with fine angular lithic lapilli; with 20 mm pale grey to white fine glassy rhyolitic ash (Rerewhakaaitu Tephra), pocketing, interbedded near base of unit
Bullot Formation (middle)	unnamed	30	3.590	Medium and fewer coarse strong brown pumice and black lithic lapilli
		30	3.620	Grey loamy coarse ash, firm
	?member L7b	60	3.680	Strong brown fine and medium pumice lapilli, with olive interiors, few grey angular lithic lapilli, and coarse sandy ash
	unnamed	20	3.700	Black and olive coarse loamy textured ash; sharp upper contact
		30	3.730	Yellowish brown loamy textured ash and few lapilli
	member L7	150	3.880	20 mm Strong brown very fine, angular, platy pumice fragments 110 mm Strong brown (7.5YR5/8) medium and fine pumice lapilli, with olive interiors, and very fine angular, platy pumice fragments and olive brown coarse ash; moderately soft pumice; reversely graded tephra; sharp basal contact 20 mm Black-olive coarse ash
Bullot Formation (?lower)	unnamed	40	3.920	Yellowish brown (10YR5/4) coarse ash and scattered lapilli
		90	4.010	Yellowish brown (10YR5/4) grading down to dark greyish brown (2.5Y4/2) coarse lithic ash; with fine lithic and pumice lapilli; ungraded tephra
		140	4.150	10 mm Andesitic pumice lapilli and interbedded reworked Kawakawa Tephra Formation 70 mm Strong brown (7.5YR5/8) very fine, fine and fewer medium pumice lapilli, with same coloured interiors, and coarse ash; reversely graded tephra, grading upward to dominantly medium lapilli; 60 mm Dominantly fine, and very fine pumice lapilli, firm and soft, and coarse ash
Te Heuheu Formation	unnamed	80	4.230	Coarse sand and lapilli, with reworked Kawakawa Tephra Formation; and scattered cobbles and pebbles; fluvial deposit
reworked Kawakawa Tephra Formation		70	4.300	20 mm Pink fine ash 50 mm Grey fine ash, pocketing; fluvially reworked tephra
Kawakawa Tephra Formation	Oruanui Ignimbrite	340	4.640	Pink fine ash with very fine and fine pumice lapilli; massive; with occasional chalazoidites; lower 50 mm mottled
	Aokautere Ash	50	4.690	30 mm Salmon-pink fine ash with many chalazoidites 20 mm Laminae of pink and grey fine ash with many chalazoidites
		85	4.775	10 mm Grey coarse crystal-rich ash and very fine pumice 30 mm Pale yellow coarse crystal-rich ash and very fine pumice 3 mm Grey fine ash 2 mm Pink fine ash 5 mm Grey fine ash 25 mm White coarse ash; with many bright orange mottles 10 mm Pale yellow coarse ash

DR10 contd

Formation	*Member*	*Unit Depth (mm)*	*Cum. Depth (m)*	*Description*	
Te Heuheu Formation	unnamed	130	4.905	40 mm	Dark grey (10YR4/1) loamy sand; sharp contacts
				50 mm	Yellowish brown (10YR5/4) medium sandy loam textured unit; massive
				20 mm	Grey medium sandy loam textured unit, with scattered fine lapilli
				20 mm	Brown medium sandy loam textured unit, with scattered fine lapilli
		60	4.965	Coarse sand with fine scattered pumice lapilli and fine subrounded lithic pebbles; ?fluvial deposit	
		80	5.045	Coarse sand with many orange and black lithic pebbles; normally graded clasts	
		450	5.045	Yellowish brown (10YR5/8) clay matrix with matrix-supported medium and coarse heterolithologic lithic pebbles, many colours, soft, weathered; with a brown firm clay band with scattered pebbles at base; wedging debris flow deposit	
		1000+	6.765	Yellowish brown (10YR5/8) coarse loamy sand and granule matrix, becoming sandier toward base; with many matrix-supported fine andesitic pebbles, many colours, and pale yellow fine pumice pebbles; soft pumice; debris flow deposit, with finer clasts than overlying deposit	

Waikato Stream Description

Section Name and Map Code: Waikato Stream Section 2 [WS2]

Grid Reference: T20/469102

Locality: Cliff face immediately east of the Desert Road and approx. 50 m north of the bridge over Waikato Stream. Description is for member L7b and older deposits only

Formation	*Member*	*Unit Depth (mm)*	*Cum. Depth (m)*	*Description*
Bullot Formation (middle)	member L7b	60	0.060	Strong brown (7.5YR5/6) fine pumice lapilli and very fine, platy, angular pumice fragments
	unnamed	20	0.080	Black coarse ash
	member L7	110	0.190	Strong brown (7.5YR5/8) fine and medium pumice lapilli, black lithic lapilli, and coarse ash; very vesicular and soft pumice lapilli.
	unnamed	40	0.230	Black coarse ash
		50	0.280	Reddish brown loamy coarse ash with abundant fine and medium lithic and pumice lapilli
		170	0.450	100 mm Strong brown fine and medium pumice lapilli with some black fine lithic lapilli and scoria; with a coarse ash matrix
				70 mm Strong brown and some olive medium and fine pumice lapilli, and many black lithic lapilli; soft pumice, and angular lithics; sharp contacts
Bullot Formation (lower)	member L1	150	0.600	Greenish grey weakly bedded coarse crystal-rich ash; some beds dominantly yellow pumiceous ash
Te Heuheu Formation	unnamed	40	0.640	Black and brown coarse ash with scattered pebbles
Bullot Formation (lower)	unnamed	70	0.710	Black to olive coarse ash
Te Heuheu Formation	unnamed	80	0.790	Yellowish brown sandy loam textured matrix, with many matrix-supported fine to very coarse pumice and lithic pebbles; ungraded; ?debris flow deposit
		150	0.940	Greyish brown sand matrix, with abundant heterolithologic andesitic pebbles
		220	1.160	Bedded sands and pebbles
Bullot Formation (lower)	unnamed	40	1.200	Brown loamy textured ash; discontinuous
Kawakawa Tephra Formation		150	1.350	White to pale grey coarse ash with finer ash base; tephra cross-cuts andesitic diamictons (described below) over a vertical extent of *c.* 4 m
Te Heuheu Formation	unnamed	180	1.530	Yellowish brown loamy sand textured matrix, with matrix-supported heterolithologic andesitic pebbles; ?debris flow deposit
		1600	3.130	Reddish brown coarse sand matrix, with weakly developed horizontal stratification, lithified; with many andesitic pebbles and occasional boulders; sharp contacts
		270	3.400	Bright orange sandy loam textured matrix, semi-lithified; with many brightly coloured andesitic pebbles, cobbles, and fewer boulders; ungraded; sharp contacts; ?debris flow deposit
		930	4.330	Lithified sand and granule matrix; with many andesitic pebbles to boulders; ?debris flow deposit
		550	4.880	Grey bedded coarse sand and pinkish brown clay beds, firm; with lenses of lithic and pumice pebbles
			4.880	Over 10⁺ m of interbedded andesitic diamictons, sands and clay to stream level

REFERENCES

Donoghue, S.L. 1991: Late Quaternary volcanic stratigraphy of the southeastern sector of Mount Ruapehu ring plain, New Zealand. Unpublished PhD. thesis, Massey University, Palmerston North.

Donoghue, S.L.; Hodgson, K.A.; Neall, V.E; Palmer, A.S. 1991a: Volcanic hazards — southwestern ring plain of Ruapehu volcano. *Geological Society of New Zealand miscellaneous publication 59B*: 56-88.

Donoghue, S.L.; Stewart, R.B.; Palmer, A.S. 1991b: Morphology and chemistry of olivine phenocrysts of Mangamate Tephra, Tongariro Volcanic Centre, New Zealand. *Journal of the Royal Society of New Zealand 21*: 225-236.

Donoghue, S.L.; Neall, V.E.; Palmer, A.S. 1994: Late Quaternary andesitic tephrostratigraphy and chronology, Tongariro Volcanic Centre, New Zealand. *Journal of the Royal Society of New Zealand* (in press).

Fergusson, G.J.; Rafter, T.A. 1959: New Zealand ^{14}C age measurements — 4. *New Zealand journal of geology and geophysics 2*: 208-241.

Froggatt, P.C.; Lowe, D.J. 1990. A review of late Quaternary silicic and some other tephra formations from New Zealand: their stratigraphy, nomenclature, distribution, volume, and age. *New Zealand journal of geology and geophysics 33*: 89-109.

Hodgson, K.A. 1993: Late Quaternary lahars from Mount Ruapehu in the Whangaehu River Valley, North Island, New Zealand. Unpublished PhD thesis, Massey University, Palmerston North (2 volumes).

Purves, A.M. 1990: Landscape ecology of the Rangipo Desert. Unpublished MSc. thesis, Massey University, Palmerston North.

Topping, W. W. 1973: Tephrostratigraphy and chronology of late Quaternary eruptives from the Tongariro Volcanic Centre, New Zealand. *New Zealand journal of geology and geophysics 16*: 397-423.

Topping, W.W. 1974: Some aspects of Quaternary history of Tongariro Volcanic Centre. Unpublished PhD thesis, Victoria University of Wellington, Wellington.

Topping, W.W.; Kohn, B.P. 1973: Rhyolitic tephra marker beds in the Tongariro area, North Island, New Zealand. *New Zealand journal of geology and geophysics 16*: 375-395.

Wilson, C.J.N. 1993: Stratigraphy, chronology, styles and dynamics of late Quaternary eruptions from Taupo volcano, New Zealand. *Philosophical transactions of the Royal Society of London A343*: 205-306.

DAY 3: TOKAANU—WANGANUI

B. J. Pillans
Department of Biogeography & Geomorphology
Research School of Pacific Studies
Australian National University
Canberra, ACT 0200, Australia

A. S. Palmer
Department of Soil Science
Massey University, Private Bag 11-222
Palmerston North, New Zealand

Pillans, B.J., Palmer, A.S. 1994. Post-conference Tour Day 3: Tokaanu-Wanganui. In: Lowe, D.J. (ed) Conference Tour Guides, Proceedings International Inter-INQUA Field Conference and Workshop on Tephrochronology, Loess, and Paleopedology, University of Waikato, Hamilton, New Zealand, 139-156.

Outline of Day 3 (Tuesday 15 February)

8.00-11.30 am	Depart Tokaanu Hotel and travel to Wanganui via National Park and Raetihi (State Highways 47 and 4)
11.30-12.30 pm	STOP 1 — Mowhanau Beach (Castleciff Section). LUNCH
12.30-1.10 pm	Travel to Kohi Road, Waverley (SH 3)
1.10-1.40 pm	STOP 2 — Kohi Road loess section
1.40-2.00 pm	Travel to Omahina Road
2.00-2.30 pm	STOP 3 — Omahina Road loess section
2.30-3.10 pm	Travel to Rangitatau East Road
3.10-4.00 pm	STOP 4 — Rangitatau East Road loess section.
4.00-4.20 pm	Travel to Brunswick Road
4.20-5.00 pm	STOP 5 — Brunswick marine terrace and Waipuru Ash
5.00-5.30 pm	Travel to Collegiate Motor Inn, Wanganui
	Evening: Dinner

INTRODUCTION TO WANGANUI BASIN

Today we travel south (Fig. 3.1) to the Wanganui Basin, a back-arc basin containing up to 4 km thickness of Plio-Pleistocene shallow marine and coastal sediments (Figs. 3.2-3.3). The basin has undergone marginal uplift and offshore subsidence as the depositional centre moved southeast. Excellent exposures of gently dipping Middle and Lower Pleistocene marine sediments occur in coastal cliffs up to 60 m high. An exceptionally well-preserved flight of marine terraces extends west from Wanganui. Airfall coverbeds of loess and tephra mantle the terraces, and provide a paleoclimate record of the last 500 ka.

STOP 1 — Mowhanau Beach (Castlecliffian Stratotype)

Coastal cliffs extending some 20 km west of Wanganui are the stratotype exposures of the New Zealand Castlecliffian (0.4-1.6 Ma) and Nukumaruan (1.6-2.4 Ma) Stages. In the cliffs, shallow marine strata dip gently southeast at dips of a few degrees (Fig. 3.4). The section was recently proposed (Pillans et al. 1991) as a possible international Lower/Middle Pleistocene boundary stratotype, at the level of the Brunhes/Matuyama boundary (0.78 Ma).

The cyclothemic nature of the Castlecliff section was established by Fleming (1953) in his benchmark study of the geology of the Wanganui area. Beu & Edwards (1984) and Kamp & Turner (1990) interpreted the cyclothems in terms of glacio-eustatic cycles, and proposed correlations with deep sea oxygen isotope stages.

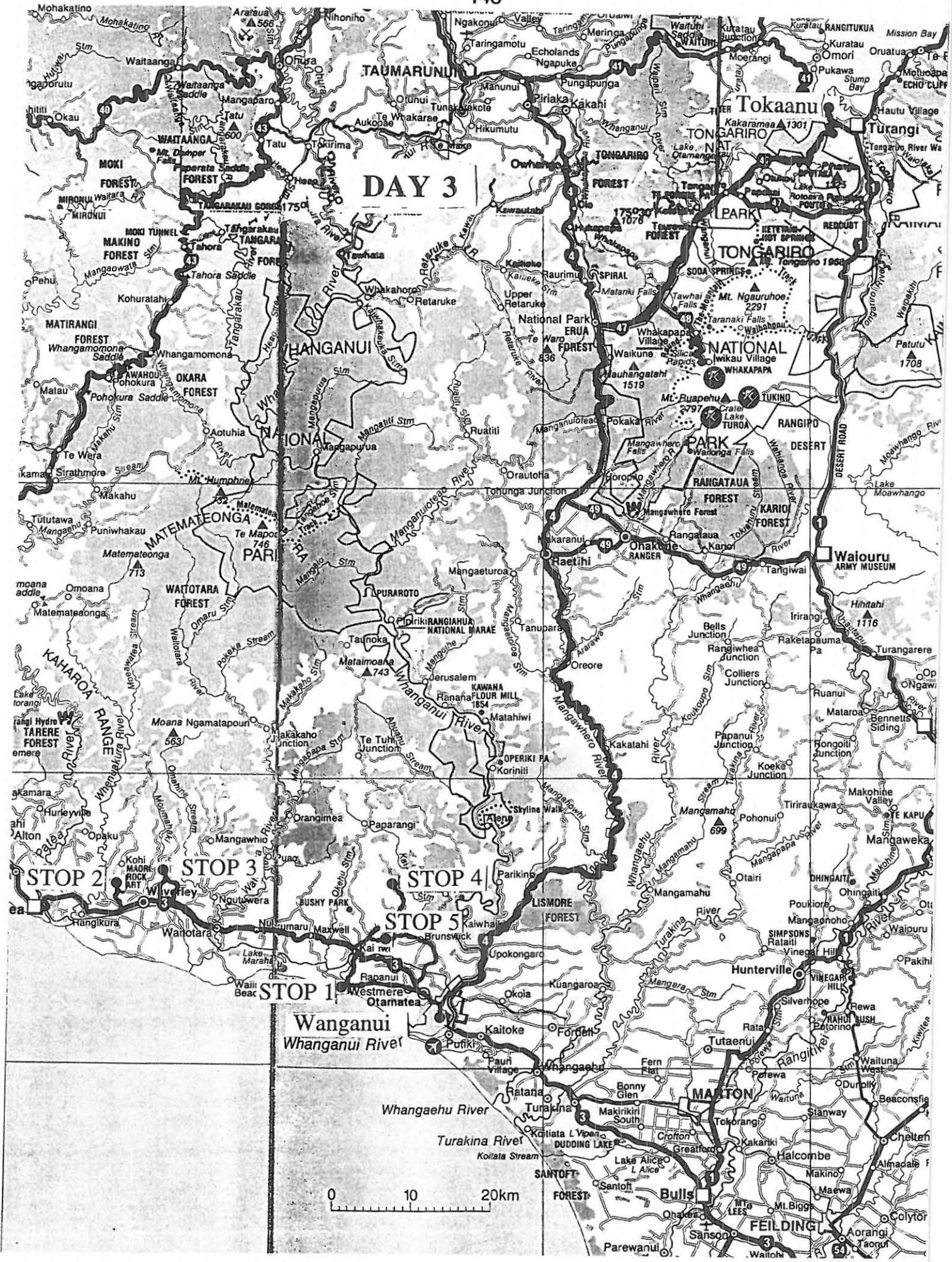

Figure 3.1: Route map for Day 3.

Abbott & Carter (in press) have shown that each cyclothem typically comprises the following elements in ascending order:

1. Basal erosional unconformity, often with evidence of boring by intertidal molluscs.
2. Sand-dominated, nearshore and beachface sediments containing pebbles and broken shallow-water molluscs.
3. A mid-cycle shellbed containing *in situ* offshore molluscs in a muddy matrix.
4. An upper massive or bedded siltstone unit containing sparse offshore molluscs.

Abbott & Carter (in press) recognise ten such cyclothems in the coastal section (Fig 3.5), and describe them in terms of the seismic sequence stratigraphy model. The sediments in each cyclothem were deposited during rising sea-level (Transgressive Systems Tract) and high sea-level (Highstand Systems Tract) phases of glacio-eustatic sea-level cycles. Abbott & Carter (in press) and Pillans et al. (in press) have also made revised correlations of the cyclothems with the oxygen isotope stages. A key tie point in the correlations is the recognition (Turner & Kamp 1990) of the Brunhes/Matuyama polarity transition at the level of the Kaikokopu Formation (Kaikokopu Shell Grit of Fleming 1953) — see Fig. 3.5.

Individual cyclothems can be traced inland across the basin some 50 km east from the Castlecliff section to the Rangitikei River valley. On Day 4 of the field trip we will examine correlative strata in the Whangaehu and Rangitikei valleys. Several cyclothems contain reworked rhyolitic tephras (tuffs), which are important for correlation and dating.

Unconformably overlying the Castlecliffian sequence at Mowhanau Beach are the type exposures of the Rapanui Formation (Fleming 1953). Rapanui Formation comprises marine and non-marine coverbeds underlying the surface of Rapanui Terrace. Erosion of the basal Rapanui wave-cut surface and deposition of the overlying marine sediments occurred during oxygen isotope stage 5e, about 120 ka (Pillans 1983, 1990).

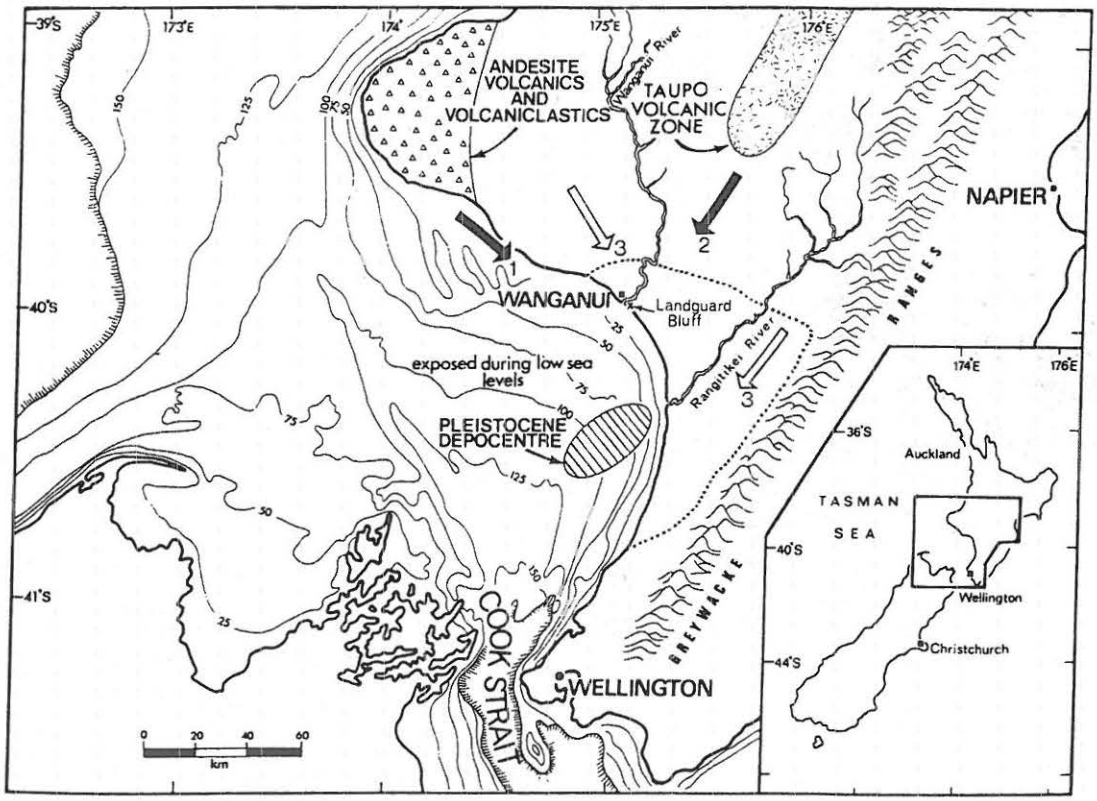

Figure 3.2: General location of the Wanganui Basin (After Pillans et al. 1988). Numbered arrows indicate main sediment sources and transport directions: 1. Taranaki andesitic volcanics; 2. Taupo Volcanic Zone andesitic and rhyolitic volcanics; 3. Tertiary/Mesozoic sedimentary and low grade metamorphic rocks.

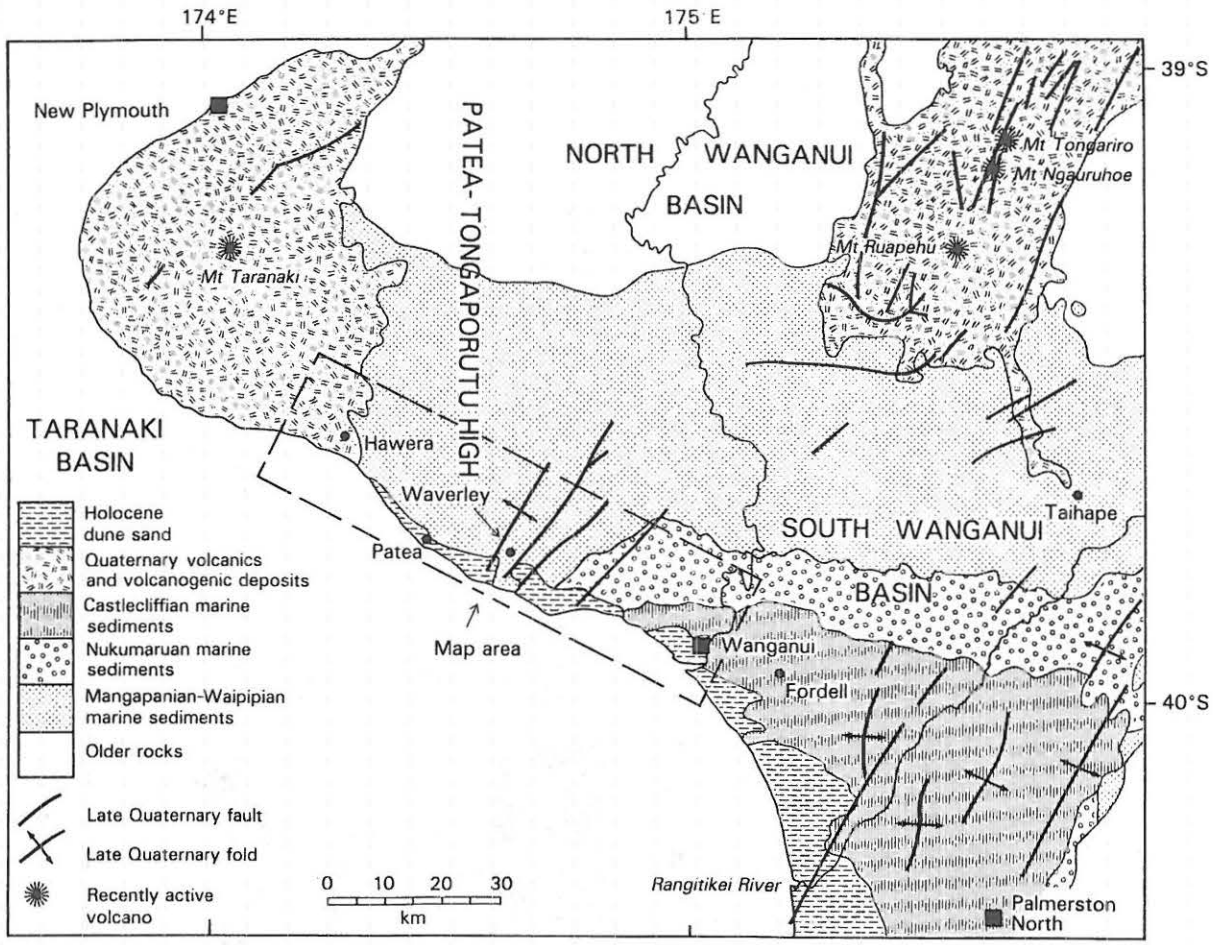

Figure 3.3: Geological setting of Wanganui Basin and location of marine terraces (map area). After Pillans (1990).

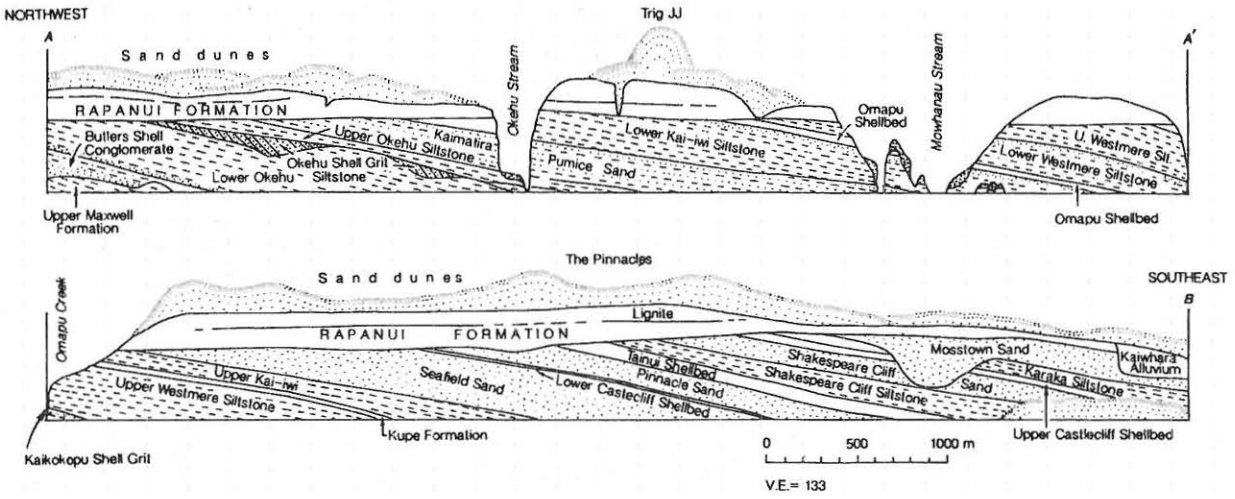

Figure 3.4: Stratigraphic sketch of the coastal Castlecliffian stratotype section west of Wanganui. After Fleming (1953) in Kamp & Turner (1990).

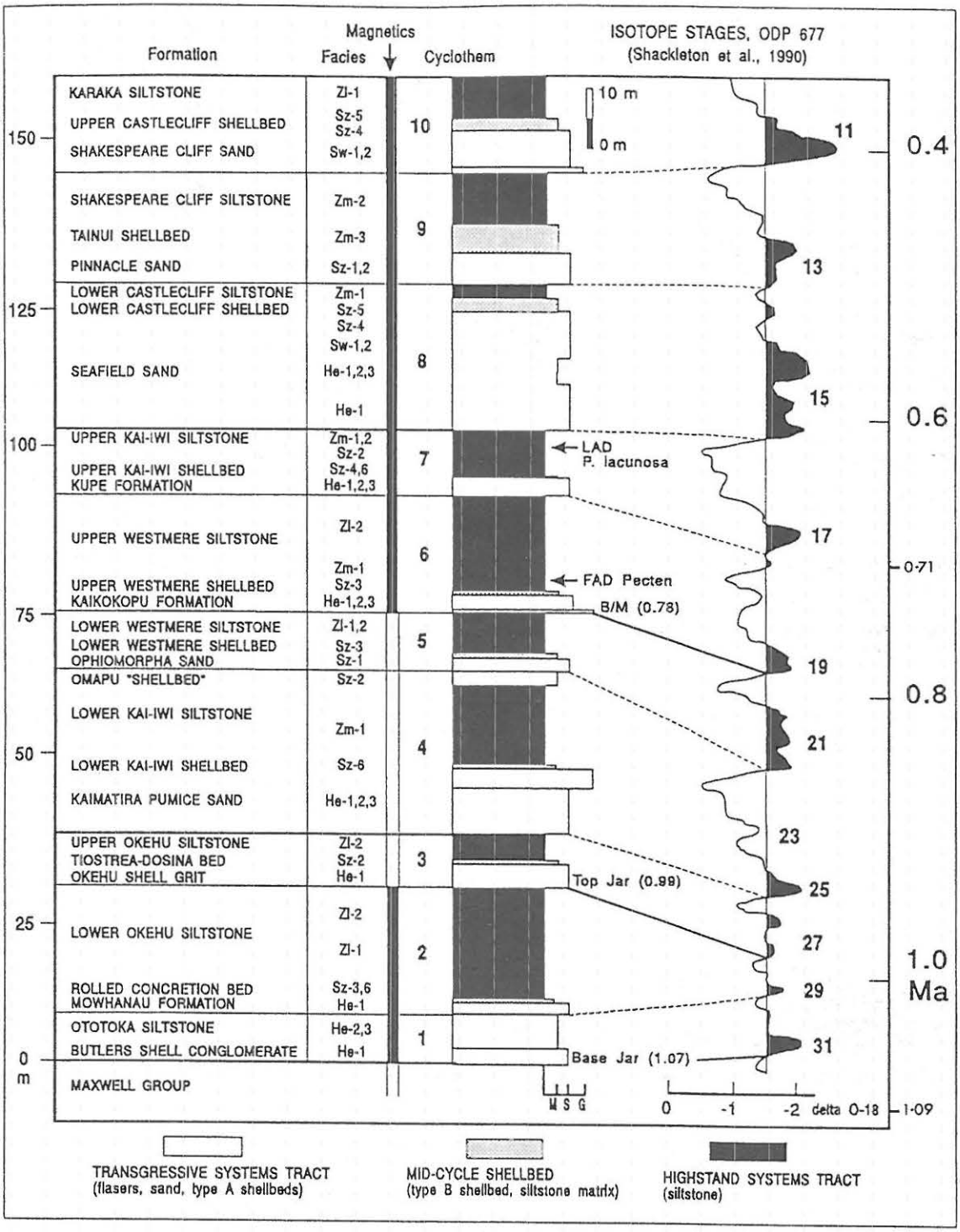

Figure 3.5: Summary stratigraphic column of the Castlecliffian section, showing lithostratigraphy, cyclothems, and correlations with the oxygen isotope timescale. After Abbott & Carter (in press).

SOUTH TARANAKI — WANGANUI MARINE TERRACES

A remarkable flight of marine terraces occurs between Hawera and Wanganui (Figs. 3.3, 3.6). The terraces run roughly parallel to the present coastline for more than 100 km, rising to over 300 m above present sea-level, and extending as much as 20 km inland (Fig. 3.6). Twelve terraces were recognised and named by Pillans (1983, 1990). Chronology for the terrace sequence was originally established by fission-track, radiocarbon, and amino acid racemization dating, coupled with a simple model of terrace deformation (Pillans 1983, 1990). Terrace names and ages, from youngest to oldest, are:

- RAKAUPIKO (60 ka; stage 3),
- HAURIRI (80 ka; stage 5a),
- INAHA (100 ka; stage 5c),
- RAPANUI (120 ka; stage 5e),
- NGARINO (210 ka; stage 7),
- BRUNSWICK (310 ka; stage 9),
- BRAEMORE (340 ka; stage 9),
- ARARATA (400 ka; stage 11),
- RANGITATAU (450 ka; stage 11?),
- BALL [=Kaiatea] (520 ka; stage 13),
- PIRI (600 ka; stage 15) and
- MARORAU (680 ka; stage 17).

The oldest 5 terraces are therefore inferred to be the shoreline equivalents of cyclothems 7-10 at Castlecliff (Fig. 3.5).

The pattern of shore-parallel deformation, which is similar for all terraces between Hawera and Wanganui (Fig. 3.7), defines a broad fold (Whangamomona Anticline), with maximum uplift in the Waverley area. Uplift rates, based on terrace strandline heights and ages, generally increase inland, and vary between 0.2 and 0.7 m/ka (Fig. 3.8). The terraces are vertically offset across several northeast trending, high angle normal faults. Some of the faults could be bending-moment faults associated with compressional folding.

From Mowhanau Beach we will travel inland across the terrace sequence to examine loess and tephra coverbeds at four localities to the north and west. The three sections at Stops 2 to 4 have been the focus of intensive study. Fifteeen centimetre undisturbed drill cores have been taken from sites adjacent to these sections. Information gained so far includes: detailed description, paleomagnetism (Pillans & Wright, 1990), bulk density, allophane content, XRF analyses of major and minor elements, extractable iron, aluminium, and silica, quartz content (A.S. Palmer et al. unpub. data), phosphate fractions, and phytolith identification. A number of thermoluminescence dates (Berger et al. 1992) and a fission-track date (Kohn et al. 1992) have also been reported from the Rangitatau East site (Stop 4). Experimental U/Th dating of pedogenic iron concretions from the Kohi Road site (Stop 2) is underway.

Figure 3.9 shows the stratigraphy and dry bulk density of the three cores taken adjacent to the roadcuts that we will examine at the next three stops (Palmer et al. unpub. data). Paleosols and modern soils have low densities because:

1. They are relatively rich in andesitic tephra (undiluted by loess).
2. The activities of soil flora and fauna create pore spaces.
3. Development of soil structure creates pore spaces.
4. Weathering produces short-range order (SRO) and crystalline clays.

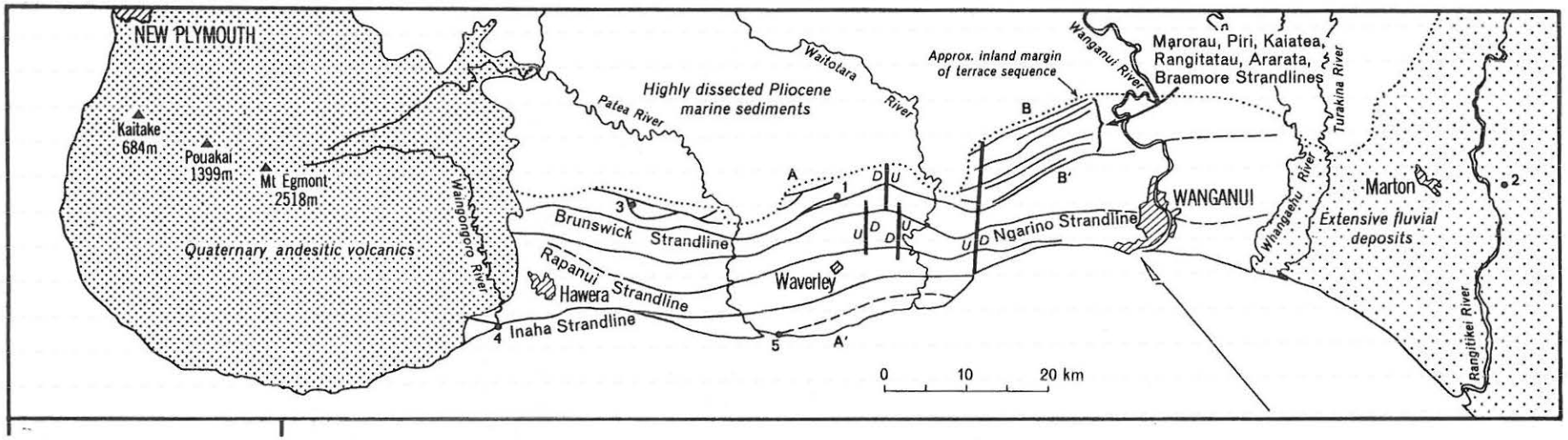

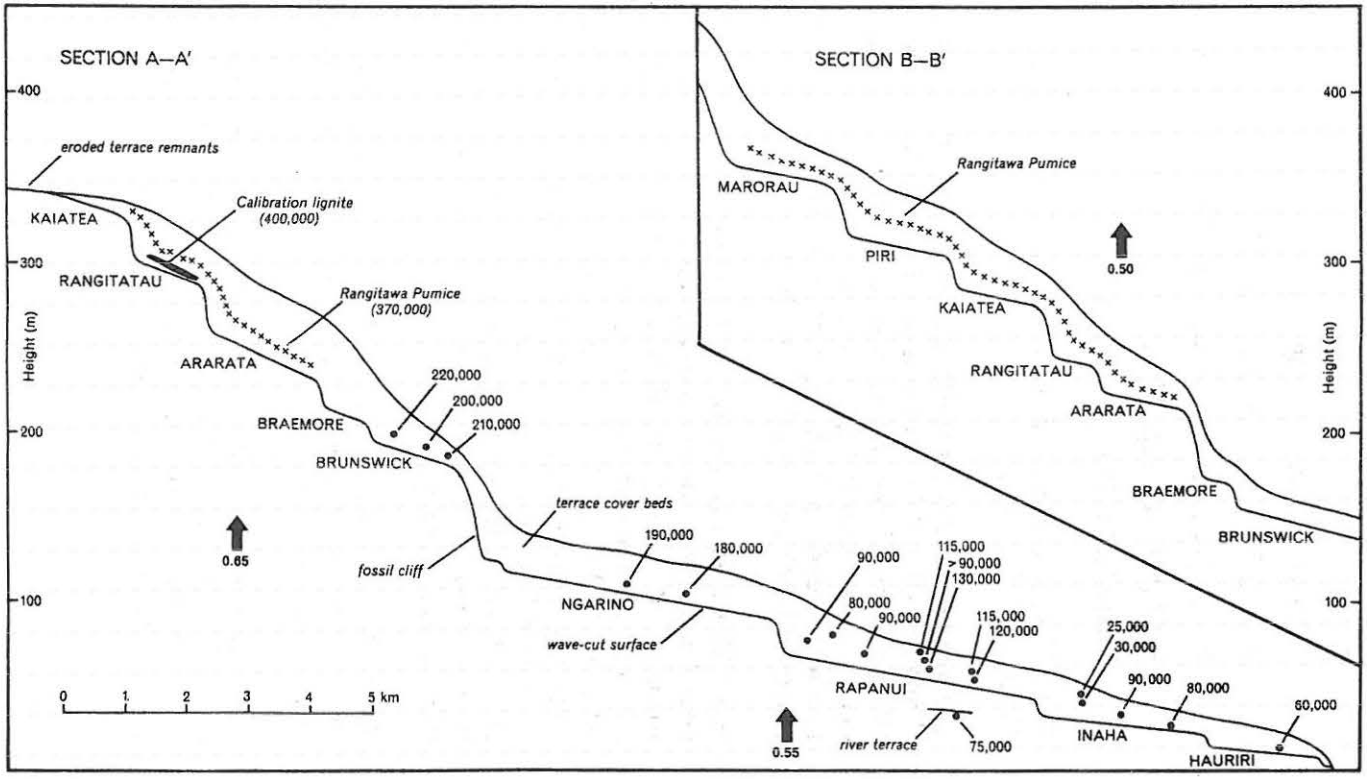

Figure 3.6:
Location of south Taranaki-Wanganui marine terraces, and generalised shore-normal cross-sections showing locations of samples dated by amino acid racemization, stratigraphic position of Rangitawa Tephra (Pumice), and uplift rates (large arrows) in m/ka.
After Pillans (1983).

Highest densities are found in unweathered quartzose-feldspathic (Q-F) loess which accumulated during glacial and stadial maxima. The Q-F loess was derived from:

1. Local gullies cut through terrace deposits into underlying Pliocene mudstones and muddy sandstones.
2. Distant fluvial aggradation surfaces, including the continental shelf which was exposed at times of low sea-level.

Volcanic loess, derived from reworked tephra and lahar surfaces of Mt Egmont/Taranaki, and older andesitic volcanoes in Taranaki, was also deposited, and generally has a low bulk density because it weathers to SRO minerals more readily than Q-F loess.

STOP 2 — Kohi Road

A road cutting on Kohi Road (Q21/465610) shows four loess layers (L1-L4) overlying dunesand and marine sediments of Rapanui Terrace (120 ka; isotope stage 5e). Loess L1, containing Kawakawa Tephra (Aokautere Ash), accumulated during isotope stage 2, Loess L2 accumulated during stage 3, Loess L3 accumulated during stage 4, and Loess L4 accumulated during substages 5b and 5d.

STOP 3 — Omahina Road

A road cutting on Omahina Road (R21/528627) shows six loess layers (L1-L5) overying fluvial sands and silts and marine sediments of Ngarino Terrace (210 ka; isotope stage 7a). Loess L5 accumulated during isotope stage 6.

STOP 4 — Rangitatau East Road

A road cutting on Rangitatau East Road (Q22/767594) shows eleven loess layers overlying dunesand on a pre-Marorau terrace surface. Rangitawa Tephra, within Loess L10, is fission track dated at 350 ± 50 ka at this locality (Kohn et al. 1992). Kawakawa Tephra (22.6 ka) occurs within loess L1. The loess/paleosol sequence is thought to span the last 500 ka.

Pillans & Wright (1990) presented paleomagnetic data from a drill core taken adjacent to the road section. The entire sequence is of normal polarity, and is therefore presumed to be younger than 780 ka. Two intervals of anomalously low inclination were recorded in L2 (30-40 ka) and at the base of L11 (490-500 ka), possibly correlating with the Mungo and Emperor events, respectively (Fig. 3.10). Magnetic susceptibility tends to be higher in paleosols than in the surrounding loess, and very high in the basal dunesand. The susceptibility peaks appear to correlate with increases in titanomagnetite from tephras, particularly andesitic tephras, which are relatively concentrated in the paleosols at times when loess accumulation slowed. The susceptibilty record is therefore partly controlled by volcanic activity and partly controlled by loess accumulation rates (and by inference, climate changes).

Figure 3.11 shows the distribution of quartz with depth in the Rangitatau East core (Palmer et al. unpub. data). Quartz is high in Q-F loess and low in paleosols, tephra, and volcanic loess. Not only do these data confirm the stratigraphic interpretation of the core, but also they give an indication of the magnitude of landscape destabilisation during glacial and stadial times. The quartz curve also allows correlation with the oxygen isotope stratigraphy of deep sea cores.

Berger et al. (1992) reported thermoluminescence (TL) dates from the section, which are in broad agreement with previous age estimates for the section. TL ages for all Wanganui Basin samples dated by Berger et al. (1992) are listed in Table 3.1.

TABLE 3.1. Thermoluminescence ages of loess in Wanganui Basin. After Berger et al. (1992).

Sample	D_E* (Gy)	Method†	Filter§	Plateau (°C)	Dose rate‡ (Gy/ka)	TL age (ka)	Expected age (ka)
RTAT-1	35.0±2.1	PB	UG11	280-350	2.149±0.076	16.3±1.3	18.5±1.5
	50.9±3.9	TB	UG11	370-420		23.7±2.2	
AOK-2	56.5±3.8	PB	UG11	270-360	2.71 ±0.14	20.8±1.7	23.0±0.5
	113.3±6.1	TB	UG11	370-420		41.8±3.1	
FERY-1	331 ±54	PB	UG11	270-340	3.88 ±0.26	85 ±15	75 ±5
RTAT-5	288 ±42	PB	UG11	290-360	2.15 ±0.16	134 ±22	110 ±10
	285 ±41	TB	UG11	310-400		133 ±21	
QTL-71A	480 ±130	PB	BG28	310-380	4.30 ±0.38	110 ±32	≤140 ±10
QTL-71H	600 ±130	PB	BG28	320-350	4.25 ±0.38	140 ±30	≥140 ±10
RTAT-13	380 ±58	PB	BG28	300-380	2.46 ±0.17	155 ±26	190 ±20
	413 ±34	TB	BG28	310-410		168 ±17	
RTAT-9	490 ±110	PB	UG11	330-380	2.10 ±0.17	234 ±56	270 ±20
GRDQ-2	396 ±66	PB	UG11	320-380	2.25 ±0.16	176 ±32	300 ±40
	436 ±41	TB	UG11	300-400		194 ±22	
	738 ±82	TB	BG28	370-440		328 ±43	
CURL-3	536 ±66	ADD	UG11	350-420	2.27 ±0.24	235 ±30	360 ±20
	790 ±140	TB	BG28	370-440		348 ±70	
RTP-2	810 ±190	PB	UG11	330-400	2.50 ±0.26	323 ±83	360 ±20
	1010 ±160	TB	UG11	350-430		403 ±76	
RTAT-20	710 ±110	TB	UG11	370-440	1.184±0.073	599 ±99	475 ±25
TMUNA-1	2340 ±740	TB	BG28	360-440	3.18 ±0.37	730 ±250	800 ±50

* Weighted mean ± average error (Berger and Huntley 1989) over temperature interval in column 4, which gives temperature range spanned by recognized plateau in D_E values. Plateau regions for PB and TB methods for samples RTAT-1 and AOK-2 are different. In spite of this difference we list the D_E values and corresponding TL ages for TB method because no plateaus were observed at lower temperatures and because any plateau region from TB method for such young loess could be interpreted as having age significance in absence of other TL data (e.g., PB experiment). All errors are 1σ.

† TL methods used to measure D_E values are partial bleach (PB), total bleach (TB), and additive dose (ADD).

§ TL emissions were recorded either through ultraviolet optical glass filter UG11 (bandpass 300-380 nm) or blue-green filter BG28 (bandpass 380-500 nm). Heating rate of 5°/s was used for TL readout.

‡ The dose rate components are calculated as outlined in Berger (1988).

Samples from Rangitatau East are:

- RTAT-1 (11 cm above Kawakawa Tephra in L1)
- RTAT-5 (base of L4)
- RTAT-13 (55 cm below top of paleosol in L6)
- RTAT-9 (in L8, 30 cm below unconformity)
- RTAT-20 (20 cm above base L11).

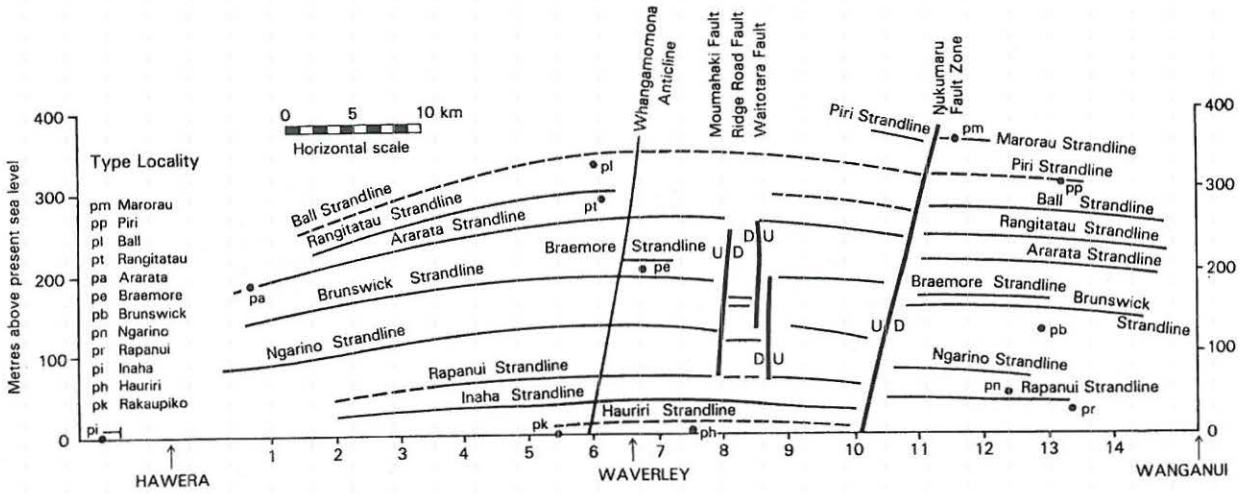

Figure 3.7: Shore-parallel deformation as shown by terrace strandline heights between Hawera and Wanganui. After Pillans (1990).

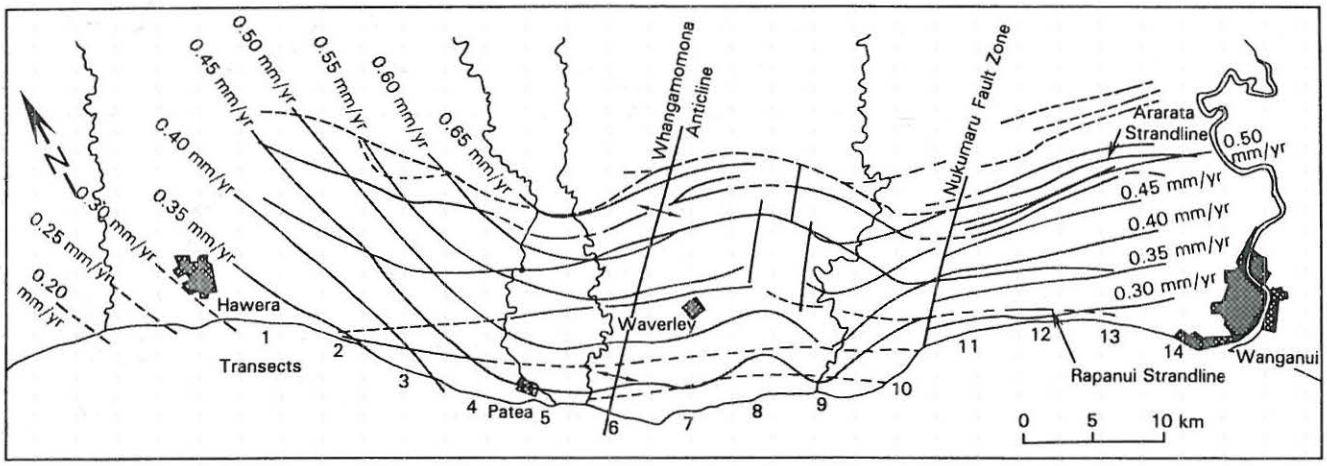

Figure 3.8: Contoured mean uplift rates based on hinging uplift model and strandline heights for each of 14 numbered shore-normal transects. After Pillans (1990).

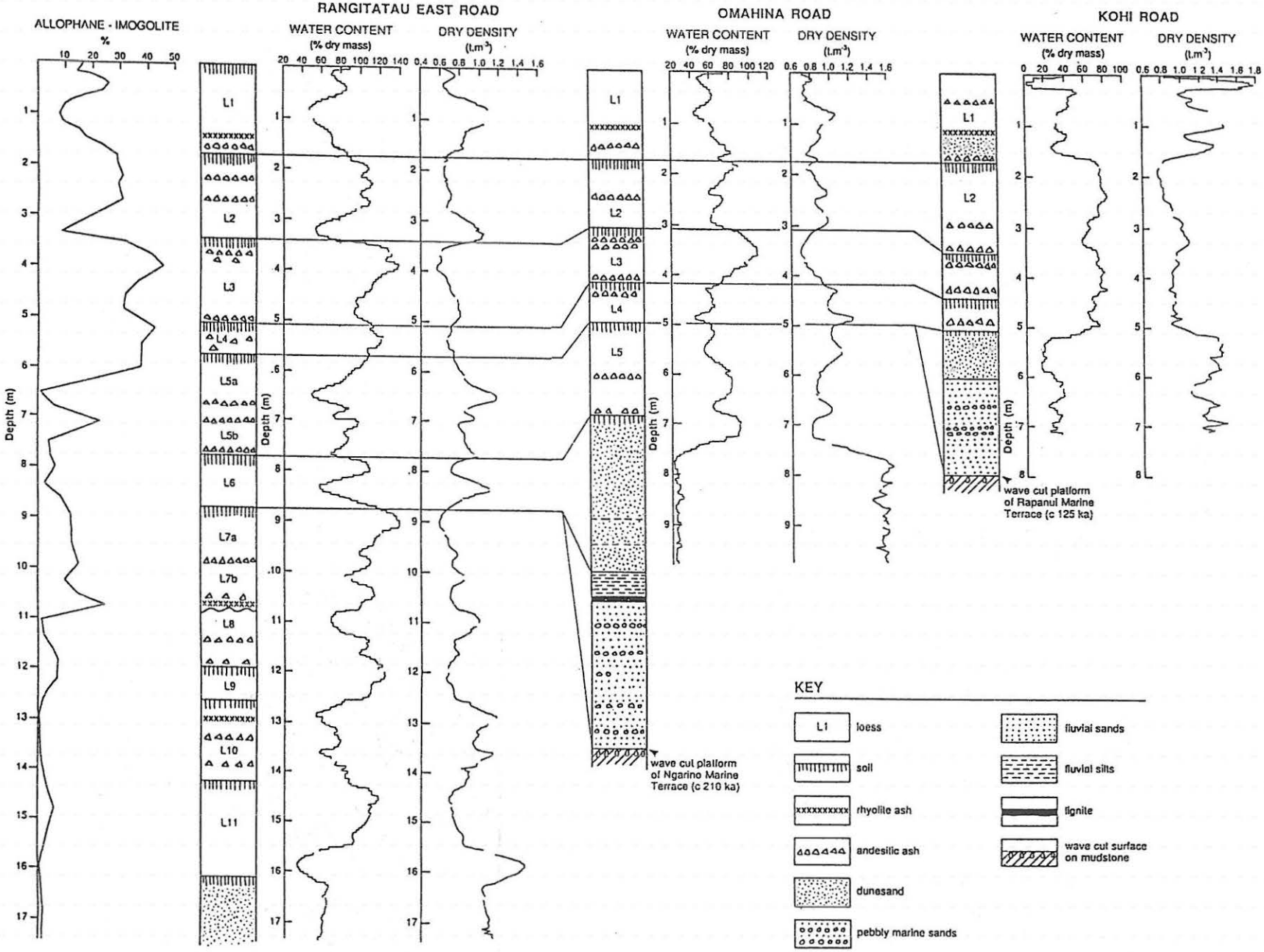

Figure 3.9: Stratigraphy, water content, and dry bulk density of cores from Kohi Road, Omahina Road, and Rangitatau East Road.

STOP 5 — Brunswick Road

A section on Brunswick Road (R22/784500) shows a sequence of terrestrial and marine sediments overlying the wave cut platform of the Brunswick Terrace (310 ka)— see Fig. 3.12. This section was nominated by Fleming (1953) as the type locality of the Brunswick Marine Terrace. The loess layers at the top of the section represent L1-L6, but are much thinner than at the Rangitatau East section. A lower rate of loess accumulation, and a lower rainfall than at Rangitatau East, have resulted in a different loess weathering facies at Brunswick Road.

The soil here is a Westmere Silt Loam (Mollic Hapludalf). Table 3.2 contains a soil profile description and selected chemical data from a nearby site (Adams & Wilde 1978). Note the texture and clay coatings (cutans) in the description, and P retention data. For comparison, Table 3.3 gives a profile description and chemical data for Egmont Black Loam (Typic Hapludand), more typical of the Omahina and Rangitatau sites to the west. Note the silt-loam texture and higher P retention of the Egmont Soil (Parfitt et al. 1980).

Beneath the Brunswick wave cut platform, a sequence of Nukumaruan (Lower Pleistocene) shallow marine sediments assigned to the Tewksbury Formation contains Waipuru Shellbed (Fleming 1953) and the rhyolitic Waipuru Ash (Fig. 3.13). Beu & Edwards (1984) reported the First Appearance Datum (FAD) of the coccolith *Geophyrocapsa sinuosa* in this section. *G. sinuosa* is thought to have evolved near the base of the Olduvai Subchron (c. 1.9 Ma) in the New Zealand region.

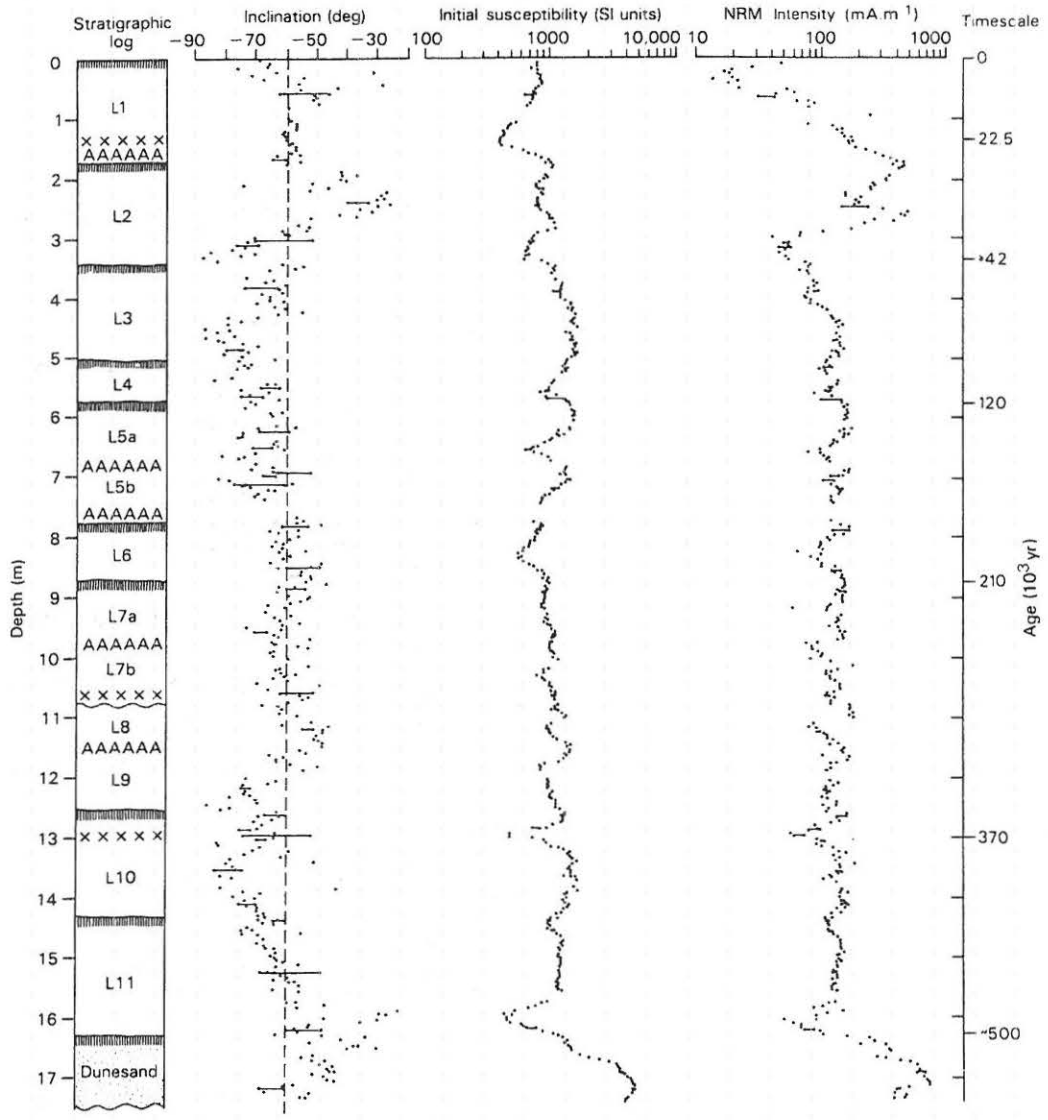

Figure 3.10: Loess stratigraphy and paleomagnetic data for Rangitatau East drill core. Rangitawa Tephra is at 13 m depth. A = andesitic tephra, X = rhyolitic tephra, vertical lines = paleosols. After Pillans & Wright (1990).

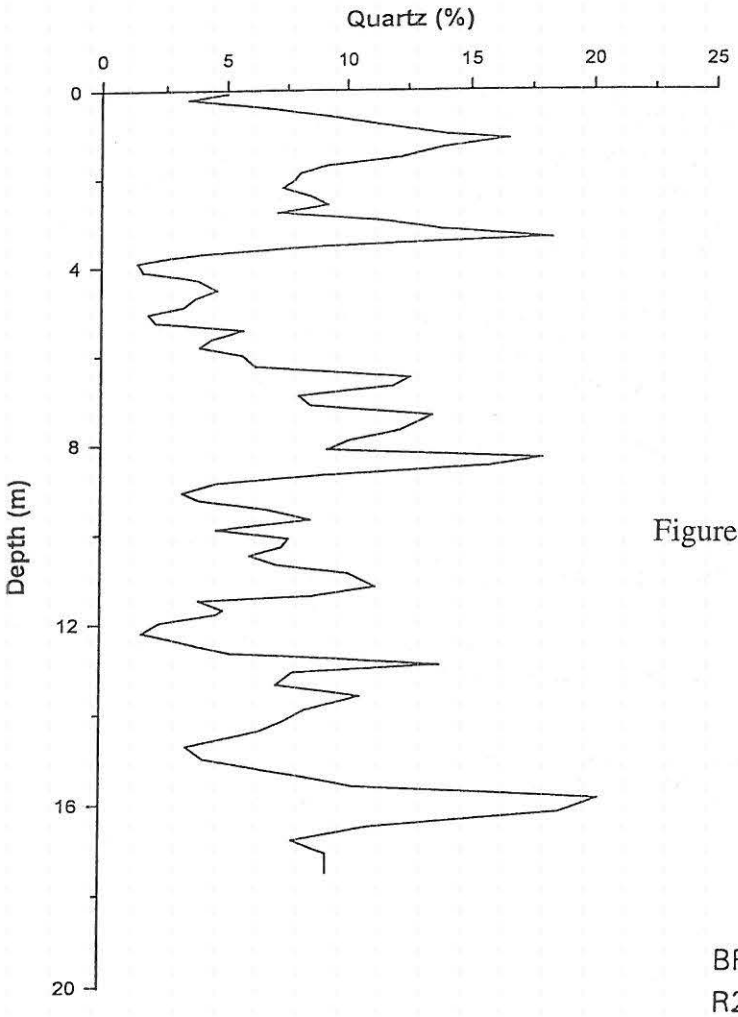

Figure 3.11: Quartz content of Rangitatau East core.

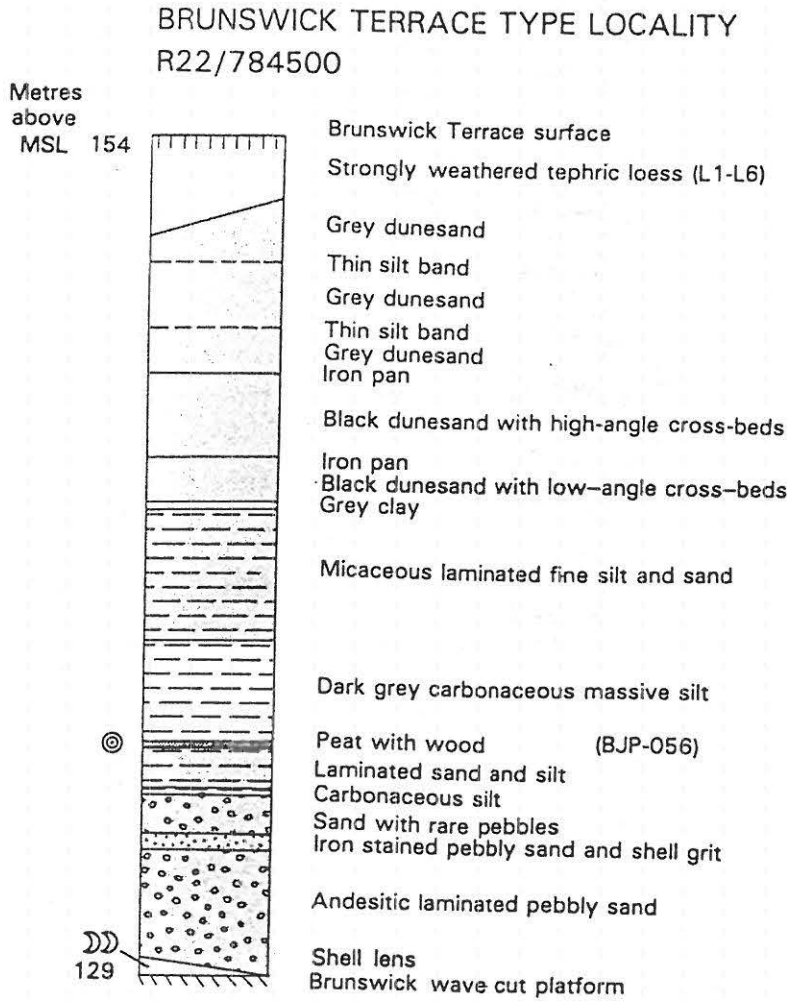

Figure 3.12: Stratigraphic section on Brunswick Road, showing coverbeds of Brunswick Terrace (310 ka) at the type locality. After Pillans (1990).

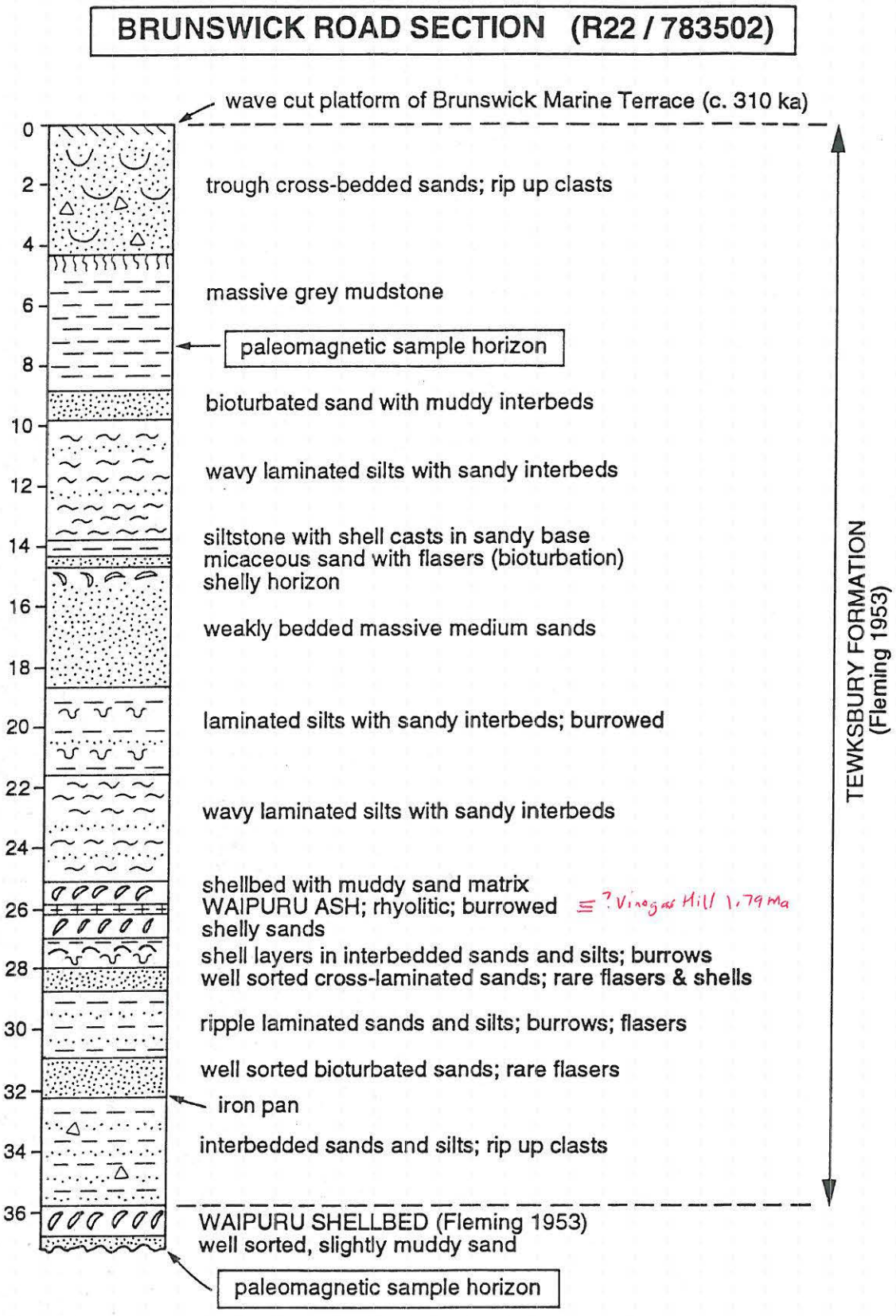

Figure 3.13: Stratigraphic section of Tewksbury Formation, Waipuru Shellbed, and Waipuru Ash on Brunswick Road.

TABLE 3.2. Soil description and chemical data for Westmere Silt Loam (Stop 5). After Adams & Wilde (1978).

WESTMERE SILT LOAM

Location: In paddock adjacent to J E Murray's house, Brunswick road, directly opposite Brunswick Hall

Grid Ref: R22/835496

Vegetation: Ryegrass-clover pasture

Drainage Class: Well drained

Land Use: Semi-intensive sheep and cattle farming. No topdressing for 20-30 years

Parent Material: Andesitic volcanic ash mixed with quartzo-feldspathic loess

Landform: Gently sloping (0-3°) uniform surface of ash-covered Brunswick marine terrace.

PROFILE DESCRIPTION

Profile Depth (cm)

A 0-20 Black (10YR 2/1) silt loam; friable; non-sticky, non-plastic; strongly-developed fine and medium nut structure; abundant roots; distinct irregular boundary,

Bwt_1 20-30 dark yellowish brown (10YR 3/4) clay loam; friable, slightly sticky, slightly plastic; moderately to strongly developed fine nut structure; few thin distinct brown to dark brown (7.5YR 4/4) cutans; many roots; indistinct boundary,

Bt_1 30-61 dark yellowish brown (10YR 4/4) clay; friable, sticky, plastic; strongly developed fine nut structure; many medium distinct brown to dark brown (7.5YR 4/4) cutans; few roots; indistinct boundary,

Profile Depth (cm)

Bt_2 61-76 dark yellowish brown (10 YR 4/4) clay loam; friable, slightly sticky, slightly plastic, moderately developed medium nut structure; few fine faint brown to dark brown (7.5YR 4/4) mottles; many medium distinct dark yellowish brown (10YR 4/4) and brown to dark brown (7.5YR 4/4) cutans,

Cu 76-90+ dark yellowish brown (10 YR 4/4)

Classification - NZSC: ?Acidic (or Pallic) Orthic Brown Soil (Hewitt 1992)
- Taxonomy: Mollic Hapludalf

Sample No	Depth (cm)	pH	Total N (%)	CEC (me %)	TEB (me %)	BS (%)	Exchangeable Cations (meq/100g)				P retn (%)	0.5M H_2SO_4-P (mg%)	Total Ca (%)	Total K (%)
							Ca (me %)	Mg (me %)	K (me. %)	Na (me. %)				
A	0-10	5.0	0.50	29.0	21.1	73	14.3	3.48	2.86	0.50	42	166	1.88	1.27
B	10-20	5.1	0.27	25.1	15.8	63	10.4	2.17	2.78	0.43	50	56	1.65	1.18
C	20-30	4.9	0.15	19.5	11.1	57	5.4	1.46	3.83	0.40	57	31	1.40	1.22
D	30-40	5.1	0.09	17.6	10.5	60	4.2	1.39	4.59	0.33	63	25	1.06	1.28
E	40-60	5.3	0.07	16.3	10.6	65	4.5	1.23	4.47	0.40	58	20	0.82	1.38
F	70-90	6.2	0.04	16.8	12.4	74	5.6	1.41	4.94	0.40	68	37	0.75	1.31

TABLE 3.3. Soil description and chemical data for Egmont Black Loam (Stops 3 and 4). After Parfitt et al. (1980).

EGMONT BLACK LOAM

Location: 1 km west of Mokoia, along main Wanganui-Hawera highway. Paddock north side of road.

Grid ref: Q21/269752

Aspect: - Altitude (m): 60 Rainfall (mm): 1010 Slope: 0-1° Landform: Ash covered marine plain

Vegetation: Ryegrass, white clover, cocksfoot, Prairie grass, Yorkshire fog

Land use: Dairying

Drainage class: Well drained

Parent material: Moderately weathered andesitic volcanic ashes of Oakura and Okato Tephras overlying tephric loess

PROFILE DESCRIPTION

Profile	Depth (cm)	
Ap	0-21	black (10YR 2/1) loam; friable; moderate fine nut structure; many fine roots; few medium and coarse roots; many fine tubular pores; sharp irregular boundary,
Bw1	21-38	dark yellowish brown (10YR 3/6) loam; very friable; weak medium nut structure breaking to fine crumb; abundant fine vesicular and interstitial pores; many medium, coarse and fine roots; many casts of Ap material in top few cms of horizon; diffuse boundary,
Bw2	38-55	dark yellowish brown (10YR 3/6) loam; very friable; weak medium nut structure breaking to fine crumb; abundant fine vesicular and interstitial pores; many medium, coarse and fine roots; diffuse boundary,
Bw3	55-89	dark yellowish brown (10YR 4/6) silt loam; friable; moderate coarse nut structure; few distinct 7.5YR 4/4 coatings on ped faces; many fine tubular pores; few fine and medium roots; indistinct boundary,
2Bw4	89-115	yellowish brown (10YR 5/4) silt loam; firm; non-sticky, slightly plastic; moderate fine and medium nut structure; many fine tubular pores; few fine roots; indistinct boundary, thin layer of dispersed weathered lapilli at boundary,
2C	115-145	yellowish brown (10YR 5/4) silt loam; slightly sandier than horizon above; firm; massive to weak coarse block structure; no roots; few fine tubular pores; distinct boundary,
3C	145+	yellowish brown (10YR 5/4-5/6) loamy sand with many small rounded hard stones; very firm; massive, no roots.

CLASSIFICATION - NZSC:Typic Orthic Allophanic Soil (Hewitt 1992)

Taxonomy: Typic Hapludand

CHEMISTRY EGMONT BLACK LOAM contd.

Sample No. SB	Depth (cm)	Hor.	pH H_2O	pH KCl	pH ΔpH	pH NaF	Exchangeable cations (meq/100 g) Ca	Mg	K	Na	H (KCl)	Al (KCl)	Extr. Acidity (pH 8.2)	Acidity-Al (meq/100 g)	CEC (meq/100 g) ECEC	NH_4OAc (pH 7)	Σ Cations (pH 8.2)	Base saturation (%) Σ bases / CEC NH_4OAc	Σ bases / Σ Cations
9557																			
A	0-21	Ap	6.6	5.9	-0.7	10.7	32	6.2	0.29	0.25		0.26	34.7	34.4	39.0	39.4	73.4	98	53
B	21-38	Bw1	6.9	6.3	-0.6	11.0	9.6	4.7	0.21	0.25		0.15	29.2	29.0	15.0	15.8	44.0	94	34
C	38-55	Bw1	6.7	6.1	-0.6	10.8	3.6	4.0	0.47	0.22		0.15	30.1	29.9	8.5	12.1	38.4	69	22
D	55-89	Bw2	6.6	5.9	-0.7	10.9	2.6	2.81	1.06	0.23		0.14	30.5	30.4	6.8	13.0	37.2	52	18
E	89-115	2Bw3	6.7	5.7	-1.0	10.7	1.7	1.16	2.64	0.26		0.12	23.3	23.2	5.9	10.7	29.1	54	20
F	115-145	2C	6.5	5.5	-1.0	10.5	1.6	1.20	1.97	0.22		0.11	21.4	21.3	5.1	9.9	26.4	51	19

Sample No. SB	Depth (cm)	Hor.	Total C (%)	Total N (%)	P (mg/100 g) H_2SO_4 (0.5 M)	P Inorg.	P Org.	P Retention (%)	Dithion. cit. (%) Fe	Dithion. cit. Al	Tamm ox. (%) Fe	Tamm ox. Al	Tamm ox. Si	Pyrophos. (%) Fe	Pyrophos. Al	Reserves (meq/100 g) K_C	Reserves Mg_r	Extractable S (ppm)
9557																		
A	0-21	Ap	10.1	0.64	143	143	156	88	1.49	0.93	1.02	3.2	1.15	0.14	0.56	0.16	3.6	22
B	21-38	Bw1	3.8	0.19	114	114	81	98	1.95	1.23	1.36	4.7	2.0	0.07	0.38	0.16	3.7	110
C	38-55	Bw1	2.2	0.12	91	91	52	99	2.2	1.09	1.40	4.9	2.3	0.04	0.31	0.18	4.9	257
D	55-89	Bw2	1.7	0.07	61	61	41	99	2.6	1.09	1.77	5.0	2.5	0.03	0.29	0.18	9.0	405
E	89-115	2Bw3	1.1	0.05	33	33	35	96	1.94	0.98	1.18	2.9	1.47	0.02	0.23	0.35	16	193
F	115-145	2C	1.0	0.04	31	31	38	91	1.51	0.81	0.81	2.8	1.45	0.02	0.17	0.33	16	142

REFERENCES

Abbott, S.T.; Carter, R.M. in press: The sequence architecture of mid-Pleistocene (c. 1.1-0.4 Ma) cyclothems from New Zealand: facies development during a period of orbital control on sea-level cyclicity. *In* de Boer, P.L; Smith, D.G. (ed) Orbital forcing and cyclic sequences. *IAS Special Publication 1.*

Adams, J.A.; Wilde, R.H. 1978: Morphological and chemical data for the Westmere Silt Loam mapping unit. *New Zealand Soil Bureau scientific report 35.*

Berger, G.W. 1988: Dating Quaternary events by luminescence. *In* Easterbrook, D.J. (ed) Dating Quaternary sediments. *Geological Society of America special paper 227*: 13-50.

Berger, G.W.; Huntley, D.J. 1989. Treatment of error in plateau values: Caveat emptor. *Ancient TL 7*: 27-29.

Berger, G.W.; Pillans, B.J.; Palmer, A.S. 1992: Dating loess up to 800 ka by thermoluminescence. *Geology 20*: 403-406.

Beu, A.G.; Edwards, A.R. 1984: New Zealand Pleistocene and late Pliocene glacio-eustatic cycles. *Palaeogeography, palaeoclimatology, palaeoecology 46*: 119-142.

Fleming, C.A. 1953: The geology of Wanganui Subdivision. *New Zealand Geological Survey bulletin 52.*

Hewitt, A.E. 1992: New Zealand Soil Classification. *New Zealand Department of Scientific and Industrial Research scientific report 19.* 133p.

Kamp, P.J.J.; Turner, G.M. 1990: Pleistocene unconformity-bounded shelf sequences (Wanganui Basin, New Zealand) correlated with global isotope record. *Sedimentary geology 68*: 155-161.

Kohn, B.P.; Pillans, B.J.; McGlone, M.S. 1992: Zircon fission track age for middle Pleistocene Rangitawa Tephra, New Zealand: stratigraphic and paleoclimatic significance. *Palaeogeography, palaeoclimatology, palaeoecology 95*: 73-94.

Parfitt, R.L.; Pollok, J.A.; Furkert, R.J. (compilers) 1980: Guidebook for Tour 1. Pre-Conference North Island, New Zealand. *Soils With Variable Charge Conference*, Palmerston North, New Zealand, February 1981: 142-143.

Pillans, B.J. 1983: Upper Quaternary marine terrace chronology and deformation, South Taranaki, New Zealand. *Geology 11*: 292-297.

Pillans, B.J. 1990: Late Quaternary marine terraces, south Taranaki-Wanganui (NZMS sheet Q22 and part sheets Q20, Q21, R21 & R22) 1:100 000. *New Zealand Geological Survey miscellaneous series map 18* (1 sheet) and notes. Wellington, New Zealand, Department of Scientific and Industrial Research.

Pillans, B.J.; Abbott, S.T.; Carter, R.M.; Beu, A.G. 1991: A possible Lower/Middle Pleistocene boundary stratotype in Wanganui Basin, New Zealand. *Abstracts*, International Union for Quaternary Research XIII International Congress, Beijing: 281.

Pillans, B.J.; Holgate, G.; McGlone, M. 1988: Climate and sea level during oxygen isotope stage 7b: on-land evidence from New Zealand. *Quaternary research 29*: 176-185.

Pillans, B.J.; Roberts, A.P.; Wilson, G.S.; Abbott, S.T.; Alloway, B.V. in press: Magnetostratigraphic, lithostratigraphic and tephrostratigraphic constraints on Lower/Middle Pleistocene sea level changes, Wanganui Basin, New Zealand. *Earth and planetary science letters.*

Pillans, B.J.; Wright, I. 1990: 500,000 year paleomagnetic record from New Zealand loess. *Quaternary research 33*: 178-187.

Shackleton, N.J.; Berger, A.; Peltier, W.R. 1990: An alternative astronomical calibration of the lower Pleistocene timescale based on ODP Site 677. *Transactions of the Royal Society of Edinburgh - earth sciences 81*: 251-261.

Turner, G.M.; Kamp, P.J.J. 1990: Paleomagnetic location of the Jaramillo Subchron and Brunhes-Matuyama transition in the Castlecliffian stratotype section, Wanganui Basin, New Zealand. *Earth and planetary science letters 100*: 42-50.

DAY 4: WANGANUI—PALMERSTON NORTH

B. J. Pillans
Department of Biogeography & Geomorphology
Research School of Pacific Studies
Australian National University
Canberra, ACT 0200, Australia

A. S. Palmer
Department of Soil Science
Massey University, Private Bag 11-222
Palmerston North, New Zealand

Pillans, B.J., Palmer, A.S. 1994. Post-conference Tour Day 4: Wanganui-Palmerston North. In: Lowe, D.J. (ed) Conference Tour Guides, Proceedings International Inter-INQUA Field Conference and Workshop on Tephrochronology, Loess, and Paleopedology, University of Waikato, Hamilton, New Zealand, 157-171.

Outline of Day 4 (Wednesday 16 February)

8.00-8.30 am	Depart Collegiate Motor Inn, Wanganui, and travel to Fordell
8.30-9.15 am	STOP 1 — Fordell Ash and Brunhes/Matuyama boundary
9.15-9.55 am	Travel to Marton
9.55-10.35 am	STOP 2 — Rangitawa Tephra (Mt Curl section)
10.35-10.50 am	Travel to Griffins Road
10.50-11.30 am	STOP 3 — Griffins Road tephras (Griffins Road Quarry)
11.30-12.00 noon	Travel to Vinegar Hill via Hunterville
12.00-1.00 pm	STOP 4 - Vinegar Hill reserve. LUNCH
1.00-1.10 pm	Travel to Pakihikura Stream
1.10- 1.30 pm	STOP 5 - Lower Pleistocene Pakihikura Pumice
1.30-1.40 pm	Travel to Mangapipi Stream
1.40-2.00 pm	STOP 6 - Lower Pleistocene Mangapipi Ash
2.00-2.10 pm	Travel to Rewa Hill
2.10-3.10 pm	STOP 7 - Lower Pleistocene Rewa and Potaka pumices (Rewa Hill section)
3.10-3.30 pm	STOP 8 - Stormy Point lookout
3.30-4.10 pm	Travel to Mt Stewart via Feilding
4.10-4.40 pm	STOP 9 - Penny Road loess section
4.40-5.10 pm	Travel to Massey University, Palmerston North
	Evening: Dinner

INTRODUCTION

Today we will make our way essentially eastward across the Wanganui Basin (Fig. 4.1), examining marine and non-marine deposits containing rhyolitic tephras erupted from the Taupo Volcanic Zone (TVZ). The rhyolitic tephras are important stratigraphic markers for correlation and dating within the basin, and also facilitate correlation to the isotope stratigraphy of deep sea cores. The tephras in non-marine sediments are dominantly airfall with some local reworking. The tephras in marine sediments are typically pumice-rich volcaniclastic sands, fluvially transported into the basin soon after eruption, and deposited in near-shore marine environments.

Most of the tephras can be geochemically fingerprinted by electron microprobe analyses of glass shards (Fig. 4.2).

STOP 1 — Kauangaroa Road, Fordell

East of Wanganui, marine terraces are somewhat obscured by fluvial and coastal dune deposits. However, the Brunswick (310 ka) and Braemore (340 ka) terraces form a broad composite surface several kilometres wide and extending some 10-15 km east of Wanganui to Fordell village. A distinctive rhyolite tephra, Fordell Ash (c. 320 ka), occurs in lignite within non-marine coverbeds of Braemore Terrace at Kauangaroa Road (S22/027378) — see Fig. 4.3. Fordell Ash also occurs stratigraphically beneath marine coverbeds of Brunswick Terrace elsewhere in the Fordell area.

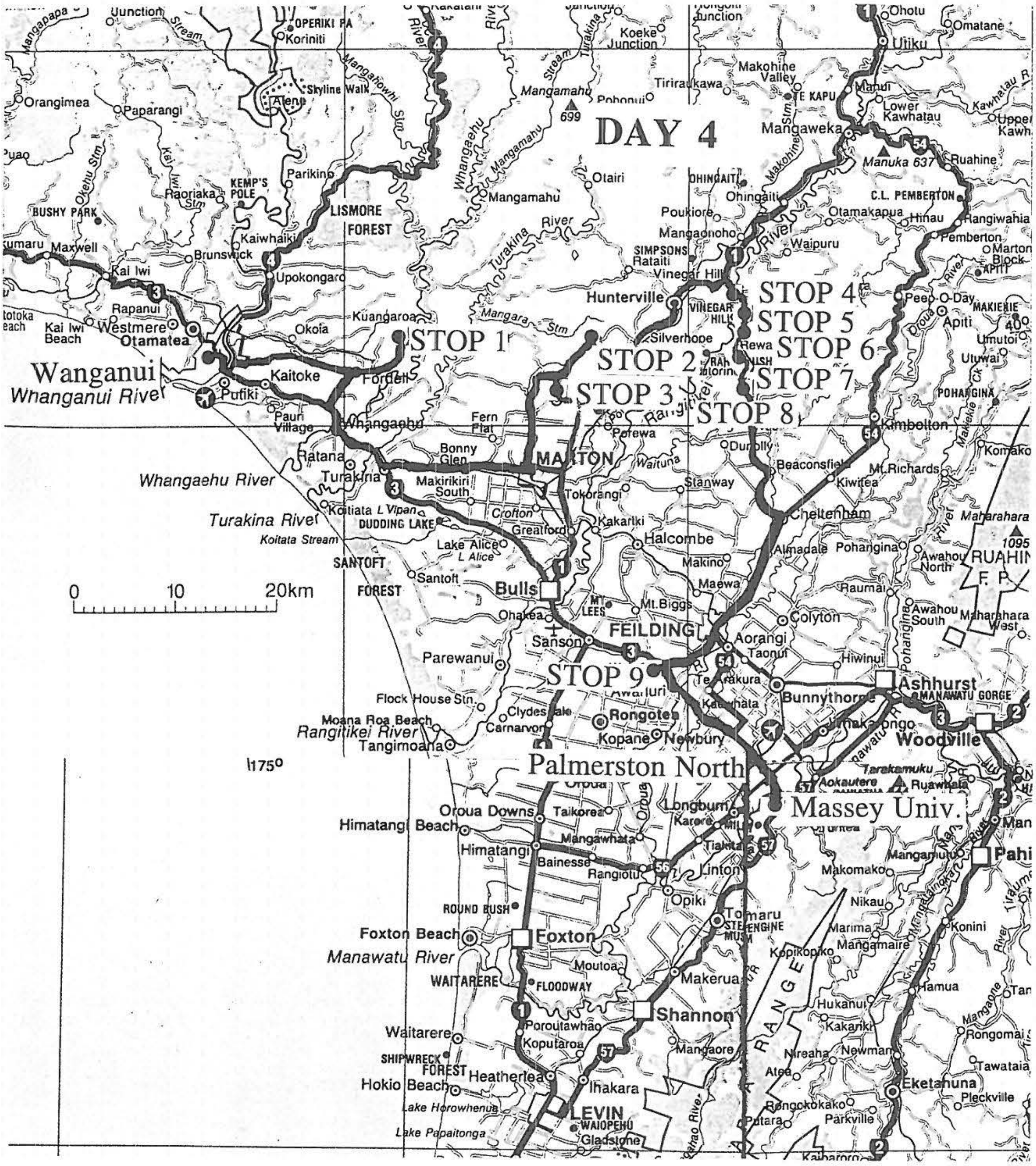

Figure 4.1: Route map for Day 4.

Pollen analyses at Kauangaroa Road (Fig. 4.4) indicate that Fordell Ash was erupted in the early part of an interglacial period, probably isotope stage 9a (Bussell & Pillans 1992) when the local vegetation was changing from *Nothofagus* (southern beech)-dominated to podocarp-dominated forest. An increase in seral taxa (particularly *Leptospermum, Nestegis, Coprosma, Neomyrtus,* and *Dicksonia squarrosa*) after the fall of the Fordell Ash suggests damage to standing vegetation, or establishment of pioneers on a new surface, or both.

The Braemore wave cut surface (162 m above present sea-level) is cut in Upper Westmere Siltstone (Cyclothem 6 at Castlecliff: Fig. 3.5). The road section below the wave cut surface has an excellent exposure of the lower part of Cyclothem 6, and underlying strata down to the distinctive Kaimatira Pumice Sand at the base of Cyclothem 4 (Fig. 4.5). Note that Cyclothems 4 and 5 appear to merge at this site, presumably because the site was in deeper water than the Castlecliff (coastal) section. Paleomagnetic measurements (Pillans et al. in press) confirm the position of the Brunhes/Matuyama boundary at the base of the Kaikokopu Formation, as at the coastal section. Kaimatira Pumice Sand contains reworked Kaukatea Ash and Potaka Pumice, the latter being fission-track dated at 1.05 ± 0.05 Ma (Alloway et al. 1993).

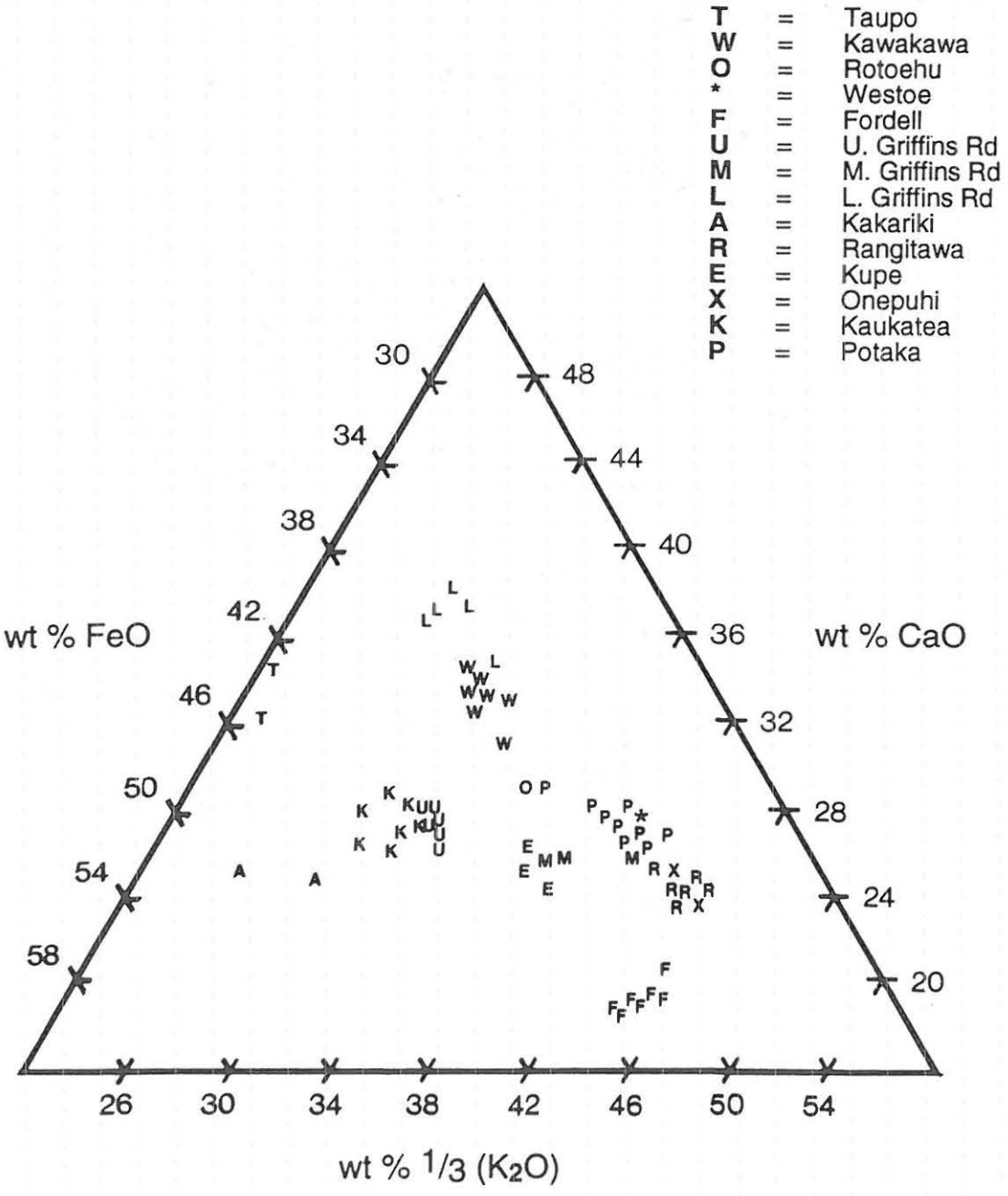

Figure 4.2: CaO-FeO-1/3K_2O plot from electron microprobe analyses of rhyolitic glass shards, Wanganui Basin. From Pillans (in press).

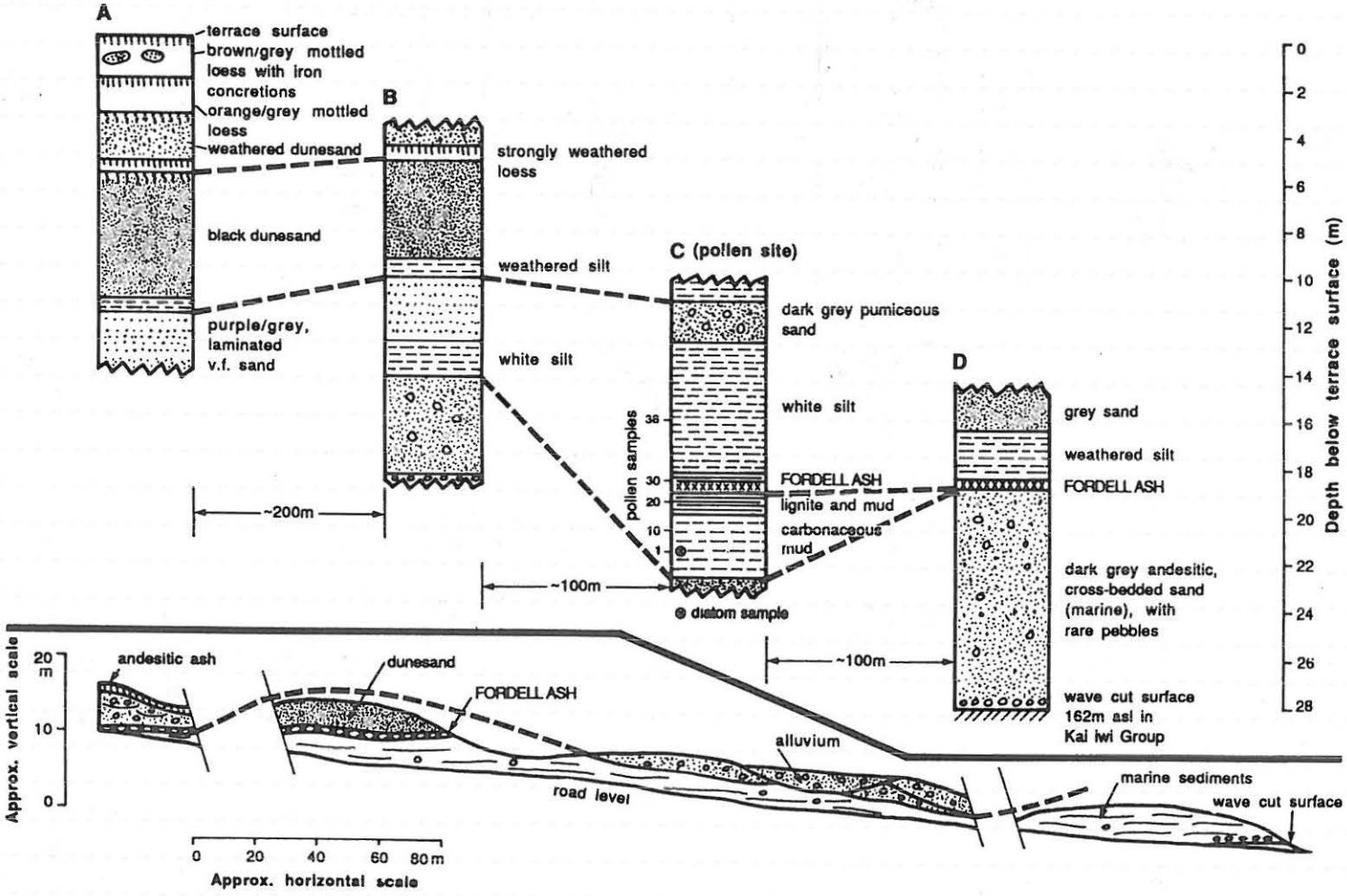

Figure 4.3: Stratigraphy of coverbeds of Braemore Terrace on Kauangaroa Road, showing the position of Fordell Ash. After Bussell & Pillans (1992).

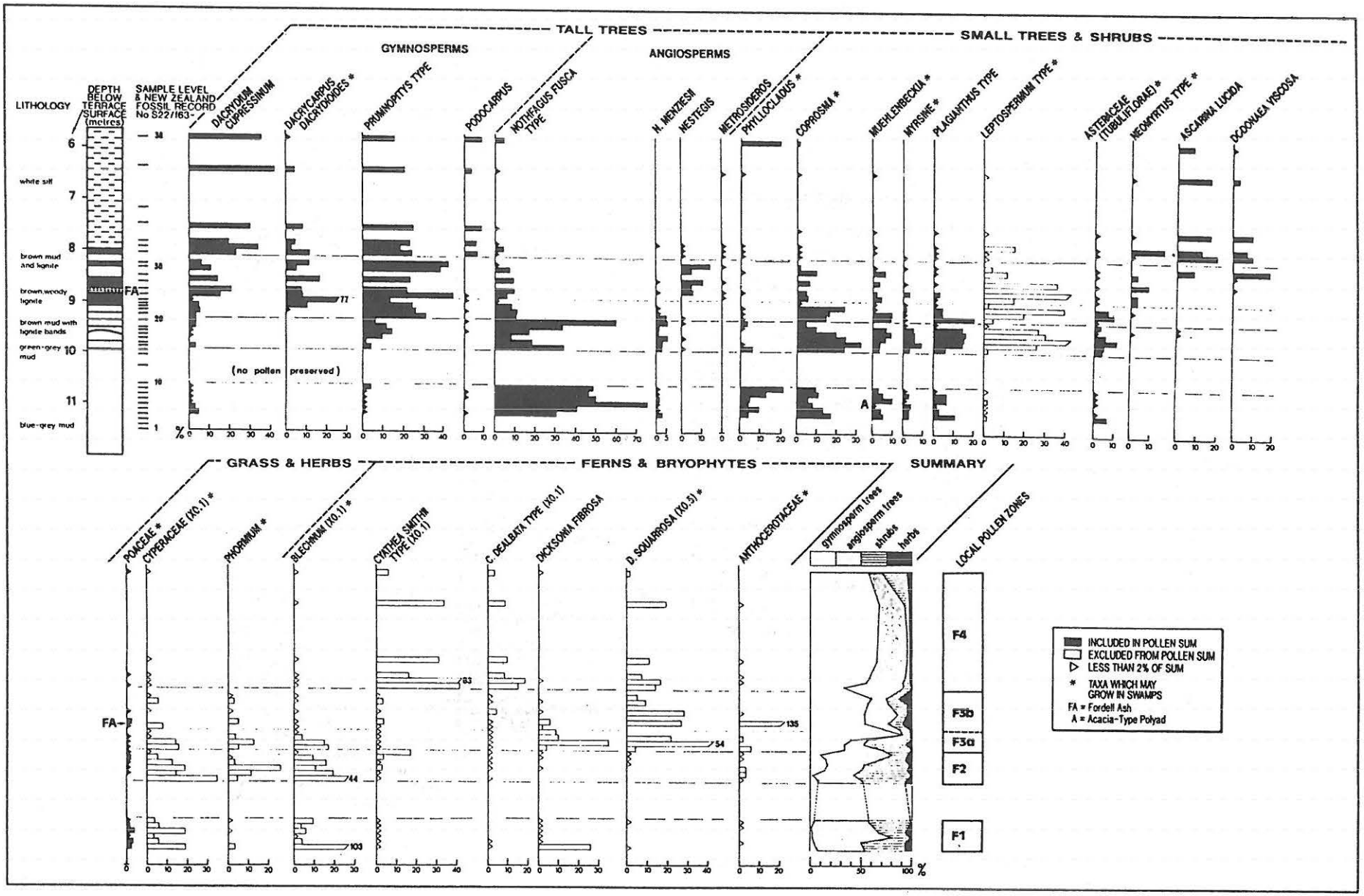

Figure 4.4: Pollen diagram from Kauangaroa Road section. After Bussell & Pillans (1992).

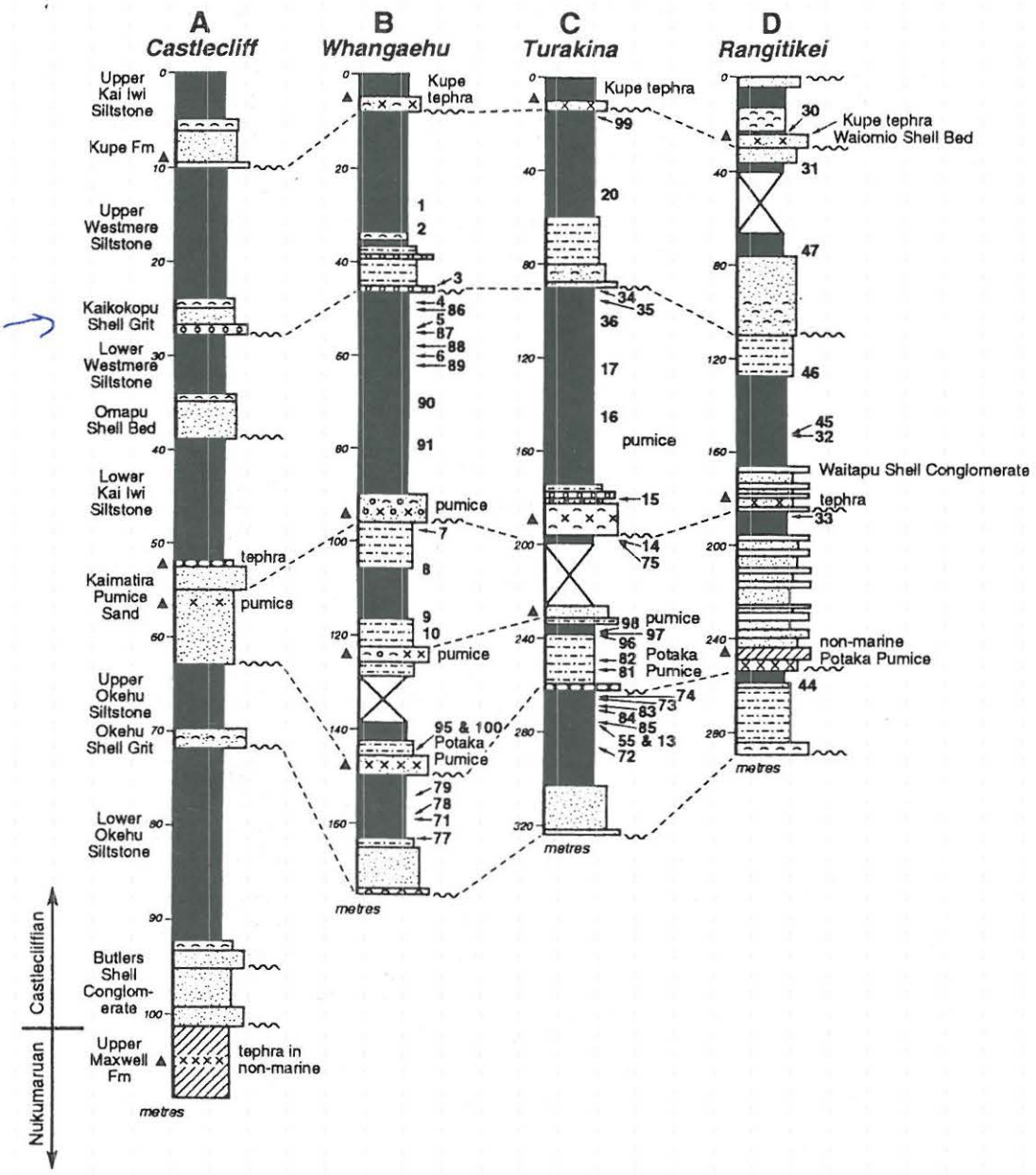

Figure 4.5: Correlation of Castlecliffian strata in four sections across Wanganui Basin (from Pillans et al. in press). Section exposed on Kauangaroa Road comprises strata between 25 and 125 m in Whangaehu column (B).

STOP 2 — Mount Curl section

A road cutting on Mount Curl Road (S22/194344) was the designated type section of Mt Curl Tephra (Milne 1973), a rhyolitic tephra some 90 cm thick (Fig. 4.6). Milne (1973) reported a fission-track age of 230 ± 30 ka for the tephra, and used the age of the tephra to underpin a loess chronology for Rangitikei valley. Recent fission-track, $^{40}Ar/^{39}Ar$, and thermoluminescence (sample CURL-3 in Table 3.1) dates from the Mt Curl section indicate an age of about 340 ka, and the Mt Curl Tephra is now correlated with Rangitawa Tephra (Kohn et al. 1992; Alloway et al. 1993).

The loess stratigraphy of the Mt Curl section is shown in Fig. 4.6, using the names of loess layers proposed by Milne (1973) and Milne & Smalley (1979). Two younger rhyolite tephras (Upper and Lower Griffins Road tephras) occur in strongly weathered loess above a ferromagnesian mineral-rich dunesand referred to as Brunswick Dunesand by Milne (1973). The dunesand is inferred to be a coastal dunesand, deposited when the shoreline was within a few km of the section. Rangitawa Tephra [= Mt Curl Tephra] was erupted during the latter part of isotope stage 10 (Black et al. 1988; Kohn et al. 1992) and so the dunesand was probably deposited during the high sea-level times of oxygen isotope stage 9.

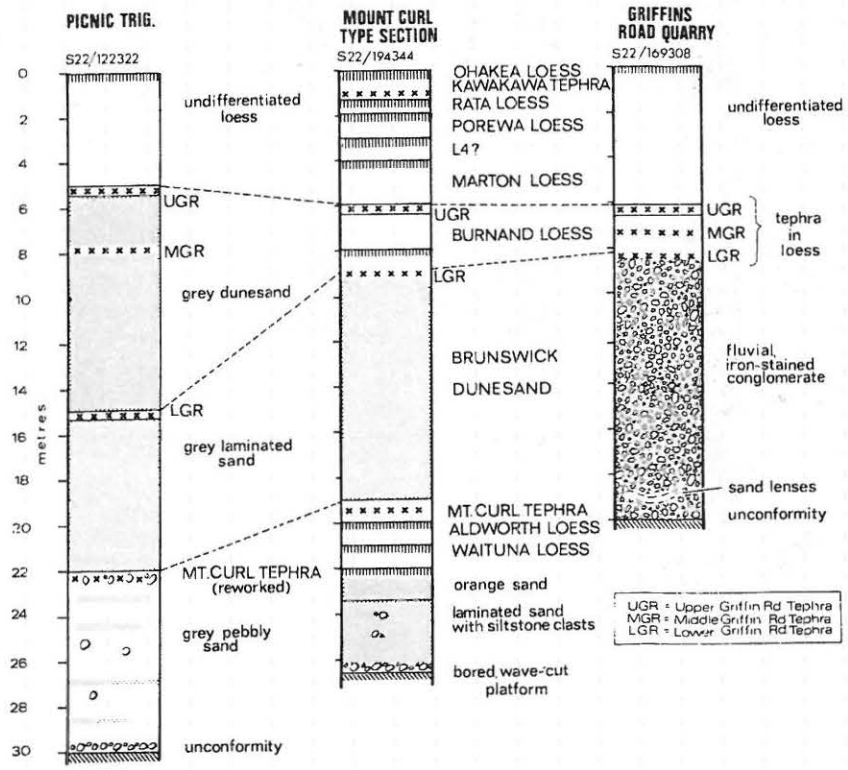

Figure 4.6: Loess and tephrostratigraphy of three sections in the Marton area. After Pillans (1988).

STOP 3 — Griffins Road Quarry

An exposure in the north face of Griffins Road Quarry shows 3 rhyolitic tepras in strongly weathered loess overlying a thick iron-stained fluvial conglomerate (Fig. 4.6). The tephras are named Upper, Middle, and Lower Griffins Road tephras (Pillans 1988), each of which is geochemically distinguishable on the basis of electron microprobe analyses of glass shards (Fig. 4.2). Berger et al. (1992) reported thermoluminescence ages of 176 ± 32, 194 ±2 2, and 328 ± 43 ka for loess 33 cm below the Upper Griffins Road tephra (sample GRDQ-2 in Table 3.1), and considered the oldest age to be the most reliable (see Berger et al. 1992 for discussion). No other numerical age determinations have been done at the site, and the loess stratigraphy is poorly exposed. However, the Griffins Road tephras occur widely in the eastern part of the Wanganui Basin, and have also been tentatively identified in South Island loess (Eden et al. 1992). The tephras may therefore have great stratigraphic potential in New Zealand loess studies.

STOP 4 — Vinegar Hill Domain

We will have a lunch stop at Vinegar Hill Domain, adjacent to the Rangitikei River. Spectacular high cliffs along the banks of the river provide excellent exposures of Upper Pliocene to Lower Pleistocene marine sediments. Waipuru Ash is exposed on the east bank of the river 1.2 km NNE of Vinegar Hill Bridge (Seward 1976), near the base of Olduvai Subchron (Seward et al. 1986).

STOPS 5,6, & 7 — Pakihikura Stream, Mangapipi Stream, Rewa Hill

Road cuttings between Pakihikura Stream and the top of Rewa Hill contain excellent exposures of four important rhyolitic tephra marker beds in the New Zealand region: Pakihikura Pumice, Mangapipi Ash, Rewa Pumice, and Potaka Pumice (Fig. 4.8). Seward (1974, 1976) reported glass fission-track ages for these and several other tephra horizons in Wanganui Basin (Fig. 4.7). The ages appeared to be consistent with the tentative identification of the Brunhes/Matuyama polarity transition between Rewa and Potaka pumices in the Rewa Hill Section. However, recent fission-track ages (Alloway et al. 1993, and new unpublished data), and paleomagnetic results (Pillans et al. in press), indicate that the ages determined by Seward (1974, 1976) are too young, probably because her glass ages were uncorrected for track annealing. The polarity transition in the Rewa Hill section is now considered to be the lower Jaramillo transition, with an astronomically-calibrated age of 1.07 Ma (Shackleton et al. 1990) — see Fig. 4.9. The revised age of 1.05 ± 0.05 Ma for Potaka Pumice (Alloway et al. 1993), which occurs within the Jaramillo Subchron, is consistent with the astronomically calibrated timescale. The revised age of 1.63 ± 0.15 Ma for Pakihikura Pumice (Alloway et al. 1993) indicates that it lies close to the Plio/Pleistocene boundary as defined in the Vrica section in Italy (Backman et al. 1983).

STOP 8 — Stormy Point Lookout

From the lookout at the top of Rewa Hill, there are spectacular views of the Rangitikei valley, and weather permitting, we may see Mt Ruapehu in the distance to the north. A broad flight of river terraces occurs within the valley, representing major fluvial aggradation surfaces from which loess was derived during glacial and stadial times. Stormy Point Lookout is on the surface of a 450 ka aggradation terrace. Analysis of the heights and ages of river terraces in the Rewa Hill area (Fig. 4.10) suggests an increasing rate of river downcutting towards the present. Emergence of Rewa Hill may have occurred about 1 Ma (Fig. 4.10).

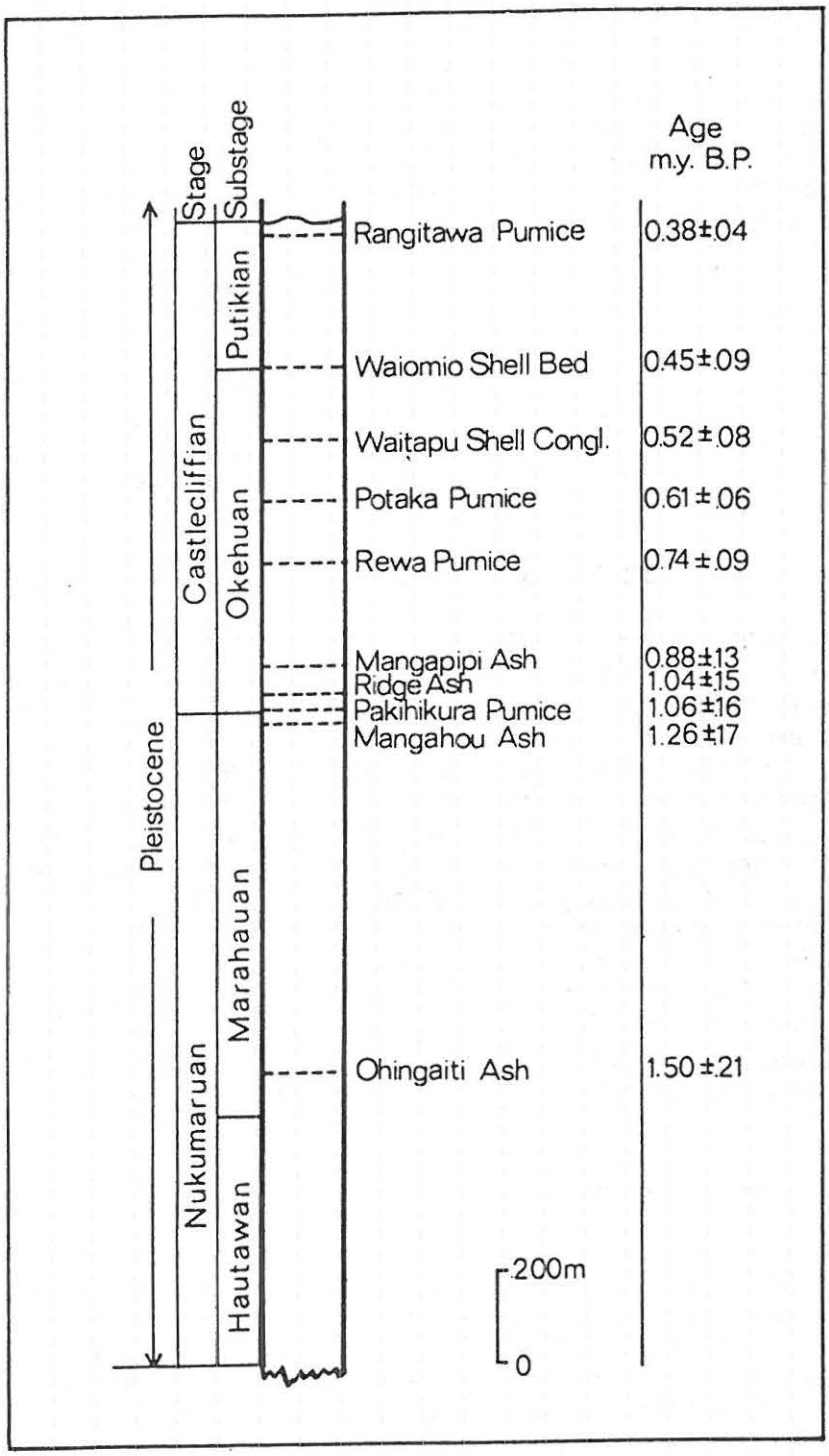

Figure 4.7: Summary of tephrostratigraphy and glass fission-track ages in Rangitikei valley (Seward 1974). Note that these ages were uncorrected for possible track annealing, and that new isothermal plateau fission-track ages (Alloway et al. 1993) for Rangitawa, Potaka, and Pakihikura pumices are 0.37 ± 0.07, 1.05 ± 0.05, and 1.63 ± 0.15 Ma, respectively.

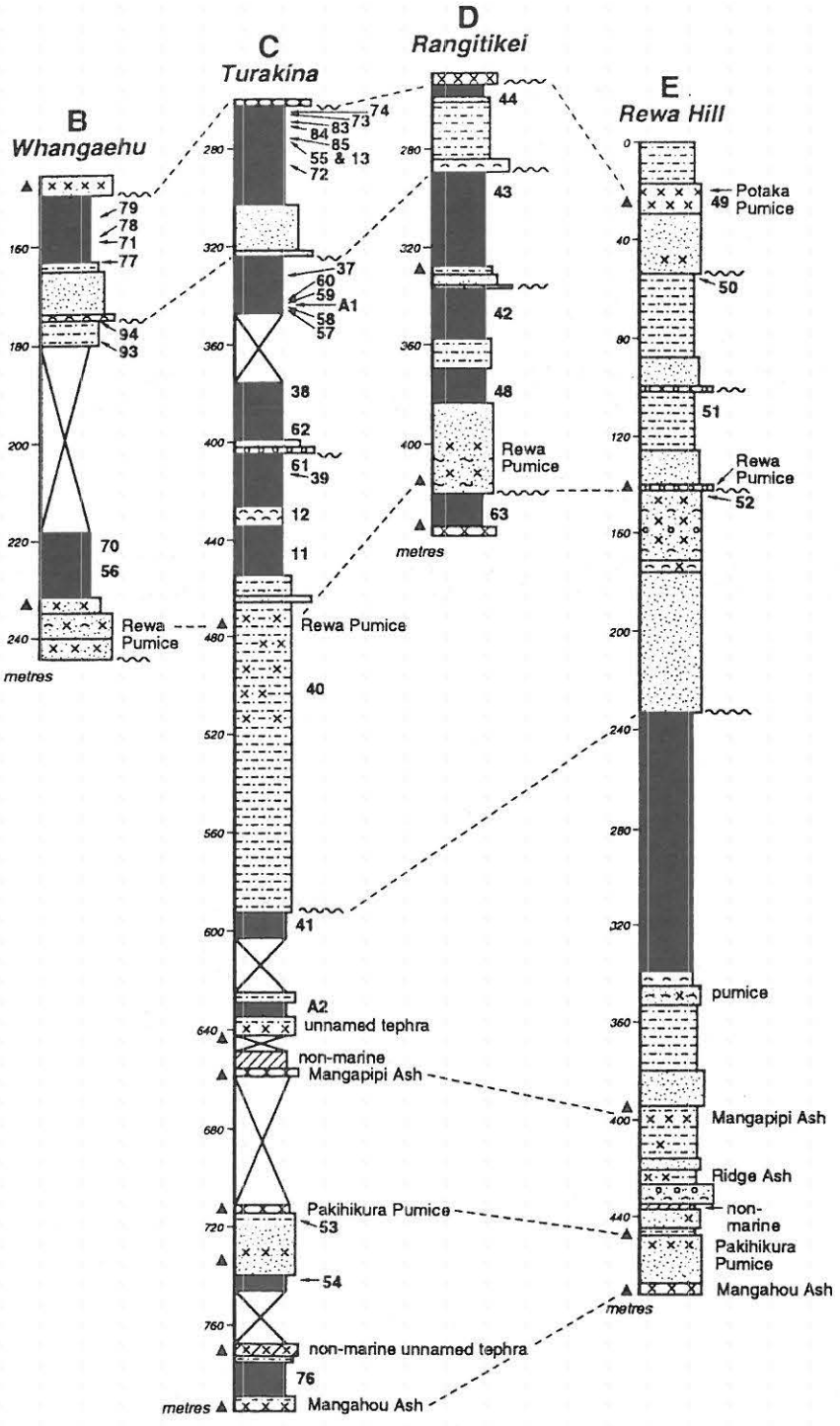

Figure 4.8: Stratigraphic summary and correlations for four sections across Wanganui Basin. Rewa Hill Section (E) is the section exposed in road cuttings between Pakihikura Stream and the top of Rewa Hill. After Pillans et al. (in press).

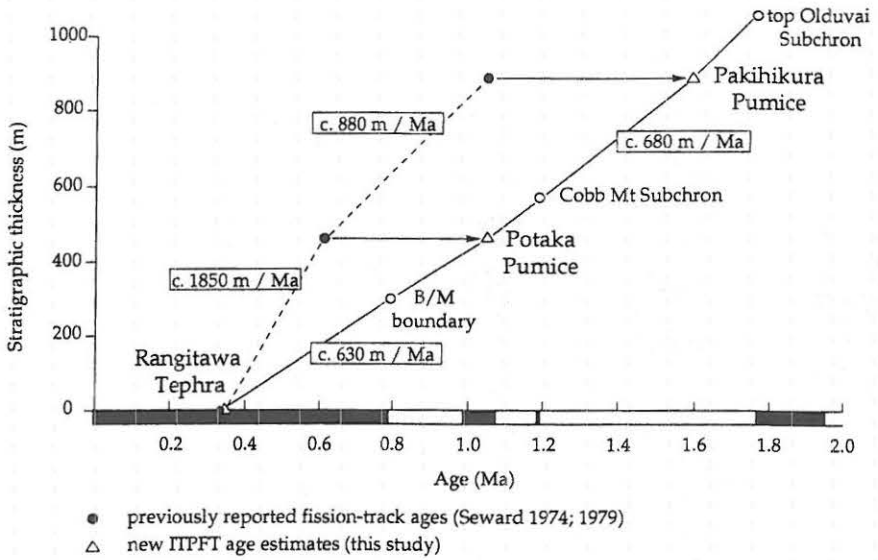

Figure 4.9: Sediment accumulation rates and magnetostratigraphy of Rangitikei River sections from Pakihikura Stream to Rangitawa Stream. After Alloway et al. (1993).

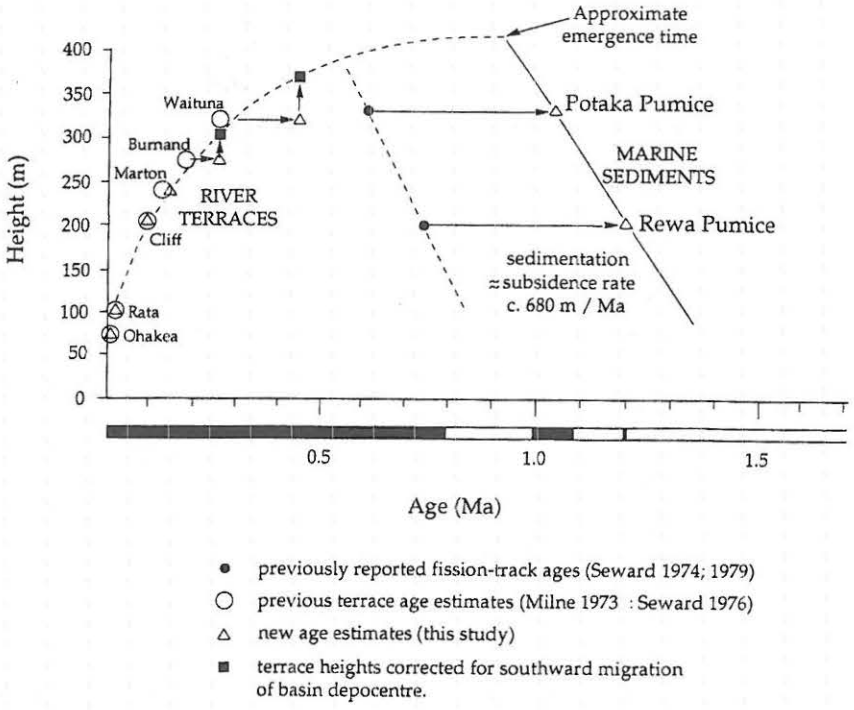

Figure 4.10: Tectonic emergence history at Rewa Hill. River terrace heights are relative to present river level. Heights of Potaka Pumice and Rewa Pumice are relative to MSL. After Alloway et al. (1993).

STOP 9 — Penny Road

A road cutting on Penny Road (S23/218038) shows 3 loess layers overlying a ferromagnesian mineral-rich dunesand (Fig. 4.11). All the sediments are strongly weathered, and contain abundant ferromanganese nodules typical of soils in this seasonally dry area with rainfall less than about 1100 mm/year. The loess layers are named, from youngest to oldest:

- Ohakea (= Loess L1)
- Rata (= Loess L2)
- Porewa (= Loess L3).

The dunesand at the base of the section is named Mount Stewart Dunesand, and is considered to be a coastal dunesand deposited during the last interglacial (isotope stage 5). Kawakawa Tephra (22.6 ka) is visible within Ohakea Loess. Pillans et al. (1993) reported TL ages of 19.8 ± 1.9 ka (partial bleach method) and 18.8 ± 1.4 ka (regeneration method) for loess [sample PNRD-1] 0.15 m below Kawakawa Tephra (Aokautere Ash) at this section.

Table 4.1 gives a soil profile description and selected chemical data from a nearby site (Parfitt et al. (1980). The soil is the Marton Silt Loam (Aquandic Endoaqualf; Soil Survey Staff 1992).

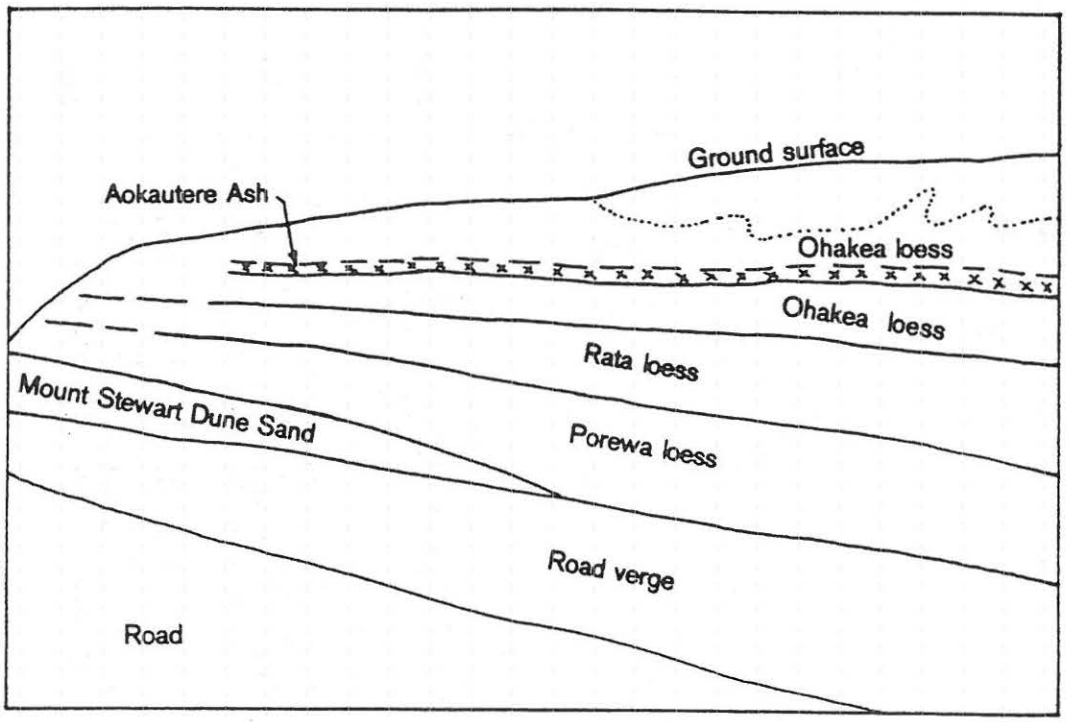

Figure 4.11: Ohakea, Rata and Porewa loesses overlying last interglacial Mount Stewart Dunesand at the north end of Penny Road (S23/218038). After Milne (1987).

TABLE 4.1. Soil description and chemical data for Marton Silt Loam. After Parfitt et al. (1980). (Stop 9)

MARTON SILT LOAM

Location: 150 metres SSE of junction of Stanway and Makara Roads, and about 30 m SW of Makara Road and 5 m E of fenceline

Grid. ref.: S23/268184

Aspect: South-west Altitude (m): 185 Rainfall (mm): 1050 Slope: 1° Landform: Planar Interfluve

Vegetation: Introduced pasture species

Drainage class: Imperfectly drained.

Land use: Pastoral farming - sheep and fat lamb, beef cattle

Parent material: Tephric loess to 51 cm, then Aokautere Ash (rhyolitic tephra) to 63 cm, then quartzo feldspathic loess to 96 cm, then tephric loess beneath.

PROFILE DESCRIPTION

Profile	Depth (cm)	
Ap	0-20	10YR 3.5/2 silt loam; soft *in situ*, friable; slightly sticky and plastic; weak very fine and fine nut and cast granular structure; 5% fine oxide nodules (<3 mm); abundant fine roots; irregular indistinct boundary,
Bgc	20-30	2.5Y 5/3 silty clay loam; stiff *in situ*, friable; sticky and plastic; moderate fine and very fine block structure; 20% fine, distinct 7.5YR 5/8 and 10% fine, faint, 5Y 6/1 mottles; many thin, prominent 7.5YR 2/1 cutans; 10% fine subangular oxide nodules (<5 mm); few fine roots; irregular indistinct boundary,
Btg1	30-51	2.5Y 5/3 clay loam; stiff *in situ*, firm; sticky and plastic; massive breaking to weak, fine block 20% fine distinct 7.5YR 4/6 and 10% fine-medium faint 5Y 6/2 mottles; few thin distinct 7.5YR 2/1 and 5YR 2/1 cutans, scattered (<1%) soft granular 5YR 2/3 and 4/6 oxide segregations (<5 mm); few fine roots; diffuse boundary,
2Btg2	51-63	2.5Y 6/3 sandy clay loam; stiff *in situ*, firm; sticky and plastic; massive; 5-7% fine distinct 5YR 4/8 and 10% fine faint 5Y 6/3 mottles; many thin prominent 5YR 2/1 cutans; rare crumbly oxide aggregations as for Btg1; few fine roots; indistinct boundary,
Btg3	63-73	2.5Y 6/3 clay loam; stiff *in situ*, firm; sticky and plastic; massive breaking to weak fine block structure; 10% fine, distinct 7.5YR 4/6 and 10% fine, faint 2.5Y 5/1 mottles; few thin distinct 5YR 2/1 cutans; indistinct boundary,
Cg	73-96	2.5Y 5/4 silt loam; very stiff *in situ*, firm; sticky, slightly plastic; moderate medium and course prismatic blocky breaking to very weak, very fine block 30% fine and medium distinct 5Y 6/2 and 10% fine, distinct 7.5YR 5/8 mottles; many thin prominent 7.5YR 3/3 and 2/1 cutans; 5-7% subangular hard oxide nodules (<2 mm); moist grey mottles in vertical veins mainly <7 mm dia. with dark cutan in centre; many pores to 0.5 mm in basal 10 cm, cutans coat pores; base defined by diffuse mod. soft subrounded 7.5YR 2/2 oxide aggregations, distinct, irregular boundary,
3Au+ 3Btg1	96-124	2.5Y 5/4 sandy clay; very stiff *in situ*, firm; sticky and plastic; massive breaking to weak very fine block; 20% fine distinct 7.5YR 5/8 and 25% fine and medium faint 5Y 6/2 mottles; thin, distinct 5YR 2/1 cutans; rare hard subrounded greywacke stones (<1 cm); indistinct boundary,
3Btg2	124-149	5Y 6/2 clay; very stiff *in situ*, very firm; slightly sticky and plastic; massive breaking to weak very fine block; 25% fine and medium distinct 7.5YR 5/8 and 15% fine, faint 2.5Y 5/4 mottles; few, thin prominent 5Y 2/1 cutans; rare granular oxide segregations at base of horizon; indistinct boundary,
4Btg	149-164	7.5YR 5/8 clay; very stiff *in situ*, very firm; sticky and plastic; weak medium platy structure breaking to weak very fine block; 20% faint 2.5Y 5/4 and 25% medium distinct 5Y 6/2 mottles.

CLASSIFICATION - NZSC: Argillic Perch-gley Pallic Soil (Hewitt 1992)

Taxonomy: Aquandic Endoaqualf

CHEMISTRY

MARTON SILT LOAM contd.

Sample No. SB	Depth (cm)	Hor.	pH H_2O	pH KCl	pH ΔpH	pH NaF	Exchangeable cations (meq/100 g) Ca	Mg	K	Na	H (KCl)	Al (KCl)	Extr. Acidity (pH 8.2)	Acidity-Al (meq/100 g)	CEC (meq/100 g) ECEC	NH_4OAc (pH 7)	Σ Cations (pH 8.2)	Base saturation (%) Σ bases / CEC NH_4OAc	Σ bases / Σ Cations
9369																			
A	0-18	Ap	5.0			8.0	9.0	1.30	0.58	0.19		0.11	13.8	13.7	11.2	14.0	24.9	79	45
B	23-28	BgC	6.0			8.2	7.3	1.87	0.33	0.33		0.11	8.7	8.6	9.9	11.7	18.5	84	53
C	33-48	Btg1	5.8			8.3	5.7	5.0	0.18	0.70		0.26	9.5	9.2	11.9	13.8	21.1	84	55
D	53-63	2Btg2	5.9			8.5	4.4	6.5	0.19	1.35		0.41	11.4	11.0	12.8	15.5	23.8	80	52
E	63-73	Btg3	6.1			8.0	4.1	6.2	0.18	1.12		0.32	8.2	7.9	11.9	13.0	19.8	89	59
F	73-94	Cg	6.6			7.9	4.2	5.8	0.16	1.18		0.22	7.7	7.5	11.5	12.1	19.0	93	59
G	99-124	3Au+3Btg	7.0			8.2	5.5	7.8	0.23	1.62		0.11	7.2	7.1	15.3	15.7	22.4	97	68
H	124-149	3Btg	7.1			8.1	6.5	8.9	0.25	1.93		0.11	9.0	8.9	17.7	18.6	26.6	95	66
I	149-164	4Btg	7.1			8.2	5.7	7.1	0.14	1.95		0.05	9.6	9.5	15.0	16.1	24.5	93	61

Sample No. SB	Depth (cm)	Hor.	Total C (%)	Total N (%)	P (mg/100 g) H_2SO_4 (0.5 M)	P Inorg.	P Org.	P Retention (%)	Dithion. cit. (%) Fe	Al	Tamm ox. (%) Fe	Al	Si	Pyrophos. (%) Fe	Al	Reserves (meq/100 g) K_c	Mg_r	Extractable S (ppm)
9369																		
A	0-18	Ap	2.8	0.26	27	32	48	27	2.9	0.20	0.60	0.14	0.05	0.18	0.05	0.27	7.3	36
B	23-28	BgC	0.8	0.09	4	10	14	32	4.3	0.22	0.68	0.12	0.08	0.06	0.01	0.29	9.1	14
C	33-48	Btg1	0.4	0.05	2	6	6	31	2.7	0.14	0.47	0.12	0.07	0.04	0.01			32
D	53-63	2Btg2	0.3	0.04	1	6	6	34	1.45	0.33	0.22	0.15	0.08	0.04	0.01			29
E	63-73	Btg3	0.2	0.02	1	5	2	15	1.08	0.08	0.10	0.06	0.03	0.03	0.01			23
F	73-94	Cg	0.2	0.02	1	7	4	14	2.5	0.03	0.12	0.05	0.03	0.02	0.00			16
G	99-124	3Au+3Btg	0.1	0.02	0.3	4	3	15	2.7	0.12	0.08	0.06	0.04	0.02	0.00			27
H	124-149	3Btg	0.1	0.02	2		1	18	3.7	0.13	0.09	0.07	0.04	0.02	0.00			39
I	149-164	4Btg	0.1	0.02	2	10	7	23	7.0	0.64	0.13	0.08	0.06	0.00	0.06			63

REFERENCES

Alloway, B.V.; Pillans, B.J.; Sandhu, A.S.; Westgate, J.A. 1993: Revision of the marine chronology in the Wanganui Basin, New Zealand, based on isothermal plateau fission-track dating of tephra horizons. *Sedimentary geology 82*: 299-310.

Backman, J.; Shackleton, N.J.; Tauxe, L. 1983: Quantitative nannofossil correlation to open ocean deep-sea sections from Plio/Pleistocene boundary at Vrica, Italy. *Nature 304*: 156-158.

Berger, G.W.; Pillans, B.; Palmer, A.S. 1992: Dating loess up to 800 ka by thermoluminescence. *Geology 20*: 403-406.

Black, K.P.; Nelson, C.S.; Hendy, C.H. 1988: A spectral analysis procedure for dating Quaternary deep-sea cores and its application to a high-resolution Bruhnes record from the southwest Pacific. *Marine geology 83*: 21-30.

Bussell, M.R.; Pillans, B. 1992: Vegetational and climatic history during isotope stage 9, Wanganui district, New Zealand, and correlation of the Fordell Ash. *Journal of the Royal Society of New Zealand 22*: 41-60.

Eden, D.N.; Froggatt, P.C.; McIntosh, P.D. 1992: The distribution and composition of volcanic glass in late Quaternary loess deposits of southern South Island, New Zealand, and some possible correlations. *New Zealand journal of geology and geophysics 35*: 69-79.

Hewitt, A.E. 1992: New Zealand Soil Classification. *New Zealand Department of Scientific and Industrial Research scientific report 19.* 133p.

Kohn, B.P.; Pillans, B.; McGlone, M.S. 1992: Zircon fission track age for middle Pleistocene Rangitawa Tephra, New Zealand: stratigraphic and paleoclimatic significance. *Palaeogeography, palaeoclimatology, palaeoecology 95*: 73-94.

Milne, J.D.G. 1973: Mount Curl Tephra, a 230 000-year-old marker bed in New Zealand, and its implications for Quaternary chronology. *New Zealand journal of geology and geophysics 16*: 519-532.

Milne, J.D.G. 1987: Tour Guide for International Symposium on Loess, 14-21 February 1987, New Zealand.

Milne, J.D.G.; Smalley, I.J. 1979: Loess deposits in the southern North Island of New Zealand: an outline stratigraphy. *Acta Geologica Academiae Scientiarum Hungaricae 22*: 197-204.

Parfitt, R.L; Pollok, J.A.; Furkert, R.J. 1980: Guidebook for Tour 1. Pre-Conference North Island, New Zealand. *Soils With Variable Charge Conference*, Palmerston North, New Zealand, February 1981: 151-152.

Pillans, B.J. 1988: Loess chronology in Wanganui Basin. *In* Eden, D.N.; Furkert, R.J. (eds) Loess, its distribution, geology and soils. Rotterdam, Balkema: 175-191.

Pillans, B.J. in press: Direct marine-terrestrial correlations, Wanganui Basin, New Zealand: the last 1 million years. *Quaternary science reviews.*

Pillans, B.J.; McGlone, M.S.; Palmer, A.S.; Mildenhall, D.; Alloway, B.V.; Berger, G.W. 1993: The last glacial maximum in central and southern North Island, New Zealand: a paleoenvironmental reconstruction using Kawakawa Tephra Formation as a chronostratigraphic marker. *Palaeogeography, palaeoclimatology, palaeoecology 101*: 283-304.

Pillans, B.J.; Roberts, A.P.; Wilson, G.S.; Abbott, S.T.; Alloway, B.V. in press: Magnetostratigraphic, lithostratigraphic and tephrostratigraphic constraints on Lower/Middle Pleistocene sea level changes, Wanganui Basin, New Zealand. *Earth and planetary science letters.*

Seward, D. 1974: Ages of New Zealand Pleistocene substages by fission-track dating of glass shards from tephra horizons. *Earth and planetary science letters 24:* 242-248.

Seward, D. 1976: Tephrostratigraphy of the marine sediments in the Wanganui Basin, New Zealand. *New Zealand journal of geology and geophysics 19*: 9-20.

Seward, D. 1979: Comparison of zircon and glass fission-track ages from tephra horizons. *Geology 7*: 479-482.

Seward, D.; Christoffel, D.A.; Lienert, B. 1986: Magnetic polarity stratigraphy of a Plio-Pleistocene marine sequence of North Island, New Zealand. *Earth and planetary science letters 80*: 353-360.

Shackleton N.J.; Berger, A.; Peltier, W.R. 1990: An alternative astronomical calibration of the lower Pleistocene timescale based on ODP Site 677. *Transactions of the Royal Society of Edinburgh - earth sciences 81*: 251-261.

Soil Survey Staff 1992: Keys to Soil Taxonomy, 5th edition. *SMSS technical monograph 19.* 566p.

DAY 5: PALMERSTON NORTH—WELLINGTON

A. S. Palmer
Department of Soil Science
Massey University, Private Bag 11-222
Palmerston North, New Zealand

Palmer, A.S. 1994. Post-conference Tour Day 5: Palmerston North-Wellington. In: Lowe, D.J. (ed) Conference Tour Guides, Proceedings International Inter-INQUA Field Conference and Workshop on Tephrochronology, Loess, and Paleopedology, University of Waikato, Hamilton, New Zealand, 172-185.

Outline of Day 5 (Thursday 17 February)

8.00 am	Depart Massey University, Palmerston North and travel to Stop 1 via the Manawatu Gorge and SH2
8.45-9.00 am	STOP 1 — View river piracy at Kakariki
9.00-10.00 am	Travel from Kakariki to Masterton
10.00-10.30 am	Travel FROM Masterton via Greytown to Stop 2
10.30-11.00 am	STOP 2 — Bidwill Hill site
11.00-11.20 am	Travel to Otaraia site
11.20-11.50 am	STOP 3 — Otaraia site
11.50-12.10 pm	Travel to Lake Ferry
12.10-1.00 pm	STOP 4 — LUNCH Lake Ferry Hotel
1.00-2.00 pm	Walk at Lake Ferry
2.00-4.00 pm	Travel to Wellington via Kumenga and Western Lake
4.00 pm	Arrive at Airport Hotel, Wellington
	Evening: Farewell Dinner Party

(Next morning [Friday 18 Feb.]: Breakfast; flights home)

INTRODUCTION

Today we have only four stops (including lunch) (Fig. 5.1) and aim to arrive in Wellington by 4 pm and the tour conclusion. During the day we will see evidence of the active tectonism that characterises this region; various other late Quaternary events and deposits (including loess, distal tephras, and paleosols) will also be seen. A map of Wairarapa's structure and a generalised cross-section are given in Fig. 5.2.

Wellington City, with a population of c. 350 000 (including Hutt Valley), has been New Zealand's capital city since 1865. Much of the city's downtown area has been rebuilt in recent years because of a high earthquake risk. Significant historical earthquakes occurred in 1848, 1855 (killing 12 people but lifting shore platforms around the harbour on which roads and railways were built), 1868, 1890, 1897, 1904, 1913, 1914, and 1942 (for further information on Wellington see Stevens 1991).

STOP 1 — River piracy at Kakariki

The ancestral Mangahao River captured the headwaters and major part of Hukanui Stream some time in the early Holocene (c. 5-10 ka) (Vella et al. 1987). Hukanui Stream used to flow east from the Tararua Range, across the Wellington Fault, and joined the Mangatainoka River (Fig. 5.3). The river emerging from the Tararua Range laterally eroded the divide on its north side to meet an insequent tributary of Mangahao River along the crush zone of Wellington Fault. Dextral movement along this fault must have aided the capture. The capture took place after 10.5 ka, the age of the youngest aggradational surface (Marden & Neall 1990), because Hukanui Stream had already incised 16 m into this surface. The height difference between Hukanui Stream at the point of capture and the Last Stadial flood plain of the Mangahao River is 21 m, although this figure is a minimum as the latter river would also have degraded by this time.

Figure 5.1: Route map for Day 5.

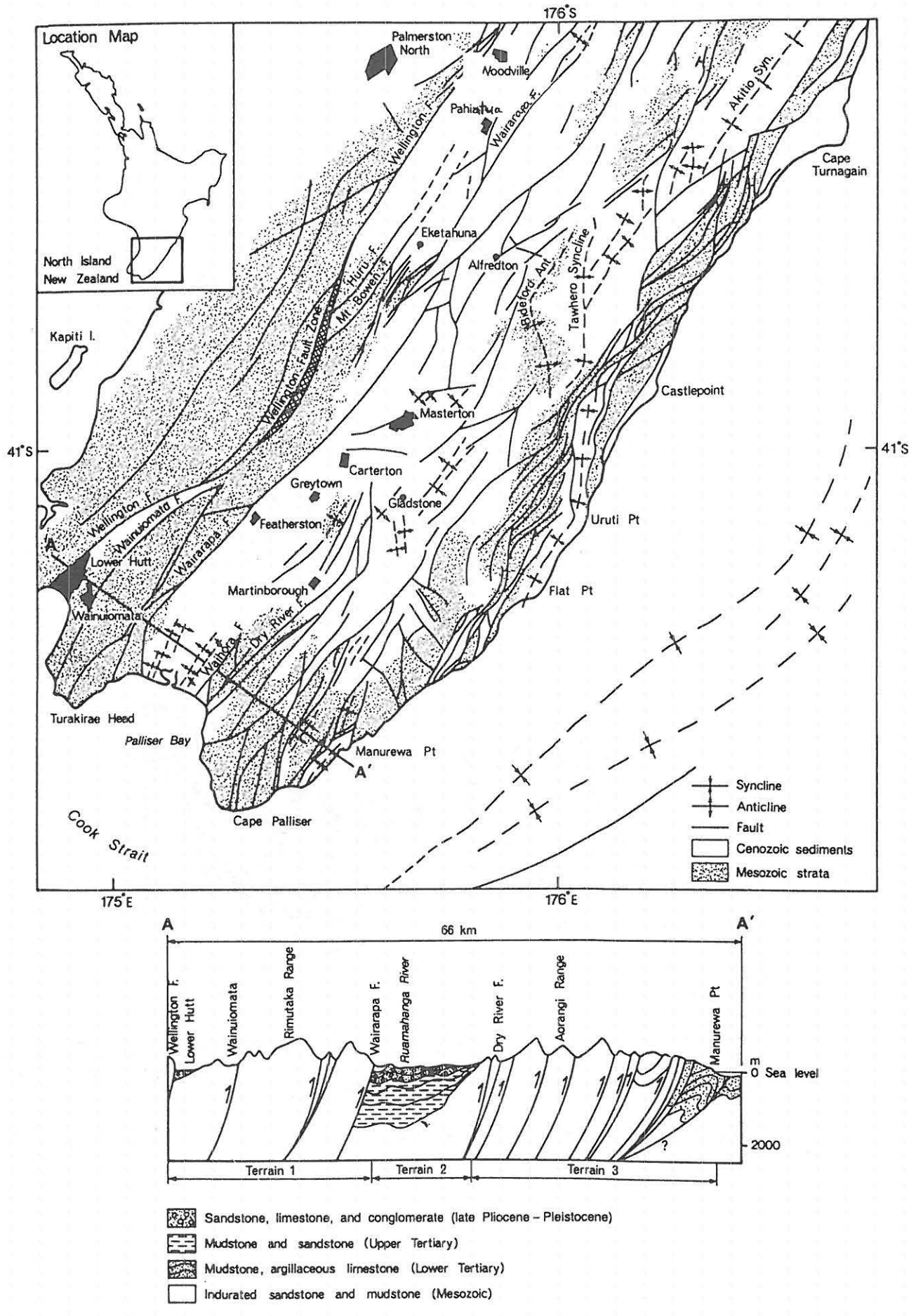

Figure 5.2: Structure of Wairarapa and a generalised cross-section (not to same scale). From Kamp (1992).

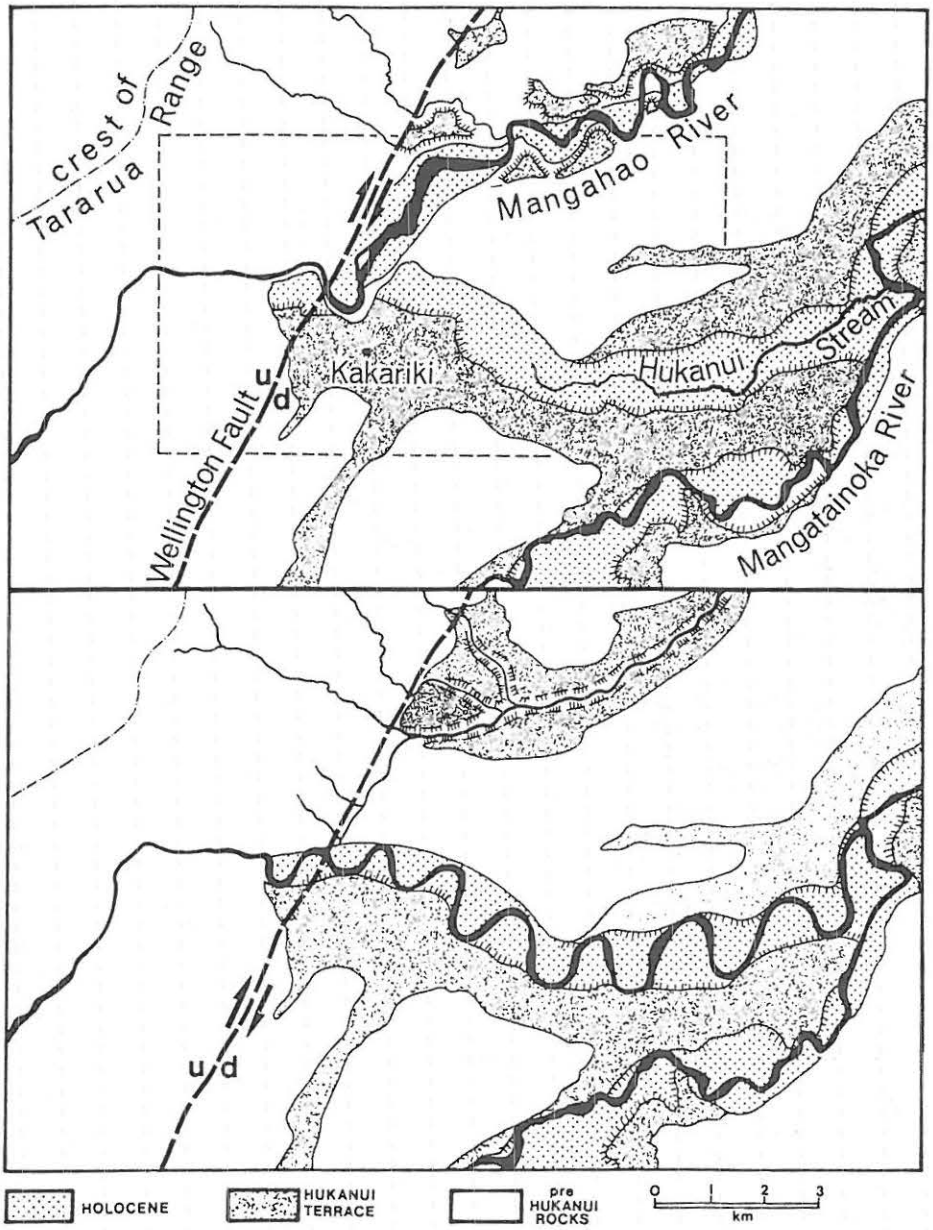

Figure 5.3: Above: The present day configuration of rivers near Kakariki (Stop 1, Fig. 5.1). Shading shows the distribution of Hukanui (Ohakean) aggradation terrace. Fine stipple is the Holocene surface formed by degradation.

Below: Reconstruction of river configuration immediately before capture (from Vella et al. 1987, p.387).

LATE QUATERNARY FAULTING

Numerous faults traverse the Eketahuna-Pahiatua region (Fig. 5.2). Major faults trend NE-SW but others trend 45-90° to this. The three most important faults involving late Quaternary movement are:

1. **Wellington Fault:** Northwards from Putara (west of Eketahuna). This fault marks the boundary between greywacke-argillite rocks of the Tararua Range and Tertiary and Quaternary rocks of the hills and plains. Between Putara and Upper Hutt, Wellington Fault is one of a number that strike along the Tararua Range. The date of last movement is unknown. However, Otway (1972) deduced a rate of average horizontal displacement of 4.8 mm/yr from geodetic monitoring, and Grapes et al. 1984 measured 4.4 mm/yr from displaced features.

2. **Wairarapa Fault:** From Palliser Bay to Masterton, this fault forms the eastern boundary of the Tararua Range. In 1855, the fault moved in the 'Wellington Earthquake' (magnitude ≥ 8.0) with 13 m dextral movement; 3 m of upthrow to the west was recorded in southern Wairarapa. The ground-break extended at least to east of Mauriceville.

3. **Alfredton Fault:** A zone of active faulting passing through the east of the district, considered to be an extension of Wairarapa Fault.

At Kakariki, the site of the Mangahao River capture, Lensen (1969) and Grapes et al. (1984) have mapped in detail features associated with the Wellington Fault (Fig. 5.4). The Wellington Fault splays to enclose a wedge. Cross faulting has produced fault ponds and a horst. These features are developed on the Hukanui Terrace, which has been offset 43 m just north of the river. Assuming a rate of horizontal offset of 4.4 mm/yr, then the Hukanui Terrace surface is this area is c. 10 000 years old (Grapes et al. 1984).

Wellington Fault has recently been trenched at several localities by the Institute of Geological and Nuclear Sciences south of Manawatu Gorge and north of the gorge by Massey University.

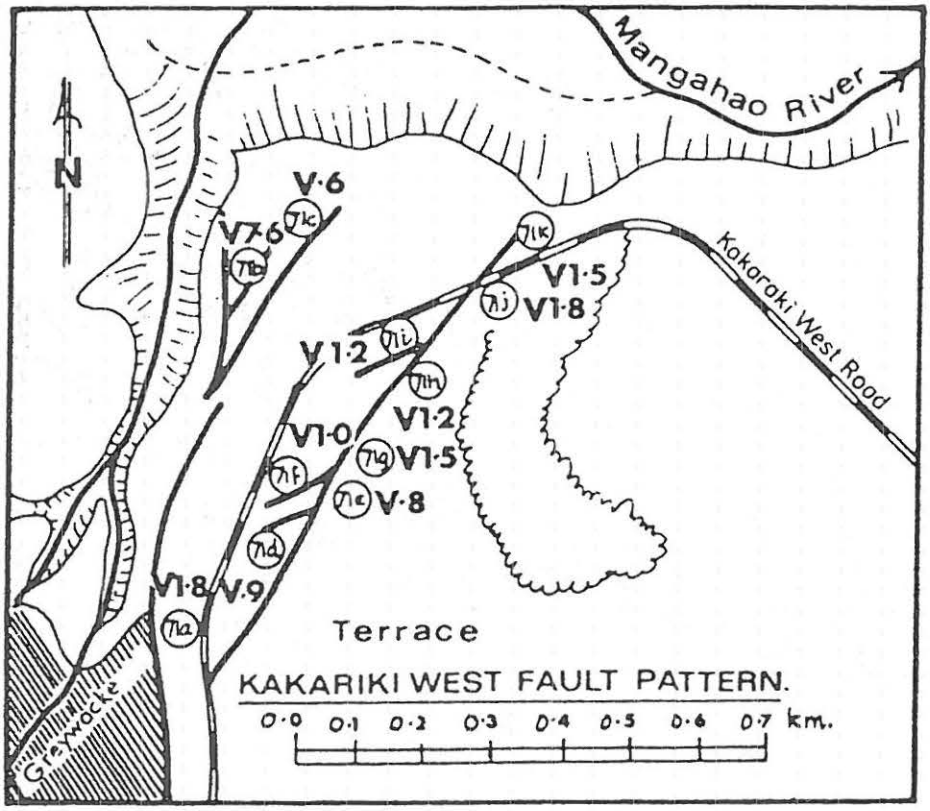

Figure 5.4: At Kakariki, Wellington Fault splays to enclose a wedge within which hinged cross-faulting has produced fault ponds and a horst.
71a, rent on aggradation surface upthrown 1.8 m to E; 71b, rent on aggradation surface upthrown 7.6 m to E; 71c = rent on bulge with 0.6 m vertical offset; 71d, trench upthrown 0.9 m to E; 71e, trench on bulge upthrown 0.8 m to E; 71f, rent and sag pond upthrown 1.0 m E; 71g, aggradational surface upthrown 1.5 m E; 71h, rent sag upthrown 1.2 m E; 71i, rent bulge upthrown 1.2 m E; 71k, rent sag upthrown 1.8 m E; 71l, rent upthrown 1.5 m E.

GEOLOGY OF WAIRARAPA VALLEY

Wairarapa Valley is within the active tectonic belt that strikes northeast through New Zealand (Fig. 5.2). Present-day physiographic features have developed in response to active faulting (including historical earth movement), tilting, and folding accompany rapid uplift (Kamp 1992).

Basement rocks are highly faulted and folded Mesozoic greywackes and argillites which form the Rimutaka - Tararua ranges and the Aorangi Mountains which are up to 1500 m high. In the valley, basement is downfallen and covered by a thick (3000 m) sequence of Cenozoic sediments. The sediment cover is thickest against the Wairarapa Fault which marks much of the western boundary between the Tararua Range and Wairarapa Valley. As well as the Wairarapa Fault, several other major faults, involving considerable displacement, strike northeast along the valley.

The tectonic regime in Wairarapa is also resulting in shortening and folding of late Quaternary deposits. As we travel between Masterton and Greytown we pass an area recently studied by Lamb & Vella (1987) and Warnes (1992) and where beds of Last Interglacial age, and younger, are being perceptibly folded (Fig. 5.5; Table 5.1).

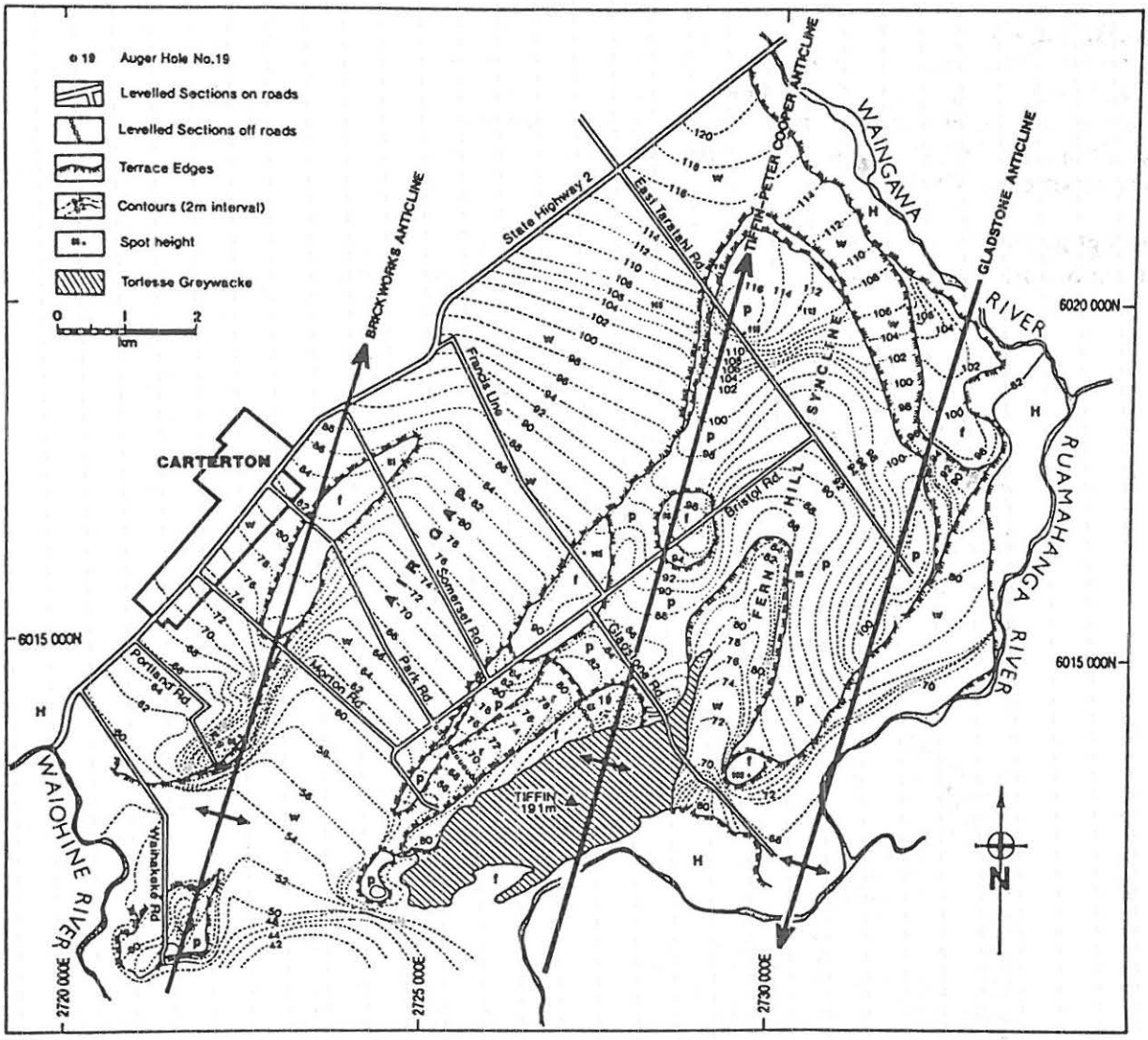

Figure 5.5: Folds in late Quaternary deposits east of Carterton. H = Holocene; w = Waiohine surface; r = Ramsley surface; p = Waipoua surface; f = Francis Line Formation (see Table 5.1). From Warnes (1992, p. 225).

TABLE 5.1. A chronology of Late Quaternary deposits and events in central and southern Wairarapa Valley.

Age yr BP	**Wairarapa**				**S.W. North Island**	**$S^{18}O$ stage**
	loess	river aggradation	Lakes Wairarapa and Onoke	marine terraces	substages	
3 500						1
6 500				Highest Holocene shoreline		1
10 000		degradation				1/2
	Waiohine	Waiohine			Ohakean	
22 590	Kawakawa Tephra					2
25 000						2
	paleosol	degradation				3
30 000						3
	Ramsley	Ramsley			Ratan	3
50 000						3
	paleosol + andesitic ash	degradation				3
60 000			lakes ?	Rakaupiko ?		4
	Waipoua	Waipoua			Porewan	4
80 000	paleosol		Francis line mudstone	Hauriri		5a
	?	?	?			5b
100 000	paleosol		Francis line mudstone	Inaha		5c
	?	?	?			5d
125 000	paleosol		Francis line mudstone	Rapanui		5e

STOP 2 — Bidwill Hill site

The Bidwill Hill site (Fig. 5.6) lies in a structural depression on a surface considered to have been cut as a marine terrace c. 100 ka (Ghani 1978). Palmer and Vucetich (1989) described three loess layers overlying lacustrine mud or peat from a core taken at this site. Only the upper two metres are visible in the road cut, but this site is typical of Ohakean loess, Kawakawa Tephra, and the Wharekaka soil (Typic Fragiaqualf) in the drier parts of Wairarapa (800-1000 mm rainfall p.a.) (Fig. 5.7). Ohakean loess is 2 m thick at this site, but 5 km farther east, adjacent to Ruamahanga River, Ohakean loess is up to 20 m thick. Pollens and diatoms in the base of the core record the cooling transition from the Last Interglacial to the first stadial of the Last Glacial. A forested landscape was replaced by grass and shrubs.

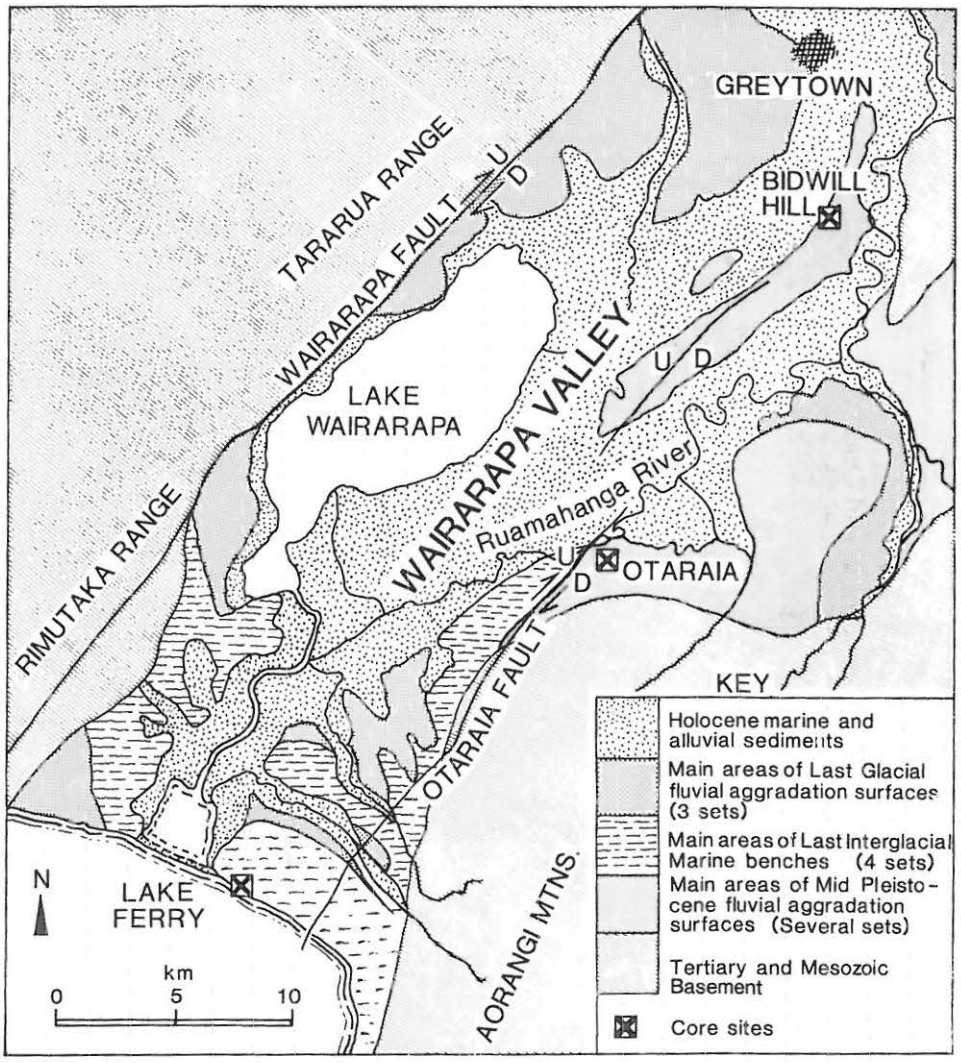

Figure 5.6: Sketch map of the main geological features and landforms in southern Wairarapa. Stop 1 = Bidwill Hill; Stop 3 = Otaraia; Stop 4 = Lake Ferry. From Palmer & Vucetich (1989, p. 501).

Wharekaka si.cl.loam (= Takamaru)

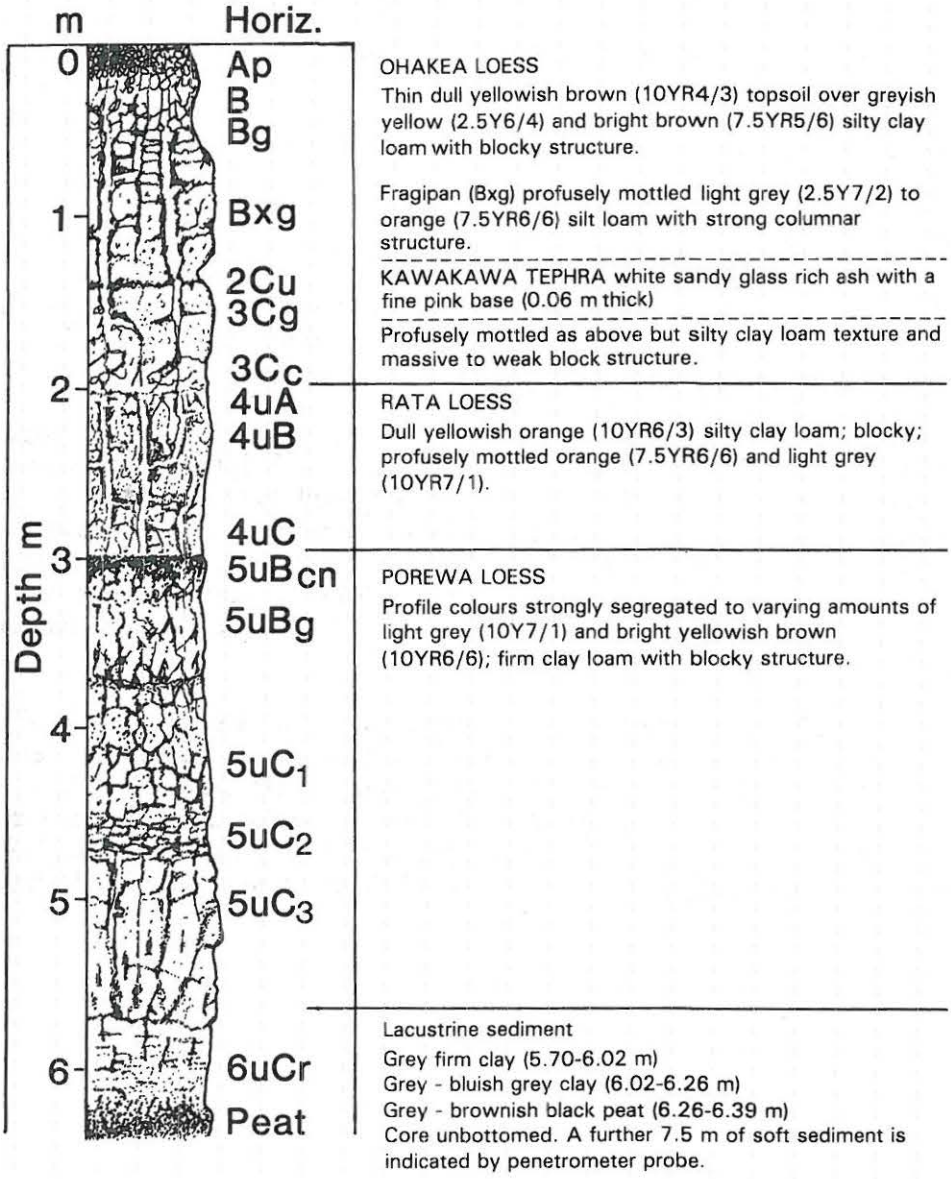

Figure 5.7: The Bidwill Hill loess column. Only the top 2.4 m is exposed above road level. From Palmer & Vucetich (1989, p. 503).

(v. large cations
Na rich in lower layers
⇒ lower exchange (as single cation
vs many smaller cations)
⇒ net -ve charge on clays
⇒ dispersion of floc.
[= dispersive

STOP 3 — Otaraia site

At Otaraia (Fig. 5.6) a much thicker loess section is visible, although Ohakean loess is now <1 m thick. The Otaraia site is on the downthrown side of Otaraia Fault on a surface that has been a sediment trap since the Last Interglacial. The Pallic Soil [= yellow-grey earths; mainly Aqualfs, Ustalfs, Aquepts — see Hewitt 1992] loess facies is very difficult to work with. Paleosols are generally unclear when soil formation from one episode is imprinted over another (Runge et al. 1974). Comparisons with present-day Pallic Soil morphologies (Tonkin et al. 1974), P distributions (Runge et al. 1974), major elements (Childs & Searle 1975), and dry bulk densities (Palmer & Barker 1984) have been successfully used to detect or confirm the presence of weathered horizons (paleosols) in the loess columns. The stratigraphy at Otaraia is similar to that at Bidwill Hill except that Ohakean loess is much thinner and Porewan loess, capped by a thick Eg horizon of a buried Aquept, is much thicker. The Interglacial sediments here consist of fluvial sands.

STOP 4 — Lake Ferry

Between Otaraia and Lake Ferry the road traverses marine terraces cut during the Last Interglacial. These were mapped by Ghani (1978) (Fig. 5.8). He assigned all four terraces to the Last Interglacial (80, 84, 100, and 125 ka) when we have seen that near Wanganui that only three marine terraces were cut during this period (Day 3). Ghani (1978) mapped the terraces by measuring heights of the **ground surface** and subtracting an arbitrary 10 m to approximate the wave-cut surface, whereas B.J. Pillans (e.g. Pillans 1983) in Wanganui measured only the height of the wave-cut surface. Exposure is generally poor but at Lake Ferry where well exposed there is up to 40 m of cover over the wave-cut surface. This leaves scope to re-interpret the marine terrace sequence by investigating loess coverbeds. If the youngest marine terrace is indeed c. 60 ka (not 80 ka) then only two loess units should be present on its surface (not three) (Palmer 1982). This question has yet to be finally resolved. Uplift rates appear to accommodate a c. 60 ka date for the lowest marine terrace and show it is less likely for the highest terrace to be older than 125 ka.

At Lake Ferry, Ghani (1978) mapped the marine terrace as his 84 ka year bench. The wave cut surface is covered by up to 10 m of marine gravels followed by 5 m of lacustrine or estuarine beds (muds, lignites, and gravels), 10 m of what look like fluvial gravels, and 5 m of loess comprising Ohakean, Ratan, and Porewan loess. If the youngest terrace is c. 60 ka, then this, the second terrace, should be c. 80 ka. The loess and cover-bed does not preclude this age. Berger et al. (1992) obtained a thermoluminescence date on a thin sand at the base of Porewan loess at 85 $\pm$ 15 ka (Table 3.1; sample FERY-1).

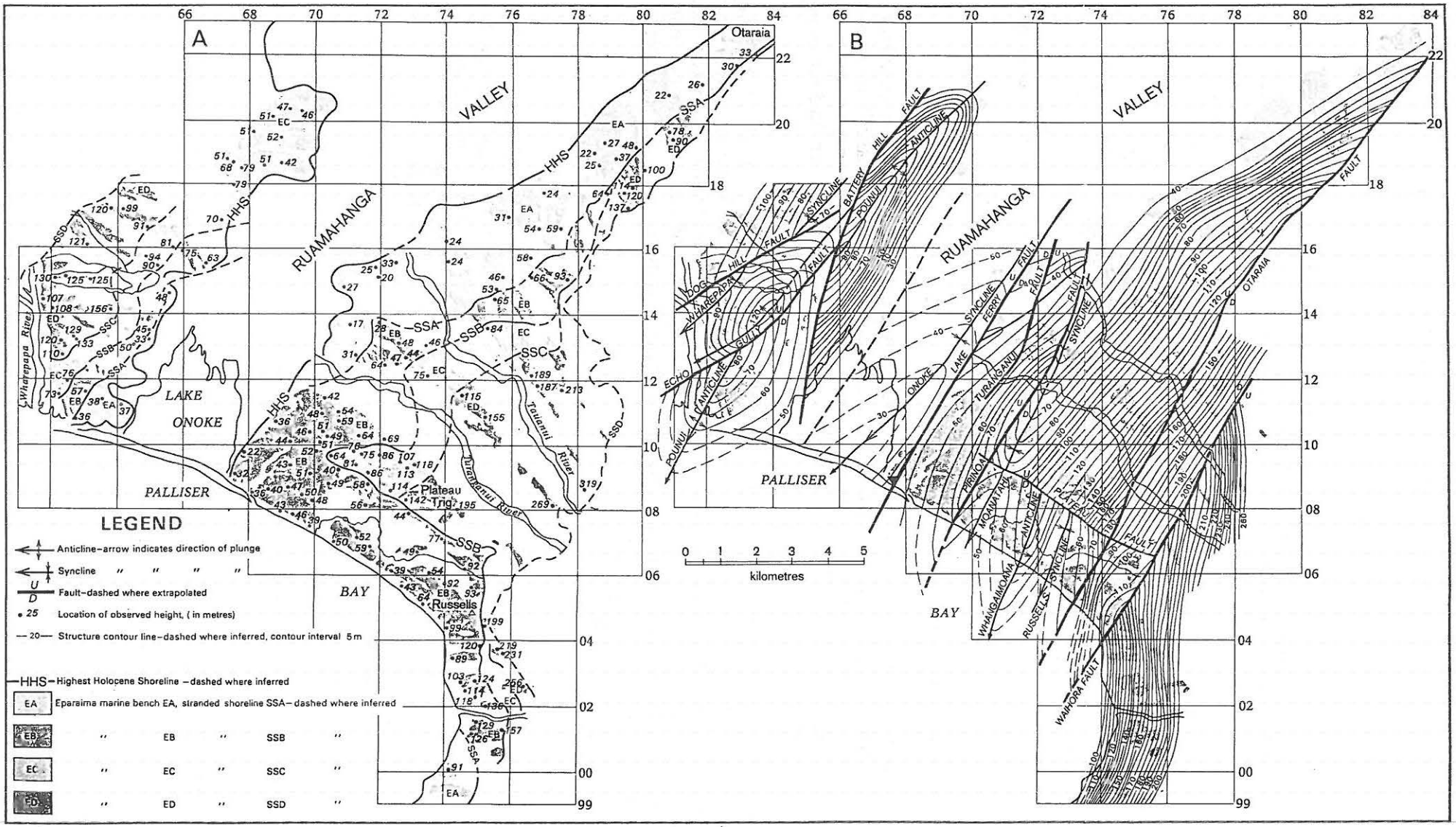

Figure 5.8: **A**. Marine terraces Ruamahunga Valley. Heights in m at points indicated. **B**. Structure contours, faults, and folds on Epiarima Marine Benches. From Ghani (1978).

THE HOLOCENE RECORD OF SOUTHERN WAIRARAPA VALLEY

Introduction

Global warming following the last stadial initiated a rise in sea level of c. 135 m in the New Zealand region, attaining near present day levels by 6. 5 ka. The rise in sea level was considerably more rapid than the rate of tectonic uplift of the land, and sediment rapidly accumulated within lower Wairarapa Valley. From 6.5 ka the uplift rate began to exceed sea level rise, and the sea gradually receded. The eustatic sea level curve constructed from New Zealand data (Gibb 1986) indicates that sea level has not varied by more than 0.5 m above or 1.0 m below present sea level since c. 6.5 ka.

The position of the highest Holocene shoreline (6.5 ka) in the southern part of Wairarapa Valley is marked by either cliffs cut into older surfaces, or a beach ridge, or sand dunes. Subsequent shorelines are marked by younger beach ridges, terraces, and sand dunes. Many of these features have been obscured by recent river erosion and sedimentation. In the early Holocene, before 6.5 ka, rivers in southern Wairarapa Valley aggraded to the rising sea level, but for the last several thousand years, aggradation from the main rivers has deposited finer deltaic sediments, gradually enclosing and silting up the lacustrine vestiges of the former estuary.

Marine sedimentary environments

By the time of the maximum marine incursion the sea was cutting back the mudstone cliffs of Palliser Bay and the greywacke cliffs at Turakirae Head. The strait between the present Lake Wairarapa and Palliser Bay was the focus of tidal currents that cliffed the tilted Last Interglacial marine benches. In the open embayment to the north (present Lake Wairarapa), the sea extended to within 5 km of both Featherston and Greytown.

Beach ridges can be traced inland through 'The Narrows' at Lake Ferry on each side of the valley. Usually the only beach ridge to be well preserved is the Highest Holocene Shoreline (HHS) which still forms barriers across the mouths of some valleys, forming swamps or small lakes. The beach ridge representing HHS is preserved around the entire west coast of Lake Wairarapa, but is recognisable mainly by morphology because the gravel forming it there is less characteristic of a coastal beach environment.

'The Narrows' entrance is now blocked by a gravel bar, 3 km long, with its crest 7 m above mean sea level, and built mainly from the headland on the western side.

Estuarine conditions persisted in Lake Wairarapa as late as 4.0 or 3.5 ka (Leach & Anderson 1974; Mitchell 1989) according to ^{14}C ages of fossil shells collected near Pirinoa. The dated shells are from sites now ambiguously at mean sea level, and there are conflicting opinions as to uplift rates in this, the axial part of the valley. Leach & Anderson (1974) reported a 20-30 cm uplift during the 1855 earthquake, but there is no evidence from historical diaries. Ghani (1978) inferred a close to zero uplift rate. Lake Wairarapa lies in a shallow structural sag but is regarded as a riverine lake (Lowe & Green 1992). It is now a mere 2 m deep and its surface is 1.2 m above sea level. With an area of 81 km^2, it is the 10th largest lake in New Zealand (Lowe & Green 1992).

Fluvial - lacustrine environments

The bar that blocks the entrance to 'The Narrows' holds back Lake Onoke, which is now held at close to mean high sea level by maintaining an open cut at Lake Ferry. Previously the bar-gap would gradually close during summer. In autumn and early winter the water would rise to 4 m above mean high sea level and flood the entire area, almost back to the HHS, making Lake Onoke and Wairarapa one, flooding the entire Kumenga and Kahautara region, and backing up the Ruamahanga River as far as Martinborough. Lacustrine sand and silt 2 m thick would be deposited over the entire region. By late winter the impounded water would break through the barrier.

The Tauherenikau and Ruamahanga Rivers have deposited large deltas of gravel, sand, and silt where they enter the lake. The Tauherenikau delta comprises the coarser material.

The vigorous rivers draining the Rimutaka and Aorangi Ranges south of Martinborough and Featherston have built large fans of greywacke gravel on the valley floor over the Ohakea Surface and older Holocene deposits. In particular, the Huangarua, Dry, Waihora, Tauanui, and Turanganui Rivers all deliver substantial amounts of gravel to the lower Ruamahanga River and pose considerable threat of flooding to farmland.

Aeolian environments

Paralleling the eastern shore of Lake Wairarapa is a series of at least 4 dune lines that mark former shorelines. Breaches and blowouts in the dune lines are aligned in the direction of the prevailing northwest wind.

The oldest dune line is often preserved above the low cliffs cut against Last Interglacial and older surfaces by the maximum sea level 6.5 ka. Thus, this dune line can not be much older than the cliff and probably is mostly younger, whereas the second main dune-line, 3 km west of Kahautara, seems to be resting on an old, low beach bar. The younger and lower dunes were possibly derived from Ruamahanga River delta sand on a lake-shore beach. The second youngest dunes are a maximum of 540 ± 50 yrs old (Mitchell 1989).

At places along the edges of terraces not covered by sand dunes are thin deposits of Holocene loess interbedded or laminated with sands. At Lake Ferry, 0.6m of Holocene loess and grit is preserved, apparently derived from the Palliser Bay beach below. A similar deposit is found on benches on the other side of 'The Narrows'. A thin veneer of Holocene loess is often encountered on the Waiohine Surface on the southeast side of the major rivers.

REFERENCES

Berger, G.W.; Pillans, B.J.; Palmer, A.S. 1992: Dating loess up to 800 ka by thermoluminescence. *Geology 20*: 403-406.

Childs, C.W.; Searle, P.L. 1975: Element distribution in loess columns at Claremont, Table Flat and Stewarts Claim, New Zealand. *New Zealand Soil Bureau scientific report 20*. 59 p.

Ghani, M.A. 1978: Late Cenozoic vertical crustal movements in southern North Island, New Zealand. *New Zealand journal of geology and geophysics 21*: 117-125.

Gibb, J.G. 1986: A New Zealand regional Holocene eustatic sea-level curve and its application to determination of vertical tectonic movements. *Royal Society of New Zealand bulletin 24*: 377-395.

Grapes, R.W.; Hardy E.F.; Wellington, A.W. 1984: The Wellington, Mohaka and Wairarapa Faults. *Publication of Geology Department, Victoria University of Wellington 28*.

Hewitt, A.E. 1992: New Zealand Soil Classification. *New Zealand Department of Scientific and Industrial Research scientific report 19*. 133p.

Kamp, P.J.J. 1992: Landforms of Wairarapa: a geological perspective. *In* Soons, J.M.; Selby, M.J. (eds) Landforms of New Zealand 2nd ed.Longman Paul, Auckland: 367-381.

Lamb, S.H.; Vella P.P 1987: The last million years of deformation in part of the New Zealand plate boundary zone. *Journal of structural geology 8*: 877-891.

Leach, B.F.; Anderson, A.J. 1974: The transformation from an estuarine to lacustrine environment in the lower Wairarapa. *Journal of the Royal Society of New Zealand 4*: 267-275.

Lensen, G.J. 1969: Sheet NI53, Eketahuna, Late Quaternary tectonic map of New Zealand. 1:63,360. New Zealand Department of Scientific and Industrial Research, Wellington, New Zealand.

Lowe, D.J.; Green, J.D. 1992: Lakes. *In* Soons, J.M.; Selby, M.J. (eds) Landforms of New Zealand 2nd ed.Longman Paul, Auckland: 107-143.

Marden, M.; Neall, V.E. 1990: Dated Okakean terraces offset by the Wellington Fault near Woodville, New Zealand. *New Zealand journal of geology and geophysics* 33: 449-453.

Mitchell, A.G. 1989: Late Quaternary deposits of the eastern shoreline of Lake Wairarapa, North Island, New Zealand. Unpublished MSc thesis, Massey University, Palmerston North.

Otway, P.M. 1972: Geodetic monitoring of earth deformation in the Wellington region. *New Zealand Geological Survey report 55*.

Palmer, A.S. 1982: The stratigraphy and selected properties of loess in Wairarapa. Unpublished PhD thesis, Victoria University of Wellington, Wellington.

Palmer, A.S.; Barker P.R. 1984: Dry bulk density, natural water content and tip penetration resistance data for four Wairarapa loess areas. *New Zealand Soil Bureau scientific report* 68. 29 p.

Palmer, A.S; Vucetich, C.G. 1989: Last Glacial loess and early Last Glacial vegetation history of Wairarapa Valley, New Zealand. *New Zealand journal of geology and geophysics 32*: 499-513.

Pillans, B.J. 1983: Upper Quaternary marine terrace chronology and deformation, South Taranaki, New Zealand. *Geology 11*: 292-297.

Runge, E.C.A.; Walker, T.W.; Howarth, D.T. 1974: A study of Late Pleistocene loess deposits, South Canterbury, New Zealand. Part 1: Forms and amounts of phosphorus compared with other techniques for identifying paleosols. *Quaternary research 4*: 76-84.

Stevens, G.R. 1991: On shaky ground - a geological guide to the Wellington Metropolitan Region. *Geological Society of New Zealand guidebook 10*. 112p.

Tonkin, P.J.; Runge E.C.A.; Ives, D.W. 1974: A study of Late Pleistocene loess deposits, South Canterbury, New Zealand. Part II: Paleosols and their stratigraphic implications. *Quaternary research 4*: 217-231.

Vella, P.; Neef, G.; Kaewyana, W. 1987: River piracy at Kakariki, north-western Wairarapa, New Zealand. *Journal of the Royal Society of New Zealand 17*: 373-380.

Warnes, P.N. 1992: Last Interglacial and last glacial stage terraces on the eastern side of Wairarapa Valley between Waiohine and Waingawa Rivers. *Journal of the Royal Society of New Zealand 22*; 217-228.